Australian Journal of

Engineering and Technology Research

VOL 2, ISSUE 1 (Jan-Jun 2017)
ISSN - 2206-5644

Published by:
Australian Research Journals, Western Australia

In collaboration with:
Research Gateway Society, Pakistan

INTRODUCTION

We are very pleased to present the third issue of **Australian Journal of Engineering and Technology Research.** Following is a brief overview of our journal, its purpose and current issue.

AJETR is a multi-disciplinary and open-access publication launched with an aim to encourage and facilitate the original research with a particular focus on developing countries. Accordingly, all publication fees are waived off for students from 28 selected universities from these countries.

Our scope covers a broad range of engineering and technology related disciplines. Research papers, book reviews, thesis and other scholarly works can be submitted for review throughout the year. Each year, **AJETR** has planned to launch two issues.

We aim to go a step ahead of other journals in terms of our commitment to nurturing the future researchers. In order to further this aim, we will be more than pleased to guide, assist and train young researchers and help them pave their way into an exciting research career. We are also very keen to form partnerships with universities in order to provide them useful research support and training.

I would like to extend my gratitude to all researchers, reviewers and others who supported Australian Research Journals in launching this research journal and presenting the current issue. We hope it comes out as a highly beneficial endeavour for the whole engineering and technology research community.

Yours Sincerely,

Muhammad Nabeel Musharraf

July 31, 2017

REVIEWERS:

Chief Editor:

Muhammad Nabeel Musharraf

Review Panel:

(Note: In addition to the following, journal may also seek assistance from external reviewers on case to case basis.)

Dr. Mohammed Abdul Rahim

(*Engineering and Technology***)**

Assistance Professor, Yanbu Industrial College, Saudi Arabia
Member, Indian Science Congress Association (ISCA).
Member, The Indian Society of Theoretical and Applied Mechanics (ISTAM),
Member, Andhra Pradesh Society for Mathematical Science (APSMS).
PhD, M.Phil, MS
(Specialization: Biofluid Dynamics)

Engineer Abdulghani A. Abied

(Information Technology, Systems Design, Technology Adoption**)**

Lecturer, Naser University, Libya.
PhD Candidate at Murdoch University, School of Information Technology, Western Australia.
M.Sc. (Computer Science)
B.Sc. (Computer Science)

Dr. Asim Saeed

(*Engineering and Technology***)**

Lecturer Australian Centre for Energy Process Training, Western Australia
PhD. Chemical Engineering
Masters in Chemical Engineering
Bachelors in Chemical Engineering
Diploma in Management

Engineer Muhammad Nabeel Musharraf

(*Mechanical, Mechatronics, Robotics, Automation, Engineering Management, IT***)**

B.E. (Mechatronics Engineering) - Recognized by Engineers Australia as eq. to 'Professional Engineer - Mechanical'
MBA (IT - Information Systems),
Certified Lean Practitioner,
Certified Six Sigma Champion,
ISO9001 Lead Auditor
Certified Internal Auditor - AU
Certified Trainer and Assessor - AU,
Diploma in WHS,
Diploma in Educational Psychology,
Diploma in Teaching
Instructional Design Master Class Training
(45+ professional certifications)

Engineer Muhammad Tariq Nazar

(*Computer Science***)**

Research and Training Associate, Information Technology University, Pakistan
Registered Member Pakistan Engineering Council
Microsoft Certified Solutions Expert (Server Infrastructure, Windows Server 2012)
Microsoft Certified Professional (Windows Server 2012 R2 and System Centre 2012)
Microsoft Specialist (Server Virtualization with Windows Server 2012 R2 Hyper-V and System Centre 2012 R2 Specialist)
Microsoft Certified Professional (Windows Server 2003 Client OS)
Cisco Certified Network Professional (CCNP IP Routing and Switching)
Cisco Certified Network Associate (CCNA R&S v2.0)
Cisco Networking Academy ID: 37330554 v5.0 with 95% plus marks)
B.Sc. Electrical Engineering (with specialization in Computer Systems)

Dr. Hafiz Usman Ahmed

(*Technology***)**

Lecturer,
Punjab University, Lahore, Pakistan
Ph.D, M.A. MBA, BA
(Gold Medallist)

Engineer. Muhammad Shakeel Ahmed

(*Engineering and Technology***)**

Lecturer Yanbu Industrial College, Saudi Arabia
Registered Member Pakistan Engineering Council
Member Mechanical Engineering Technology Quality Assurance and Accreditation
B.Sc. Mechanical Engineering

Engineer Adil Amjad Ashraf Sheikh

(*Software Engineering and IT, Embedded Systems, Systems Engineering***)**

Project Manager/Researcher,
UMM AL QURA UNIVERSITY,
MAKKAH, SAUDI ARABIA
Erasmus Mundus - European Masters in Informatics
(RWTH-Aachen and University of Trento, Aachen-Germany and Trento-Italy)
MS (Software Systems Engineering) from RWTH
MS (Embedded Systems Informatics) from University of Trento
B. E. Computer Systems (Honours) from NUST, Pakistan (Gold Medallist)

Table of Contents:

1. COMPARISON OF CONTROLLERS FOR SHIP AUTOPILOTS

   Raheel Ahmed Nizamani, Mukhtiar Ali Unar
   PP. 1-10
   DOI: https://doi.org/10.6084/m9.figshare.4909376.v1

2. PROSPECTS OF UTILIZATION OF MODIFIED DISH TYPE SOLAR COOKER IN RURAL AREAS OF SIND, PAKISTAN

   S.A. Shah, Syed Zulqarnain, Fawad Ahmed, S. Faraz, B. Asadullah, P. Ubedullah, P. Inamullah
   PP. 11-18
   DOI: https://doi.org/10.6084/m9.figshare.4909379.v1

3. ENHANCED SOLAR PV MPPT SYSTEM FOR 12V BATTERY CHARGER

   Shoaib Ahmed Siddique, Kashif Ishaque, Hooma Amjad, Mubashir Irshad
   PP. 19-28
   DOI: https://doi.org/10.6084/m9.figshare.4909391.v1

4. AUTOMATION OF SUPPLY CHAIN MANAGEMENT BY RFID AND XBEE NETWORK

   Aftab Ahmed, Qadir Bakhsh, Kamran Latif
   PP. 29-36
   DOI: https://doi.org/10.6084/m9.figshare.4909397.v1

5. REAL TIME MONITORING OF SUPPLY CHAIN MANAGEMENT NETWORK

   Aftab Ahmed, Qadir Bakhsh, Kamran Latif
   PP. 37-48
   DOI: https://doi.org/10.6084/m9.figshare.4909418.v1

6. COMBUSTION ANALYSIS OF COAL USING COAL WATER SLURRY TECHNIQUE

   Javaid Iqbal, Liaquat Ali Lehri, S. Mushtaq Shah, Mohammed Nadeem
   PP. 49-57
   DOI: https://doi.org/10.6084/m9.figshare.4909421.v1

7. CASE STUDY ON LEAN MANUFACTURING FOR MINIMIZATION OF DEFECTS IN THE FABRICATION PROCESS OF SHIPBUILDING

   A.N Sanjrani, S.A. Shah
   PP. 58-64
   DOI: https://doi.org/10.6084/m9.figshare.4909427.v1

8. COAL BED METHANE IN PAKISTAN: DIFFICULTIES AND PROSPECTS

Tahir Hussain Soomro, Abdul Samad Shaikh, Zeeshan Ali Lashari
PP. 65-72
DOI: https://doi.org/10.6084/m9.figshare.4909445.v1

9. ENVIRONMENTAL IMPACTS OF SHALE GAS EXPLOITATION

Tahir Hussain Soomro, Asadullah Memon, Zeeshan Ali Lashari
PP. 73-80
DOI: https://doi.org/10.6084/m9.figshare.4909448.v1

10. AN ADVANCED APPROACH FOR BETTER MECHANICAL PROPERTIES OF EPOXY BASED CARBON COMPOSITES USING DOUBLE VACUUM BAG INFUSION TECHNIQUE

Ashfaq Hussain, M.Faizan Siddique Awan, Kalsoom Bhagat, Laraib Alam Khan
PP. 81-88
DOI: https://doi.org/10.6084/m9.figshare.4909451.v1

11. DYNAMIC STRUCTURAL AND MODAL ANALYSIS OF TYRE COUPLING ON UNSTRUCTURED MESH

Intizar Ali, Dileep Kumar, Imran Mir, Ishfaque Ali Qazi
PP. 89-98
DOI: https://doi.org/10.6084/m9.figshare.4909457.v1

12. DETERMINATION OF TECHNICALLY FEASIBLE DEVELOPMENT STRATEGY TO PRODUCE UNCONVENTIONAL TIGHT GAS SAND RESERVOIR

Temoor Muther, Naveed Ahmed Ghirano, Saleem Qadir Tunio, Asadullah Memon, Abdul Haque Tunio
PP. 99-108
DOI: https://doi.org/10.6084/m9.figshare.5005070.v1

13. SHAPE MEMORY EFFECT AND PERFORMANCE OF A NITINOL ENGINE
Pranav A. Vyavahare, C. P. Karthikeyan
PP. 109-119
DOI: https://doi.org/10.6084/m9.figshare.5005832.v2

14. MULTI-AREA LOAD FREQUENCY CONTROL (LFC) FOR POWER SYSTEM USING LINEAR QUADRATIC GAUSSIAN (LQG) CONTROLLER

Muddasar Ali, Muhammad Ejaz Hassan
PP. 120-132
DOI: https://doi.org/10.6084/m9.figshare.5103226.v1

15. DESIGN OF ROBUST CONTROLLER FOR AUTOMATIC VOLTAGE REGULATOR (AVR) IN POWER SYSTEM

Khadija Jalal, Muhammad Ejaz Hassan
PP. 133-148
DOI: https://doi.org/10.6084/m9.figshare.5198275.v2

AUSTRALIAN JOURNAL OF ENGINEERING AND TECHNOLOGY RESEARCH (AJMFR)
Vol. 2, Issue 1 - 2017

COMPARISON OF CONTROLLERS FOR SHIP AUTOPILOTS

Raheel Ahmed Nizamani
Institute of Information and Communication Technologies, Mehran University of Engineering and Technology, Jamshoro

Mukhtiar Ali Unar
Institute of Information and Communication Technologies, Mehran University of Engineering and Technology, Jamshoro

Note: This paper has been accepted for publication from the submissions made at the 2nd National Conference on *Intelligent Manufacturing & Sustainable Energy Systems (IMSES 2016) - Pakistan*

Abstract

Majority of vessels at sea employ traditional Proportional Integral Derivative (PID) controller for manoeuvring. A vast majority of control algorithms are available; however, most designers use old Ziegler-Nichols tuned PID control which was proposed in 1942. Although some of the recent methods have been used in other areas of engineering yet hardly any of them have been utilized for a ship steering. This paper compares the performance of four of the more recent controllers for ship steering. Zeefakkel ferry and Mariner class ship are chosen to test the performance of the given controllers. Ship models are selected such that the performance of controllers may be evaluated for both open loop stable as well as open loop unstable ships. The controllers are tested through simulation studies.

Comparison study shows that Internal Model Controller performs better but it is suitable only for open-loop stable ships. For ships with open-loop instability Astrom method provides better results. Neural Network based controller should have performed best amongst all but it requires relatively large training data at varying speed.

Keywords:

Ship Steering, PID Control, Internal Model Control, Neural Network based Control, Ship Autopilot.

1. INTRODUCTION

The design of ship autopilots has remained challenge for more than a century. Almost all types of control algorithms including the PID [1], Least Squares Gaussian (LQG) [2-4], Pole placement [5], Fuzzy logic [6,7], Neural Networks [8,9], and many more have been investigated.

However, almost all commercial ships and more than 95% of closed-loop industrial processes use the controllers based on conventional PID algorithm. The measured heading of the ship is compared with desired heading and the resultant error is fed as input to the controller. The rudder angle commanded by the controller is then fed to ship steering machine which moves the rudder accordingly, the result of which is ship following its due course. The automatic ship steering is to fulfil two requirements i.e.,

course keeping and course changing. Course changing requires the controllers to change the heading of ship to desired heading in the shortest possible time without any oscillations in heading. This requirement of fast and accurate response is especially useful in crowded areas to avoid collision. The other requirement to be fulfilled by the ship controller is course keeping. This requires that the ship maintain its fixed course with minimum rudder activity and yaw effects as otherwise fuel consumption and wear on propeller blades would rise.

The performance of an automatic ship steering control depends upon type of ship under consideration, environmental conditions, performance criterion (eg. Fast or economical response) among other things. A vast majority of controllers are available. Some of them are better than others. The main purpose of this article is to explore any four best controllers for two types of ships, namely a ferry and Mariner Class Ship.

2. MATHEMATICAL MODEL OF THE SHIP

To derive equations of motion of ship an inertial (earth-fixed) and a body-fixed coordinate systems are chosen to describe the dynamics of motion of a ship. The nomenclature of ships' horizontal motion is described using Fig. 1.

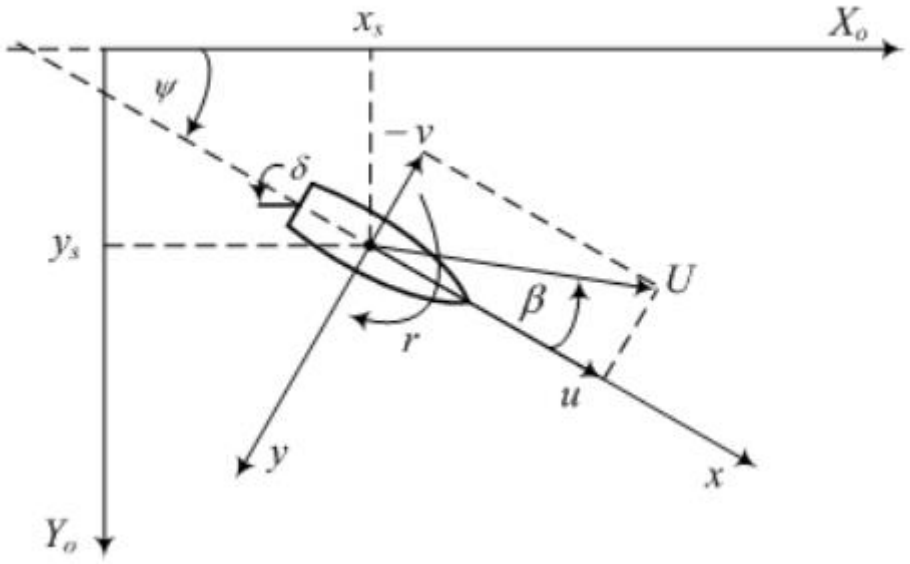

Fig. 1. Variables used to describe the horizontal motion of ship

2.1 Nomoto's Model

According to Nomoto's Second order model the yaw angle is related to rudder angle as [10]

$$\frac{\Psi(s)}{\delta(s)} = \frac{K(T_3 s + 1)}{s(T_1 s + 1)(T_2 s + 1)}$$

The parameters K, T_1,T_2 and T_3 are called "steering quality indices"

A first order approximation can be obtained by setting $T = T_1 + T_2 - T_3$

$$\frac{\Psi(s)}{\delta(s)} = \frac{K}{s(Ts+1)}$$

In this article two ships are considered namely a Zeefakkel Ferry and Mariner ship. Different model parameters of the two ships are given in Table 1 [10, 11]

Table: Parameters of the ships under consideration

Ship	**Zeefakkel**	**Mariner**
Length	45	161
Speed	5m/s	7.7m/s
K	0.5	-0.187
T	31	-402.83
b	0.016129	-0.000227
a	0.0322	-0.00248

2.2 Effect of Feed Forward Speed

The effect of forward speed U on ship parameters can be eliminated using non-dimensional quantities. If K_o and T_o are the gain and time constant respectively of Nomoto's first order model at speed U_o then

$$K = \left(\frac{U}{U_o}\right) K_o$$

$$T = \left(\frac{U_o}{U}\right) T_o$$

In this article, the ships are tested at a speed of 5m/s.

2.3 Norrbin's Model

Nomoto's model discussed above is a linear model suitable for constant feed forward speed and small rudder angles. Norrbin's proposed model does not make any such assumption and is given as [11]

$$\delta = m\ddot{\Psi} + d_1\dot{\Psi} + d_3\dot{\Psi}^3$$

where $m = \frac{T}{K}, d_1 = \frac{\alpha_1}{K}$ and $d_3 = \frac{\alpha_3}{K}$

2.4 Steering Machine

The function of steering machine is to move the rudder to desired heading when commanded by control system [10]. A simplified Simulink model is shown in figure. Rudder limiter and rudder rate limiter are in the ranges

$$\delta_{max} = \pm 35^{o} \text{ and } \dot{\delta}_{max} = \pm 5^{o}$$

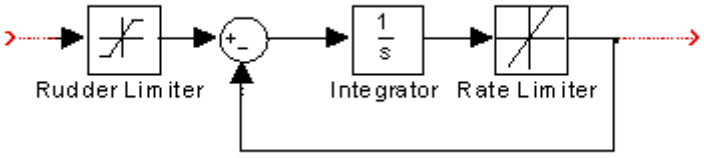

Fig. 2. Ship Steering Machine

3. SHIP COURSE CONTROL

The generalized block diagram of ship steering control system is shown in Fig. 3

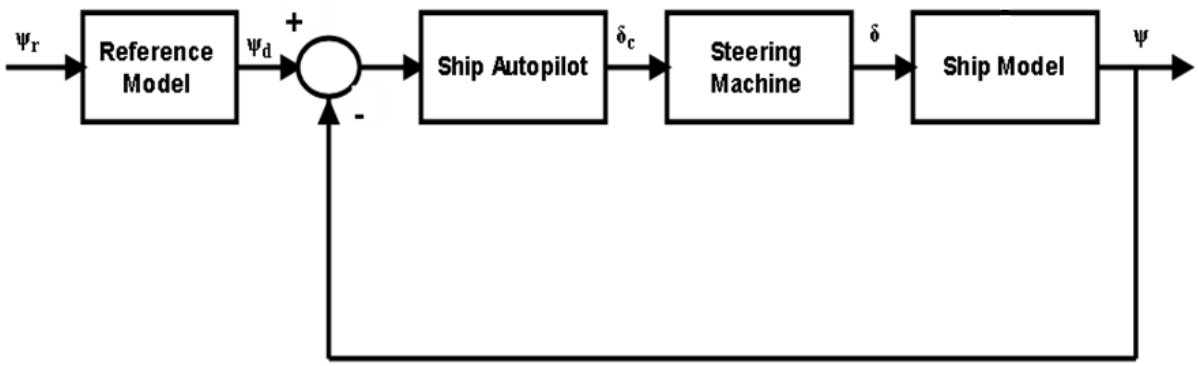

Fig. 3. Block diagram of complete Ship Steering system

In this article, four course changing controllers of the ship are considered

3.1 Fossen Controller

The controller proposed by Fossen [10] relates controller parameters with damping ratio ζ and natural frequency ω_n of a closed loop ship controller

$$K_p = \frac{T{\omega_n}^2}{K} K_d = \frac{2T\zeta\omega_n - 1}{K}$$

$$\frac{K_i}{K_p} \approx \frac{\omega_n}{10} = \frac{\omega_n K_p}{10} = \frac{{\omega_n}^3 T}{10K}$$

3.2 Astrom Controller

Astrom Controller is based on Optimal Control Theory which minimize certain performance index. Stability and maneuverability over a wide operating range, and minimizing propulsion loss due to

rudder movement are the two parameters chosen for the desired performance index expressed as [11]

$$J = \frac{1}{T}\int_0^T \left(\widetilde{\Psi^2} + \chi\delta^2\right)dt$$

Then the controller parameters which minimize the above performance index are given as

$$K_p = \begin{Bmatrix} \frac{1}{\sqrt{x}} & b > 0 \\ -\frac{1}{\sqrt{x}} & b < 0 \end{Bmatrix}$$

$$K_d = \begin{Bmatrix} \sqrt{\left(\frac{a}{b}\right)^2 + \frac{2}{b\sqrt{x}}} - \frac{a}{b} & b > 0 \\ -\sqrt{\left(\frac{a}{b}\right)^2 - \frac{2}{b\sqrt{x}}} + \frac{a}{b} & b < 0 \end{Bmatrix}$$

Where $a = \frac{1}{T}$ and $b = \frac{K}{T}$

3.3 Internal Model Controller

The Internal Model Control philosophy relies on the internal model principle, which states: "Accurate control can be achieved only if the control systems encapsulates (either implicitly or explicitly) some representation of the process to be controlled." The Internal Model Control structure has a controller implementation which includes model of the plant itself.

For a PID controller represented as

$$G_e = K_p\left(1 + \frac{1}{T_i s} + T_d s\right)$$

PID parameters for a wide variety of process models are given in Table 2 [12]

Table 2: PID controller Using Internal Model Controller

Model	Kp	Ti	Td
$\frac{K}{Ts+1}$	$\frac{T}{K\Omega}$	T	---
$\frac{K}{(T_1 s+1)(T_2 s+1)}$	$\frac{T_1+T_2}{K\Omega}$	T1+T2	$\frac{T_1 T_2}{T_1+T_2}$
$\frac{K(-ks+1)}{T^2 s^2+2\zeta T s+1}$	$\frac{2\zeta T}{K(k+\Omega)}$	$2\zeta T$	$\frac{T}{2\zeta}$
$\frac{K}{s(Ts+1)}$	$\frac{1}{K\Omega}$	---	T

Nomoto's first order model is given by $\frac{K}{s(Ts+1)}$, the PD parameters, as evident from the table above, can be calculated as

$$K_p = \frac{1}{K\Omega}$$

$$K_d = T$$

The integral term is calculated using the rule of thumb

$$K_i = \frac{\omega_n K_p}{10} = \frac{{\omega_n}^3 T}{10K}$$

3.4 Artificial Neural Network

Artificial Neural Networks (ANNs) have been popular choice for control of those problems whose parameters vary with operating conditions. ANNs are universal approximators and mimic the behaviour of the system to any degree of accuracy. In this work, a feedforward ANN has been trained to behave like a PID controller. This a a three layer network which is trained by using the well known error back propagation algorithm. Seven neurons have been used in the hidden layer. Each neuron in the hidden layer uses the tangent hyperbolic function and output neuron uses a linear transfer function. There are three input to the ANN which are the heading error, derivative of heading error and integral of the hidden layer. The only output is the rudder angle. It is possible to use the forward speed as an additional input so that the network can yield robust performance under varying speeds. However, this is a preliminary work in which forward speed has not been taken as an additional input.

4. SIMULATION STUDY

The Fossen controller, Astrom controller, Internal Model Controller and Neural Network Controller described in the article are implemented in Matlab/Simulink. The model is simulated for 100 seconds. The block diagram of the complete ship steering model, shown in figure, is implemented using Simulink.

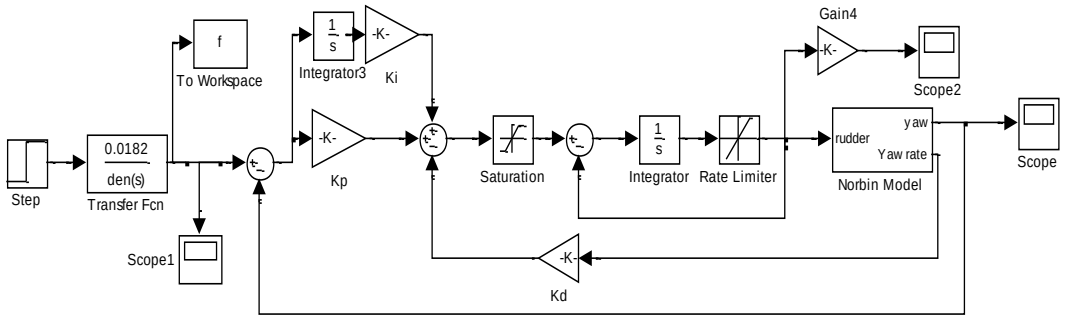

Fig. 5. Actual simulation model implemented in Simulink

The values of controller parameters of different controllers are tuned for best possible results. Natural frequency and damping ratio respectively for Fossen controller are $\omega_n = 0.03$ and $\zeta = 1$ respectively.

$x = 0.08$ for Astrom controller and $\Omega = 0.035$ for Internal Model Controller. Seven neurons are used to create the Neural Network. A step input of 7 degree heading change is given to the model and simulation is run for 100 seconds.

5. RESULTS AND DISCUSSION

In this section, the results of different controllers for ship autopilot are compared. In addition to heading response by different controllers, rudder responses are also compared with each other to check for saturation. Fig. 6 compares the course followed by Zeefakkel Ferry as generated by different controllers and Fig. 8 compares the course followed by Mariner Class ship. Fig. 7 and Fig. 9 compares the rudder response of all four controllers for Zeefakkel Ferry and Mariner Class Ship respectively.

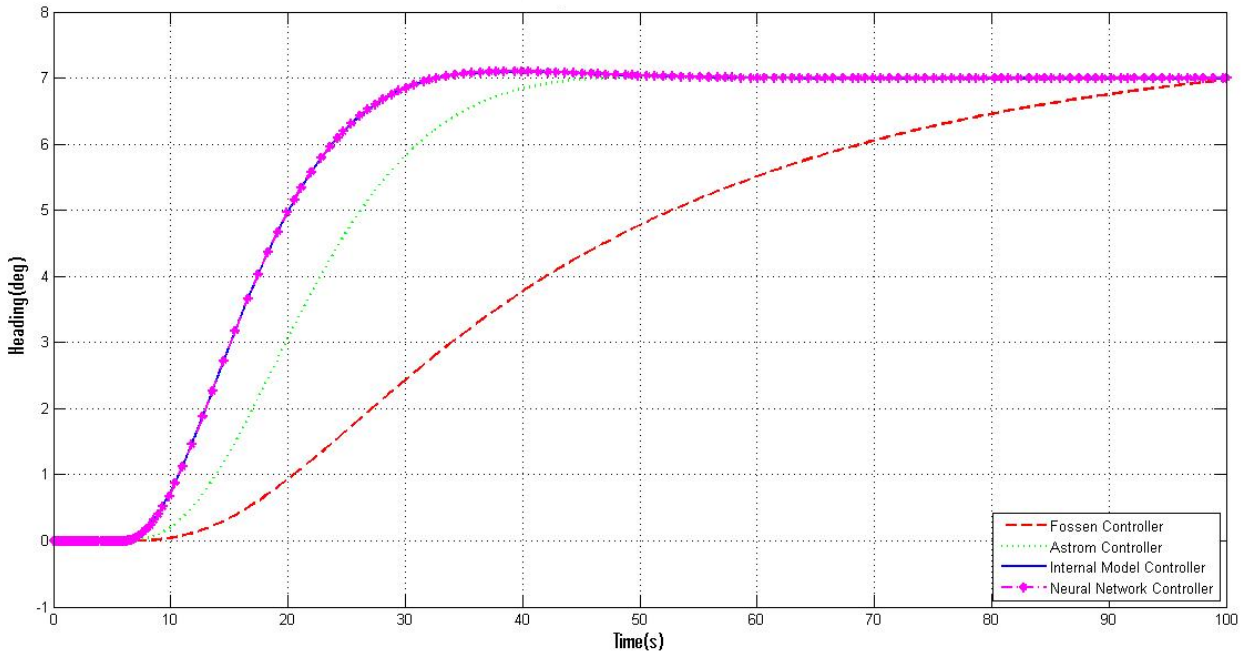

Fig. 6. Comparison of Heading Response for different controllers on Zeefakkel Ferry

During the initial 10 sec in Fig. 6, there is hardly any response by all controllers. This is due to the presence of reference model which smoothes out abrupt step input and provides the input to system gradually. For the next part of the response, as illustrated in Fig. 6 all three controllers except Fossen controller move the Ferry to desired heading of 7 deg in reasonable time. However the Fossen controller takes full 100 seconds to reach the desired heading. If the simulation time is increased it would be found that there is a large overshoot by Fossen controller and it almost takes a 1000 seconds to reach the desired heading.

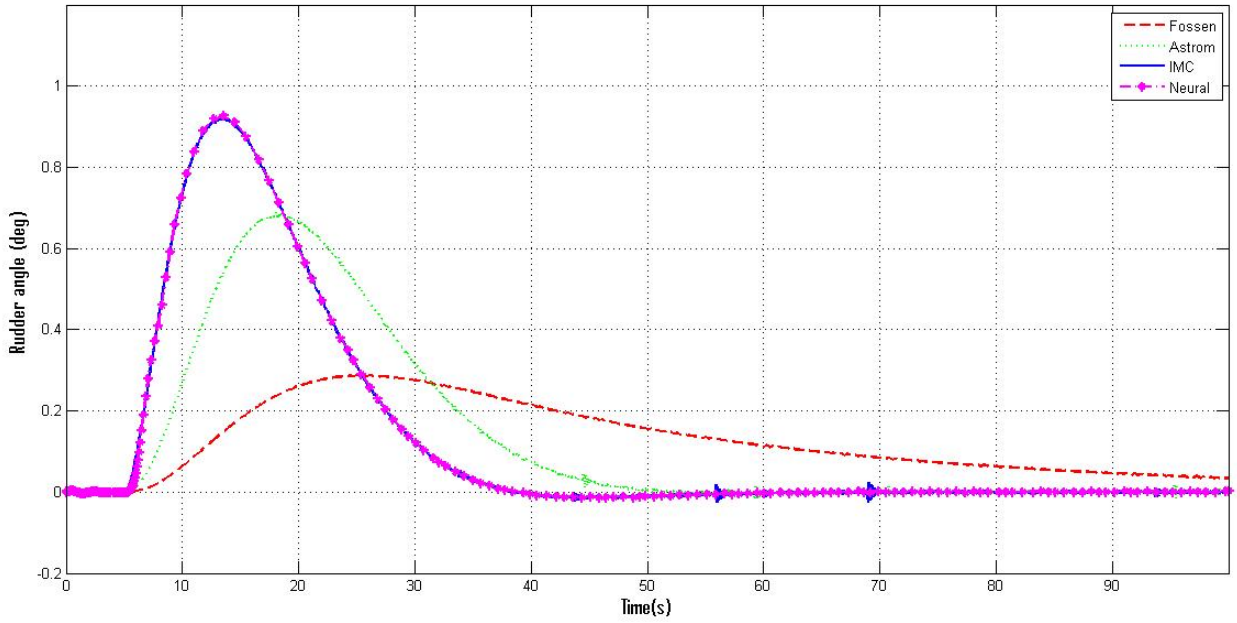

Fig. 7. Comparison of Rudder Response for different controllers on Zeefakkel Ferry

Fig. 7 illustrates the rudder responses by all four controllers. As is evident from Fig. 7 the rudder responses from all the controllers stayed within prescribed limits of saturation. However the rudder response of Fossen controller hardly showed any movement which proves the sluggishness of Fossen controller.

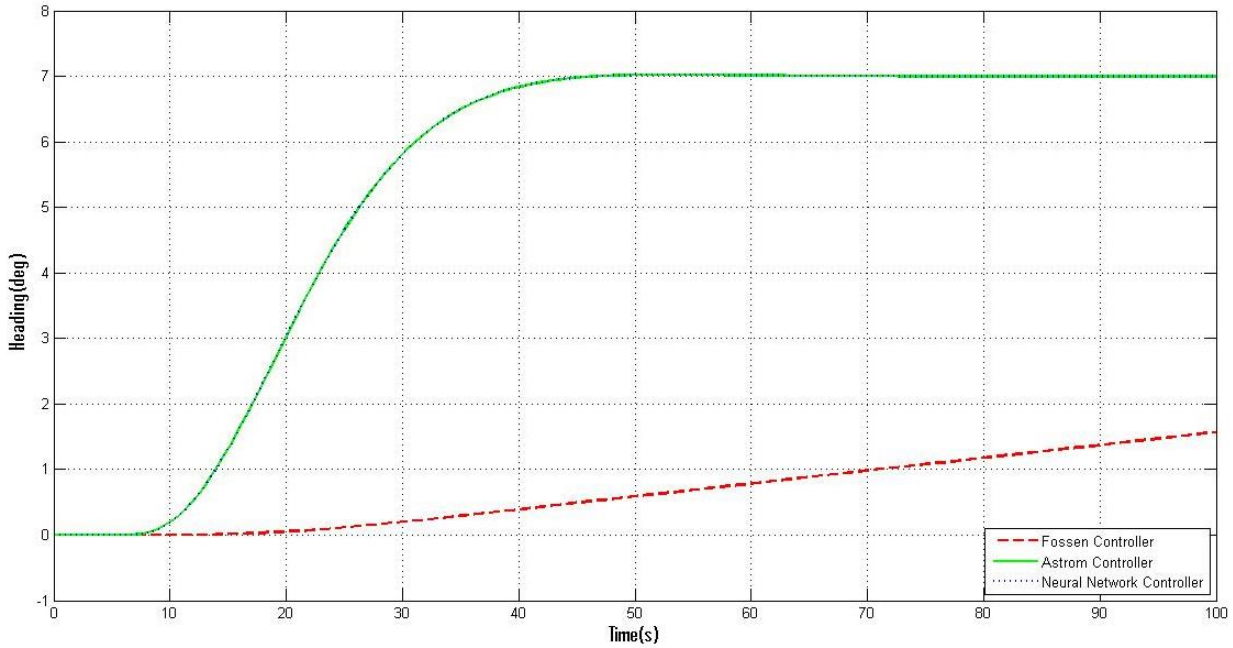

Fig. 8. Comparison of Heading Response for different controllers on Mariner Ship

Fig. 8 compares the heading response of different controllers for Mariner Class Ship. Internal Model Control on Mariner produces dangerously large oscillations and has therefore been neglected from

the comparison. This is due to the fact that IMC is only applicable on those ships which are open loop stable and the Mariner is open-loop unstable. Here again Fossen controller shows extremely sluggish response. Neural Network controller was trained using Astrom controller's data, therefore, their curves coincide.

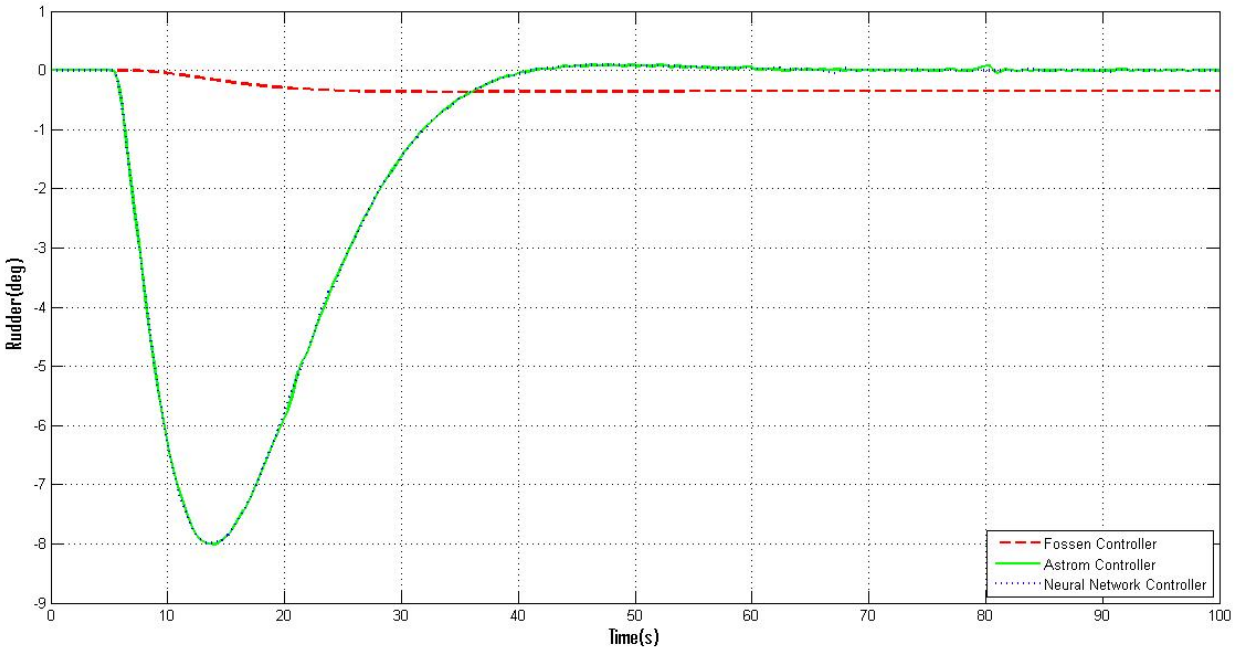

Fig. 9. Comparison of Rudder Response for different controllers on Mariner Ship

6. CONCLUSION

In this study, four types of controllers are used as autopilot for Zeefakkel Ferry and Mariner Class ship and their responses are compared. The complete models are simulated in Matlab/Simulink. Heading and rudder responses are compared against each other. The comparison reveals that Fossen controller performed worst for both the ships as it was very sluggish and had a dangerously large overshoot (not shown in diagram below due to small time range). Astrom controller performed relatively better but it also took longer time to reach steady state for Zeefakkel Ferry. For Mariner Class Ship Astrom controller performed best. Internal model controller and neural network controller trained using data set of IMC performed best in case of Zeefakkel Ferry but for Mariner Ship, IMC was not tested as it only can be used for open-loop stable ships whereas Mariner is open-loop unstable. Neural Network performed good for all cases and will continue to do so provided it has sufficiently large data set to be trained.

References:

1. Katebi R., Saeed Q., Non-Linear Predictive PID Control Design for Ship Maneuvering, IFAC Proceedings, Vol. 42, No. 18, pp. 86-90, 2009.
2. Rostgaard M., Poulsen N.K., Thygesen B.G., Ravn O., Stochastic Modeling and AdaptiveLQG Control of a Ship, Control Engineering Practice, Vol. 2, No. 6, 1994.

3. Holzhuter T., LQG Approach for the High-Precision Track Control of Ships, IEEE Proceedings - Control Theory and Applications, Vol. 144, No.2, pp. 121-127, 1997.

4. Katebi M. R.; Byrne J.; Marshall R., LQG Adaptive Autopilot Design, IEE Colloquium on Control in the Marine Industry, London, 1988.

5. Alfaro-Cid E.; McGookin E.W.; Murray-Smith D.J.; GA-optimised PID and pole placement real and simulated performance when controlling the dynamics of a supply ship, IEE Proceedings - Control Theory and Applications, Vol. 153, No. 2, 2006.

6. Larrazabal J.M., Santos Peñas M.; Intelligent Rudder Control of an Unmanned Surface Vessel, *Expert Systems with Applications,* Vol. 55, 2016, pp. 106-117, August 2016.
7. Pathan D.M., Unar M.A., Memon Z.A., Fuzzy Logic Trajectory Tracking Controller for a Tanker, Mehran University Research Journal of Engineering and Technology, Vol.31, No. 2,pp. 315-324, April 2012.
8. Unar M.A., Murray-Smith D.J., Automatic Steering of Ships Using Neural Networks, International Journal of Adaptive Control and Signal Processing, Vol. 13, No.4, pp. 203-218, 1999.
9. Khizer AN, Yaping D, Unar MA., Design of Heading Controller for Cargo Ship using Feed Forward Artificial Neural Network., International Journal of Advancements in Computing Technology, Vol. 5, No. 9, pp. 556-566, 2013.
10. Fossen T.I., Guidance and Control of Ocean Vehicles, John Wiley & Sons, 1994.
11. Unar M.A., Ship Steering Control Using Feedforward Neural Networks, PhD Thesis, University of Glasgow, Glasgow, Scotland, UK, 1999.
12. Unar M.A., Multi Loop PID Control Design, MSc Thesis, University of Glasgow, Glasgow, Scotland, UK.

AUSTRALIAN JOURNAL OF ENGINEERING AND TECHNOLOGY RESEARCH (AJMFR)
Vol. 2, Issue 1 - 2017

PROSPECTS OF UTILIZATION OF MODIFIED DISH TYPE SOLAR COOKER IN RURAL AREAS OF SIND, PAKISTAN

Shah, S.A.; Zulqarnain, Syed; Ahmed, Fawad; Faraz, S.; Asadullah, B.; Ubedullah, P.; Inamullah, P.

Department of Mechanical Engineering MUET SZAB,
Khairpur Mir's 66020, Pakistan

Note: This paper has been accepted for publication from the submissions made at 2nd National Conference on *Intelligent Manufacturing & Sustainable Energy Systems (IMSES 2016) - Pakistan*

Abstract:
Fossil fuels such as coal, natural gas, liquefied petroleum gas and biomass energy sources and residues are generally used to cater energy needs for cooking in rural and urban areas of Pakistan. However, natural gas and liquefied petroleum gas and coal are finite and are incapable to cope up with growing energy needs of population. Solar energy can be utilized as an alternative fuel for cooking using solar cookers in Sind, Pakistan. A Dish Type Solar Cooker of 4ft (122cm) with a collector covering its surface with a reflective Chrome-Silver-Mirror-Tint –Film is developed and is tested in two modes, one with bare and covered pot. A solar mechanical tracker is adjusted for changing the angle of collector every 20-30 minutes, which yielded promising results in terms of cooking food in efficient and effective manner.

Keywords: *Solar Cooker, Dish type, Portable, Collector*

1. INTRODUCTION:

Due to the finite nature of fossil fuel and their Environmental Hazards, which are used traditionally used for meeting cooking energy needs on small, medium and large scale, gradual switching over to renewable Energy is considered a feasible option and is the key energy issue in the world. Among renewable energy sources solar energy is considered a sustainable and reliable energy source in tropical parts of the world [1]. Fortunately, Pakistan lies in the tropic region and is replete with solar energy and seems feasible option to cater various energy needs, as is illustrated in annual solar irradiance data, which shown in figure 1.

There are various dimensions of solar energy utilization. Solar energy can be utilized as a source for electrical power generation, space heating, space cooling, drying and cooking [2]. Solar energy can be utilized using solar cookers to cook food on small, medium and large scale in the world. Solar Cookers have the potential to replace traditional cooking fuels in Sind, Pakistan because of abundance of solar Energy available in these areas throughout the day and round the year in environment friendly manner.

There are various types of solar cookers, which are used worldwide to cater cooking energy needs. The two most common designs include box type and parabolic concentrator type. Various developments are made worldwide on the utilization of solar cookers. Box and parabolic Type solar cookers designs are largely used for cooking food on small scale [1]. Cylindrical trough shape solar cooker designs are also used for cooking on both community and domestic levels [3,4]. Ssatellite dish

technology is also used for solar cooking applications [5]. Portable solar cooker and water heater with parabolic dish concentrator are also used, which have better energy and exergy efficiencies [6]. The efficiency of the solar cookers can be increased and cooking time can be reduced by modification in the design parameters [7].

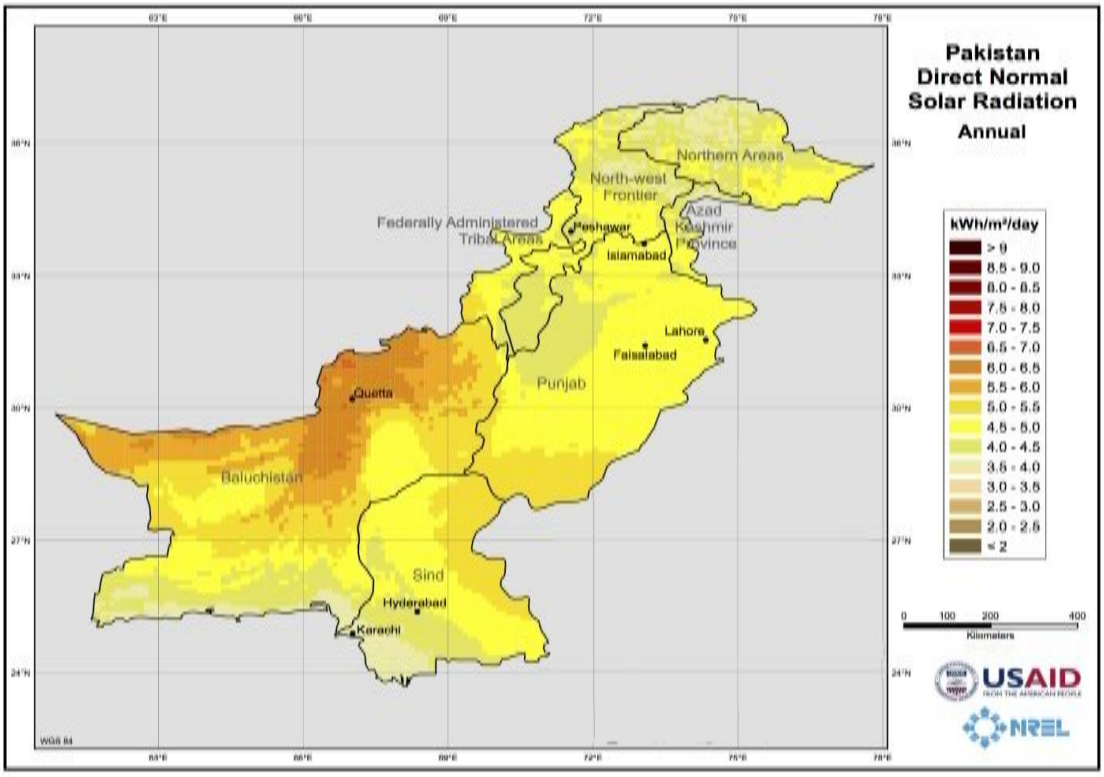

Figure 1: Annual Solar Irradiance data of Pakistan

Since cooking needs of people in Pakistan are met by the use wood burning, natural gas liquefied petroleum gas. However, these entire energy sources are unsustainable and cannot be considered as affordable option for meeting cooking energy needs of the people. There is dire need of an alternative renewable and sustainable energy source, which can cater not only cooking energy needs reliably but also is accessible to the people living equally in rural and urban areas of Sind, Pakistan.

The prospects of modified design of dish type solar cooker utilization are analyzed. A slight variation in one of the design parameters i.e. in the curvature of the concentrator is made in order to investigate its effect on the performance of solar cooker both in covered and uncovered pot mode.

2. Materials and Methodology

The material, which are used for frame/stand is mild steel. Dish/Concentrator is mounted on the central mild steel having rod of length 150cm, which is supported by a frame/stand. The focal length of pot holder/absorber is 37cm from the center of concentrator/dish and has diameter of 25cm.The angle of the dish is adjustable manually by tightening/losing the bolt on either side of the dish. Proposed dish type solar collectors is shown in figure 3 and 4.

The dish type solar cooker parameters comprise of focal length, concentration ratio, aperture area, cooking power and efficiency. These parameters are calculated theoretically on basis of the input data obtained on proposed site at Khairpur, Sind Pakistan.

A software "parabolic calculator 2.0 is also used for the calculation of these parameters and their results are compared with the results of theoretical design parameters.

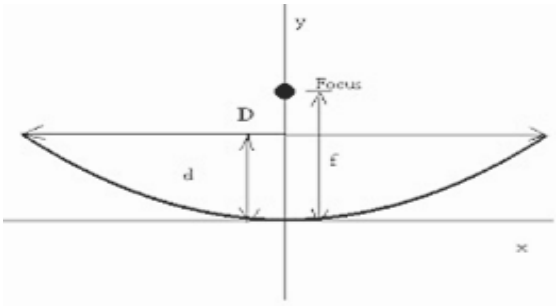

Figure 2: illustrate Diameter, Focus and Depth of Parabola

3. Results and Discussion:

The first design parameters, of proposed dish type solar cooker is focal length/distance, which is Distance from the Focus to the Vertex of Parabola, and is calculated by the following expression;

$$f = \frac{Da^2}{16h}$$

Where D_a is the aperture diameter and h is the height. The other parameter of dish type solar cooker is concentration ratio, which is the ratio of Aperture area to absorber area and is calculated by using the following expression;

$$C_{area} = \frac{A_a}{A_{abs}}$$

Where D_a is the aperture diameter and h is the height. The other parameter of dish type solar cooker is concentration ratio, which is the ratio of Aperture area to absorber area and is calculated by using the following expression;

$$A_a = \frac{\pi Da^2}{4}$$

Where *Da* is the diameter of the absorber. The cooking Power is an important parameter in solar cooker and is calculated by using the following relationship.

$$P = \frac{mC_p\Delta T}{t}$$

Where m is the mass of the liquid in the pot $C_p$isthe Specific heat and $\Delta T$is rise in the temperature of water and *t* is the cooking time of the test. The efficiency of the cooking process is calculated by using the following expression:

$$\eta = \frac{mC_p\Delta T}{tA_a\mathrm{G}} = \frac{P}{A_a\mathrm{G}}$$

Where G is the Solar Irradiance in W/m^2.

Following results are obtained by using above formulas

- ✓ D= 122cm
- ✓ Depth = 25cm
- ✓ $f = 37.21$
- ✓ $C_{area} = 23.63$
- ✓ $A_a = 1.16m^2$
- ✓ $A_{abs} = 0.049m^2$

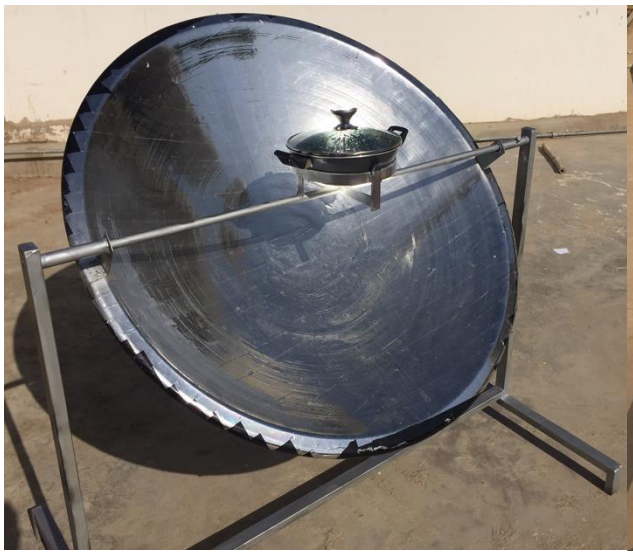

Figure 3: The Solar Cooker while cooking

Figure 4: The Solar Cooker

Cooking Power and Efficiencies of solar cooker were calculated as shown in table.1 and table.2 and their corresponding graphs shown in figure 5 and figure 6.

Table 1. Power required v/s Output

Sr. #	Time (min)	Mass of Water (kg)	Power Required (W)	Power Output (W)
01	20	1	259.8566667	191.8833333
02	35	2	296.9790476	231.0333333
03	50	3	311.828	262.9333333
04	65	4	319.8235897	302.0833333
05	80	5	324.8208333	320.9333333
06	95	6	328.24	325.2833333
07	110	7	330.7266667	300.15
08	125	8	332.6165333	280.8166667
09	140	9	334.1014286	273.5666667
10	155	10	335.2989247	241.1833333
11	170	11	336.285098	199.1333333
12	185	12	337.1113514	175.9333333

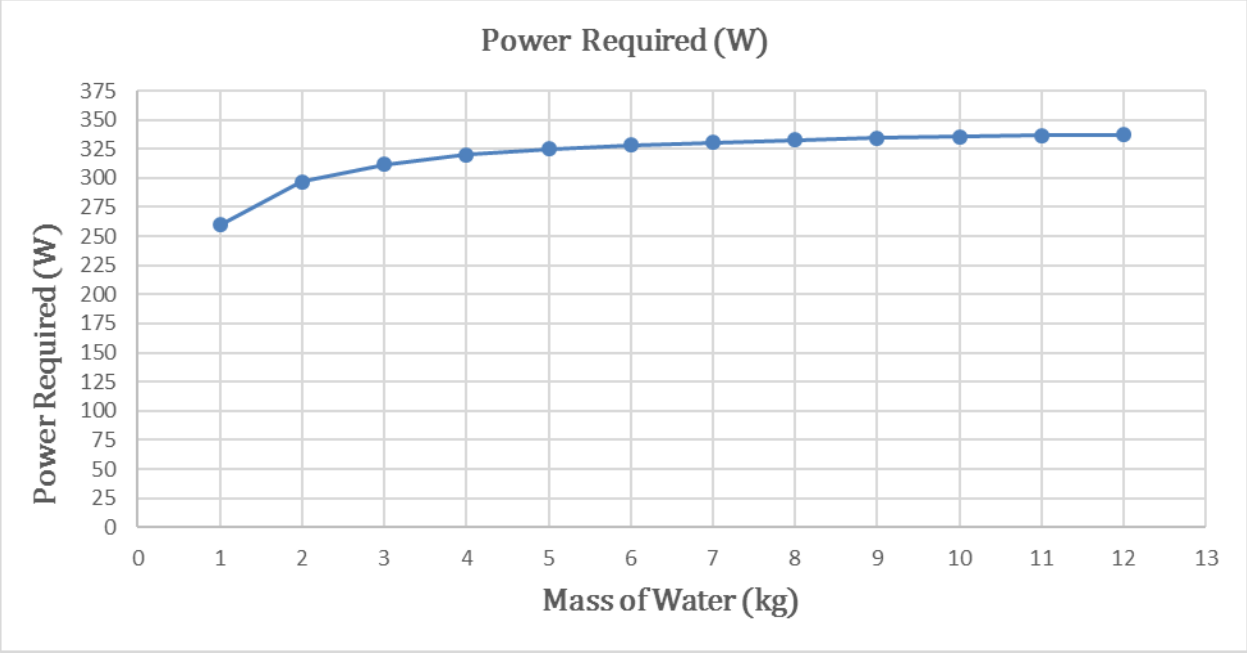

Figure 5: Power v/s Mass of Water

Table 2. Annual Efficiency

Sr. #	Month	Efficiency
01	January	0.580187063
02	February	0.698562761
03	March	0.795017033
04	April	0.913392731
05	May	0.970388438
06	June	0.983541293
07	July	0.907547018
08	August	0.849089883
09	September	0.827168457
10	October	0.729252757
11	November	0.602108488
12	December	0.531959927

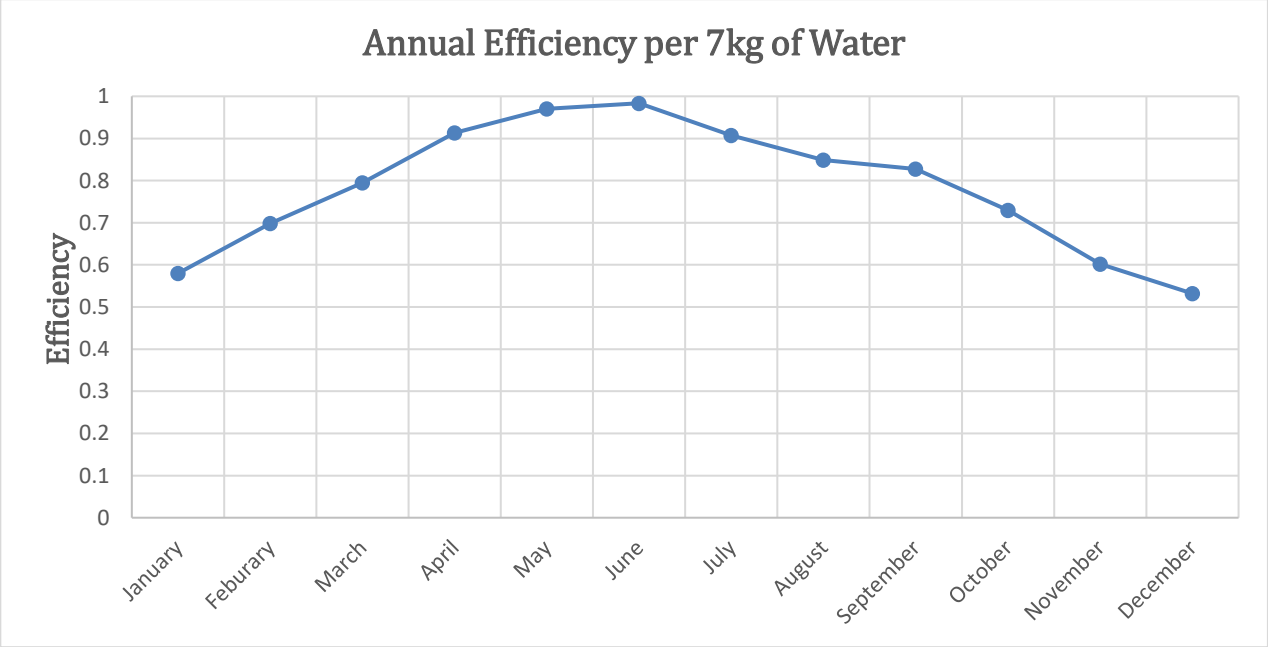

Figure 6: Annual Efficiency for Cooking

High efficiency and power can be obtained as per the monthly solar irradiance data of the place. By analyzing Table 2, it can be said that power obtained during the month of May & June is increased by 45 % compared to the month of December due to the available maximum solar irradiance value.

The proposed dish type solar cookers have potential to produce required amount of cooking energy and is capable to replace traditional fuel and cooking appliances in rural and urban areas of Sindh, Pakistan. There is considerable scope of solar cookers in Sindh, Pakistan and these can be used in those underdeveloped areas, where traditional fuels have failed miserably.

4. Conclusion:

It was found that 7 Kg of water at 25 ^{o}C with pot covered was bought to boil at approximately 99.6 ^{o}C in 110 min which is very high compare to conventional flat-plate Designs. An increase in efficiency as much as 45 % was found during the month of June with an uncertainty of ±1.7%. Using glass box for pot during cooking, it was found that efficiency and cooking power increased by 38% & 275% respectively. If considerable support is provided in terms of material resources portable dish type solar cookers can be manufactured on small, medium and large scale.

References:

1. Shah,S.A.Abbasi A.F and Daudpoto J.”Energy and emission benefit analysis of solar powered electrical power generation in Pakistan", Sind University Research Journal Vol:46, June (2013)
2. Shah,S.A.,Abbasi,A.F.and Daudpoto J.”Case Study of Electrical Energy Requirement for meeting various needs in a desert dwelling" Mehran University Research Journal, Vol:32 July,(2013)
3. H.H Ozturk,” Energy and exergy efficiencies of a solar box-cooker”, “International Journal of Exergy (IJEX)”, Vol. 1, No. 2, 2004.
4. R.Petela,” Exergy analysis of the solar cylindrical-parabolic cooker”, “Solar Energy”, Volume 79, Issue 3, Pages 221–233, September 2005.
5. S.C. Kaushik, M.K. Gupta, “Energy and exergy efficiency comparison of community-size and domestic-size paraboloidal solar cooker performance”, “Energy for Sustainable Development”, Volume 12, Issue 3, Pages 60-64, September 2008.
6. Saleh A, Badran A. “Solar cooker utilizing satellite dish technology”, “In: Proceedings of the global conference on renewable energy approaches for desert regions (GCREADER)”, Amman; 18–22 September 2006.
7. Ali A. Badran, “Portable solar cooker and water heater”, “Energy Conversion and Management”, Volume 51, Issue 8, Pages 1605–1609, August 2010.
8. N. L. Panwar, S. C. Kaushik, Surendra Kothari,” Experimental investigation of energy and exergy efficiencies of domestic size parabolic dish solar cooker” “AIP/Journal of Renewable and Sustainable Energy” Volume 4, Issue 2, doi: 10.1063/1.3699615, (2012).
9. Joudeh Noureddin K, Modified portable solar cooker, B.Sc. Graduation Project, Department of Mechanical Engineering, Faculty of Engineering and Technology, University of Jordan; May 2007.
10. A. K. PandeyV. V. TyagiS. R. ParkS. K. Tyagi,” Comparative experimental study of solar cookers using exergy analysis”, “Journal of Thermal Analysis and Calorimetry”, Volume 109, Issue 1, pp 425–431, July 2012,

11. H.H Ozturk," Experimental determination of energy and exergy efficiency of the solar parabolic-cooker", "Solar Energy", Volume 77, Issue 1, Pages 67–71, 2004.
12. "NASA Surface meteorology and Solar Energy: RETScreen Data", Eosweb.larc.nasa.gov, 2016. [Online]. Available: https://eosweb.larc.nasa.gov/sse/RETScreen/.
13. "NREL: International Activities - Pakistan Resource Maps and Toolkit", Nrel.gov, 2016. [Online]. Available: http://www.nrel.gov/international/ra_pakistan.html.
14. " Parabola Calculator version 2.0", Mscir.tripod.com, 2016. [Online]. Available: http://mscir.tripod.com/parabola/.

AUSTRALIAN JOURNAL OF ENGINEERING AND TECHNOLOGY RESEARCH (AJMFR)
Vol. 2, Issue 1 - 2017

ENHANCED SOLAR PV MPPT SYSTEM FOR 12V BATTERY CHARGER

SHOAIB AHMED SIDDIQUE,
Department of Electrical Engineering, Mohammad Ali Jinnah University-Karachi

KASHIF ISHAQUE,
Department of Electrical Engineering, Mohammad Ali Jinnah University-Karachi

HOOMA AMJAD,
College of Engineering, Pakistan Air Force - Karachi Institute of Economics & Technology

MUBASHIR IRSHAD,
College of Engineering, Pakistan Air Force - Karachi Institute of Economics & Technology

Note: This paper has been accepted for publication from the submissions made at the 2nd National Conference on *Intelligent Manufacturing & Sustainable Energy Systems (IMSES 2016) - Pakistan*

ABSTRACT:

When a Photovoltaic (PV) panel is exposed to sunlight an I-V characteristic curve of that panel is observed. The I-V characteristics of the PV panel continuously change with the change in insolation and temperature of the surroundings which also alters the maximum power point MPP of the PV panels. This affects the charging process of the batteries connected with the PV panels. This paper presents the solution to an efficient designed Solar PV system for charging the batteries. The system uses Perturb & Observe (P&O) algorithm to track the MPP. The MPP tracking algorithm works in conjunction with a DC-DC Buck (step-down) converter. The power from the PV panels is fed into a charge controller, which equals the PV voltages to the battery voltages with maximum power being delivered from PV panels to the batteries. A dsPIC microcontroller is used which continuously tracks the MPP even with the changing conditions and handles the charging battery voltages. A MATLAB based modelling and simulation is also designed and is first used to test the algorithm along with the charge controller under the changing conditions and then it is implemented on the hardware. The simulation results show that the algorithm tracks the MPP point of the PV panels, including the hardware results which verifies the efficient working of the proposed design.

Keywords: Maximum Power Point Tracking (MPPT), Perturb and Observe (P&O), MATLAB, DC-DC Converter.

1. INTRODUCTION:

With the increasing crisis in the availability of energy and its resources; like fossil fuels, solar energy has become one of the most demanding resources for the production of electrical energy. Solar panels need to be operated at maximum power point (MPP) in order to extract maximum power out of it. This is done with the help of a power dc-dc converter allowing the panels to thoroughly operate at maximum power point. PV Panels when being operated at the maximum power point gives the highest efficiency. There are various algorithms for MPP tracking, the one used here is hill-climbing algorithm commonly known as Perturb and Observe (P&O), which is one of the most extensively used algorithm due to its simplicity and ease of implementation [1] [2]. It operates by perturbing the operating voltages of the PV array. The P&O works well under slight variations in irradiance [3].

The solar panel used is JC120S-12/Zb and the characteristics are enlisted below:

Table 1: Parameters of JC120S-12/Zb Module under STC

Maximum Power at STC	P_{max}	120 Wp
Open Circuit Voltage	V_{oc}	19.8 V
Optimum Operating voltage	V_{mp}	16.0 V
Short circuit current	I_{sc}	8.03 A
Optimum operating current	I_{mp}	7.50 A

For a battery with lower voltages the power rate of charging losses increases when directly connected to the solar panels, which is catered by this MPPT charger. These losses occur because of the current-voltage (I-V) characteristics curve of the solar panels. Every PV module has its own I-V curve which gives information about the characteristics of the module. The proposed power converter for this project is a step-down DC-DC converter known as Buck Converter, which steps down the input DC voltages. This paper focuses throughout on efficient battery charging through solar panels with minimal losses. Establish the research background in this section.

2. MPPT BATTERY CHARGING SYSTEM MODEL:

PV panels provides dc output voltages with a certain I-V curve characteristics, each panel has its own curve characteristics depending upon the design. This dc voltage is not stable enough to directly charge the batteries therefore they need to be converted up to a voltage level to stably charge the batteries. This is done with the help of a dc-dc converter which is a buck converter in this case. A MPP tracking algorithm is implemented using a dsPIC microcontroller. This controller keeps tracking the MPP and operates the panels at this point. A simple block diagram of this model is shown in figure 1.

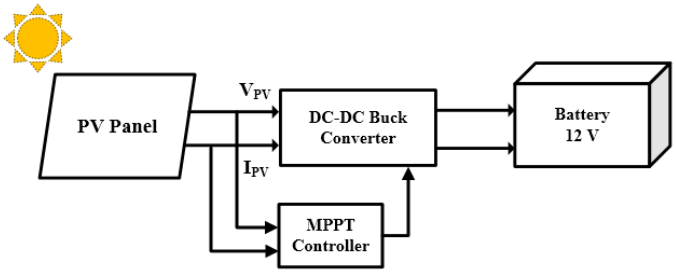

Figure 1 MPPT Battery Charging system model

3. MAXIMUM POWER POINT TRACKING (MPPT)

Maximum Power Point Tracking as the name suggests is an algorithm used for the tracking of maximum power of the solar panels being used. MPP can easily be understood referring to a non-MPPT based system; in which if we talk about a non-MPPT based battery charger means that the solar panels are directly connected to the battery terminals without any kind of circuitry in between them. In this case, the panels operate only on the battery voltages thereby not delivering their maximum power.

Contrary to it a MPPT charger ensures solar panel to function on voltages at which it is able to supply maximum power to the batteries for charging. A solar panel comes with the specs including Voc and Isc and each panel have different I-V Curve under constant irradiance as discussed. The real-time I-V curve of two *JC120S-12/Zb* solar panels in series is shown in figure 2.

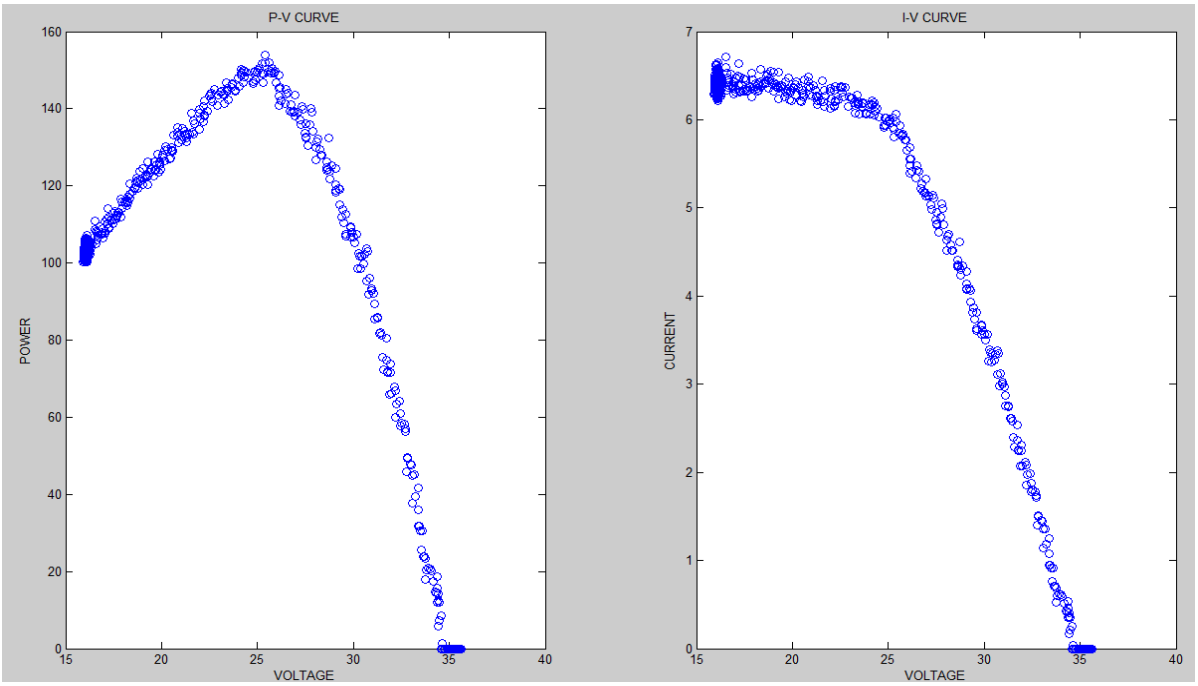

Figure 2 Real-Time P-V & I-V curve of 2 series connected solar panels.

The I-V curve in figure 2 is a real-time graph plotted on MATLAB. The V_{oc} and I_{sc} are 35 volts and 6.5 Amperes respectively. The maximum power point MPP lies on the knee of this curve which is around the point where I_{pv}=5.8A & V_{pv} = 25V. The basic objective of MPP algorithm is to track this knee. The maximum power can be seen from the PV curve which is at 145 Watt.

A number of researches have took place in this field for efficiently tracking the MPP of a panel. There are a number of ways to track the MPP, out which few are listed below:

i- Perturb and Observe
ii- Incremental Conductance
iii- Current Sweep
iv- Constant Voltage

The method used here is Perturb and Observe MPPT algorithm.

4. PERTURB & OBSERVE (P&O)

Perturb and Observe, an MPPT algorithm commonly known as P&O algorithm; in this method, the voltages in small amount from the PV panel are set by the controller, the controller calculates the power and if there is an increase in power the controller makes further adjustments in that direction until the power no longer changes [4].
The P&O algorithm measures the voltage, current and calculates the power of the PV panels and then perturbs the voltage to estimate the changing direction. Figure 3 shows a PV curve of a PV panel.

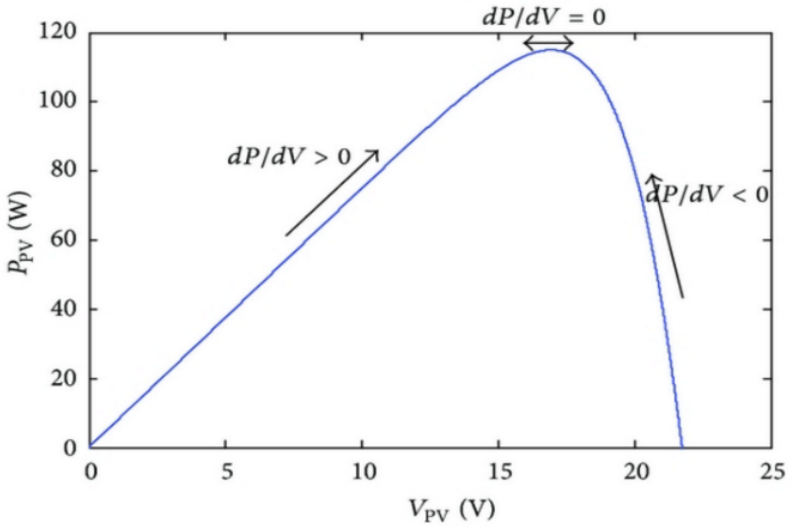

Figure 3 P-V Curve of a Solar Panel.

It can be witnessed from the left side the PV panel power increases with the increase in panel voltages and after the maximum power point (MPP) at the right-hand side the power starts decreasing. This concludes that if he power is increasing in a certain direction the perturbation must also be performed in the same direction either from left to right or right to left. Contrary to it if there is a decrement in power reverse perturbation must be performed [5].

The MPP is achieved when the ratio of change in power and change in voltage is equal to zero i.e. dP/dV =0. The functional operation of P&O algorithm can be summarized with the help of the table below:

Table 2: P&O Operation Table

ΔP_{PV}	ΔV_{PV}	Perturbation
>0	>0	Increase V
>0	<0	Decrease V
<0	>0	Decrease V
<0	<0	Increase V

Table 2 with reference to figure 3; when the change in power and voltage of the panels is greater than 0 the perturbation must be done so as to increase the panel voltages. If the change in power is greater than 0 and the change in voltage is less than 0, the perturbation must be done in a manner to decrease the voltage of the panels. A flow chart representing the flow of P&O algorithm is shown in figure 4.

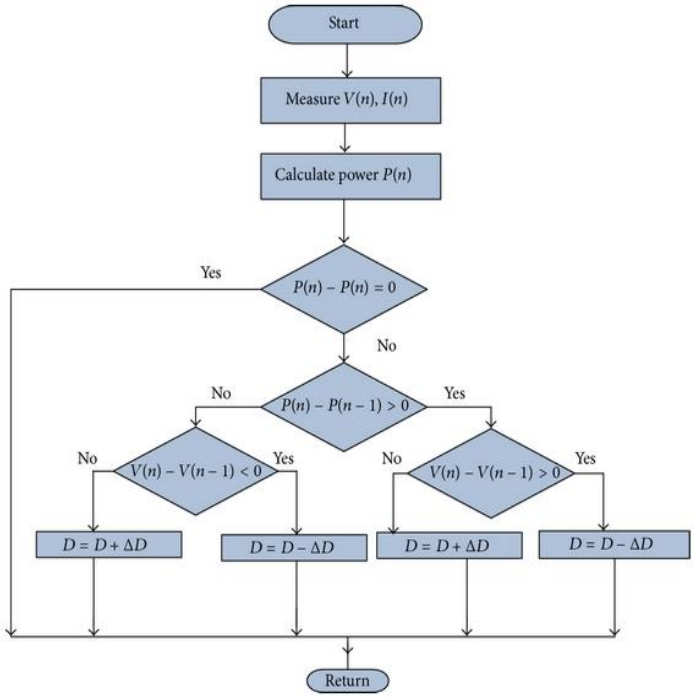

Figure 4 P&O Algorithm Flow Chart

The solar panel voltage and current is initially measured and the power is then calculated. The change in power ΔP_{PV} and change in panel voltages ΔV_{PV} are then calculated after this the panel voltages are perturbed by a constant value. If this perturbation causes the power to increase the perturbation must be done in the same direction else if the case is opposite then reverse perturbation must be applied. This P&O algorithm is also known as hill climbing algorithm [6].

5. DC-DC Converter

It is a power electronic circuitry that converts DC voltages from one level to another. It can be either a step-up (boost) or a step-down (buck) converter and is a class of power converters. Depending upon the applications there are a wide range of DC-DC converters. There are a variety of DC-DC converters depending on the method of voltage level conversion two of them are:

i- Linear DC-DC Converters
ii- Switched mode DC-DC Converter

The dc-dc converter is the main circuitry responsible for the tracking of MPP [7] [8]. There are some drawbacks of linear DC-DC regulator in terms of power losses; like they can only output lower voltages than the input supplied to them. Considering the efficiency of the switched mode converters (75-98%) we will be using these for MPPT purpose to charge the battery.

The dc-dc converter used here for the MPP tracking is a Buck Converter.

6. DC-DC BUCK Converter

A buck converter is a step-down DC to DC converter which reduces the voltages applied to its input by a certain factor. A general circuit diagram of buck converter is shown in figure 5.

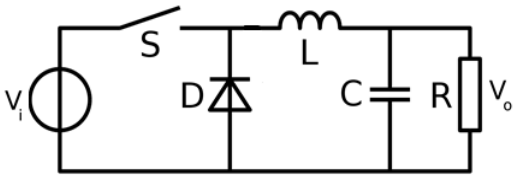

Figure 5 Circuit Diagram of a Buck Converter.

Where V_i is input voltage, V_o is the output voltage, S is an active switching device, D is a diode, L is an inductor and C is the capacitor.

7. WORKING OF BUCK CONVERTER

A switch mode converter; buck converter in this case contains a switch which is usually a mosfet an active device. When a switching device is introduced there exist a dual state of operation; namely ON state and OFF state. These states are named with reference to the switching device in the converter, a mosfet.

During the ON state, when the mosfet is on the circuit in figure 5 becomes as shown below:

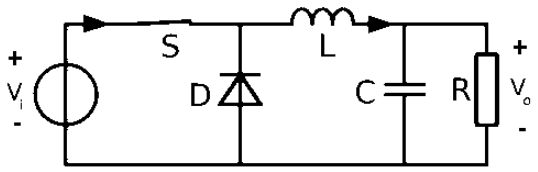

Figure 6 Buck Converter in ON State.

In this state the switch S is on, the current from the input voltage source passes through the switch, the inductor and capacitor finally it flows through the load. Initially the current does not pass to the load directly when the switch is on because the inductor stores the charge in itself. And as the diode is in parallel with the Vi source therefore a positive voltage occurs on it reverse biasing the diode, hence it acts as if it is not present in the circuit.

During the OFF state the Buck converter looks as shown in figure 7.

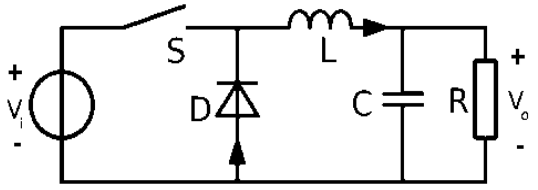

Figure 7 Buck Converter during OFF state.

In this state the switching device (mosfet) is switched off, now the energy stored in the inductor L comes into play this energy is released in the circuit. The voltages developed across the inductor known as electromagnetic force (emf) causes the current to flow in the circuit through the diode D and the load R. The diode in this case is forward biased. When all the energy stored in the inductor is supplied then the capacitor becomes the source for current. Now the current flows till the next ON state occurs.

The major portion here is the switching part for the converter, without which the converter is of no use to us. The switching is done through an external source through a controller or a function generator which supplies a square wave generated at 20 KHz or above. Below 20 KHz is an audible range and the inductor starts producing noise as it gets saturated [9].

8. EQUATION ANALYSIS OF BUCK CONVERTER

The transfer function of the buck converter elaborates the functioning of the buck converter. In order to derive a T.F for this converter we will have to consider both the cases i.e. the ON state and the OFF state.

Referring to figure 6; the ON state, we can observe the inductor voltages are:

$$v_L(t) = Vi - v_C(t)$$
$$v_L(t) = Vi - v(t)$$
$$v(t) = V - v_{ripple}$$

Where;

$$| v_{ripple} | << V$$

$$v_L(t) = Vi - V$$

Now referring to figure 7; the OFF state, we can observe that the inductor voltages are:

$$v_L(t) = - v_C(t)$$
$$v_L(t) = - v(t)$$
$$v_L(t) = - V$$

The ON time is represented by [DT_s] and OFF time is represented by [$D'T_s$] where D is the duty cycle, T_s is the switching time which is the inverse of switching frequency and D'+D = 1 which is the complete duty cycle. Using the area formula we get the equation below:

$$(Vi - V)\, DT_s + (-V)\, D'T_s = 0$$
$$Vi\, D - V\, D - V\, D' = 0$$
$$Vi\, D - V\, (D+D') = 0$$
$$Vi\, D - V = 0$$
$$Vi\, D = V$$

$$V = D \times Vi \quad \textit{(Equation A)}$$

Equation *A* above is the final transfer function of an ideal buck converter.

9. EQUATION ANALYSIS OF BUCK CONVERTER

The MATLAB model for 12V battery charger is shown in figure 8 is simulated at different values of irradiance at standard temperature conditions STC of 25ºC. The PV simulator simulates the PV characteristics which gives us the P-V curve of the panels. The MPPT controller when comes into play the PV curve shows the red dots on the P_{max} points which indicates that the P&O algorithm is being processed and it tracks the MPP. The P&O algorithm works in combination with the buck converter. The result of processed P&O algorithm is shown in figure 9.

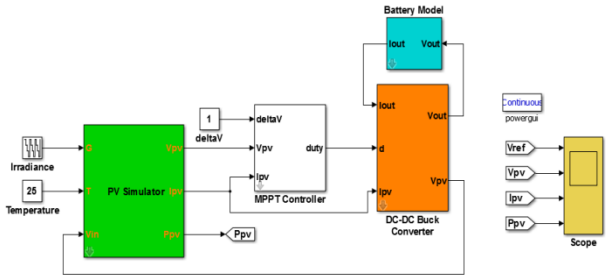

Figure 8 MATLAB model for MPPT Battery Charger

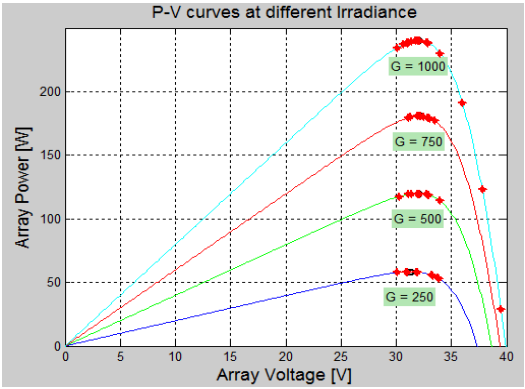

Figure 9 Processing and output of P&O Algorithm.

The red dots in figure 9 shows that the hill top or in other words the maximum power has been tracked, and that too not only for a single irradiance but for all changes in irradiance.

10. HARDWARE RESULTS & DISCUSSIONS:

The complete hardware setup designed for this project is shown in figure 10.

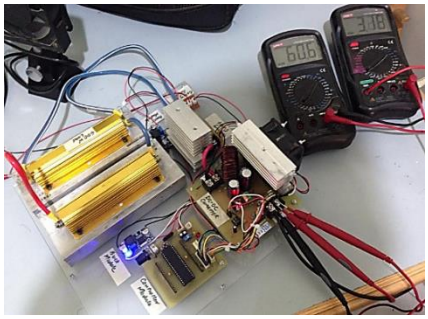

Figure 10 Hardware setup for MPPT Charger.

The real time result of P-V and I-V curve is shown in figure 2. The maximum power point MPP lies on the knee of this curve which is around the point where I_{pv}=5.8A & V_{pv} = 25V, the P-V curve also shows that the maximum power is 145 Watts, the MPP tracking algorithm is implemented in a dsPIC30F4013 microcontroller which is responsible for the tracking of MPP throughout the entire function of the designed battery charger. The MPP tracking graph for this system is shown in fig 11.

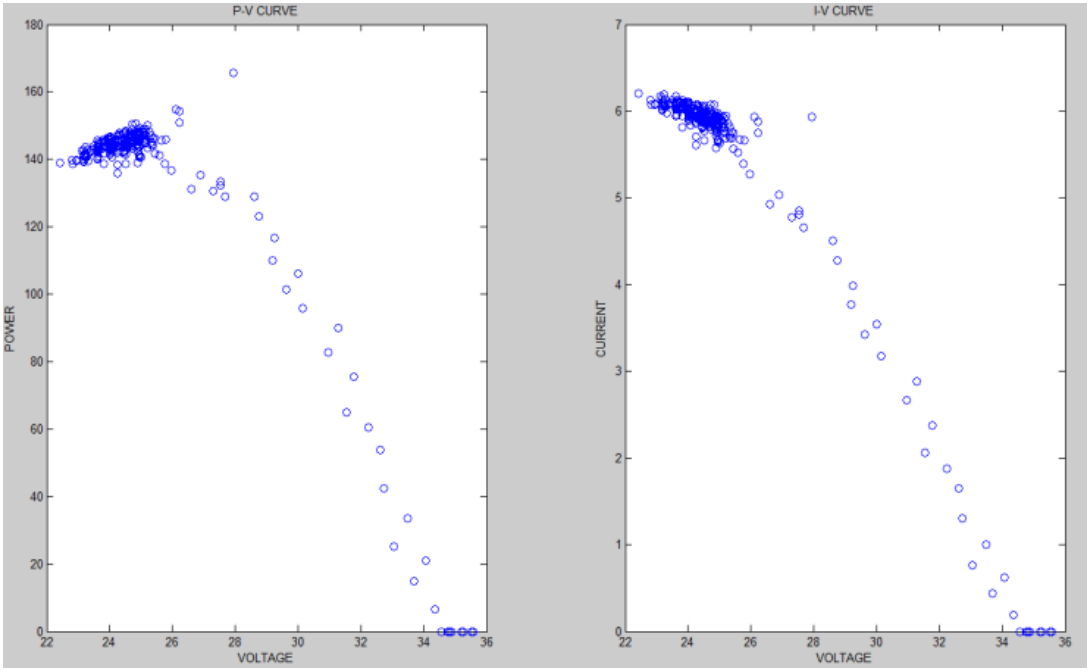

Figure 11 Real-Time p-V & I-V Curve of MPP Tracking.

The MPP algorithm tracks the MPP of the solar panel in real time which can be observed by the dense blue dots at the top left corner of the P-V & I-V curves of the hardware results plotted on MATLAB. The result is more evident in the left graph of figure 11 which shows the P-V curve of tracked MPP at 145 Watts.

11. CONCLUSION:

In this paper, P&O algorithm is used for the application of battery charging with MPP tracking for efficient charging of batteries while maximum power is being delivered for the charging process, which increases the efficiency of the system reducing the losses which occurs in the case of direct connectivity of the batteries for charging purpose. The paper shows the results of MATLAB simulations and its implementation on actual hardware.

REFERENCES:

1. D. G. S. a. M. V. N.Femia, "Predictive & adaptive MPPT perturb and observe method," IEEE Trans. Aerosp Electron. Syst.,, Vols. vol. 43, no. 3, p. pp. 934–950, Jul, 2007.
2. W. C. a. R.Ramesh, "Comparative Study of P&O and InC MPPT Algorithms," AJER.
3. S. R. C.Thulasiyammal, "Performance Analysis of Converters Using Solar Powered Maximum Power Point Tracking (MPPT) Algorithms," International Journal of Advance Research in Computer Science and Management Studies.

4. K. E. Abdullah M.Noman, "DSPACE Real-Time Implementation of MPPT- Based FLC Method," International Journal of Photoenergy, 2013.
5. S. S. T. S.Gomathy, "Design and Implementation of Maximum Power Point Tracking (MPPT) Algorithm for a Standalone PV System," IJSER.
6. K. M. M. V R Bharambe, "Implementation of P&O MPPT for PV System with using Buck and Buck-Boost Converters".
7. R. Saxena, "DC-DC Buck-Converter for MPPT of PV System".
8. Z. S. A. S. Kashif Ishaque, "Application of Particle Swarm Optimization for Maximum Power Point Tracking of PV System With Direct Control Method," IEEE, 2011.
9. M. A. R. Dr. B.J. Ranganath, "Design of DC/DC Buck-Boost Converter Charge Controller for Solar Power Applications".

AUSTRALIAN JOURNAL OF ENGINEERING AND TECHNOLOGY RESEARCH (AJMFR)
Vol. 2, Issue 1 - 2017

AUTOMATION OF SUPPLY CHAIN MANAGEMENT BY RFID AND XBEE NETWORK

Aftab Ahmed,
Sindh Technical Education and Vocational Training Authority, Karachi, Pakistan

Qadir Bakhsh,
Universiti Tun Hussein Onn Malaysia (UTHM), Faculty of Mechanical and Manufacturing Engineering, Batu Pahat, Parit Raja, 86400, Malaysia

Kamran Latif
International college of Automotive (ICAM), Kawasan Perindustrian Peramu Jaya, 26600 Pekan, Pahang, Malaysia

Note: This paper has been accepted for publication from the submissions made at the 2nd National Conference on *Intelligent Manufacturing & Sustainable Energy Systems (IMSES 2016) - Pakistan*

ABSTRACT:

All organizations aim to increase productivity and minimize wastes in terms of expenditure, energy, movements, time and other factors. Scope of this aim is not only limited to manufacturing sector but also includes services and transport/ logistics industry. Barcode technology is used for scanning items in various processes and industries due to easy implementation and low cost. But, it needs human intervention to scan each item individually. It cannot scan dirty, damaged or moving items. To overcome this problem, Radio Frequency Identification (RFID) wireless technology is used for items identification. It does not need human intervention. It can scan multiple and moving items at once. Integration of RFID with Xbee wireless communication network is easy to implement and can be able to increase the communication range. In this paper, a novel approach of Laboratory Virtual Instrument Engineering Workbench (LabVIEW) control platform integrated with RFID system has been presented. This system provides visibility of items at various stages of supply chain on real time basis.

1. INTRODUCTION:

Supply chain management (SCM) is the efficient control of the transaction of goods and services. It comprises the movement and raw materials storage, inventory in process and finished products from initial stage to the end point. The SCM is the cycle of raw material supplier to the manufacturer followed by distributor, retailer and customer [1] as shown in Fig 1.1.

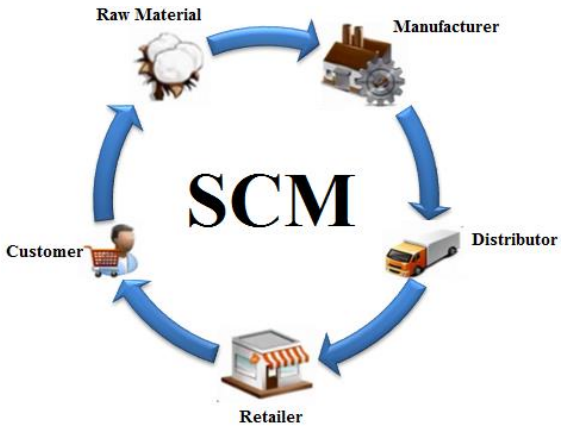

Fig. 1.1 Supply Chain Management (SCM) Cycle

The aim of every SCM is to reduce operational cost minimize wastage and increase profit. It can be achieved by real-time flow of information, product, and funds. It needs an advanced technology to monitor and control. RFID is an advanced auto-ID wireless technology used for real-time tracking and identification of an items without human intervention [2].

Most of the countries are using barcode technology for identification of items, which needs human intervention to scan each item individually. It's a time-consuming activity and may happen a chance of human error by missing of an item during scanning process. To overcome this problem RFID wireless technology is used to scan items automatically by radio frequency. Its further advantages are to scan multiple and moving items at once [3]. It also can scan in dirty and harsh environment. It can scan at longer distance and waves are passing inside the human body as well as non-metallic materials. RFID tag has large data storage capacity. The efficiency is higher in terms of accuracy, speed, quality and flexibility of operation.

1.1. RADIO FREQUENCY IDENTIFICATION (RFID) TECHNOLOGY:

Radio frequency identification (RFID) is a wireless technology used for automatically tracking or identifying the entities by radio waves without line of sight in real time visibility of enterprise operations in an indoor system. RFID works on dissimilar frequencies such as LF, HF, UHF and Microwave to fulfill the different requirement. RFID system has three basic components. 1) RFID tag (data carrying device), 2) RFID reader (transceiver) and 3) middleware as shown Fig 1.2. The working principle begins when RFID reader transmits radio frequency wave signal to the tagged items, which contains the microchip (data storage device). When it receives the radio wave signal, immediately activates and send response back radio wave signal along with data towards RFID reader. That data drives to the middleware, which filters and sort the data and send important information to the main business software to monitor and control the SCM [4]. It provides real-time information of each item in SCM at various stages [5].

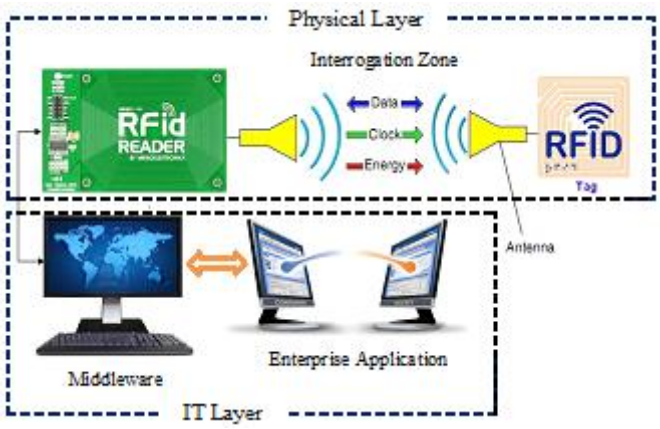

Fig.1.2. Typical RFID System [12]

There are various application areas of RFID including manufacturing, logistics, asset tracking, retailing, warehousing, healthcare and SCM etc [6].

1.1.1. RFID TAG

The basic function of RFID tag is to identify the item similar to the barcode tag. RFID tag comprises of an antenna and an integrated circuit called microchip, which is used for sending a response back to the reader. Microchip stores items information including Model No, serial No and other characteristics of object, it may comprises price, weight, size, color and date of manufacture etc [7]. Tags are classified by power usage, storage memory and communication method between tag and reader as shown in Table 1.

TABLE 1. Classification of RFID tags [8]

Type of tag	**Power usage**
Passive	Power receiving from RFID reader called as 'reflective powered'. It is small and virtually unlimited life span.
Semi-passive	Battery is used as a power source to retain memory in the tag and to modulate the reflected signal.
Active	Powered by Internal battery having longer read range and more expensive than passive tags due to (read/write) provision. Batteries are periodically replaced
Memory	Application
Read-only	Memory is programmed by factory once manufactured cannot be modified. Limited data can store commonly 96 bits of information
Read-write	Read and write provision. Store larger data from 32 kb to 128 kb, more expensive than read-only chips, used only for tracking expensive items
Method	Communication process
Induction	Electromagnetic proximity or near field inductive coupling. Generally, use LF and HF
Propagation	Far field or broadcasting electromagnetic waves Operates on UHF and microwaves frequency bands

The data of item stored into the tag memory as unique Electronic Product Code (EPC). It is used to signal back to the reader to identify the object to which the tag is attached. Tag might be attached to a pallet, case, and entity etc. The environmental sensors can be attached to the tag to measure environmental constraints like temperature and humidity. The sensors information may communicate with the integrated circuit, and then sends to RFID reader.

1.1.2. RFID READER

RFID reader is a device which communicates with tags. It consists one or more than one antennas and the interrogator circuitry (IC). Antenna is used to transmit or receive radio wave signal along with the data to/from the tag to identify the object. The reader integrated circuit is an intermediate between the reader antenna and the IT layer [7]. Reader circuit is used to transmit and receive data through reader antenna and send back for processing. It coordinates between various reader's antennas for efficient tags reading. The interrogation zone is the three-dimensional space between reader and tag which is used for communication.

1.1.3. MIDDLEWARE

Wired or wireless physical network is used to sends and collects data directly from RFID reader. It executes a business-related process concerning the data. It carries, stores and sends to the enterprise applications as needed. Middleware is the intermediate between the reader and the enterprise application [9].

1.1.4. ENTERPRISE APPLICATION

It is the special designed software used for various features of a firm's operation and processes including finance, inventory control, manufacturing, human resources, marketing, sales and resource planning [10]. The supply chain management sustainability can be controlled by decent mechanism throughout the life span of goods and services. The aims of supply chain sustainability is to produce, protect and develop long-term planning of environmental, social and economic issues for all entrepreneurs which are involved in bringing products and services into market. This objective can be achieved by real-time exchange of information using RFID system. This system can easily add with the Xbee wireless network to enhance the communication range.

2. XBEE (ZIGBEE) WIRELESS MESH NETWORK:

Xbee is the low cost, low power eating and low rate of data transmission wireless communication device working as mesh network. It is used to enhance the communication range. Wireless transceivers technologies generally operates on frequency bands to share with numerous users at different Radio Frequency (RF) schemes. In specific WiFi, Bluetooth and latest Zigbee, these technologies are used to enhance communication range of the RFID reader. They all three operate on the unlicensed 2.4 GHz Industrial, Scientific and Medical (ISM) band [11]. Table 2. shows the comparison of wireless technologies [12].

TABLE 2. Comparison of wireless technologies

Characteristics	Zigbee	Wi-Fi (802.11n)	Blue Tooth
Data Rate	20,40 and 250 Kbps	2 to 200Mbps	24Mbps
Range (meters)	1-300	1-100	1-10
Frequency	868MHz, 900-928MHz, 2.4GHz	2.4 & 5 GHz	2.4GHz
Complexity	Low	High	High
Battery life (days)	100-1000+	1-5	1-7
Nodes per network	255/65000+	30	7
Topology	Star, Tree, Mesh	Tree	Tree
Standby Current	3 x 10 -6 amps	20 x 10 -3 amps	200 x 10 -6 amps
Memory	32-60KB	100KB	100KB
Protocol Stack Size	4"32KB	100+KB	~100+KB
Stronghold	Long battery life, low cost, low data rate	High data rate	Interoperability, cable replacement
Applications	Remote control, battery-operated products, sensors	Internet browsing, PC networking, file transfers	Wireless USB, handset, headset

It provides high flexibility in node placement, which is based on IEEE 802.15.4 standard. Its benefit is to increase large wireless network at any stage [13-15].

3. RESEARCH AIMS:

To minimize efforts in terms of operational cost, reduce wastage and maximize profit within allocated resources.

4. RESEARCH APPROACH:

The novel approach of LabVIEW Graphical User Interface (GUI) system works on single control platform to monitor visibility of items in SCM on real-time basis according to the following steps.
Step 1. Make three control tabs at front panel window of LabVIEW platform named “indicator” tab, “parameter setting” tab and “address source file” tab.
Step 2. Browse the established UDL file at “Address Source File” tab and fill-up the names of vehicle table and items table in required fields to linkage with M.S Access database.
Step 3. Select the tab “Parameter Setting” and to fill up all the fields by required parameters.
Step 4. Select “Indicators” tab and press run button to operate integrated system. The RFID-Xbee wireless setup being worked according to the algorithm into the developed system. The RFID tag is attached with vehicle of raw material. During entrance into the door of factory, the RFID reader identifies it by unique product code as vehicle No. only those vehicles which are registered in the database. It shows status as “Available” with green light signal and its complete data below the green

light signal at the control panel, if vehicle is not registered in the database, it indicates red signal with status “Not Available”.

Step 5. Keep it register the vehicle by inputting the data of vehicle in required fields, e.g. (Registration No, Type of Vehicle, Company name, Driver Name, Driver IC and License) as mentioned in Fig 1.3. After filling up the data of vehicle in the mentioned fields at front panel within permitted time, keep it identity again to move the tagged vehicle in the range of RFID reader, it indicates green light signal along with full data and it shows the status as “Available”.

Step 6. Keep it continue for items identification, the RFID reader identifies it with unique ID code and shows the status in the field of “Item code”; also indicates green light signal along with data showing below the green light indicator. The status shown as “Available” at the front panel, otherwise shows red light signal with status “Not Available”, in case of items data not available in the database.

Step 7. The LabVIEW program has provision for data entry of item within programmed period for updating the database, to ensure keep it update.

Step 8. Keep the items identify again by moving the RFID tagged item slowly near the RFID reader range, it instantaneously identify the item, if it shows green light signal at the control panel with full data, it means the item in the database updated, if it shows red light signal, repeat the earlier procedure until shows green light signal. When all items identifies with green light signal, it shows the database updated for items identification. This system proves the real time information of items identification and data updating during identification or tracking process.

This system can be applicable for sustainable manufacturing, supply chain management, car parking, office automation and hypermarket for item pricing. This system can be modified according to the need-based approach. The benefit of this system is to provide visibility of items at a single control platform. The visibility offered by system could help to reduce losses in terms of wastage of time expenditure and services. It also can lower inventory levels, distribution and handling costs. Integrated system allows products to be followed in real-time scanning across the supply chain providing accurate and detailed information of all items with increased efficiency. Inventory visibility can be used to achieve gains in areas such as faster response to customer demands and market trends, improving the ability to have the right product in the right place at the right time.

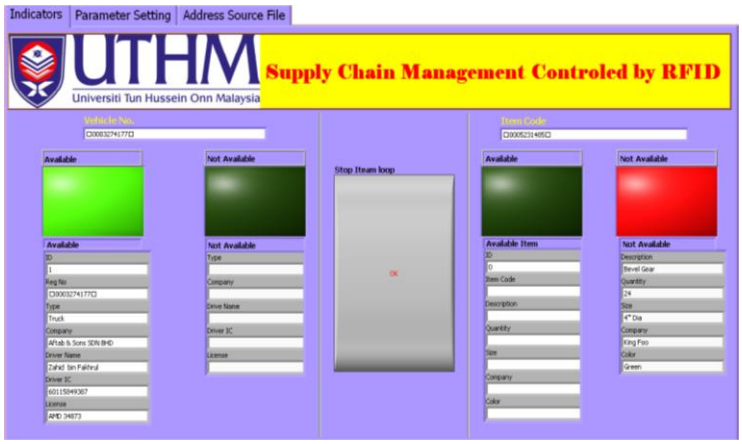

Fig. 1.3. Monitoring by LabVIEW Control panel

5. SUMMARY:

RFID-Xbee wireless network system integrates with LabVIEW GUI, which provide complete picture of visibility of items at a single control platform. This system has great provision to identify entities on real time basis. It decreases human error, optimize inventory control and escalate productivity as well as information accuracy at indoor heterogeneous network of sustainable economic advantage. Moreover, the power eating of the system is minimized by using low power hardware. The tracking range of RFID reader can also be improved with Xbee wireless devices; so that beyond range items can be tracked easily without additional RFID readers.

For future work, the Global Positioning System (GPS) and WSN can be joined with the above system which can observe indoor as well as outdoor real-time tracking and identification of items features. It also can sensing environmental parameters with more visibility which reduce the tracking time span.

6. ACKNOWLEDGEMENTS:

This research is financially supported by the Postgraduate Incentive Research Grant of University Tun Hussein Onn Malaysia (UTHM). The authors would like to thank (UTHM) Malaysia.

7. REFERENCES:

[1] H. Khalid et al., Optimization of RFID network planning using Zigbee and WSN, AIP Conference Proceedings 1660, 090008 (2015);

[2] L. Claudia, RFID Technology and Applications in the Retail Supply Chain, The Early Metro Group Pilot, 18th Bled eConference eIntegration in Action, Bled, Slovenia, 2005, pp 6 - 8,

[3] S. C Xiaoyong et. al., On The Creation of Automatic Identification and Data Capture Infrastructure via RFID 1 Introduction 2 Identification Automation Technologies, 2007, pp 1-19

[4] N. Zarokostas et al., RFID Middleware Design for Enhancing Traceability in the Supply Chain Management, EEE 18th International Symposium on Personal, Indoor and Mobile Radio Communications, 2007, pp 1-5

[5] M. Sumi et al., Design of a Zigbee-based RFID network for industry applications, Proceedings of the 2nd international conference on Security of information and networks - SIN, 2009, pp 111-116

[6] H. Khalid., et al., Study of RFID application with Zigbee Network in supply chain management. Proceedings of the International Conference on Mechanical, Automotive, and Aerospace Engineering (ICMAAE), 2013.

[7] A. Ahmed, et al., Integration of Value Stream Mapping with RFID, WSN and ZigbeeNetwork, Applied Mechanics and Materials, 2014, Vol. 465-466, pp 769-773

[8] C. Linda and F. W. Samuel, AN INSIDE LOOK AT RFID TECHNOLOGY, Journal of Technology Management and Innovation, 2007, Vol. 2, pp 128-141

[9] N.C. Karmakar, Handbook of smart antennas for RFID systems, John Wiley & Sons, Inc., Hoboken, New Jersey, 2010, pp 620

[10] L. Ruiz-Garcia et al., A review of wireless sensor technologies and applications in agriculture and food industry: state of the art and current trends, Sensors, 2009, Vol. 9, pp 4728-4750

[11] Optimization of RFID Real-time Locating System, Australian Journal of Basic and Applied Sciences, 2014, Vol. 8, pp 662-668

[12] G. Goncalo and S. Helena., Indoor Location System Using Zigbee Technology, Third International Conference on Sensor Technologies and Applications, 2009, pp 152-157

[13] S. Wen-Ts and T. Ming-Han, Data fusion of multi-sensor for IOT precise measurement based on improved PSO algorithms, Computers & Mathematics with Applications, 2012, 64, pp 1450-1461

[14] A. Ahmed et al. Impact of RFID and Xbee Communication Network on Supply Chain Management. Applied Mechanics and Materials, 2014, Vol. 660, pp 983–987

[15] H. K. Cho and B. Y. Jongdeok, Large-scale active RFID system utilizing Zigbee networks, IEEE Transactions on Consumer Electronics, 2011, Vol. 57, pp 379-385

AUSTRALIAN JOURNAL OF ENGINEERING AND TECHNOLOGY RESEARCH (AJMFR)
Vol. 2, Issue 1 - 2017

REAL TIME MONITORING OF SUPPLY CHAIN MANAGEMENT NETWORK

Aftab Ahmed,
Sindh Technical Education and Vocational Training Authority, Karachi, Pakistan

Qadir Bakhsh,
Universiti Tun Hussein Onn Malaysia (UTHM), Faculty of Mechanical and Manufacturing Engineering, Batu Pahat, Parit Raja, 86400, Malaysia

Kamran Latif
International college of Automotive (ICAM), Kawasan Perindustrian Peramu Jaya, 26600 Pekan, Pahang, Malaysia

Note: This paper has been accepted for publication from the submissions made at the 2nd National Conference on *Intelligent Manufacturing & Sustainable Energy Systems (IMSES 2016) - Pakistan*

ABSTRACT:

The organizations that produce, distribute, handle or sell various goods are continuously searching for ways to increase profits, minimize operational costs and reduce wastage in order to accomplish a sustainable supply chain competitive advantage in terms of cost and other important factors. Among other optimizations in the process, Radio Frequency Identification (RFID) and WSN are increasingly being used in place of the more traditional barcode technology. RFID is used for real-time tracking and identification of people, animals, and items without human intervention. It can scan multiple and moving items at once through human body and non-metallic materials. Xbee (Zigbee) wireless communication network is easy to integrate with RFID-WSN system. It is able to increase the communication range as well as measure environmental parameters. This system provides smart identification of items on real time basis at a single control platform. It gives complete picture of items features and environmental constraints like temperature and humidity etc. Efficiency of this structure is higher in terms of accuracy, speed, quality and flexibility of operation.

1. INTRODUCTION:

Supply chain management (SCM) is the effective control of the movement of goods, finance, and provision of amenities. It includes the transaction of raw materials storage, inventory in process and finished items produce from initial stage to the final point where it is to be used. SCM cycle begins by the flow of raw materials from storage followed by manufacturing, warehousing, and retailer; finally, product sells to the customer [1-2] as shown in Fig 1.1.

Fig. 1.1. Supply Chain Management (SCM) Cycle

Aim of every SCM is to reduce operational cost, minimize wastage and increase profit. It can be achieved by real-time flow of information, product, and funds.The real-time information is the backbone of every supply chain. It needs an advance auto-ID technology to monitor and control.

2. AUTO-ID TECHNOLOGY:

The automatic identification and data capture (AIDC) technologies used for automatically identifying objects, data collection and to transmit that data directly into computer systems without human intervention [3]. AIDC include the following technologies such as bar codes, biometrics, Smart Cards, Optical Character Recognition (OCR) and Radio Frequency Identification (RFID) [4] as shown in Fig 1.2.

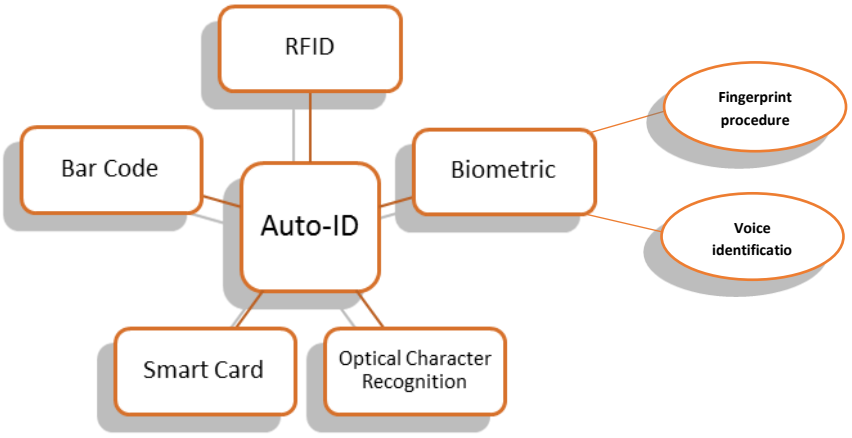

Figure 1.2. Important Auto-ID technologies [3]

Automatic identification (Auto-ID) technologies are very popular at present; it provides information about, people, animals and items in transit. Among all identification technologies, barcode is the most

widely used for identification of items, because it has very low cost. It needs human intervention to scan each item individually. It's a time-consuming activity and may happen a chance of human error by missing of an item during scanning process. To overcome this problem an advance RFID auto-ID wireless technology is used to scan items automatically by radio frequency without human intervention [5]. Its further advantages are to scan multiple and moving items at once [6]. It also can scan in dirty and harsh environment. It can scan at longer distance, radio waves can passing inside human body and non-metallic materials. RFID tag has large data storage capacity. The efficiency is higher in terms of accuracy, speed, quality and flexibility of operation.

The objectives of supply chain management is to exploit customer value, minimizing cost and wastage to achieve a sustainable economic advantage by real-time flow of information with increased efficiency, speed, and accuracy [7]. The numbers of organizations make production, arrange distribution and selling several items. Organizations are exploring what is the provision of RFID to increase operating efficiency, product quality, cut-down inventory level, shrinkage and bullwhip effect also drive further income opportunities in supply chain [8]. Decreasing of tag cost has been widely recognized as the important aspect impelling the extensive usage of RFID technology [9]. The widespread implementation of RFID across the supply chain will bring substantial benefits leading to condensed operational costs and improved profits [10]. Numerous experts in financial matters suggested that it will happen in following basic areas.

i. Minimize inventory and shrinkage
ii. Reduce labor expenses in store, warehouse and on shop floor to get benefit.
iii. Minimize out-of-stock items
iv. Bullwhip effect

Various researchers and scientists believe that application of RFID technology would never be failed; if following issues are to be resolved.

i. Tag prices and efficiencies
ii. RFID standards must be harmonize,
iii. Interoperability throughout the supply chain
iv. Large volumes of data handle by IT infrastructure
v. Modification or variation of work and labor performs
vi. Cost of placement correctly shared
vii. Privacy matters

According to Alinean Research Company, the new developed RFID schemes could cut supply chain expenses by 3-5% and attain 2-7% increase in income. RFID provides accurate and instantaneous visibility of entities in the supply chain. It can make every project as sustainable to get benefits on long-term basis. Usually, 90% of plans need a official business case validation in order to get approval of projects. RFID wireless technology gives promise of bottom-line positive business benefits and a tangible Return of Investment (ROI) [11] as shown in Table 1.1.

Table 1.1: Tangible ROI (bottom-line positive business benefits) [11]

Overall project summary	Benefits
Total investment:	$17M
Net Present Value (NPV) of profits:	$26M
Scheme time span:	3 years
ROI:	188%
Payback period:	11 months

The main issue in the supply chain control is the product loss or shrinkage. The shrinkage is the variation between documented and actual inventory [12]. The loss of inventory is caused by some factors, including shoplifting, employee theft, vendor fraud, administrative error and breaking in transit or in store and cashier mistakes that advantage to the customer. As per record of National Retail Security Investigation led by the University of Florida, reduction in the United States during 2009 denoted 1.44% of retail sales [13]. This fraction is amounting to the billions of dollars is missing in record each year for U.S. retailers only. Therefore, security services including guards, tags, and cameras are used by retailers as an exertion to reduce shrinkage. Radio-Frequency Identification (RFID) as an evolving technology has produced tremendous amount of interest in the supply chain domain to reduce the loss. RFID technology has been used to provide more effective way to identify and track items at the several stages throughout the supply chain in huge retail industry.

3. RADIO FREQUENCY IDENTIFICATION (RFID) TECHNOLOGY:

Radio frequency identification (RFID) is a wireless technology. It is used for spontaneously tracking, locating or identifying and data capture of items by radio frequency waves with no line of sight in real time picture of business operations in an indoor environment. RFID works on radio wave frequencies according to the necessity such as LF, HF, UHF, and Microwave. The RFID system has three basic components. 1) RFID tag (data carrying device), 2) RFID reader (transceiver) and 3) middleware as shown Fig 1.3.

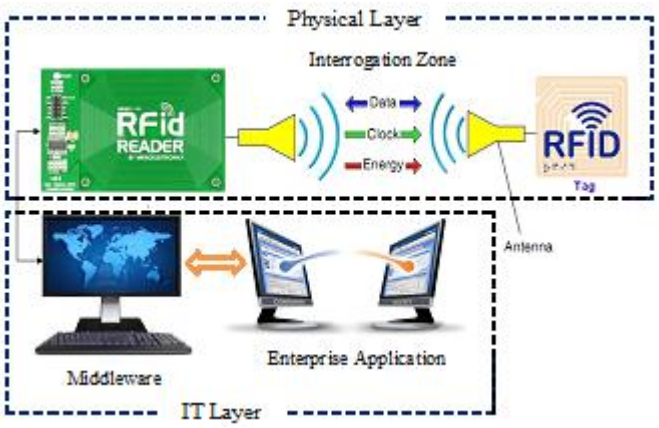

Fig.1.3. Typical RFID System [16]

The working principle begins when RFID reader transmits radio frequency wave signal to the tagged items, which contains the microchip (data storage device). Each tag has a unique identification code number and may optionally hold additional information about the object. When it receives the radio wave signal, immediately activates and send response back radio wave signal along with data towards RFID interrogator. The captured data sends to the middleware, which filters and sort the data and send important information to the main business software to monitor and control the SCM [14]. It provides real-time information of each item in SCM at various stages [15].

There are various application areas of RFID including manufacturing, logistics, asset tracking, retailing, warehousing, healthcare, and SCM etc.

3.1 RFID TAG:

The basic function of RFID tag is to identify the item similar to the barcode tag. RFID tag comprises of an antenna and an integrated circuit called microchip, which is used for sending a response back to the reader. It stores items data or other characteristics of object for identification purpose e.g TAG = [Type of product | Subtype | Product-ID | Position | Date | Size | Color | Price] [16]. There are various types of tags in shape and size according to different application areas are shown in Fig 1.4. It can be assembled into basic categories such as power source, memory type, operating frequencies, functionality, protocol, energy transfer and communication as shown in Table 1.2. It may be active (powered by battery) or passive (unpowered and reactively propagating a radio wave frequency signal) [17].

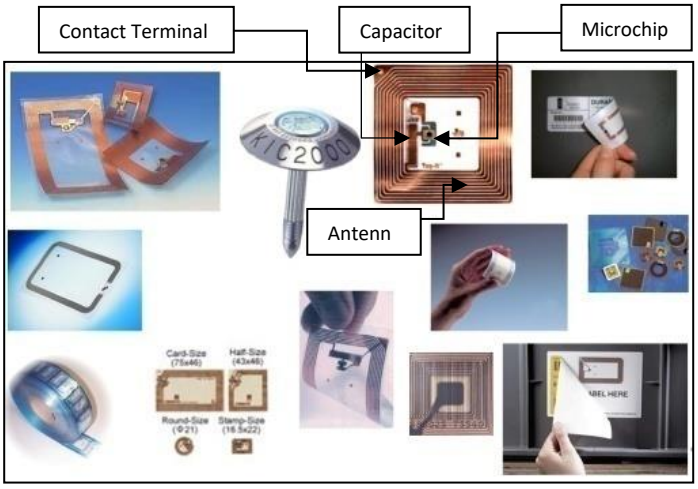

Fig. 1.4. Various RFID Tags [16]

TABLE 1.2 Classification of RFID tags [5]

Type of tag	Power usage
Passive	Power receiving from RFID reader called as 'reflective powered'. It is small and virtually unlimited life span.
Semi-passive	Battery is used as a power source to retain memory in the tag and to modulate the reflected signal.
Active	Power received by an internal battery, read range is greater and more expensive than passive tags due to read & write provision. Batteries are periodically replaced

Memory type	**Application**	
Read-only	Memory is programmed by factory once manufactured can't be modified. Limited data can store commonly 96 bits of information	
Read-write	Read and write provision. Store larger data from 32 kb to 128 kb, more expensive than read-only chips, used only for tracking expensive items	
Frequency	**Range**	
LF	125 kHz -134 kHz, generally tags are passive, have short read ranges of few inches	
HF	13.56 MHz, passive tags use near field inductive coupling, read range is about 3 ft	
UHF	433 MHz (active tags- read range 100 ft) or 860 MHz – 960 MHz (passive and semi-passive tags- read range about 20 ft)	
Microwave	2.4 GHz and 5.8 GHz frequency using ISM band. Read range of passive, semi-passive and active tags (15, 100, and 350 ft) respectively	
Class	**Functionality (EPC Global Classes)**	
Class 0	Passive tags during manufacture of IC chips having Write Once Read Many (WORM)	
Class 1	Passive tags with WORM chips, writing first time can be done at the factory or at site of operation	
Class 2	Passive tags, read/write capability in available memory for user and possibility of data encryption	
Class 3	Semi-passive tags with on-board environmental sensors, read/write capability, and memory space availability for user	
Class 4	Active tags onboard sensors having read/write capability, user memory, and provision for peer communication with other active tags and readers	
Class 5	Define reader which communicate and power the tags belonging up to the aforesaid classes	
Protocol	**Working Standard**	
Open Protocols	Developed by ISO 18000-6(A/B) and are available in equal terms globally for those who want to use them	**Air Interface Protocols** Decide how the tag data communicate using EM waves and include frequency of operation, emission levels, bit rate, anti- collision algorithms, modulation, encoding, and so on **Data Content Protocols** Division, definition, and layout of the memory in the IC, mandatory information that should be included there with their specific locations,
Proprietary Protocols	Developed by manufacturers for their own business purpose; e.g, Texas Instrument's, Alien, TI Tag-IT, Intermec, Intelli Tag.	
Energy Transfer	**Communication of tag and reader**	
Near field	Proximity electromagnetic, or inductive coupling. Generally, use LF and HF frequency bands	
Far field	Propagating electromagnetic waves called as Backscatter coupling. Operates on UHF and microwaves frequency bands	
Transmitter in Tag (Active Tag)	Battery powered having longer read range of operation as compared to passive tags. At powered ON it transmits 16 bit unique ID code on 433 MHz frequency at each 6 seconds. Transmission time is 100ms then goes to sleep for saving battery. After each	

	6 second it wakes up automatically and transmits its unique 16 bit code. It remains ON as long as the tag is powered ON. Battery life is 2 months with continuous on position.

The data of item stored into the tag memory as unique Electronic Product Code (EPC). It is used to signal back to the reader to identify the object to which the tag is attached. Tag can be attached to a pallet, case or item etc. The environmental sensors can be attached to the tag which measure environmental parameters like humidity and temperature. The sensors information may communicate with the integrated circuit, and then sends to RFID reader.

3.2 RFID READER:

RFID reader communicates with tags in the interrogation zone between reader and tag. It consists one or more than one antennas and the interrogator circuitry (IC). Antenna is used to transmit or receive radio wave signal along with the data to/from the tag to identify the object. The interrogator circuit is a transition among the reader antenna and IT layer. Reader circuit is used to send and receive data by the reader antenna and then sending back end for processing. It also coordinates between different reader's antennas for the efficient reading of tags. RFID readers are categorized according to the design, power supply, communication, mobility, protocol, frequency spectrum and data encoding protocol as shown in Table 1.3.

Table 1.3: Classification of RFID readers [18]

Type	**Application**
Design	
Read	Reads data from the tag.
Read/write	Reads data from the tag and writes on the tag
Power supply	
From Network	Get power from external source by using power cord, mostly stationary readers. Power supply range (5V to 12V and 24V).
Battery Assisted	Portable, light weight, battery power supply to the motherboard. Both handheld and stationary, use 5V to 12V for power supply.
Communication Interface	
Serial	Connected to host computers for using serial communication link by RS-485, RS-232, USB or IC2; limited no. of serial ports at host computer, low data transfer than network readers.
Network	Associated to host computer by wire or wireless, it supports multiple network protocols (Ethernet, TCP/IP, UDP/IP, HTTP, LAN, WLAN, and others) as a network device, large number of readers can connect small number of computers
Mobility	
Stationary	Fixed at the walls, portals, entrance and exit gate etc. Power supply range (12V to 24V), weight 1.5 kg to 5 kg, reading range up to 300 m
Mobile	Reader is a handy, moveable device have built-in antennas, battery powered, light weight (82-700g), reading range up to 100m, working wirelessly having memory block to save data and then transfer data in

	the database via wire. It can integrate with barcode scanner for both tag and barcode identification
Interrogation protocol	
Passive	Limited to only "listening and data transmission techniques called transponder-driven protocols for communication
Active	According communication protocols number of tags to be talked, it is more capable and faster than passive
Frequency spectrum	
Non-unique	Two Radio frequencies used by the reader for fast, reliable and full-duplex communication
Unique	unique frequency range is used (short bandwidth <80 MHz) for both transmission and reception
Data encoding protocol	
Simple	Unique protocol is used for data transmission between tags and the reader
Agile	Multiple protocols is used for data transmission between tags and readers include EPC Gen1, EPC Gen2, ISO 18000, and TIRIS Bus Protocol

3.3 MIDDLEWARE:

It is the physical network may be wired and or wireless that sends and collects data directly from the interrogator. It performs a business-related process regarding the data which carries, store and sends to the enterprise applications as needed. It is the intermediate between the interrogator and the enterprise application [18].

3.4 ENTERPRISE APPLICATION:

The enterprise application is the process of data collection from middleware using IoT and used in relevant business processes, depending on the business process involved. It is the special designed software used for various features of a firm's operations including purchase, inventory control, manufacturing, human resources, marketing, sales and resource planning [19]. In this application selection of RFID devices such as tags, readers and middleware for particular application is very important. The selection criteria depend upon protocol, electromagnetic power, read range, frequency, shape, and size of the tags and so on. Interoperability of the different components in a single system as well as between different systems is very important in business process operating globally. Interoperability, quality, privacy and safety depend upon standard. Standard is well-defined set of instructions to follow throughout the world for any specific operation. RFID technology is working on ISO and EPC global standard, where each and every aspect of the system and its working are well-defined. ISO and EPC global standard is regulated by the authorities such as Federal Communication Commission (FCC) (USA), European Radiocommunications Office (ERO) (Europe), Australian Communication Authority (Australia), and so on. The responsibility of all above-mentioned authorities to confirm that the standard to be followed properly.

The supply chain management sustainability can be controlled by proper management practices throughout the lifecycles of products using enterprise application. The objective of supply chain sustainability is a long-term planning including economic, social and environmental aspects of production management. This objective can be achieved by real-time exchange of information using

RFID system. This system has provision to integrate with the Xbee wireless network to enhance the communication range.

4. XBEE (ZIGBEE) WIRELESS MESH NETWORK:

Xbee wireless devices are designed for less power eating, low data flow, least cost, low latency, high level of security and less complicate than those from present offered standards. It is simple to use and easy to configure having longer battery life and is able to self-healing and self-organizing large network. It is highly reliable in both normal and harsh environments [20-21]. ZigBee is built on IEEE 802.15.4 standard and firmly follows rules to confirm abiding sustainability and consistent operation. It is regulated by ZigBee Alliance. ZigBee Alliance defines additional stack layers including (PHY, MAC and NWK layer) which are based on the (7- layer) Open Systems Interconnection Reference Model (OSI/RM). Zigbee works on 2.4GHz unlicensed Industrial Scientific and Medical (ISM) band [22].

The economic cost permits the technology to be widely used in wireless control and monitoring applications, use low power permits longer battery life and the mesh networking provides high consistency and longer transmission range.

In multi-hop wireless mesh networks, one or more intermediate nodes available along the path that receive and forward packets via wireless links. Multi-hop wireless networks have numerous benefits associated to networks with single wireless links. Multi-hop wireless networks can extend the exposure of a network and improve connectivity. Multiple “short” links might require less transmission power which reduce energy consumption than over “long” links. It enables higher data rates resulting in higher throughput and more efficient use of the wireless medium. Multi-hop wireless networks avoid wide placement of cables in a cost-efficient way. In case of dense multi-hop networks having number of paths might become available that can be used to increase robustness of the network.

Wireless communication technologies generally operates on frequency bands to share information with several users at different Radio Frequency (RF) schemes. Specifically, WiFi, Bluetooth and currently Zigbee technologies are used to extend the communication range of the RFID reader as shown in Table 1.4.

Table 1.4: Comparison of wireless technologies [5]

Characteristics	ZigBee (WPAN)	Wi-Fi (802.11) (WLAN)	Blue Tooth (WLAN/WPAN)
IEEE Specification	802.15.4	802.11 a/b/g/n	802.15.1
Industry Organizations	ZigBee Alliance	Wi-Fi Alliance	Bluetooth SIG (Special Interest Group)
Data Rate	20,40 and 250 Kbps	2 to 200Mbps	24Mbps
Range (meters)	1-300	1-100	1-10
Frequency	868MHz, 900-928MHz, 2.4GHz	2.4 & 5 GHz	2.4GHz
Complexity	Low (simple)	High (very complex)	High (complex)
Battery life (days)	100-7000	1-5	1-7
Establishment segment speed	30 msec	3 sec	10 sec
Power Consumption	~ 1 mW	~ 160 mW – 600W	~ 40 -100 mW
Cost ($ US)	~ 2-5	~ 20-50	~ 4-5
Nodes per network	255/65000+	30	7
Topology	Star, Tree, Mesh	Tree	Tree
Standby Current	3 x 10 -6 amps	20 x 10 -3 amps	200 x 10 -6 amps
Memory	32-60KB	100KB	100KB
Security	128 bit AES and key define	SSID	64bit, 128bit
Spreading	DSSS	DSSS, CCK, OFDM	FHSS
Protocol Stack Size	4"32KB	100+KB	~100+KB
Strong hold	Long battery life, low cost, low data rate	High data rate	Interoperability, cable replacement
Applications Focus	(Monitoring & Control) Remote control, battery-operated products, sensors	(Web, Email, Video) Internet browsing, PC networking, file transfers	(Cable replacement) Wireless USB, handset, headset

5. RESEARCH AIMS:

To optimize the business within available resources in Supply Chain Management by achieving sustainable competitive advantage.

6. RESEARCH APPROACH:

Step1: Attach RFID tags with each item for tracking and updating the information of items characteristics in the tags memory.
Step2: Deploy RFID readers at each section depending upon the planned area according to business requirement as shown in Fig 1.5.
Step3: Configure one Xbee device as coordinator and attach with the computer using Ethernet interface link to LAN.
Step4: Configure number of routers as well as end nodes (module) then remotely attach with large number of active RFID readers system based on multi-hop placement using dual radio frequency to overcome the range of radio areas to capture information from the RFID readers and drive it to the main server through coordinator and intermediate routers.
Step5: Attach wireless sensors with RFID tags wherever required to monitor the parameters like temperature, light, and humidity etc.
Step6: The established RFID-WSN system has provision to communicate to the main server by ZigBee network.
This system is able to provide real-time identification of item's characteristics and environmental parameters at single control platform, which can enhance the overall efficacy of supply chain.

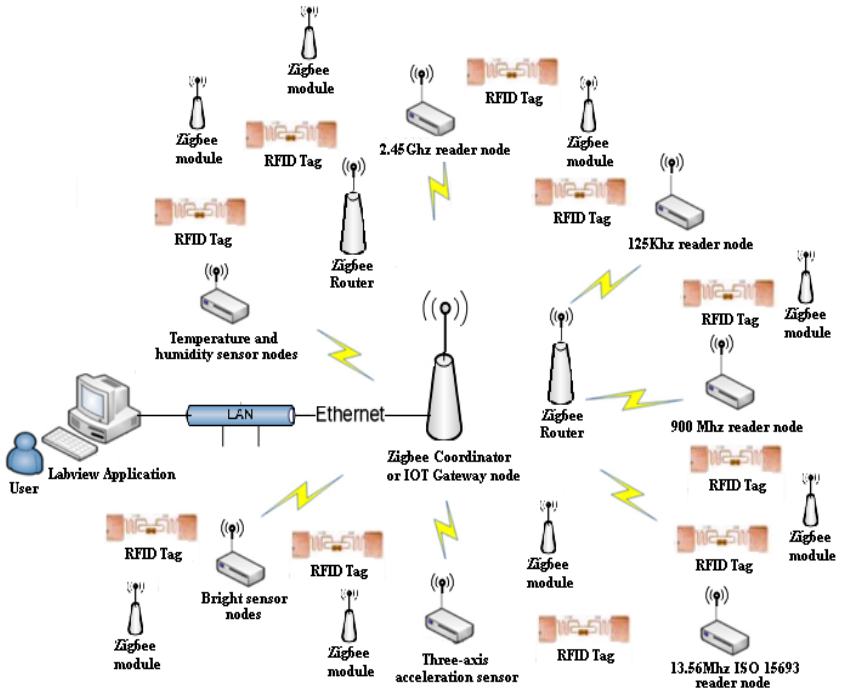

Fig. 1.5. IOT system architecture [6]

This system can be applicable for sustainable manufacturing, supply chain management, car parking, office automation and supermarket for item pricing. This system can be modified according to the need-based approach. The benefit of this system is to provide visibility of items at a single control

platform. That visible picture offered by system could guide to shrink losses in terms of wastage of time expenditure and services. It also can lower inventory levels, distribution and handling costs. Integrated system permits items to be scanned on real-time basis through the supply chain providing accurate and complete information of all items with greater efficiency. Inventory visibility provide gains in areas such as quick response to consumer demands and market tendencies. Now it is easy to decide to make provision right product in the right place at the right time.

7. SUMMARY:

Integrated RFID-WSN and Xbee wireless network system has significant potential of tracking of items identification and data capture on real time basis. It also measures the environmental parameters. Xbee devices have great provision to increase the range of data transmission of RFID readers to main business software by multi-hop communication. The main business software is worked on LabVIEW GUI which can provide visibility of items at each stage of supply chain on a single control platform. The advantage of this system is to lessen human error, minimizes wastage in terms of energy, expenditure, time, out of stock inventory and services. It also improves productivity and information accuracy at indoor environment of sustainable advantage.
The above system can be integrated with Global Positioning System (GPS) for future work, which can monitor both indoor as well as outdoor real time information.

8. ACKNOWLEDGEMENTS:

This research is financially supported by the Postgraduate Incentive Research Grant of University Tun Hussein Onn Malaysia (UTHM). The authors would like to thank (UTHM) Malaysia.

9. REFERENCES:

[1] R. Barton & A. Thomas, Implementation of intelligent systems, enabling integration of SMEs to high-value supply chain networks. Engineering Applications of Artificial Intelligence, (2009), Vol. 22(6), pp 929–938

[2] A. Zaheeruddin and M. Munir., Integrating the supply chain with RFID -A technical and business analysis, Communications of the Association for Information Systems (2005), Vol. 15, pp 393-427

[3] F. Klaus, RFID handbook: Fundamentals and applications in contactless smart Cards, Radio Frequency Identification and Near-Field Communication, John Wiley & Sons, Ltd, (2010).

[4] X. Su, et al., On The Creation of Automatic Identification and Data Capture Infrastructure via RFID. Pervasive Networked Systems, (2007), pp 1–19

[5] H. Khalid., et al., Optimization of RFID network planning using Zigbee and WSN, AIP Conference Proceedings (2015), 1660, 090008 pp 1-9

[6] H. Khalid., et al., Optimization of RFID Real-time Locating System. Australian Journal of Basic and Applied Sciences, (2014), Vol.8(4), pp 662-668

[7] M. Yüksel, & A. Yüksel, RFID technology in business systems and supply chain management. Journal of Economic and Social Studies, (2011), Vol.1(1), pp 53–71

[8] E. Bottani, et al., The impact of RFID and EPC network on the bullwhip effect in the Italian FMCG supply chain. International Journal of Production Economics, (2010), Vol. 124(2), pp 426–432

[9] C.-Y. Lin, & Y.-H. Ho, RFID technology adoption and supply chain performance: an empirical study in China's logistics industry. Supply Chain Management. An International Journal, (2009), Vol. 14(5), pp 369–378

[10] S. Mueller, & C. Tinnefeld, Using RFID to Improve Supply Chain Management. New Age Marketing: Emerging Realities, (2008), pp 1-12

[11] T. Pisello, Shrinking the supply chain expands the return the ROI of RFID in the supply chain. Orlando, FL, Alinean White Paper, (2006), pp 1-16

[12] S.A. Elshayeb et al., Improving Supply Chain Traceability Using RFID Technology. International Journal of Network and Mobile Technologies, (2010), Vol. 1(1), pp 22–27

[13] A. G. Kok et al., A break-even analysis of RFID technology for inventory sensitive to shrinkage. International Journal of Production Economics, (2008), Vol. 112(2), pp 521–531

[14] A. Ahmed et al. Impact of RFID and Xbee Communication Network on Supply Chain Management. Applied Mechanics and Materials, (2014), Vol. 660, pp 983–987

[15] H. K. Cho and B. Y. Jongdeok, Large-scale active RFID system utilizing Zigbee networks, IEEE Transactions on Consumer Electronics, (2011), Vol. 57, pp 379-385

[16] A. Ahmed, et al., Integration of Value Stream Mapping with RFID, WSN and ZigbeeNetwork, Applied Mechanics and Materials, (2014), Vol. 465-466, pp 769-773

[17] I. Bhattacharya, Tracking and Monitoring of Tagged Objects employing Particle Swarm Optimization algorithm in a Departmental Store. IIUM Engineering Journal, (2011), Vol. 12(1), pp 1–12

[18] N.C. Karmakar, Handbook of smart antennas for RFID systems, John Wiley & Sons, Inc., Hoboken, New Jersey, (2010), pp 620

[19] L. Ruiz-Garcia et al., A review of wireless sensor technologies and applications in agriculture and food industry: state of the art and current trends, Sensors, (2009), Vol. 9, pp 4728-4750

[20] M. Agarwal, et al., A study of ZigBee technology. International Journal on Recent and Innovation Trends in Computing and Communication, (2013), Vol. 1(4), pp 287–292

[21] W.-T.Sung & Y.-C. Hsu, Designing an industrial real-time measurement and monitoring system based on embedded system and ZigBee. Expert Systems with Applications, (2011), 38(4), pp 4522–4529

[22] K. Shuaib et al. Co-existence of Zigbee and WLAN, A performance study. In Wireless Telecommunications Symposium, WTS. (2006), pp 1–6

AUSTRALIAN JOURNAL OF ENGINEERING AND TECHNOLOGY RESEARCH (AJMFR)
Vol. 2, Issue 1 - 2017

COMBUSTION ANALYSIS OF COAL USING COAL WATER SLURRY TECHNIQUE

Javaid Iqbal
Mechanical Engineering Department, Balochistan University of Engineering and Technology, Pakistan

Liaquat Ali Lehri
Mechanical Engineering Department, Balochistan University of Engineering and Technology, Pakistan

S. Mushtaq Shah
Mechanical Engineering Department, Balochistan University of Engineering and Technology, Pakistan

Mohammed Nadeem
Mechanical Engineering Department, Balochistan University of Engineering and Technology, Pakistan

Note: This paper has been accepted for publication from the submissions made at the 2nd National Conference on *Intelligent Manufacturing & Sustainable Energy Systems (IMSES 2016) - Pakistan*

Abstract

Geographically, Baluchistan is largest province of Pakistan and contain numerous energy resources, including natural gas and coal. This work focuses on the coal resources of Baluchistan considering their quantity and importance in the overall potential energy portfolio of the country. The available coal can be used by different methods, and the slurry technique is one of them. The energy crises create serious problems for development and growth of any country so to fulfill energy requirements of growing population, to overcome this problem and also for the environmental effects of the coal the coal water slurry is best technique of combustion. Coal water slurry is best alternative and creates 78% less pollution than other methods, and referred as clean coal technology. The experimental investigation using coal-water slurry technique for different coal Particle size has been compared and presented here in this research work.

Keywords: Coal, Combustion, Slurry, Environment, Investigation, size

1. WORLD ENERGY RESOURCES AND IMPACT ON THE ENVIRONMENT

The living standard of people of a country depends on basic needs like water, electricity and energy resources. Today the world energy demands are met by using fossil fuels and renewable energy resources. The energy resources can be visualized in terms of various parameters. The world population during current century may increase between 6 and 11 billion and the energy demand has been increased 35 times during last two centuries. [1] The main drivers of the alternative energy search are the population growth, economy, technology, and agriculture. The potential of renewable energy source is enormous as they can meet the world's energy demand. Renewable energy sources such as biomass, wind, solar, hydropower, and geothermal can provide sustainable energy services

based on the use of routinely available, indigenous resources. Renewable energy sources currently supply somewhere between 15% and 20% of world's total energy demand. [2] Non-renewable energy resources are the conventional energy sources based on oil, coal, and natural gas have proven to be highly effective drivers of economic progress, but at the same time damaging the environment.

2. PRIMARY AND SECONDARY ENERGY

The primary energy is new energy entering the system, and the energy that is transformed within the system is called secondary. [2] The Primary energy is used to designate those sources that only involve in extraction or capture with or without separation from contiguous material, cleaning or grading, before the energy embodied in that source can be converted into heat or mechanical work. [2]

3. NON-RENEWABLE ENERGY RESOURCES

A non-renewable resource is a natural resource that cannot be re-made or re-grown at a scale comparable to its consumption. Most of our energies come from non-renewable energy sources such as Coal, petroleum, natural gas, propane, and uranium are non-renewable energy sources. They are used to make electricity, to heat our homes, to move our cars, and to manufacture all kinds of products. There are many sources of energy in our world. We can get energy from the sun, from wind, and from falling water. We can also get energy from materials that contain stored energy. We call these materials "fuels." One of our most important sources of non-renewable energy today is fossil fuels. Fossil fuels take a long time to form. If we go back in geological history, we find that it took millions of years for our fossil fuels to come to be. Because of the time needed to form these fuels, and because the conditions for formation must be just right, most geologists feel that little or no new fossil fuel is being produced. For this reason, we call fossil fuels "non-renewable." They were formed between 50 million and 350 million years ago. The processes by which they formed are not totally understood. Decayed remains of ancient plants and/or animals were buried by sediments. Through the action of heat and pressure over millions of centuries, they were chemically changed. Coal, oil, and natural gas are the results [3]. Coal was formed from the remains of ferns, trees, and grasses that grew in great swamps 345 million years ago. These remains formed layers as they sank under the water of the swamps. The plant material partially decayed as these layers formed beds of peat, a soft brown substance that is up to 30% carbon. Peat is the earliest stage of coal formation. Shallow seas later covered the swamps and slowly deposited layers of sand and mud over the peat. These sediments exerted pressure on the peat over thousands of years. Slowly chemical changes took place transforming it to lignite or brown coal.

4. COAL

Coal is a non-renewable energy source. The energy in coal comes from plants that lived hundreds of years ago under the swamps. [3] Coal is one of the energy source that can be used in solid, liquid or gaseous form depending on the situation demands. Coal is the most abundant fossil fuel available worldwide. The global distribution of coal is non-uniform like any other mineral deposits or for that matter petroleum. For instance, one-half of the world’s known reserves of coal are in the United States of America. The primary use for coal is in the generation of electrical power. In Missouri State, more than 85% of generation is done by coal-fired power plants. Pakistan is a coal-rich country, but,

unfortunately, use of coal has not been developed for power due to lack of modern techniques expertise in power plant technology and coal mining. Other than this the financial problem was the main problem. Pakistan is fourth coal richest country of the world and has coal field in almost all provinces such as Harnai coal, mach coal, and Dukki coal in Balochistan has not been used for this purpose.

5. ENVIRONMENTAL IMPACT OF NON- RENEWABLE ENERGY RESOURCES

During combustion process, the fossil fuels release carbon dioxide, carbon monoxide, SOx and NOx. This results in the environment damage, and global warming. The emission of greenhouse gases is main factor for global warming, Carbon dioxide is one of those gases and has major role in global warming. Energy demand is increasing throughout the world and in order to get more energy, the more power plants need to be built. As it is known that thermal power plants burn different fuels like gas, oil, and coal called fossil fuels release different greenhouse gases as flue gas. In future, the rapid increase in demand will cause limitations in availability of fossil fuels, the resources available may decay. This increase in demand and flue gases emission will also have a major impact on the environment. Carbon dioxide is the main culprit for global warming; all fossil fuels on burning release carbon dioxide. Carbon dioxide emissions can be reduced by different techniques like adding biomass with fossil fuels and others. The coal water slurry technique is one of them.

6. BALOCHISTAN COALRESOURCES

Following coal, coal mining areas are active in Baluchistan

- Dukki,
- Khost
- Sharig
- Harnai
- Sor Range
- Degari
- Pir Ismail
- Ziyarat
- Mach
- Kingri

Producing about 50% of the coal production in Pakistan. The total coal reserves are about 217 million tons, of which 32 million tons are considered mineable. The thickness of coal seams ranges from 0.3 to 2.3 meters. Baluchistan coal is classified as sub-bituminous to bituminous and the heating value ranges from 9,637 to 15,499 Btu/lb. It has low ash and high sulfur coal and is considered suitable for power generation by co-firing with biomass because high sulfur may produce pollution [3]. Small power plants up to 25 MW can be set up in each coal field.

6.1. MACH COAL

Mach coal field lies in topo sheet No. 34 O/5 within a few kilometres radius of Mach railway station Bolan and Kalat Districts, having about 50 sq. km. of presently known coalfield area. The station is

situated 65 km from Quetta of Sibi-Quetta railroad which passes through the historic Bolan Pass. Coal in Mach area has been known since pre-partition times. Several coal seams are present in ranging in thickness from 0.3 m – 1.5 m but only 3 beds with an average thickness of 0.75m are commercially workable. The quality of coal is sub bituminous. The coal can be subjected to spontaneous combustion and is suitable for power generation of 21 to 24 MW. [3]

6.2. KHOST, SHAHRAG AND HARNAI COAL

Khost, Sharag and Harnai coal fields cover an area of 200 sq. km in the Sibi the District of Baluchistan. It is located at a distance of 160 km to the East and North East of Quetta. The Sibi-Khost extension of Pakistan railway runs along the coal fields. The coalfields are also connected by an unmetalled road. The coal is of Bituminous to Sub-bituminous quality. Coal beds are generally thin, and dipping at 60 degrees. The coal is considered suitable for power generation. Small power plants up to 50 MW can be set up, based on coal produced from these three small coalfields. [4]

6.3. SOR RANGE AND DEGARI COAL

The Sor-Range and Degari coal-fields are located about 12 km South of Quetta city, and extend southeast for a distance of 26 km, covering an area of about 50 sq. km. The northern half of the field is known as Sor-Range and the southern as Degari. Quetta is the nearest railhead for the Sor-Range mines and Spezand railway station for the Degari mines. There are the largest coal-producing fields Of Baluchistan. The coal field is approachable by a metaled road which encircles the entire coalfield joining the Quetta-Sibi highway near Spezand. The coal-bearing area is a doubly plunging symmetrical syncline. The coal seems generally dipped at angles of 45 to 50 degrees. The coal field lies in an arid to semi-arid region with an extreme temperature changes. It experiences that heavy snowfall and rain during winter, but little rain during summer. The thickness of the coal bed ranges from 0.3 m to 1.3 m. The total coal reserves are estimated about 50 million tons. The coal is sub-bituminous in quality and is considered suitable for power generation. Small power plants up to 25 MW can be set up in each Sor-Range and Degari coalfield.

7. COAL WATER SLURRY FUEL (CWSF)

Coal-water slurry fuel is a combustible mixture of fine coal particles suspended in water. It can be used to power the boilers, gas turbines, diesel engines and heating and power stations. CWSF has inherent advantages over solid coal. It may be stored by different methods like in tanks. It can also be transported by a variety of methods like pipelines it can also be pumped or atomized. It can be burnt like a heavy fuel oil [5]. There is no dust explosion hazards and less space than pulverized or solid coal. Unlike pulverized coal, there is no need for expensive drying of the cleaned coal [5]. Recently, limestone has been added to slurries to capture sulphur oxides during the combustion process and reduce emissions [4]. Due to the high moisture content of CWSF, flame temperatures are considerably lower than in pulverized coal flames. This results in lower nitrogen oxide emissions [5]. However, since coals usually contain more fuel nitrogen than fuel oils, CWSF's nitrogen oxide emissions are correspondingly higher (report) than for fuel oil [5].

7.1. OBJECTIVE AND BURNER DESIGN

The objective of this research study is combustion analysis of coal available in Baluchistan, using CWSF technique with different coal particle sizes. The dimensions of nozzle are under:

- Length of Nozzle = 1 inch
- Internal diameter = 1.3 inches
- Outlet diameter = 0.6 inch

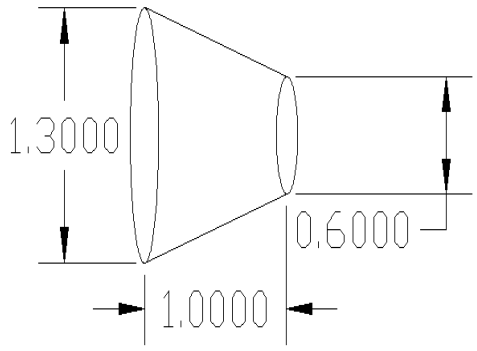

(a)

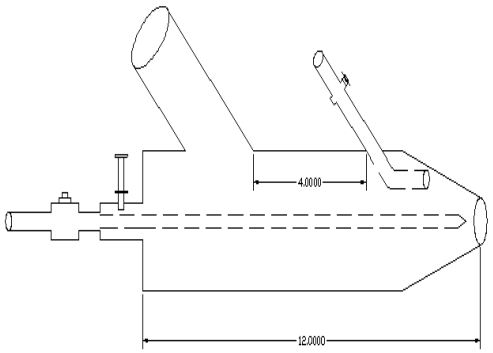

(b)

Fig. 2. Pulverized coal Burner

Fig. 3. Various size of sieves

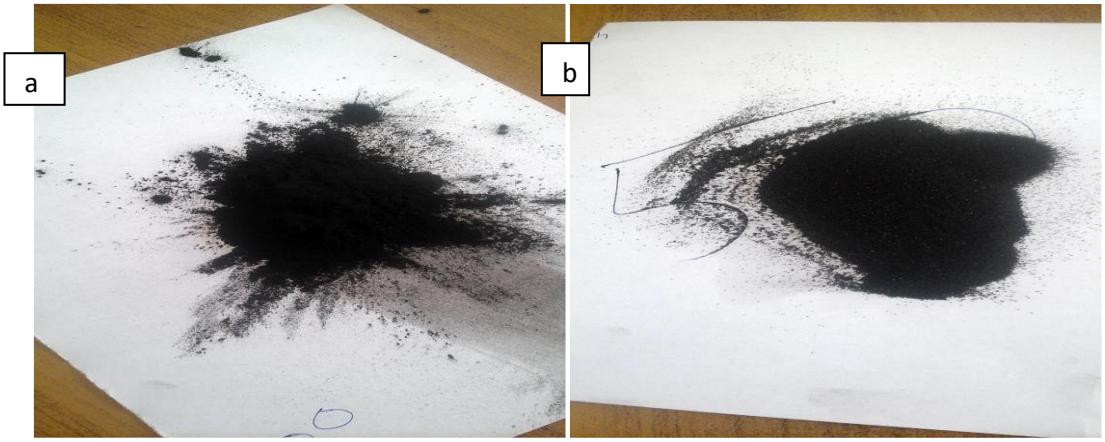

Fig. 4. (a) 200 micron coal particle size **(b)** 50 micron coal particle

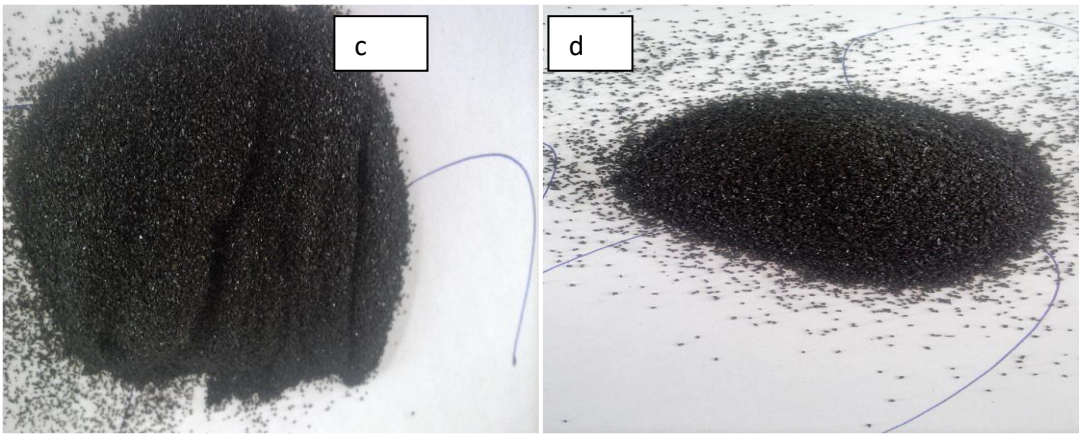

Fig 4. (c) 40 micron coal particle size **(d)** 30 micron coal particle size

7.2. PRODUCTION METHOD

The coal is grinded and mixed with water, then milled in microns using a roller mill (the mass media diameter or "mind" is typically 30 to 50 microns) and beneficiated to remove ash. After being dewatered, flow and stability improvers like grinded lime stone are added to yield the final product (report). Dispersants (surfactants, such as calcium lignosul phonate) help to wet and separate

individual coal particles and reduce the slurry viscosity, while stabilizers prevent the particles from settling into a hard-packed bed by suspending them in a weak gel. Stabilizers are generally starches, gums, salts, or clays (report). Other additives include freezing point depressants, biocides, and caustics (to control the pH of the product).

8. EXPERIMENTAL WORK

Sample of sub-bituminous coal was taken from the Sor Range of Baluchistan mines. Collected different particles size coal; for measurement, the several types of sieves with their respective numbers were used in the laboratory.

8.1. RESULTS

Adding 70% coal and 30% water; adding some other chemical additive such as wasted moble-oil, kerosene-oil, etc increases the efficiency of fuel [4]. For sustainable suspension of particles in water it is also essential that the mixture may be continuously agitated and in present study, it was agitated at 7000 to 9000 rpm. Particles size which were used are as under:

- 30 Microns particle size.
- 40 Microns particle size.
- 50 Microns particle size.
- 100 Microns particle size.
- 200 Microns particle size

Table 1. Combustion behavior of CSWF at different water and coal ratios

Coal ratio	Water ratio	Combustion Behavior
50	50	Not sustainable
60	40	Not sustainable
70	30	Sustainable
80	20	Fluctuating

Table 2. Combustion behavior of CSWF at different water and coal ratio

Coal Size	Weight (Gram)	Combustion
200 Micron	60	Not Stable
100 Micron	60	Not stable
50 Micron	60	Stable
40 Micron	60	Stable
30 Micron	60	Stable

Figure 5. Stability time of different particle sizes

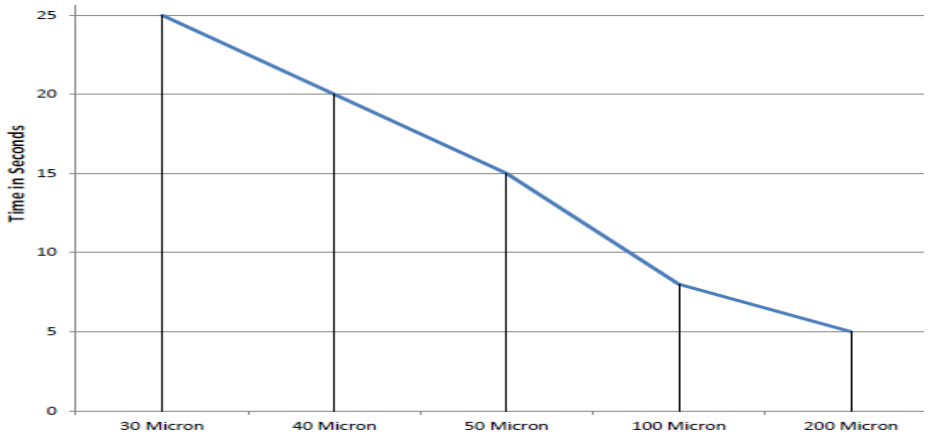

Particle Size

9. DISCISSION ANDCONCLUSIONS

Basically, the research is on bituminous coal available in Baluchistan Pakistan using coal-water slurry technique because the coal water slurry fuel has many advantages than the solid fuel. It can also be transported in easy way like pumping, pipelines and can easily be stored. This technique reduces the greenhouse gases releasing from the solid coal. So, the experimental work was done on different particle sizes of coal like 200,100,50,40 and 30 Micron. Also, the different water ratio and coal ratio was used to test. The results are given in the table 1, table 2 and Figure 5.

We can accordingly draw following conclusions:

- 30 Micron particle size of coal can be successfully combusted using technique
- 40 Micron particle size of coal can be successfully combusted using coal-water slurry technique.
- 50 Micron Particle size of coal can be successfully combusted using coal-water slurry technique.
- 30:70 coal water ratios could be used for sustainable combustion.
- The Baluchistan coal is best for power plants using coal-water slurry technique.

ACKNOWLEDGEMENT

The efforts taken by the author would not have been possible without the kind support of co-authors, Baluchistan University of Engineering & technology, Khuzdar, Pakistan Lab/workshop staff of BUETK, and Mines and minerals department, government of Baluchistan, Pakistan who provided us the services to do this research work. Authors would like to extend our thanks to all of them.

References

[1] Department of Economic and Social Affairs. (2004). *World Population To 2300.* United Nations, Department of Economic and Social Affair. Newyork: United Nations.

[2] A.K. Akella, R.P. Saini, M.P. Sharma., "Social, economical and environmental impacts of renewable energy systems" Renewable Energy 34, PP390–396, 2009

[3] Aroussi, A., and Iqbal, J., "Solid Fuel Biomass cofiring with coal", 4th International symposium on hydrocarbon and chemistry,pp.2-10, Ghardaia, March 24-26,2008.

[4] Overgaard, S., "Definition of primary and secondary energy", Standard International Energy Classification (SIEC), pp. 1-7, 1999

[5] Abeba, A., "Investment Opportunity in Coal of Ethiopia", Geological Survey of Ethiopia (GSE), pp. 1-40,2009

[6] Michael, D. "Impact of Energy Development on the Environment", report, University of Alaska, National Geographic, 2013

[7] Prakash, Ramachandran., Ching.Yi., Tsai and Gary. W.,Schanche., "An Evaluation of Coal Water Slurry Fuel Burners and Technology". ,USACERL TECHNICAL REPORT,coal Use Technologies,US Army Construction Engineering Research Laboratories, 1992

AUSTRALIAN JOURNAL OF ENGINEERING AND TECHNOLOGY RESEARCH (AJMFR)
Vol. 2, Issue 1 - 2017

CASE STUDY ON LEAN MANUFACTURING FOR MINIMIZATION OF DEFECCTS IN THE FABRICATION PROCESS OF SHIPBUILDING

A.N Sanjrani,
Department of Mechanical Engineering, Mehran University of Engineering & Technology, SZAB Campus, Khairpur Mir's

S.A. Shah,
Department of Mechanical Engineering, Mehran University of Engineering & Technology, SZAB Campus, Khairpur Mir's

Note: This paper has been accepted for publication from the submissions made at the 2nd National Conference on *Intelligent Manufacturing & Sustainable Energy Systems (IMSES 2016) - Pakistan*

ABSTRACT:

There are **Note:** This paper has been accepted for publication from the submissions made at the 2nd National Conference on *Intelligent Manufacturing & Sustainable Energy Systems (IMSES 2016) - Pakistan*

There are various common problems in the traditional fabrication process of certain components of ship. These problems not only result in poor performance but also hamper the process of attaining quality assurance standards of the shipbuilding industry. However, application of more efficient processes can overcome such problems in the shipbuilding and fabrication processes. In this regard, lean manufacturing approach based defect analysis can be a feasible option to resolve such problems of poor quality. In this work, lean manufacturing technique based defect analysis approach is applied at certain stages of fabrication process of shipbuilding for bringing better quality and results. The results reveal that a considerable improvement in the quality of fabrication process of ship can be achieved in terms of reduction in the number of defects, which is not possible under traditional manufacturing process. The paper accordingly highlights an opportunity and methodology to improve the current manufacturing and shipbuilding processes in the light of productivity improvement initiatives implemented in other industries (under the umbrella of lean).

1. INTRODUCTION:

The shipbuilding industry generates millions of dollars for the support and development of country and hence enjoys a prominent position in country's economy. Without the value-added process of company, the life cycle of product does not carry any wealth. That is why the shipbuilding industries are also implementing lean manufacturing techniques in their manufacturing systems to avoid the delay in completion product and to reduce the wastage of material. The fabrication is the main value added process of the manufacturing of ship blocks and the inspection of the surveyor is key component to ensure integral structural members of ship to complete as per given specification without defect. However, it is not possible that every ship did not contain any defect in the fabrication Process. The first world countries have the robust facilities in their shipbuilding yards for lean

production and repair facilities on account of having the leading-edge shipyards and contribute considerable revenues to their economy by Guido Perla at al [1]. Further the shipbuilding industry not only earns heavy revenue and profit but also enable countries to enhance their defence capability for protection of their geographic location in sea by manufacturing the warships and submarines as Tsuji Zhangjiagang in China, Flensburger Schiffbau Gesellschaft Germany, two shipyard of Spain Gondan Asturias and H.J. Barreras Vigo and one of shipyard from Turkey Besiktas Yalova.

The geographic location of Shipyards has the great impact on sale and purchase of products according to strategic clients purchasing needs and power. The Europe is shown in the left side of according to Google map and Asia reflected on the right side of picture, therefore, both of regions have a separate market of business but the China in this region is current world leader of the shipbuilding industry as shown in (Figure 1).

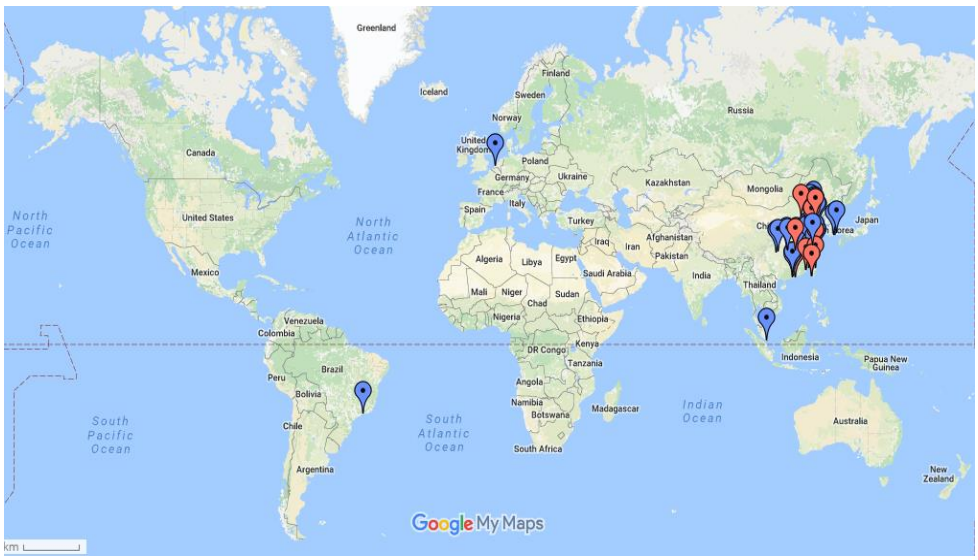

Figure 1. Strategically Contribution of Shipyards

Historically, most of countries has been played a prominent role such as Europe, Asia, South Korea and Japan since 19th to 20th century. The product development cycle has been improved by this competition in between these shipyard and most of lean shipyards belongs to Europe, Japan, and China in reduction of defects in the fabrication processes. The major junk of shipyards are existing with Asia 34% and Europe 31% and rest with other regions as shown in (Figure 2).

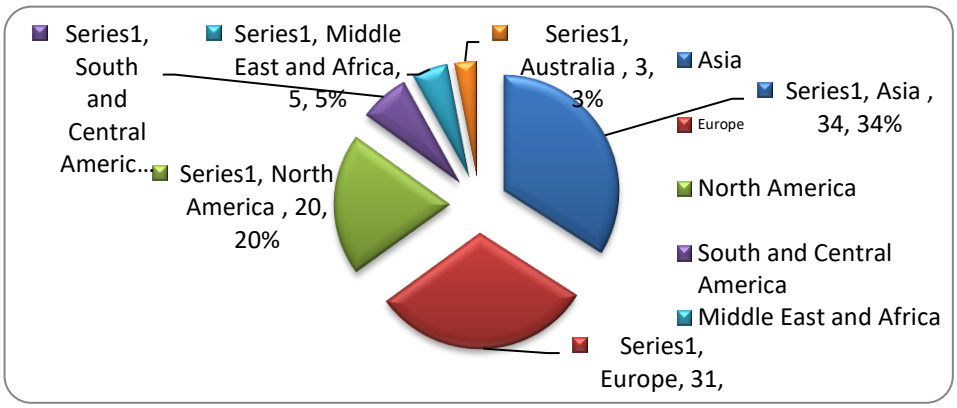

Figure 2. Contribution of Shipyards according to regions

As every shipyard want to be the cost and quality assurance and control effective to ensure the product development cycle during product realization. So in that regards shipyards are focusing for professional trainings, standardization, and sustainability in the product cycle. The inspection manager has to face and manage inspection to control the defects in the fabrication process but that was not possible as research and development changes the profile of ships varying in different sizes and functions. The considerable asset taken into account in atomization in the product development cycle to minimize the defects and time delays. This is how the traditional shipyard are closing day by day due to latest development in the production facilities. The model of lean manufacturing as resembling to Toyota motors was implemented is the one of the source for the sustainability of shipyard in manufacturing of ships due to provision of flexibility in modification because of R&D in design, in jig and fixture over a production cycle according to clients.

Most of traditional shipyards are closing due to their financial crises and competitiveness as compared to advanced lean shipyards. Generally, manufacturing businesses have to alter from a traditional mass manufacturing practices to a healthier and well-organized and flexible production technique such as lean production. In order to decrease costs and to enhance quality certain innovative techniques are introduced in manufacturing processes. Lean manufacturing is one of such useful technique and it is implemented with the objective to reduce time from source to destination of a product by reducing sources of unwanted processes in the production stream by Liker, J.K [2].

There are certain stages in the fabrication process where the product process is hindered in-between value-added activities and non-value added activities. The rework due to defects and repair in welding of block fabrication, machinery installation, erection of blocks, deck and superstructure as well as electrical installation causes to increase the size of non-value added activities which enhance the cost of production. Shipyards can further enhance their competitiveness and efficiency by organizing the most operative professional systems and controlling techniques using lean manufacturing processes.

Lean manufacturing system enable the manufacturer to consume less resource as in input to produce a higher performance which in principle building the customer satisfaction and improvement greater market stake than those of its competitors by Katayama and Bennett [3].

Hypothetically, lean production is the industrialized system without waste, although waste is anything which is unused leftover or overused over processing of resources within the product lead time in the production by Shahram [4].

Similarly, lean production is the organized elimination of waste by all members of the industry from the working areas of the value stream of product cycle, whereby the value stream activities are contributing to the transformation of a product from raw material to finished product by Worley and Doolen [5].

Moreover, lean production is the calculated realization to manufacturing having an objective to eliminate or reduce the waste while emphasizing the need of continuous improvement by Papadopoulou and Ozbayrak [6].

Lean production is the intangible framework which has established principles and techniques such as multi-functional teams, elimination of zero-value activities, continuous improvement and supplier

integration to gain production efficiency and effectiveness and delivering a raw material on the basis of just-in-time by Sanchez and Perez [7].

Likewise, lean production has the multi-dimensional approach that include several management tools as just-in-time, quality management system, workforce, cellular manufacturing, and supplier management which is known to be integrated system by Shah and Ward [8] but all industries are now focusing on the importance of technology and innovation in lean production. Manufacturing corporations do not retain with lean production that would lose out to competitors. Manufacturing corporations contest only on new technological, creative, and innovative and hallmark quality of products to achieve high profit of the market by Agus and Hajinoor [9]. Shipbuilding industry can generate massive revenue by implementing the best lean practices of ship building to reduce defect and rework.

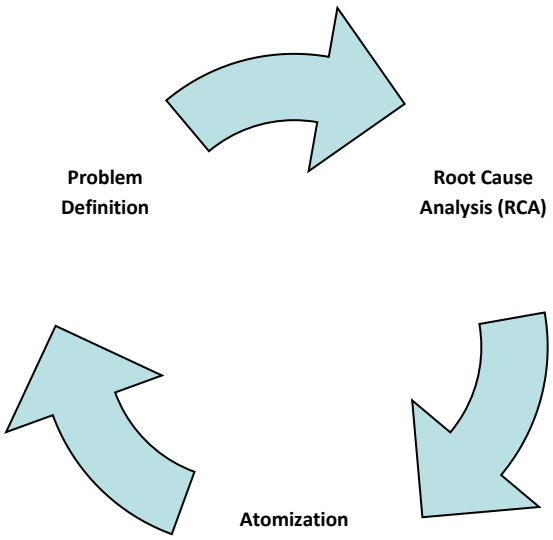

Figure 3 Defect Based Production Cycle

2. RESEARCH AIMS:

This study is projected on Defects based production cycle (DBPC) to deliver assistance to both academicians and professional engineers and practitioners to reduce the delays in work orders. The study will explore fabrication defects and their reduction in production of ships by implementing of lean manufacturing techniques. In the manufacturing sector where most of employees has a knowledge of engineering but they did not care about the defects, repair, rework, and their associated causes. This study embraces the scholars, policy makers and producers how to increase the performance and reduce the wastages from the production processes to improve the whole product cycle.

3. RESEARCH APPROACH:

This research presents the methodology that is based on new lean techniques in which it covers the listed areas as the Model designing, target population, data collection and data analysis.

The designed model is based on Defects based production cycle (DBPC) in which lean manufacturing based defect analysis approach is applied at four processes such as hull fabrication and erection, birth

and machinery outfit, paint and electric power generation of shipbuilding/fabrication processes and variance in the performance is evaluated with the objective to enhance quality and to reduce the total costs. Defect base production cycle for implementing is the new tool to improve the manufacturing processes, as is illustrated in Fig.3.

This cycle is defined as when problems arises at the production area such as defects, repair or rework all are associated with the 6Ms which include Man, Material, Machine, Measuring, Method and mobility of workers. In order to find the root cause of problem the defect is processed and scrutinizes to obtain the outcome of analysis. As the outcome is achieved by the RCA that requires engineering mistake proof atomization system shall be implemented to avoid the reoccurrence of the similar defect.

It is difficult to work on the defects where you have very limited ships are in the process of manufacturing and fabrication. In order to validate the DBPC model, the population data of two same types' ships were taken into account. A ship when it is completed all defects were analyzed and then automated system was introduced based on 6 Ms to encounter similar defects to reduce the repair and rework in order to reduce the delays.

4. Results

The application of this technique caters to speed up the processes and minimize the repair rework in hull, paint and electrical during construction of ship. The results of hull and machinery reveal that there is considerable reduction of defects in hull and outfit the defects includes welding defects, electrical connectivity defects, machinery alignment defects.

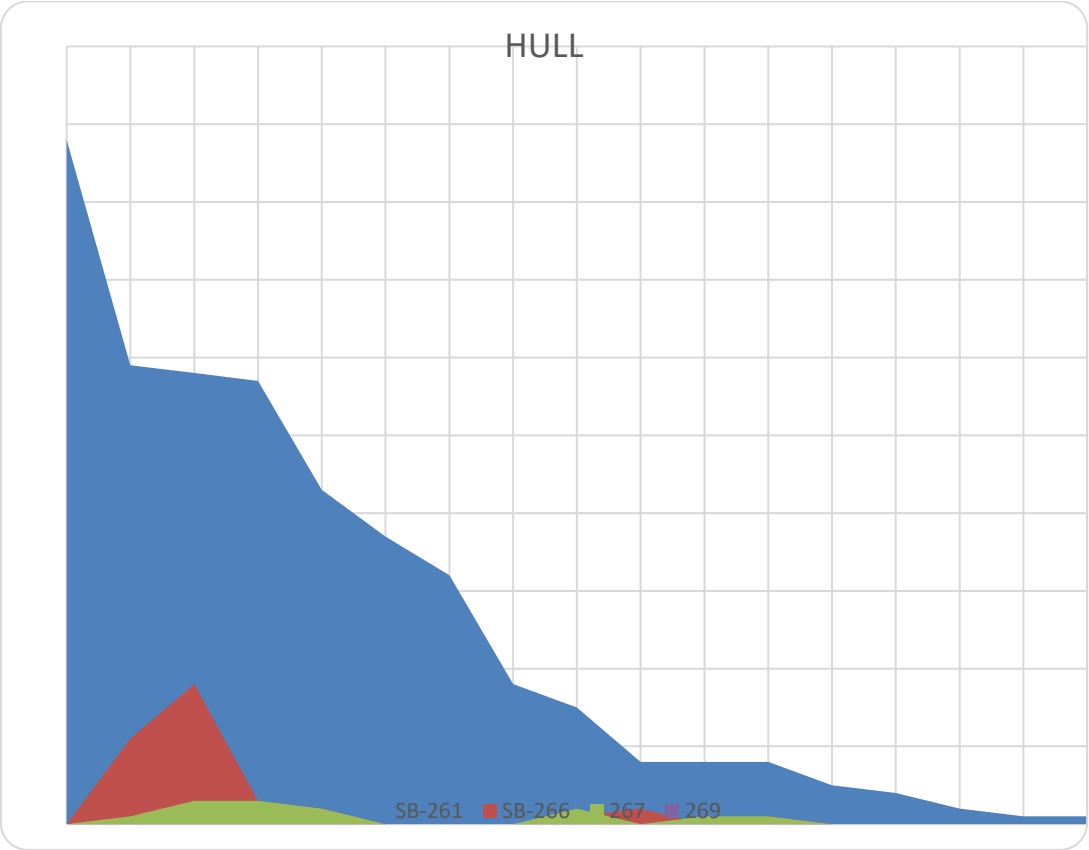

This chart reveals that the amount of defect in hull section are reduced and also eliminated from the production development cycles. The defects include over grinding, excessive welding, undercut pin holes, cavity, incorrect assembly, misalignment, incomplete welding as per joint design, incomplete work on inspection, self-check, not as per drawing, uneven fabrication, corner edge welds, non-systematic processes, deformation, cleaning, reworks, wrong equipment, penetration and marking all defect are reduced or eliminated after implementing Defect-based production cycle (DBPC).

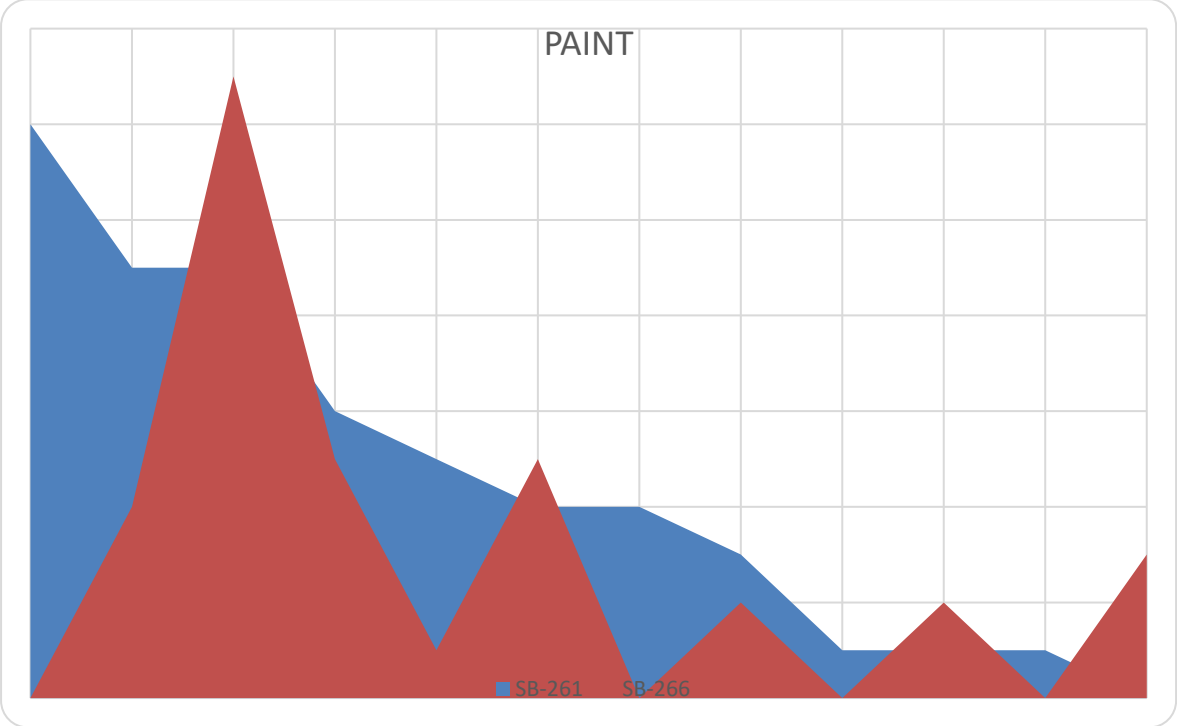

The results of paint based defects like cleaning, sagging, derusting, pinholes, low dry film thickness, incorrect paint code, missing paint, cavities, rework, expired paint related problems and peel off problems are minimized after implementing the DBPC.

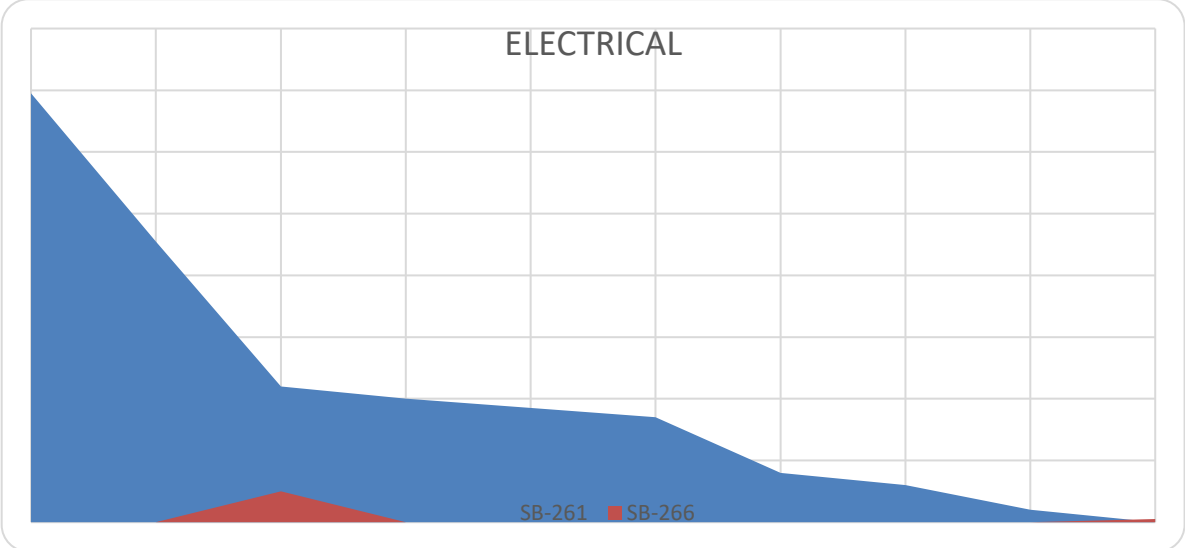

The results of electrical process expose that problems of in secured loose cabling, incorrect cable laying, missing instruments, resistance and earthing, self-check, incorrect panel connections, not as per specifications, insulations, fuse indication of light, defects are reduced and eliminated.

5. CONCLUSIONS:

Defect Base Production Cycle with 6Ms is the new Lean manufacturing tool which will enable engineers and manufacturer to minimize of non-value added activities. This cycle will reduces the defects, over-processing, manual inspections, mobility of products, manual operations, repairs, saves production man-hours, material costs up to 15% of overall costs of production and ensures effective utilization of resources. Future work of this study shall be carried out on maintenance of machinery which can validated to check the possible outcomes on basis of implementing Defect base production cycle (DBPC). This model has worth for engineers, manufacturer, scholars and industrialist to enhance their productivity in shipbuilding and the manufacturing sector.

6. REFERENCES:

1. Guido Perla, Stuart Clark, Peter E. Dahl, 2012 “BC Shipbuilding and Repair Competitiveness and Productivity Road Map Project” © Economic Growth Solution Inc.
2. Liker, J.K. (1996), “Becoming Lean” © New York, NY: Free Press, p. 481.
3. H. Katayama and D. Bennett, “Lean production in a changing competitive world: a Japanese perspective,” *International Journal of Operations & Production Management,* vol. 16, no. 2, pp. 8-23, 1996.
4. T. Shahram, “Lean manufacturing performance in China: assessment of 65 manufacturing plants,” *Journal of Manufacturing Technology Management*, vol. 19, no. 2, pp. 217-234, 2008.
5. J. M. Worley and T. L Doolen, “The role of communication and management support in a lean manufacturing implementation,” *Management Decision*, vol. 44, no. 2, pp. 228-245, 2006.
6. T. C. Papadopoulou and M. Ozbayrak, “Leaness: experience from the journey to date,” *Journal of Manufacturing Technology Management*.vol. 16, no. 7, pp. 784-807, 2005.
7. A. Sanchez and M. P. Perez, “Lean indicators and manufacturing strategies,” *International Journal of Operations & Production Management,* vol. 21, no. 11, pp. 1433 1451, 2001.
8. R. Shah and P. T. Ward, “Lean manufacturing: context, practice bundles, and performance,” *Journal of Operations Management,* vol. 21, no. 1, pp. 129–149, 2003.
9. A. Agus and M. S. Hajinoor, “Lean production supply chain management as driver towards enhancing product quality and business performance: Case study of manufacturing companies in Malaysia,” *International Journal of Quality and Reliability Management, (Emerald),* vol. 29, no. 1, pp. 92-121, 2012.

AUSTRALIAN JOURNAL OF ENGINEERING AND TECHNOLOGY RESEARCH (AJMFR)
Vol. 2, Issue 1 - 2017

COAL BED METHANE IN PAKISTAN: DIFFICULTIES AND PROSPECTS

Tahir Hussain Soomro
Department of Petroleum & N. Gas Engineering, Mehran UET Shaheed Z.A Bhutto Campus, Khairpur Mirs, Pakistan

Abdul Samad Shaikh
Department of Petroleum & N.Gas Engineering, Mehran UET Shaheed Z.A Bhutto Campus, Khairpur Mirs, Pakistan

Zeeshan Ali Lashari
Department of Petroleum & N.Gas Engineering, Mehran UET Shaheed Z.A Bhutto Campus, Khairpur Mirs, Pakistan

Note: This paper has been accepted for publication from the submissions made at the 2nd National Conference on *Intelligent Manufacturing & Sustainable Energy Systems (IMSES 2016) - Pakistan*

ABSTRACT:

The availability of energy resources is of prominent importance to society. The greatest challenge, the energy sector is facing today, is how to meet the rising demand of energy. On the other hand, the depletion of natural resources is also posing a concern. To meet the rapidly increasing demand for energy and faster depletion of conventional energy resources, Pakistan with other countries is desperately searching for alternate energy resources like coal bed methane (CBM), shale gas, and gas hydrate. CBM is considered to be the most viable resource of these and Pakistan is indeed blessed with vast yet untapped resources waiting to be explored. Pakistan with 185 billion tons is the 7th largest country of the world in terms of coal reserves and Pakistan makes 4.5% of the total world's coal reserves. The present paper discusses the prospects of CBM as a clean energy source, difficulty involved in production of CBM, and enhanced recovery techniques. In this regard, one Pakistani coal field is selected and coal contents are determined by analyzing the collected samples.

1. INTRODUCTION:

Depletion of conventional resources, and rising demand for clean energy challenges Pakistan to hunt for alternatives resources. Intense importance has been given for searching out more and more energy resources; significantly non-conventional ones like CBM, shale gas & gas hydrates, as gas is more favorable compared to oil or coal. CBM is considered to be one of the most viable alternatives to deal the situation. With increasing demand and rising oil and gas prices, CBM is definitely a feasible alternative energy source. Coal bed methane is generated during coalification process which gets adsorbed on coal at higher pressure. However, it is a mining hazard. Presence of CBM in underground mine not only makes mining works difficult and dangerous but also makes it very expensive and not economical.

However, CBM is a significantly clean fuel if utilized properly. CBM is a clean gas having heating value

of approximately 8500 KCal/kg compared to 9000 KCal/kg of natural gas. It is of pipeline quality; hence can be fed directly to national pipeline grid without enough treatment. Methane gas production from coalbed would lead to de-methanation of coal beds and avoidance of methane emissions into the environment, thus turning an atmospheric hazard into a clean energy resource. Pakistan in the field of coal as seventh largest in the world, Pakistan has good prospects for commercial production of coalbed methane. Methane may be a possible alternative to compressed natural gas (CNG) and its use as automotive fuel will certainly help reducing pollution levels.

India is one of the select countries which have undertaken steps through a transparent policy to harness domestic CBM resources. The Government of India has received overwhelming responses from prospective producers with several big players starting operations on exploration and development of CBM in India and set to become the fourth after US, Australia, and China in terms of exploration and production of coal bed methane.

However, in order to fully develop India's CBM potential, delineation of prospective CBM blocks is necessary. There are other measures like provision of technical training, promotion of research and development, and transfer of CBM development technologies that can further the growth of the sector.

India lacks in CBM related services which delayed the scheduled production. Efficient production of CBM is becoming a real challenge to the E & P companies due to lack in detailed reservoir characterization. So far, the most investigations have been limited to measurement of adsorption isotherms under static conditions and is deficient in providing information of gas pressure-driven and concentration-driven conditions. More care should be taken on measurement of porosity and permeability also. To produce more methane from the coal enhanced technology like CO2 sequestration may be implemented. This process can not only reduce the emission of this gas to atmosphere, will also help in extra production of methane gas [2]. Though, presently, CO2 is not an implemented much because of high cost. But the necessity to reduce greenhouse gas emissions has provided a dual role for coal beds - as a source of natural gas and as a repository for CO2.

S. No	Province	Coal Reserves
1	Sindh	184,623
2	Balochistan	217
3	Punjab	235
4	Khyber Pakhtun Khuwa	91 5
5	Azad Jamu kashmir	9
Total		185,175

Coal Reserves of Pakistan

In the present investigation, Thar coal field has been selected as the study area. Samples have been collected from various locations & depths. Standard methods have been followed to characterize the collected coal samples and evaluation gas reserve.

2. GLOBAL AND PAKISTANI SCENARIO:

Global Scenario: The largest CBM resource bases lie in the former Soviet Union, Canada, China, Australia and the United States. However, much of the world's CBM recovery potential remains untapped. In 2006, it was estimated that of global resources totaling 143 trillion cubic meters, only 1 trillion cubic meters was actually recovered from reserves.

This is due to a lack of incentive in some countries to fully exploit the resource base, particularly in parts of the former Soviet Union where conventional natural gas is abundant. The United States has demonstrated a strong drive to utilize its resource base. Exploitation in Canada has been somewhat slower than in the US but is expected to increase with the development of new exploration and extraction technologies. The global CBM activities are shown in Fig. 1. The potential for supplementing significant proportions of natural gas supply with CBM is also growing in China, where demand for natural gas was set to outstrip domestic production by 2010.

Pakistani scenario: In Pakistan, coal deposits presence was known before of independence. Its economic value was highlighted in the late 80's when large reserves of coal were discovered in the Lakhra and Sonda area of Sindh. In 1992 deposits of 175.5 Billion tonnes was discovered in an area of 9000 sq. km in Tharparkar Desert [3, 4]. Coal reserves exits in Sindh, Baluchistan, Punjab, Khyber Paktun Khuwa (formerly known as NWPF) and Azad Jammu Kashmir, estimated about 185.5 billion tons of Lignite to sub-bituminous ranks details are shown in Table. The importance of coal as industrial fuel is well known in the industrialists, because of its low price and good heating value, but the high emission of the coal flame is a distinct advantage. Initially, coal was not used as fuel in the cement plants, now cement industry realized the importance of Coal as a fuel and started using the coal. It is used for direct firing in the manufacture of cement, bricks, pipes, glass tanks and metal smelting, and as boiler fuel for the supply of steam to process plant in the paper, chemical and food processing industries. In the brick kiln, it is estimated that one ton of coal have same energy potential as of one tonne oil. Pakistan coal consumption by industrial sector wise is given as under:

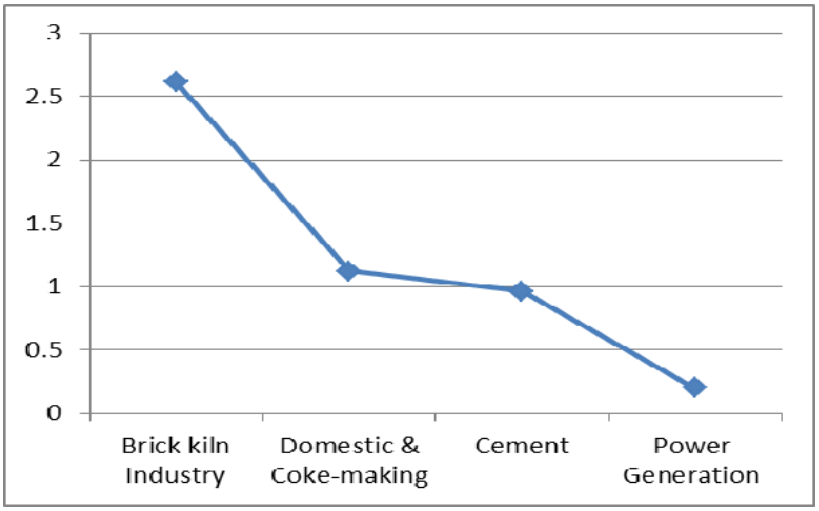

Coal Consumption by sector wise in Pakistan

MATERIALS AND METHOD

A. Sample collection and characterization

As coal is not exposed on the surface the core samples and borehole logs were collected by Geological survey of Pakistan from VV-14, SV-13, VV-12 boreholes at Block # 1, after detail core examination at Block # 1 is divided into Sinhar Vikian and varvai sub-blocks and borehole codes are given after the sub-blocks. The shallowest and deepest of coal samples are obtained at 143.8m (VV-12) and 245.28 (SV-13) depths. Efforts were made to sample all major verities within coal seams and more than one sample was taken from thick seams.

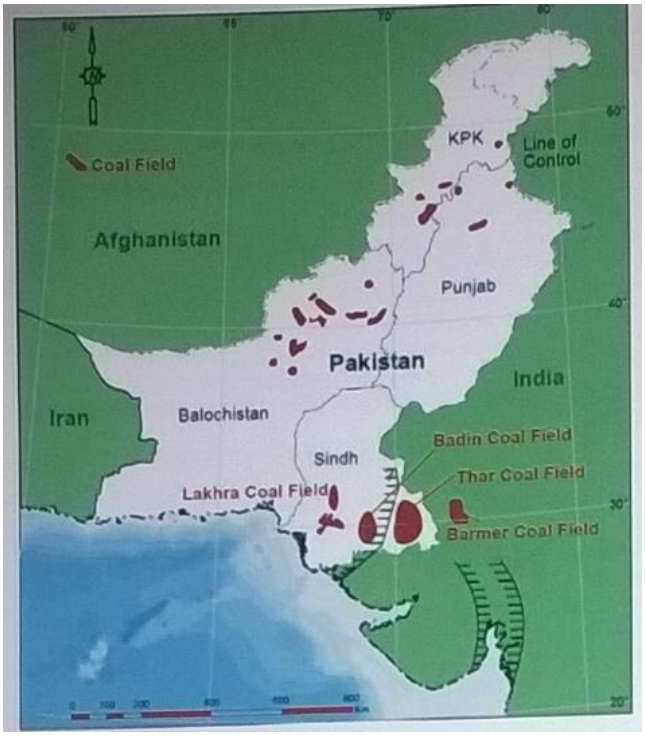

ANALYTICAL METHODS

The following analytical techniques were applied for the study

1. For organic petrography, polished blocks were prepared according to ISO 7404 (2004) procedure. Maceral analyses and vitrinite/huminite reflectance measurements (Rr %) were carried out using a Zeiss MPV3 microscopic equipped with a photomultiplier. For maceral analysis, at least 500 points on each polished block were counted under incident white light and blue light excitation. The maceral nomenclature applied was this of the Stoped- Heerien System as modified by ICCP and Sykorova.
2. For Geochemical analysis, the core sample was crushed and grinded to 200m mesh size. Total organic carbon (TOC) and sulphur content was measured by combustion of sample in Leco Carbon sulphur Analysis CS 244 after carbonate removal with 5% Hcl.
3. Extraction of bitumen or extractable organic matter (EOM) was assessed using Soxhlet Apparatus and dicholoro methane as solvent. EOM was fractioned into saturated, aromatic hydrocarbons and non-hydrocarbons by liquid column chromatography on silica gel/aluminium oxide by eluting with n-hexane and dichloromethane, respectively.
4. Rock Eval Pyrolysis is applied to identify the type and maturity of organic matter and to assess petroleum potential in sediments.
5. Pyrolysis was carried out using a closed steel vessel of 100 ml volume capacity with airtight facility. About 11.26g of grinded coal with double water amount were added in a steel vessel, air was evacuated by nitrogen flushing and tight vessel was kept in a muffle furnace at a temperature of 350-degree centigrade for 24 hours. It was removed and extracted with dichloromethane.

Formation	Age	Thickness	Lithology
Dune Sand	Recent	14-93 m	Sand, Silt & Clay
----------Unconformity----------			
Alluvial Deposits	Sub-Recent	11-209 m	Sandstone, Siltstone, Claystone, mottled
----------Unconformity----------			
Bara Formation	Middle Palaeocene to Early Eocene	0-185 m	Claystone, Shale, Coal, Sandstone, Carbonaceous Claystone
----------Unconformity----------			
Nagar Parkar Granite	Pre-Cambrian		Granite, Gabbro & Diorite

Stratigraphic sequence of Thar Coal Field of Pakistan

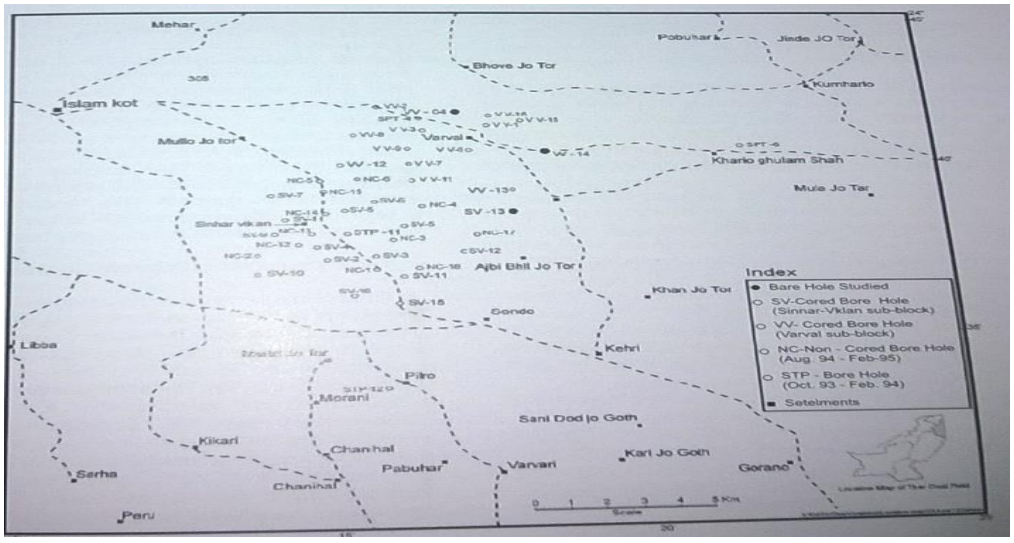

Location map of boreholes studied and drilled in Block No.1

RESULTS

The extractable organic matter (EOM), saturated (SHC) and Aeromatic (AHC) fractions

S.No	Sample No	Borehole	TOC %	EOM ppm	EOM g	NSO %
1	553-V	SV-13	19.38	1396.8	0.35	79.95
2	615-V	VV-14	51.83	10563.2	2.64	85.50
3	618-V	VV-14	66.71	10324.8	2.16	57.92
4	621-V	VV-14	55.32	5456.0	1.36	87.40
5	626-V	VV-14	53.33	9503.6	2.38	79.60
6	649-V	VV-14	56.42	2759.7	0.97	65.50
7	650-V	VV-12	28.12	2346.8	0.82	65.00
8	660-V	VV-12	57.34	3799.7	1.33	57.40

The Results of the Rock–Eval Pyrolysis of Thar Coal

S.No	Sample	TOC %	S %	Tmax ^{0}C	Gp mg HC/g
Bore Hole # VV-04					
1	V-643	26.13	8.93	364	28.09
2	V-644	54.59	0.8	406	126.17
3	V-645	61.04	0.87	341	56.84
Borehole # VV-14					
1	V-612	46.48	1.12	408	142.62
2	V-613	31.64	5.95	392	198.48
3	V-614	52.9	1.39	406	244.36
Bore Hole # SV-13					
1	553-V	19.86	4.01	419	75.13
2	554-V	64.4	6.71	400	185.58
3	555-V	49.21	8.63	418	184.32

IMPORTANCE

Gas is a more desirable fossil fuel because its use is considered to be better for the environment as the nation's demand increases and reserves continue to decrease. Coal bed methane fill as important niche in the domestic production portfolio. The term conventional gas includes many different types and compositions of natural gas with wide variations in its associated development and operations. CBM and other unconventional gas resources (e.g. shale gas, tight gas) are not as well defined, generally they are less productive and economically viable conventional gas.

Conventional process of extraction

Extraction of coal bed methane is not without controversy. CBM extraction involves pumping large volumes of water from coal seams in order to release water pressure that traps gas with the coal. The quality and dispersal of this water is a source of much debate. Each well is expected to produce approximately 5-20 gallons of water per minute.

A coal seam may best be visualized as a heterogeneous porous medium consisting of a bulk matrix system of homogenous low porosity, low permeability through which the gas may diffuse quite large; so parallelepiped surrounded by an orthogonal system of continuous uniform fractures of high permeability and porosity. The classical view of mass transport in the coal model has been that in the coal model has been that of a two-step process consisting of gas diffusion from the matrix into the matrix into the fractures and laminar flow of fluid through the fractures.The primary recovery leads to only 20-60% of the total recovery of methane from coal bed so to achieve maximum recovery ECBM is introduced

Enhanced Coal Bed Methane Recovery

New technologies have been proposed for extraction and recovery of CBM due to its growing importance. Enhanced coal bed methane recovery is to recover a larger fraction of gas in place. The two principle methods of ECBM recovery are 1) Use of nitrogen injection 2) Displacement desorption employing carbon dioxide injection. One important aspect of ECBM is the adsorption and desorption behaviour of gas mixtures. Primary recovery using depressurization techniques induces desorption of the CBM by lowering the overall pressure of the reservoir. On the other hand, a second gas maintains overall reservoir pressure while lowering the partial pressure of the CBM in the free gas. Injected gas also sweeps the desorbed gas through the CBM reservoir. Nitrogen is a natural choice as an injection gas because of its availability. Carbon dioxide is also promising because of benefit of greenhouse sequestration.

CONCLUSION

CBM technology is proceeding with good space to prove itself as a cleaner energy security to Pakistan as well as the World. However, production strategy of methane from CBM is very much different from conventional gas reservoir. The study revealed that the coal type, rank, volatile matter, and fixed carbon are strongly influence the adsorption capacity of methane into the coal bed. With increasing depth maturation of coal increases and generation of methane gas also increases. From the studies, it is observed that in future this field may be considered for methane extraction using advanced technology and in emergency condition. Sequestration of CO2 helps in mitigation of global warming, at the same time helps in recovery of methane gas from coal bed unveiled otherwise. However, detailed and intensive studies are required for efficient and economic production of coal bed methane.

Role of Natural gas, oil and other resources of energy is more than 99% for power generation and coal has contributed merely less than 1%. Reservoirs of conventional natural gas are depleting which are raising question for availability of energy for power generation. Compatibility of Coal can justify Underground Coal gasification technique for gasification and its utilization in Combined Cycle Station for power generation.

Technological development suggests the enhancement of non-renewable energy resources. In the current situation the energy consumption is increasing every year .the energy crises and price escalation have led to other alternative resources to compete daily increasing energy demand Coal bed Methane is an important aspect considering nation growth. CBM is a clean burning energy source which can be used as a boiler fuel and vehicle fuel. CBM is a non-conventional hydrocarbon fundamentally different in its formation processes and production technology so attention should be taken to put on development of this resource in order to meet the current crises of energy.

REFERENCES

[1] Khursheed Anwar, “Economic and Social Commission for Asia and the Pacific”, Country Paper Pakistan, Regional Seminar on Commercialization of Biomass Technology, Guangzhou, China, 2001, pp 1-4.

[2] Syed Zafar Ilyas, A Case Study to Bottle the Biogas in Cylinders as a Source of Power for Rural Industries Development In Pakistan, world Applied Science Journal, IDOSI Publications, 2006, pp127-130.

[3] Pakistan Coal Power Generation Potential, Private Power and Infrastructure Board, Ministry of Water and Power Government of Pakistan, 2004, pp 9-11.
[4] Pakistan's Thar Coal power Generation Potential, Private Power and Infrastructure Board, Ministry of Water and Power, Government of Pakistan, June 2008 pp 3.
[5] Balochistan Conservation Strategy, IUCN, Pakistan & Government of Pakistan, 2000, pp 122-138
[6] Engr. Abdul Waheed Bhutto, "Developing Coal Resources", The Dawn, Dated June 13, 2005
[7] Nazar-ul-Islam, Anwar Mohsin, Marzban Joozer and Habibullah, Mineral Statistics of Pakistan, Government of Pakistan Ministry of Petroleum and Natural Resources, Geological Survey of Pakistan, 2005, pp 2-18
[8] Engr. Abdul Waheed Bhutto, "Pakistan's coal resources" The Dawn, dated September 20, 2004
[9] Water and Power Development Authority (WAPDA) Brochure, 150 MW Lakhra Power Station Near Khanote (1993)
[10] S. Aziz, M. I. Pathan and S. A. Soomro, Erosion Problems in FBC Power Plant Based On Lakhra Coal, J. Appl. & Emerg. Sc., 2006 pp. 145
[11] S. Aziz, S. A. Soomro and M. A. Zeenat, Particle Size Analysis Of Coal & Limestone Used in FBC Power Plant at Lakhra, Mehran University Journal of Engineering & Technology, 50 (2008) 20
[12] S. Aziz, Study of technical aspects for improving the efficiency of FBC power plant at Khanot, M. E. Thesis, Chemical Engineering Department, Mehran University of Engineering & Technology, Jamshoro, (1999).
[13] Changdu and Sichvan, 3x50 MW FBC Lakhra power plant Near Khanote, Dong Fang Electric Corporation, R. of China, (1993).

AUSTRALIAN JOURNAL OF ENGINEERING AND TECHNOLOGY RESEARCH (AJMFR)
Vol. 2, Issue 1 - 2017

ENVIRONMENTAL IMPACTS OF SHALE GAS EXPLOITATION

Tahir Hussain Soomro
Department of Petroleum & N. Gas Engineering, Mehran UET Shaheed Z.A Bhutto Campus, Khairpur Mirs, Pakistan

Asadullah Memon
Department of Petroleum & N. Gas Engineering, Mehran UET Shaheed Z.A Bhutto Campus, Khairpur Mirs, Pakistan

Zeeshan Ali Lashari
Department of Petroleum & N. Gas Engineering, Mehran UET Shaheed Z.A Bhutto Campus, Khairpur Mirs, Pakistan

Note: This paper has been accepted for publication from the submissions made at the 2nd National Conference on *Intelligent Manufacturing & Sustainable Energy Systems (IMSES 2016) - Pakistan*

ABSTRACT:

Due to ever increasing energy demands and depleting conventional reservoirs, world is focusing towards the exploitation of unconventional reservoirs with the help of advanced technology that has been developed over the period. Exploitation of shale is one such development among others that has recently been witnessed, although the exploitation of shale has posed certain environmental challenges that need to be known and properly addressed.

The technology that has been employed for the development of shale is hydraulic fracturing, horizontal drilling, multi fracking etc that are the most significant sources of environmental destruction along with some others. This has posed a significant challenge to the companies that are involved in these operations. Civil society is reacting sharply to the consequences of such operations and the effects they are going to generate on environment. Different environmental laws have been breached and due to which certain areas are banned for the shale hydraulic fracturing like New York, Vermont states etc in America. Different documentaries on the subject had been made like “Gas land by Josh fox” that certainly shows the level of concern it has generated among the civil society who is at stake.

Hence a comprehensive study has been performed on the potential threats on environment due to shale gas exploitation and what could be done to minimize such adverse effects. Some of the findings of the study are that the environmental threats may be reduced with the help of careful planning of operations that needs to be carried out and the employment of technology that has been developed specially for the minimization of adverse environmental aspects of shale exploitation. Further, there is a need of a further research into this matter to make it as environment-friendly as possible.

1. INTRODUCTION:

From the last decades, the oil and gas has been explored and produced through conventional resources as they are available, easy to develop and economical as well.

The oil and gas as a fuel is typically found in permeable formation like as sandstone, limestone etc. The oil or gas produced through conventional extraction method are becoming increasingly limited to meet the current market demand. Therefore, in order to meet the market demand, the world is moving from conventional to unconventional natural gas sources or alternative. The shale gas, coalbed methane, and tight gas are the common examples of unconventional natural gas sources.

In unconventional extraction, the gas is extracted from reservoir by alteration of reservoir characteristics like as porosity, permeability, fluid trapping mechanism etc or rock characteristic. The hydraulic fracturing is the technique that helps to alter the characteristics of reservoir and rock and enables gas to flow in the borehole.

Due to extensive amount of unconventional reservoirs present, world is focusing towards the development of shale reservoirs which has posed certain environmental hazards as well that needs to be addressed and controlled [1]. This study focused on many health risk and various environmental issues connected with the unconventional extraction methods i.e growth and development of high volume hydraulic fracturing.

2. Shale Gas Extraction

Two most importance technologies has been used to deliver the potential to unlock tighter shale gas formations.

These technologies are “Horizontal drilling” and “hydraulic fracturing”. Both technologies are used combined to extract gas from shale formation see Fig 1. [2].

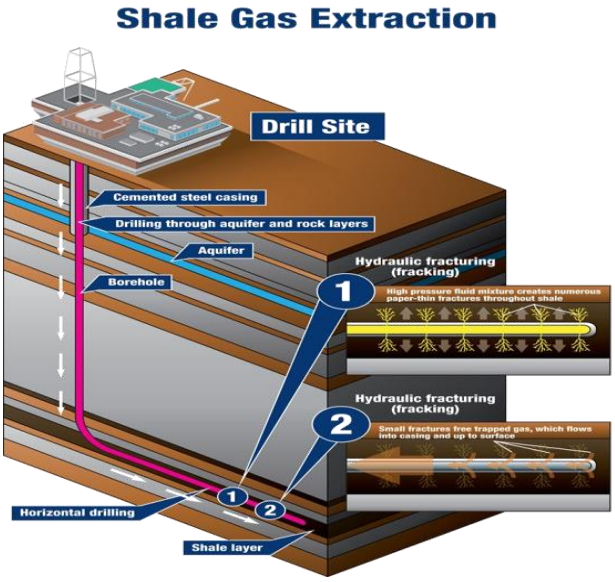

Fig. 1. Shale Gas Extraction process.

For shale gas extraction, the horizontal well is drilled which allows the well to pass through toward the hydrocarbon bearing rock seam, which may not be greater than 90m thick. Basically, this type of drilling has an advantage to maximize the contact area between the wellbore and formation. After that hydraulic fracturing or fracking to be done which may maximizes the well production i.e flow and volume of the produced gas.

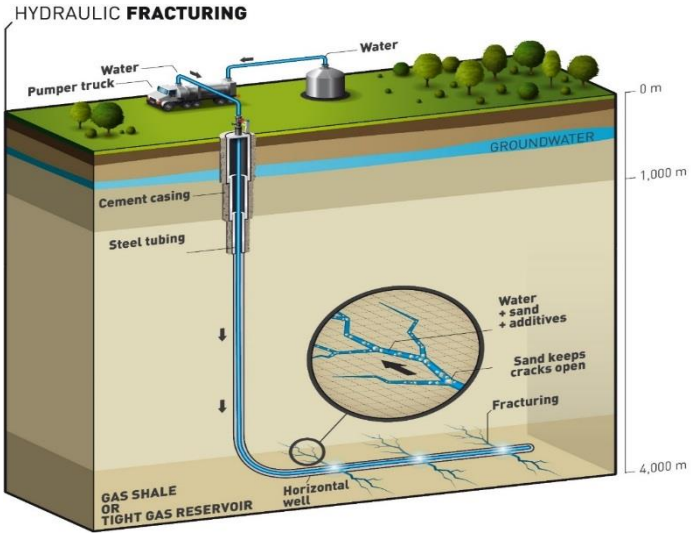

Fig. 2. Hydraulic fracturing process.

Well, stimulation technique such as hydraulic fracturing, acidizing can be used in the well bore to increase the permeability of the fluid and are implemented to extract the shale reserves. Hydraulic fracturing or fracking is helps to build a fractures in the rock bearing hydrocarbon formation[3]. The size of these fractures may as few 100 meters into the reservoir rock and commence at horizontal departure see Fig 2.

3. Water Usage

It is very difficult to create fractures in the well without water. Usually, two to five million gallons water required to complete each fracture job. Therefore, water is essential for fracturing job. In some case, the water can be used as recycled but the water recycle treatment process desires a major recession from the aquifer or other water resources [4].

Passage to plentiful water is critic to shale gas development and it directly effects on the sources of plenty water and therefore, secession must be managed. Nowadays, most of industry is working on this hazard and taken tremendous efforts as well in managing the water secession, water treatment and use the produced water as this reducing the water demands of shale gas drilling.

4. Environmental Hazards

The main environmental hazards associated with the shale gas extraction are defined as under:

4.1 Surface & grand water contamination

The high risk of water contamination has been seen at different steps of the well site preparation, fracking process, fluids flow toward the surface, and during well abandonment as well in surface and ground level.

The surface water contamination may be result of runoff and erosion during early site preparation. After runoff and erosion, most of silt particles are accumulated in surface waters and contaminants penetrating streams, water bodies, and groundwater. This is the common problem which has been seen in entire large-scale mining as well as activities of extraction[5].

In extraction activities especially unconventional gas extraction which carries a higher risk as it requires high-volume processes per installation and the risks increase with respect to multiple installations. Shale gas installations are expected to generate greater stormwater runoff, which could affect natural habitats through sediment build up, stream erosion, flooding, and water degradation.

This study considered the water contamination risks due to following reasons:

- Poor well design or poor casing structure.
- Well, kick or mechanical equipment failure.
- Movement of combustible natural gas towards the water storage/supplies.
- Geological conditions are inadequate.
- Inadequate planning and site preparation and management.

4.2 Air emissions

It is found from literature that the natural gas produced during the fracking operations can be bad for the atmosphere as compared with coal [6]. Because this natural gas discharge into the atmosphere. Further, study suggested that the emissions from shale gas are between 20-100% more than the coal through life cycle greenhouse gas (GHG) on a 20-year timeframe basis [7].

Most of natural gas industries are taken effort to reducing the methane emissions during shale gas operation along with emissions of carbon dioxide, sulphur dioxide, hydrogen sulphide from treating and other process of sour water for hydraulic fracture job. The emission produced from this fracking operations are harmful for the environment.

4.3 Land and Take

Some of the study shows that the land used in shale gas extraction has a significant risk of impacts because small size of land required for production stage while large size of land required for fracking process.

4.4 Noise pollution

There are many sources of noise in shale gas extraction i.e during excavation, installation and drilling,

generator, process and transport etc and its level varies from stage to stage i.e preparation and production cycle.

4.5 Bioversity Impacts

The effect of biodiversity on unconventional gas extraction has seen and it may causes of degradation or splitting up or complete removal of a habitat as a result of site construction or excessive water absorption etc.

Other affect biodiversity occurs due to the operations of well drilling through noise, traffic and site management and hydraulic fracturing through sediment runoff, waste water, and contamination.

4.6 Traffic

Movements of truck is initially very high due to site development but these movements can be reduced by temporary setup i.e use of pipelines for water supply, drainage etc. The movements of truck may also be affecting on road damage, road safety issues, and other related infrastructure. The risk is may also increase as traffic increase due to spillages and accidents involving hazardous materials.

4.7 Visual Impacts

The effect of visual is to be considered as low during well-pad site identification and preparation. The risk of visual impacts connected with fracking is little bit important, with the essential diversity to the landscape in here of little bit visually invasive appearance.

4.8 Seismicity

The effect of seismic associated with fracking process is minor as up to 3 magnitude on the earthquake magnitude scale has been used and this would not be disturb to the public and undetectable as well. Therefore, the risk of this hazard is low [8].

The summary of risk level at various stages of field development o individual site and Cumulative are shown in table.1 & 2.

Table. 4.1. Level of risk at various stages of field development (Individual Site).

Aspects of Environmental hazards		**(a)**	**(b)**	**(c)**	**(d)**	**(e)**	**(f)**	**(g)**
		Site starts- up	Well design	Fracturing operations	Well Completion	Production	Well abandonment (Pre and post)	Overall rating
Water contamination	Ground	N.A	Low	Moderate-High	High	Moderate-High	N.C	High
	Surface	Low	Moderate	Moderate-High	High	Low	N.A	High
Resources of Water		N.A	N.A	Moderate	N.A	Moderate	N.A	Moderate
Air impact		Low	Moderate	Moderate	Moderate	Moderate	Low	Moderate
Land and take impact		Moderate	N.A	N.A	N.A	Moderate	N.C	Moderate
Biodiversity impact		N.C	Low	Low	Low	Moderate	N.C	Moderate

Noise impact	Low	Moderate	Moderate	N.C	Low	N.A	Moderate-High
Visual Impact	Low	Low	Low	N.A	Low	Low-Moderate	Low-Moderate
Seismicity impact	N.A	N.A	Low	Low	N.A	N.A	Low
Traffic impact	Low	Low	Moderate	Low	Low	N.A	Moderate

Table. 4.2. Level of risk at various stages of field development (Cumulative).

Aspects of Environmental hazards		**(a)**	**(b)**	**(c)**	**(d)**	**(e)**	**(f)**	**(g)**
		Site starts- up	Well design	Fracturing operations	Well Completion	Production	Well abandonment (Pre and post)	Overall rating across all phases
Water contamination	Ground	N.A	Low	Moderate-High	High	High	N.C	High
	Surface	Moderate	Moderate	Moderate-High	High	Moderate	N.A	High
Resources of Water		N.A	N.A	High	N.A	High	N.A	High
Air impact		Low	High	High	High	High	Low	High
Land and take impact		Very-High	N.A	N.A	N.A	High	N.C	High
Biodiversity impact		N.C	Low	Moderate	Moderate	High	N.C	High
Noise impact		Low	High	Moderate	N.C	Low	N.A	High
Visual Impact		Moderate	Moderate	Moderate	N.A	Low	Low-Moderate	Moderate
Seismicity impact		N.A	N.A	Low	Low	N.A	N.A	Low
Traffic impact		High	High	High	Moderate	Low	N.A	High

Note:

- Not applicable (N.A): Impact not relevant to this stage of development.
- Not classifiable (N.C): Insufficient information available for the significance of this impact to be assessed.

5. Control

5.1 Fracture Monitoring

The effects of fracking can be control through monitoring the fracturing design, process, treatment, and analysis. The monitoring technologies can be used for fracking treatment such as tiltmeter measurements and microseismic fracture mapping [9]. These both technologies are helps to map fracking location orientation and depth.

Micro-seismic is the monitoring technology in which seismic waves are generated during the fracking job and then monitor the generated fractures. This type of monitoring help to engineers by providing the capability to oversee the resource via brilliant placing of additional wells to yield benefits of understanding the subsurface conditions and its behavior and may also be expected fracture results in newly wells [10].

5.2 Change in Standard

The effects of fracking may also be controlled through change in standard like as "Green" or "Reduced Emissions Completions," in which both gas and liquid hydrocarbons are abstracted from flow back, would need to be occupied during completions and recompletions of fracking in gas wells.

The following change in standard may be used to reduce the effects on fracking operation [11]:

- Use of compressors for natural gas flow through pipelines.
- Centrifugal units is to be equipped with dry seal systems.
- Uses of pneumatic controllers during all process.
- Uses of condensate and crude oil storage tanks for reduction in VOC emissions.

6. Conclusion

- It is observed in this study that the risk is high on unconventional extraction method as compared with conventional but can be reduce by reducing the effect which affecting on unconventional extraction method.
- Above study shows that there are many potential threats on environment due to shale gas exploitation and could be minimize by careful planning of operation, proper monitoring, and control system.
- Environment-friendly methods can be adopted during fracking operation for success of the project.

Recommendations

From this study, it is recommended that:

- Overview on environment threat or potential risks should be considered before commence of any project.
- Adopting effective technologies for reducing the adverse effects especially in those areas where sensitivity is high related to the biodiversity, community etc.
- Measures and approaches to reduce land disturbance and land-take, pressure on biodiversity, noise (during drilling, fracturing, and completion), traffic movements, risk of ground and surface water Contamination.

Acknowledgement

We would like to express our gratitude to MUET S.Z.A.B Campus, Khairpur Mirs for granting us the permission to publish this paper.

References

1. Arthur. James Daniel, Coughlin. Bobbi Jo, Bohm. Brian K, "Summary of Environmental Issues, Mitigation Strategies, and Regulatory Challenges Associated With Shale Gas Development in the United States and Applicability to Development and Operations in Canada", 138977-MS SPE Conference paper, 2010.

2. Connor, J. A., Molofsky, L. J., Richardson, S. D., Bianchi-Mosquera, G. C., "Environmental Issues and Answers Related to Shale Gas Development", 174164-MS SPE , Conference Paper, 2015.

3. Arthur. James Daniel, Bohm. Brian K., Cornue. David, "Environmental Considerations of Modern Shale Gas Development", 122931-MS SPE Conference Paper, 2009.

4. Reza Rezaee, "Fundamentals of Gas Shale Reservoirs", Wiley: John Wiley & Sons, Inc., 2015.

5. Stephen G. Osborn, Avner Vengosh, Nathaniel R. Warner, Robert B. Jackson, "Methane Contamination of Drinking Water Accompanying Gas-Well Drilling and Hydraulic Fracturing",

6. Proceedings of the National Academy of Sciences 108(20):8172-6, May 2011.

7. Hsue-Peng. Loh, Nancy. Loh "Hydraulic Fracturing and Shale Gas: Environmental and Health Impacts" Advances in Water Resources Management, pp.293-337, 2016.
8. Cornell's. Robert. Howarth, "Methane and the greenhouse-gas footprint of natural gas from shale formations," Climatic Change, March 13, 2011,

9. Chanpura. Rajesh. A., Germanovich. Leonid. N., "Faulting and seismicity associated with fluid extraction", 01-0885 ARMA Conference Paper, 2001.

10. Quirein. John A., Grable. Jeff, Cornish. Bruce, Stamm. Ron, Perkins. Tegwyn, "Microseismic Fracture Monitoring", VV SPWLA Conference Paper, 2006.

11. Cipolla. Craig L., Williams. Michael John, Weng. Xiaowei, Mark. Gavin, Maxwell. Shawn C., "Hydraulic Fracture Monitoring to Reservoir Simulation: Maximizing Value", 133877-MS SPE Conference Paper, 2010.

12. Laffin. Michael, Blake. Kariya, Michael. Blake, "Shale Gas and Hydraulic Fracking", 20-3262 WPC Conference Paper , 2011.

AUSTRALIAN JOURNAL OF ENGINEERING AND TECHNOLOGY RESEARCH (AJMFR)
Vol. 2, Issue 1 - 2017

AN ADVANCED APPROACH FOR BETTER MECHANICAL PROPERTIES OF EPOXY BASED CARBON COMPOSITES USING DOUBLE VACUUM BAG INFUSION TECHNIQUE

Ashfaq Hussain
Composite Research Center, Department of Materials Science and Engineering, Institute of Space Technology, Islamabad, Pakistan
School of Mechanical Engineering, Xian Jiaotong University, Shaanxi, Xian P.R.China

M.Faizan Siddique Awan
[a]Composite Research Center, Department of Materials Science and Engineering, Institute of Space Technology, Islamabad, Pakistan

Kalsoom Bhagat
Department of Electrical Engineering, MUET SZAB Campus Khairpur, Sindh, Pakistan

Laraib Alam Khan
[a]Composite Research Center, Department of Materials Science and Engineering, Institute of Space Technology, Islamabad, Pakistan

Kashif Naveed
[a]Composite Research Center, Department of Materials Science and Engineering, Institute of Space Technology, Islamabad, Pakistan

Tayyab Subhani
[a]Composite Research Center, Department of Materials Science and Engineering, Institute of Space Technology, Islamabad, Pakistan

Note: This paper has been accepted for publication from the submissions made at the 2nd National Conference on *Intelligent Manufacturing & Sustainable Energy Systems (IMSES 2016) - Pakistan*

Abstract
Double vacuum bag (DVB) infusion process is used for the manufacturing of carbon fiber epoxy matrix composites for aerospace applications. For reference, carbon fiber epoxy matrix composites were also prepared by single vacuum bag (SVB) infusion process. The composites manufactured by DVB showed less void contents and more fiber volume fraction together with good impregnation of carbon fibers with resin. An increase in mechanical properties including shear and flexural moduli was also observed than composite processed by SVB. DVB infusion process is a promising technique for the manufacturing of polymeric matrix composites for aerospace and automobile industries.

Keywords: Double vacuum bag; Single vacuum bag; Carbon fiber; Epoxy resin.

1 INTRODUCTION

Polymer matrix composites (PMCs) are an important class of engineering materials. PMCs are successfully replacing traditional structural materials and offer an opportunity to compete metallic materials[1]. In particular, carbon fiber epoxy matrix composites are especially used for aerospace applications due to their better specific properties than traditional materials. Carbon fiber epoxy matrix composites have gained importance due to their higher strength-to-weight ratio. Carbon fibers may exist in short fibers or continuous forms. The structure may be amorphous, crystalline or partly crystalline. Moreover, carbon fibers do not impart health hazards [1].

The properties of PMCs are dependent on the mode of fabrication. Tooling design is vital for the production of cost-effective and durable composite products[2].A range of processes have been developed to prepare PMCs such as hand layup, spray up, compression moulding, transfer moulding, vacuum infusion and vacuum bagging[3].In particular, close mould techniques were developed to fabricate composite parts with less damage to human health and better functional and structural properties[4, 5]. Close mould methods utilize two counterparts, i.e. a male part and a female part. A variant of closed mould process is resin transfer moulding, which has further variants such as vacuum assisted resin transfer moulding. Another variant is controlled atmospheric pressure resin infusion[6, 7].

Among different manufacturing techniques, vacuum infusion is a process widely used to prepare PMCs, which offers a safer and affordable alternative to produce composites otherwise prepared by autoclave processes[8]. In this technique, consolidation force is applied via vacuum, which derives low viscosity resin into the mould cavity. Like other techniques, vacuum infusion also has limitations associated with it such as the presence of voids in composites, bag relaxation defects and non-uniformity and permeability issues.

Double Vacuum Bag (DVB) infusion technique is an easy and cheap technique to fabricate quality PMCs than other techniques. In single vacuum bag (SVB) process, the polymeric bag provides compaction which is not sufficient to achieve good densification of composites. The parts fabricated from SVB process are found to have high void contents. The properties of a composite are detrimentally affected by voids introduced during the manufacturing process. SVB process along with the porosity factor produce composites having fiber volume fraction in the range of 40-43%. As the main properties of PMCs are derived from fibers, therefore, their increased content in composites is advantageous. Higher the fiber volume fraction in a composite, higher will be the strength and modulus; thus, increased efficiency and performance of the composite. DVB works on the same principle of infusion and utilizes two separate bags under two vacuum levels. The actual infusion takes place in the inner bag. The second bag seals the mould and envelops the first bag and provides extra pressure on the infused composite part. As the resin enters the first bag the absolute pressure drops with the increase in the volume. The double bag tries to compensate by providing full vacuum pressure to the part, hence allowing the removal of extra resin, increased fiber content and a lower void content.

In this paper work on DVB technique is used to prepare composites. The aim is to produce void-free composites and to increase their integrity thus producing parts with higher fiber volume fraction. A comparison between DVB and SVB was made on the basis of physical and mechanical properties i.e. void content, fiber volume fraction, shear modulus, flexural modulus. Carbon fibers were impregnated in epoxy resin to prepare composites by the both techniques for comparison. Microstructural and mechanical characterization was performed to evaluate the composites with reference to their manufacturing techniques.

2 EXPERIMENTAL

Materials

Commercially available, high-strength polyacrylonitrile-based 2-D woven carbon fabric with average fiber diameter of 7 µm was procured from CNME International, China. Epoxy resin (Araldite 5052) with its hardener (Aradur 5052) was purchased from Huntsman Advanced Materials. Airtech peel ply, distribution media, and polymeric nylon bag were used for composite manufacturing. Caul plate was used to acquire even compaction upon carbon fabrics; two rotary vacuum pumps were used.

Manufacturing

Flat and rectangular composite panels of dimensions 500x400 mm were fabricated using DVB and SVB processes. The mould was cleaned with acetone, which was followed by the application of demolding material, i.e. wax. Peel-ply was first placed in the mould cavity, which served as a debonding media and helped to debond the final composite specimen from the mould without sticking. The carbon fabrics in desired dimensions were later stacked in the mould. After placing the desired layers of carbon fabrics, another layer of peel-ply was stacked above the carbon fabrics; as a matter of fact, carbon fibers were sandwiched between two peel-plies. Highly permeable distribution/flow media was placed over peel ply, which is a mesh-like structure and helps the resin to distribute homogeneously over the preform, i.e. carbon fabrics. Subsequently, a polymeric bag covered the mould containing carbon fabric; the bag was attached with the substrate using a tacky tape.

A perforated metal plate with smooth surface finish was placed over the bag, which served as caul plate. Ideally, caul plate should be equal in size to the size of fabrics to distribute equal pressure upon the composite to be manufactured. Another polymeric bag was used, which covered the existing setup and was also attached to the substrate using a tacky tape. In the inner bag, an inlet and an outlet were prepared for the infusion of the resin. Inlet port was connected to the resin pot via a plastic pipe. The outlet port connected with the resin reservoir has two holes: one connected with the vacuum pump and other with outlet pipe. The present setup ensured the backflow of resin to vacuum pump, which might cause failure of the pump. For outer bag, a single outlet was connected to a second vacuum pump through a pipe.

Before the infusion to start, the valve on the inlet pipe was closed. The vacuum pump was switched on to evacuate the air from the setup. When mold was completely degassed, the setup was checked for any leakages. The resin was also degassed for 15 min. After complete checking and degassing, the inlet pipe was placed in the resin pot and inlet was opened. Due to the action of atmospheric pressure resin started flowing into the mold. Due to high compaction and use of permeable flow media, the resin was equally distributed over the whole composite specimen and complete wetting of the fabric was obtained. Vacuum pump sucked the excess resin while the process continued for 2h to remove excess resin from the part. Finally, the vacuum pump was switched off. After curing of composites for 24h, these were removed from the mold and post-cured in an oven at 100^{o}C for 1h. Figure 1 shows the schematic of the composite manufacturing process. For comparison composites with conventional SVB process were also prepared.

Characterization

Images of the composites were captured using an optical microscope. To determine void concentration and fiber volume fraction, image processing of the composite images was carried out using Image J software. Moreover, the void size, shape, and spatial distribution were also determined using the composite images.

Mechanical properties of the prepared composites were evaluated from interlaminar shear and three-point bend tests. Shear test was performed according to ASTM D2344 standard with specimen size of 15x10x10 mm. Three-point bend test was performed using ASTM D790 standard with specimen size of 80x15x10 mm. At least ten specimens were prepared for the two testing techniques to acquire reliable data.

3 RESULTS AND DISCUSSIONS

Optical micrographs of the composites processed by DVB and SVB and their image processing are shown in Figures 2 and 3, respectively. The difference in the void contents can be seen. Indeed, the presence of defects in composites such as porosity and voids reduces their mechanical performance, as discussed further below.

Table 1 enlists the physical and mechanical properties of the composites manufactured by DVB and SVB processes i.e. void content, shear, and flexural moduli. In comparison to SVB, the process of DVB offers better compaction and higher loading of fibers. It can be seen in Figure 4 that the average void content in SVB-processed composites is 11±2, which reduced to 4±2 in DVB-processed composites. The decrease in void content was achieved after increased infusion of resin under high pressure in DVB process. Moreover, the fiber volume fraction also increased under high pressure. After proper impregnation of fibers, the excess resin was rejected by the process. Figure 5 shows the increase in the fiber volume fraction in the two manufacturing processes. It can be seen that the fiber volume fraction increased from 42±3 to 54±3, when DVB process was used.

It was obvious that composites containing less porosity and increased fiber contents possessed better mechanical properties, which was evidenced in mechanical testing. The composites processed by DVB offered higher flexural modulus, i.e. 51±3GPa than reference composites, i.e. 44±3MPa (Figure 6a). Similarly, shear modulus of the composites manufactured by DVB was higher, i.e. 44±3GPa than reference composites processed by SVB, i.e. 37±3GPa (Figure 6b). It can be inferred that the composites fabricated by DVB offered more control over vacuum and resulted in better mechanical properties. Moreover, low void content means better structural properties due to better integrity of manufactured composites.

When resin enters the dry carbon fabrics under pressure, it may displace fibers. Hence the void concentration in such areas will be high, which was verified by optical images (not shown here) that void concentration is different at different locations of the composites. The resin flow is uniform in the middle of the composites while the edges have increased void contents. The same trend was observed in the composites processed by both techniques though the effect was diluted in DVB process, as observed in Figure 7, which shows the void content measurement from one edge of the composite specimen to the other edge with a distance of 500mm. Vacuum leakages may occur at the edges and result in high void content but DVB process provided better vacuum control and therefore the void concentration was much lower than SVB process.

4 CONCLUSIONS

Double vacuum bag (DVB) infusion process was adopted for the fabrication of polymeric matrix composites. Carbon fiber epoxy matrix composites were selected for the fabrication of composites and a comprehensive comparison was drawn between the physical and mechanical properties of the composites prepared by DVB and single vacuum bag (SVB) infusion processes. An increase in the mechanical properties, i.e. shear and flexural moduli, was noticed using DVB process. The void contents also decreased by using this novel process along with an increase in the fiber volume fraction in the composites. Finally, it was observed that the application of double bags reduced the difference in void contents at the middle and edges of the composites and provided materials with better resin impregnation and thus uniform resultant properties.

TABLES

Table 1. Mechanical properties for SVB and DVB samples

Samples	Void Content (%)	Shear Modulus (GPa)	Flexural Modulus (GPa)
SVB	10±3	37±3	44±3
DVB	4±2	44±3	51±3

FIGURES

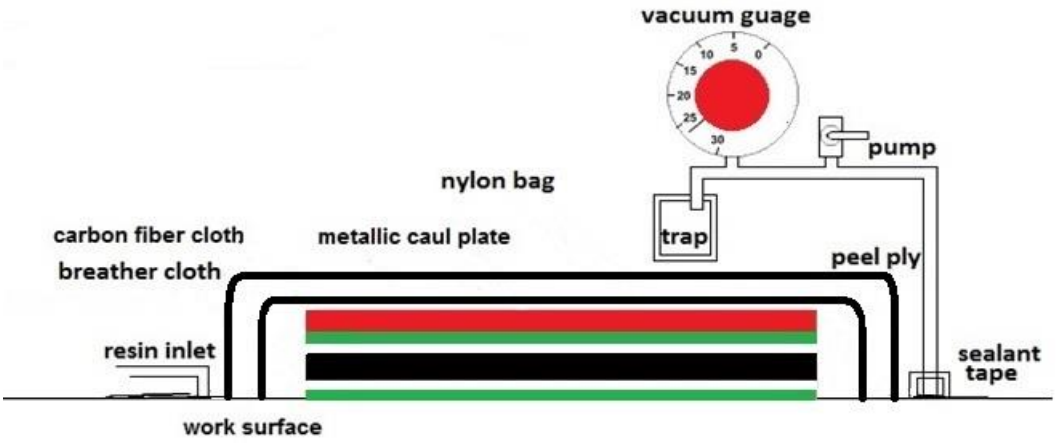

Figure 1 Schematic illustration of double vacuum bag infusion process

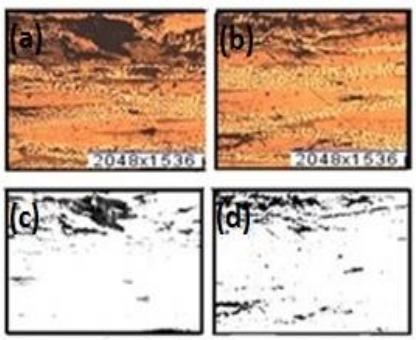

Figure 2(a,b) Optical micrograph of composites prepared by SVB and (c,d) their image processing

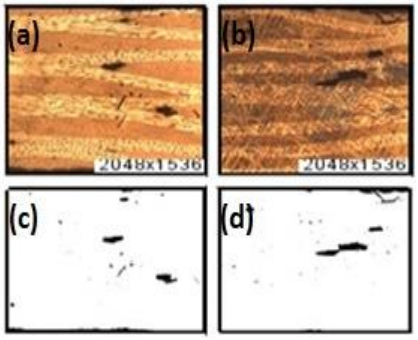

Figure 3 (a,b) Optical micrograph of composites prepared by SVB and (c,d) their image processing

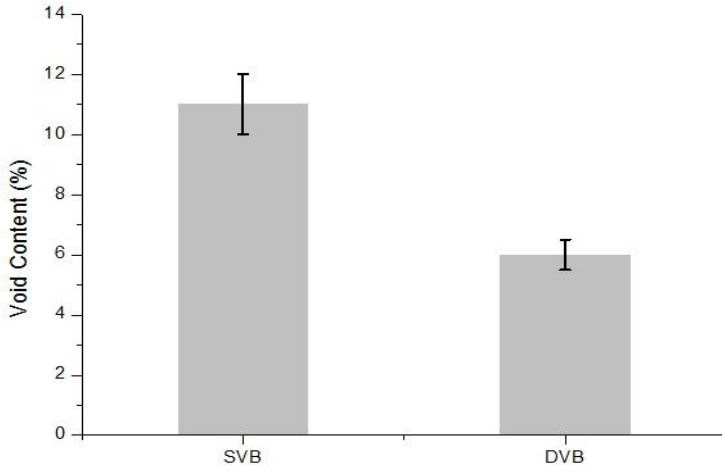

Figure 4 Void concentration in DVB and SVB process

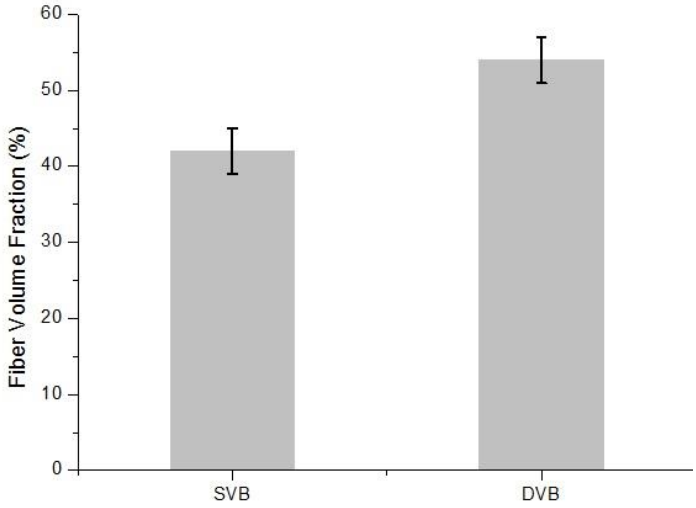

Figure 5 Fibre volume fraction comparison graph

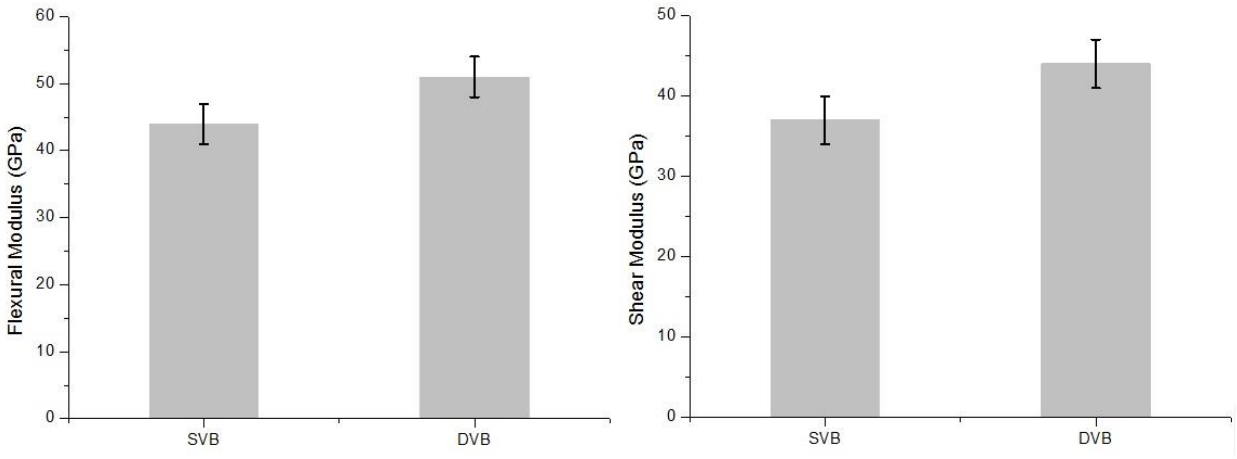

Figure 6 Modulus comparison for DVB and SVB process (a) flexural modulus (b) shear modulus

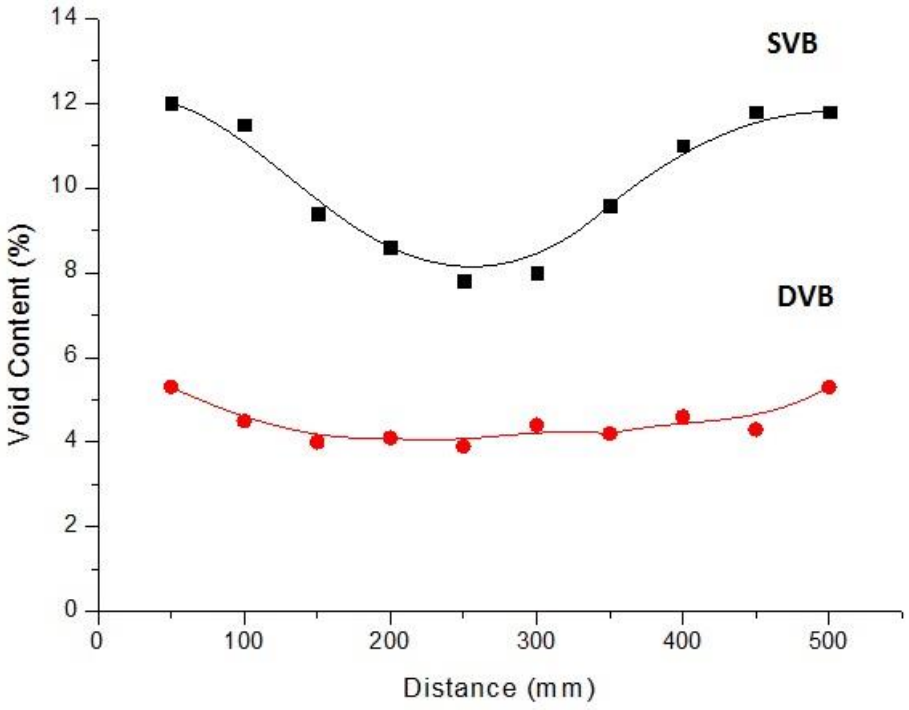

Figure 7 **The spatial distribution of void contents in composites manufactured by SVB and DVB processes**

References

1. Singha, K., A Short Review on Basalt Fibre International Journal of Textile Science 2012.

2. Abdalrahman, r., design, and analysis of integrally-heated tooling for polymer composites. 2015.

3. McIlhagger, A., E. Archer, and R. McIlhagger, Manufacturing processes for composite materials and components for aerospace applications. Polymer Composites in the Aerospace Industry, 2014. 53.

4. Ho, M.-p., et al., Critical factors on manufacturing processes of natural fiber composites. Composites Part B: Engineering, 2012. 43(8): p. 3549-3562.

5. Michaud, V. and A. Mortensen, Infiltration processing of fiber reinforced composites: governing phenomena. Composites Part A: applied science and manufacturing, 2001. 32(8): p. 981-996.

6. Rudd, C., et al., Liquid moulding technologies: Resin transfer moulding, structural reaction injection moulding and related processing techniques. 1997: Elsevier.

7. Niggemann, C., et al., Experimental investigation of the controlled atmospheric pressure resin infusion (CAPRI) process. Journal of Composite materials, 2008. 42(11): p. 1049-1061.

8. de Almeida, S.F.M. and Z.d.S.N. Neto, Effect of void content on the strength of composite laminates. Composite structures, 1994. 28(2): p. 139-148.

AUSTRALIAN JOURNAL OF ENGINEERING AND TECHNOLOGY RESEARCH (AJMFR)
Vol. 2, Issue 1 - 2017

DYNAMIC STRUCTURAL AND MODAL ANALYSIS OF TYRE COUPLING ON UNSTRUCTURED MESH

INTIZAR ALI,
Department of Mechanical Engineering, Humdard University, Karachi, Pakistan

DILEEP KUMAR,
Department of Mechanical Engineering, Mehran University of Engineering and Technology Shaheed Zulfiqar Ali Bhutto Campus, Khairpur Mir's, Pakistan

Imran Mir
Directorate of Postgraduates Studies, Mehran University of Engineering and Technology, Jamshoro, Pakistan

Ishfaque Ali Qazi
Department of Mechanical Engineering, Qauid-e-Awam UCET, Larkano, Pakistan

Note: This paper has been accepted for publication from the submissions made at the 2nd National Conference on *Intelligent Manufacturing & Sustainable Energy Systems (IMSES 2016) - Pakistan*

ABSTRACT:

The coupling is one of a key component of power transmission systems where it is subjected to highly fluctuating loads resulting in over-stressing undesired vibration and shocks. Tyre coupling have capability to absorb sudden jerks and vibration, therefore, it provides safe and efficient operation. In this research, transient structural and modal analysis of tyre, coupling is carried out by using ANSYS structural code on unstructured mesh. To predict deformation, stresses as well as natural frequencies of structure under time-dependent loads to avoid structure failure and resonance. Unstructured mesh is used to reduce discretization error. Research results reveal that the existing tyre coupling design is safe from strength and vibration point of view but it undergoes very large deformation which becomes major cause of fatigue failure. It is also concluded that there is enough potential of weight reduction is available in existing design of coupling which increase system performance.

Keywords: Tyre coupling, transient structural analysis, modal analysis and fatigue failure.

INTRODUCTION:

The couplings are widely used in various engineering applications for power transmission and to increase shaft length to achieve intended function. Shafts are usually available in length varying from 6 to 10 meters, so that they can be easily handled, transported and precisely manufactured. But in most of engineering applications shafts of large lengths are required to transmit the torque which can be obtained by joining two or more shafts in order to obtain the required length (Patel, Oza, Gohel, Parmar, & Kadivar, 2014) & (Johnson, 1996). Then coupling is used to get required length, for that purpose several types of coupling are used, tyre coupling is one of them. Tyre coupling is used to connect two shafts which are co-linear; it will make up the misalignment and withstand the backlash. Since misalignment during assembly can be reduced but can't be eliminated. Misalignment is major

problem in most of application several research are being conducted to detect and analyse its cause and remedies (McGinnity & Mancuso, 2005; Veale & Roberts, 2011). Study is done to detect misalignment between motor and load developed. The developed model equation shows that because of misalignment forcing frequencies come even multiple frequencies of motor speed (Xu & Marangoni, 1994). (Sekhar & Prabhu, 1995) modelled rotor-bearing system to understand effect of (Bossio, Bossio, & De Angelo, 2009). In order to understand the effects of shaft misalignment and rotor unbalance, a theoretical model of complete motor flexible coupling rotor system is misaligned and location of coupling along shaft is determined by using finite element method. Study concluded that coupling location with respect to bending mode shape affects vibration.

Misalignment and unbalance have got extreme focus in design of high speed rotating machinery because they experience unwarranted vibrations and torsional stresses. To get rid of this phenomenon we need a coupling with appreciable elasticity and flexibility. Study was conducted on design and life enhancement of structural components of an aircraft by using flexible coupling, (Nagesh, Basha, & Singh, 2015) and the effects misalignment of jaw, flexible and rigid flange coupling is analysed experimentally by frequency spectrum of unbalance of shaft coupling and compared with available literature and experimental results are very close to them (Pathan & Khaire, 2014). As from above literature, it is concluded that misalignment, as well as vibration, are until serious issues. To solve these types of problems tyre coupling offers intangible benefits through taking angular misalignment, parallel misalignment and absorbing torsional vibration. Tyre coupling is sometimes called self-aligning coupling (Vibration control, 2015).

1. RESEARCH AIMS:

Despite of all these benefits and providing solution to such serious problems tyre coupling is remain less area of interest for designers. Therefore, in this research, very little effort is done to bridge this gap. Research is conducted to analyse the behaviour of tyre coupling under transient loading to get knowledge about structural integrity of coupling and potential of weight reduction. Finally, various structure parameters such as deformation stresses as well as on natural frequencies are analysed through finite element method.

2. RESEARCH APPROACH:

In order to carry out tyre coupling simulation, three-dimensional models are developed in Pro-engineering software. Model is developed according to given specification. All the three components are first modelled in Pro-engineering modelling than they are assembled. In order to carry out structural analysis, finite element discretization method is used to completely discretise physical domain. Simulation is conducted on unstructured mesh by using tetrahedron mesh elements to reduce discretization error. Patch conforming algorithm is used to refine mesh at critical points and to obtained high orthogonal mesh quality. Transient structural analysis of tyre coupling is carried out in ANSYS 12.0 structural code. Material for flange and tyre are Grey Cast Iron and Neoprene respectively.

3. FEA GOVERNING EQUATIONS

Finite element analysis is a numerical technique which solves complex continuous structural problem by discretising into small segments known as element. All the elements are connected at one point

called node, in between two nodes the element is considered as elastic spring. The whole system behaviour is governed by following governing equations.

$$\{F\} = [K]\{u\}$$

In the equation *F* denotes applied external load, *U* represent system behaviour and *K* is the property of material known as stiffness. In case of finite element analysis, each element is represented by different equation and finally makes thousand equations. For all cases, two variables are known and third one has to be determined therefore equation can be written as.

$$\{u\} = [K]^{-1}\{F\}$$

In this form above equation looks very easy and can be solved easily but these equations are interconnected at each node and their displacement, as well as force transmission, affects each other. The given below is case of single spring loaded and distort at both nodes by force f_1 f_2 and distorts by displacement u_1 *and* u_2 then equation can be written as

$$f_1 = -k(u_2 - u_1)$$
$$f_2 = k(u_2 - u_1)$$

These equations can be written in matrix form as

$$\begin{pmatrix} k & -k \\ -k & k \end{pmatrix}\begin{pmatrix} u_1 \\ u_2 \end{pmatrix} = \begin{pmatrix} f_1 \\ f_2 \end{pmatrix}$$

Or

$$[k_e]\{\mathrm{u}\} = \{F\} \quad \text{Whereas} \quad k_e = \begin{pmatrix} k & -k \\ -k & k \end{pmatrix}$$

Therefore for three springs in combination then,

$$\begin{pmatrix} k_1 & -k_1 & 0 \\ -k_1 & k_1 + k_2 & -k_2 \\ 0 & -k_2 & k_2 \end{pmatrix}\begin{pmatrix} U_1 \\ U_2 \\ U_3 \end{pmatrix} = \begin{pmatrix} F_1 \\ F_2 \\ F_3 \end{pmatrix}$$

In this way all the equation of discretised domain are connected, solved by Newton-Raphson method as follow.

$$X_{n+1} = x_n - \frac{f(x_n)}{f'(x_n)}$$

4. DESIGN AND MODELING

Tyre coupling offers main advantage that it maintains high torque to lower weight ratio. The operating torque bearing capacity is around 12000 Nm. The considered model is capable of withstanding axial, lateral and angular misalignment up to 6 mm and 5 degrees. They can absorb abnormal shocks as well as minimize effect of misalignment and increase machines life. The torsional stresses are absorbed during the rotational motion of the shaft and smooth power transmission is achieved with less deflections. The flexible tyre coupling consists of two flanges and tyre is fixed between them. It has greater damping values as compared to rigid couplings. In order to carry out tyre coupling simulation three-dimensional models is developed in Pro-engineering software. Model is developed according to given specification. All the three components are first modelled in Pro-engineering modelling than they are assembled. The proposed system consists of a tyre coupling, assembling two flanges together and tyre attached in between. The design parameters of the CAD model are as under:

Table.1 shows specifications of Tyre coupling

Maximum Bore	Length	Diameter	E	Weight	M	Screws
90	230	194.5	89	67.2	26	8

Figure 1. Design of Assembly of tyre coupling.

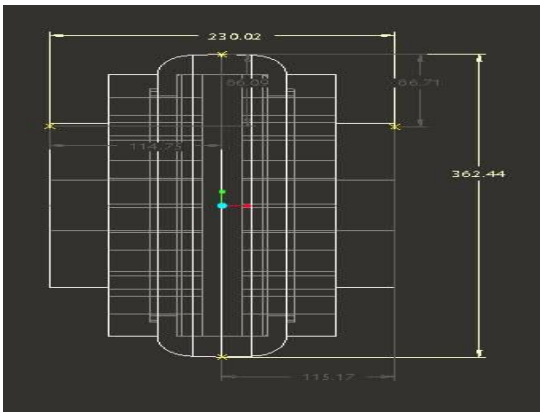

Figure 2. Two-dimensional model of tyre coupling.

5. MESHING AND TRANSIENT ANALYSIS

Finite element analyst and designers should be confident in the results of their analyses before sending a product to prototype or production. For that, it is mandatory to minimize errors in numerical solution. Among all the error discretization error is the major type of error because it greatly affects simulation results. In order to carry out structural analysis, finite element discretization method is

used to completely discretise physical domain. Simulation is conducted on unstructured mesh by using tetrahedron mesh elements to reduce discretization error. Patch conforming algorithm is used to refine mesh at critical points and to obtained high orthogonal mesh quality. Good orthogonal quality is achieved for getting accurate solution.

Finite element method uses numerical method to solve stiffness-displacement equations for every element iteratively. Newton-Raphson method is used to solve structural equations. For the simulation is tyre coupling is selected of which have rotational speed of 1800 rpm and the nominal torque values of 1881 Nm respectively. The maximum allowable misalignment cannot exceed 6 mm in parallel for this particular design. Transient structural analysis of tyre coupling is carried out in ANSYS 12.0 structural code. Material for flange and tyre are Grey Cast Iron Neoprene respectively. Since function of coupling is to transmit power by connecting two shafts, therefore, it is also designed like shaft. In order to conduct structural analysis, one end of coupling is fixed and moment is applied on other end then various parameters are determined. Moment is applied non-linearly with increasing time steps which is shown in Figure 3.

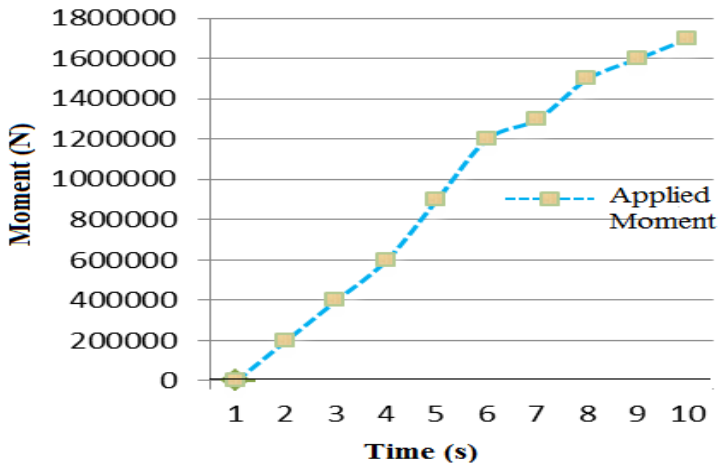

Figure 3. Applied moment variation

6. MODEL ANALYSIS

As coupling is highly important component of rotating system because its failure causes disaster of the system. There are several ways which can become cause of coupling failure such as excessive loading, misalignment, unbalance in system component and resonance. Therefore, coupling should be designed to withstand all these failure conditions. In this research, dynamic structural analysis is conducted to analyse structural integrity. As on structural analysis is not enough for safe, efficient and durable design of tyre coupling, therefore modal analysis is conducted to analyse effect of material damping, rotational speed as well as design of tyre coupling in order to resonance. Through modal analysis system mode shapes, natural frequencies, as well as the actual vibration response under this frequency range, can be predicted. Determination of natural frequencies is helpful to operate system at safer external frequencies to occurrence of resonance. The results from modal analysis can be used as reference value for other dynamic analysis like random analysis, harmonic analysis, etc. It is

analysed with different mode frequencies to prevent it from failure resulted by elastic strain. Hence the deformation and misalignment of the shaft is easily calculated. The following frequency input is given to the model:

6. RESULT AND DISCUSSIONS

Transient structural analysis of tyre coupling is carried out in ANSYS 12.0 structural code for flange and tyre are made up of grey cast iron and neoprene. The variation of maximum principal stresses incurred on tyre coupling is illustrated on Figure 4 whereas variation maximum shear stresses are demonstrated on Figure 5. The deformation in tyre coupling caused by applied load is illustrated on Figure 6 and its corresponding variation with time is shown in Figure 7. The von-Mises criteria of tyre coupling are illustrated on Figure 8 and 10 and variation in different stresses with time span are shown in Figure 9. The variation of tyre coupling frequency with span of time is illustrated on Figure 11.

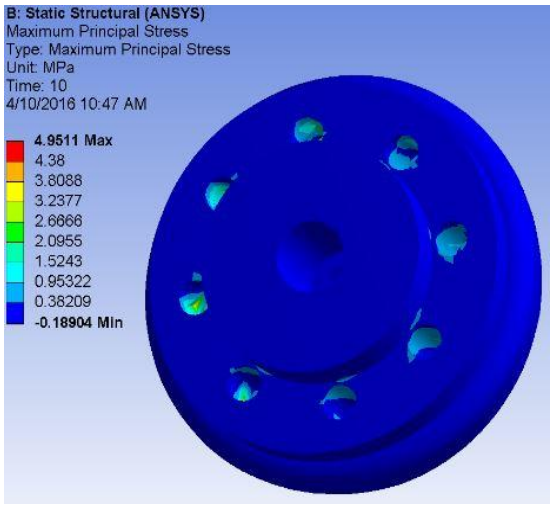

Figure 4. Principal stresses in tyre coupling

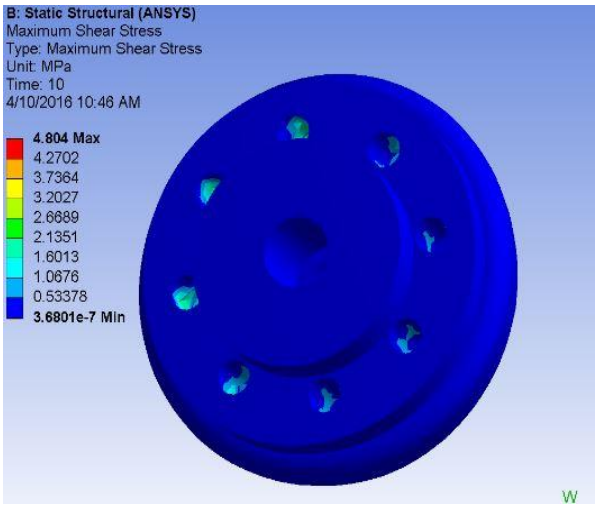

Figure 5. Shear stress variation

Fig. 4 exhibits the stress distribution in various sections of tyre coupling. In correspondence with maximum principal stress theory which holds for the brittle materials only where the grey cast iron behaves more or less likely brittle material. The theory states that the material will fail if principal stresses exceed the ultimate compressive and tensile stresses. In the light of this tyre coupling is subjected to 4.9511 MPa, which is very low as compared to maximum stress values hence it will remain safe for these specifications.

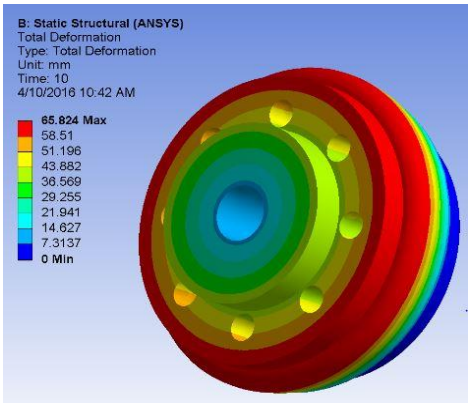

Figure 6. Deformation results in tyre coupling

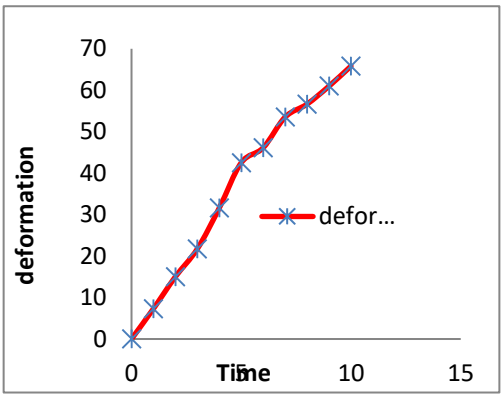

Figure 7. Variation in deformation V/s time.

Figure 5 shows the maximum shear stresses acting on coupling. According to the maximum shear stress theory criterion, a given structural Component is safe as long as the maximum value of the shearing stress in that component remains smaller than the corresponding value of the shearing stress. Therefore, it is clear in from analysis that tyre coupling is subjected to very shear stress as compared to maximum shearing stress of material, therefore, it remains safe.

Finite element analyses of tyre coupling results are shown in Figure 7 exhibits the deformation is caused by an applied load. In order to make conclusion about structure integrity St. Venants criteria is applied. Saint Venant's criterion states that structural component will remain safe as long as deformation or strain in that component will remain smaller than the ultimate strain at which tensile test specimen of the material might fail. The maximum deformation that the above test specimen can undergo is 65.82 mm which is quite less than the ultimate strain. Hence material will sustain the above load.

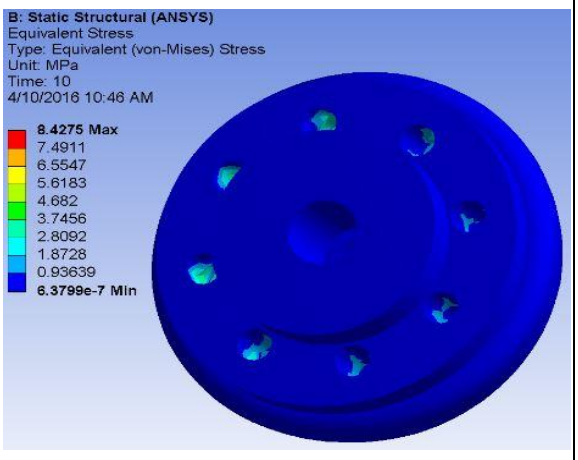

Fig 8. Analysis of equivalent stress occurs in tyre coupling.

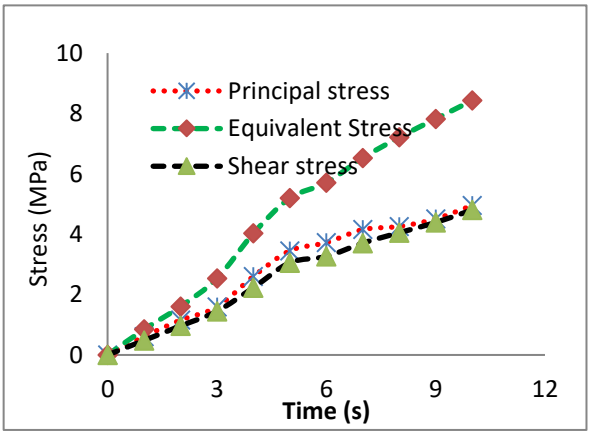

Figure 9. Variation in stresses against time.

Figure 8 shows the equivalent stresses acting on tyre coupling. From the values of stresses shown in figure indicate that given structural component is safe as long as the maximum value of the distortion energy per unit volume in above material remains smaller than the distortion energy per unit volume required causing yield in a tensile test specimen of the material. The distortion energy per unit volume in an isotropic material under plane stress corresponds to the principal stresses that are produced and are negligible comparatively the ultimate strength. It is shown in Figure 9 that the different types of stresses with the span of time increases as applied moment increases.

From the simulation, von-Mises, stresses are calculated in modal analysis which shows that with increase in operating frequencies the stress will increases proportionally. At the given mode frequencies, the induced stresses won't cause any failure as the maximum stress-bearing capacity of the material is very high.

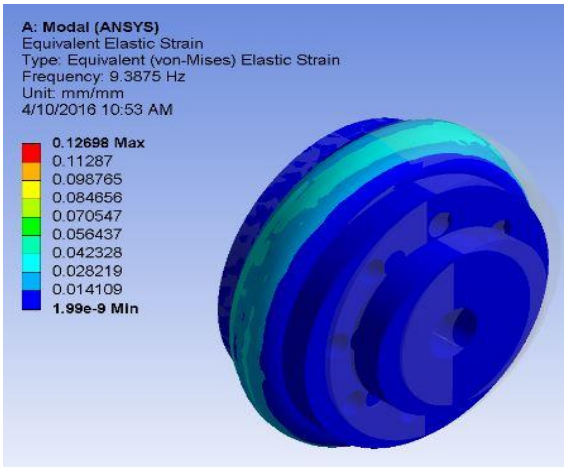

Fig 10. Analysis of elastic strain of tyre coupling.

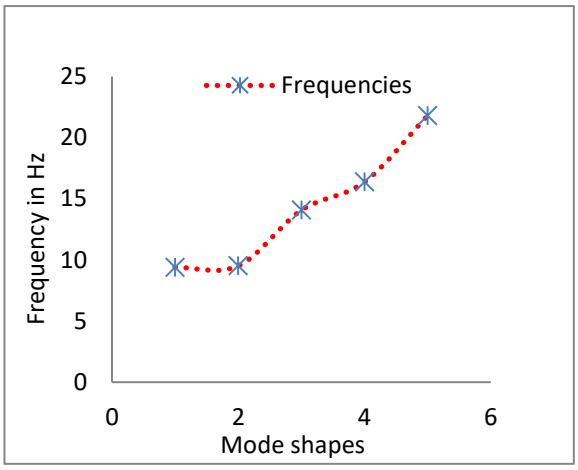

Fig 11. Effects of mode shapes on frequency.

In modal analysis, the input of moment is applied at the number of discrete frequencies over the range of our frequency interest. As the structure is excited its response will exhibit sharp peak at resonance frequency that is the input frequency. Meanwhile, the induced vibration will cause misalignment of shaft and the maximum misalignment turns out to be 0.12 mm under the above mode frequency.

In the Finite element modal analysis, tyre coupling is exposed to range of frequencies that induces stresses far less than the ultimate stresses. Moreover, total deformation obtained at the one mode frequency is 0.12 mm, whereas this type of coupling will operate nominally till 6 mm deformation. In order to prevent failures, the operating frequencies must not coincide with the input frequencies. However, the higher mode frequencies will prove to be critical as it can distort to the maximum strain of the coupling.

CONCLUSION

The realistic tyre coupling model is presented and simulated in this study. The tyre between two flanges has been analysed while transmitting the torque and power. This study is conducted for transient loading to analyse structural as well as vibration behaviour of the tyre coupling in specific

for Neoprene material. Dynamic analysis of tyre coupling reveals that the considered tyre coupling design is safe from strength and vibration point of view. Because it is found that very small amount of stresses developed and natural frequencies are far away from external exciting frequencies. But the existing design and used material have very large deformation which became major cause of fatigue failure. It is also concluded that there is enough potential of weight reduction is available in existing design of coupling which increase system performance.

ACKNOWLEDGMENT

This research work is jointly supported by Department of Mechanical Engineering, Humdard University, Karachi, Pakistan and Department of Mechanical Engineering, Mehran University of Engineering and Technology Shaheed Zulfiqar Ali Bhutto Campus, Khairpur Mir's, Pakistan.

REFERENCES

Bossio, J. M., Bossio, G. R., & De Angelo, C. H. (2009). *Angular misalignment in induction motors with flexible coupling.* Paper presented at the Industrial Electronics, 2009. IECON'09. 35th Annual Conference of IEEE.

Johnson, C. M. (1996). An introduction to flexible couplings. *World Pumps, 1996*(363), 38-43. doi: 10.1016/S0262-1762(99)81001-3

McGinnity, M., & Mancuso, J. (2005). New pump coupling reduces effects of torque, misalignment and unbalance. *World Pumps, 2005*(464), 34-37. doi: 10.1016/s0262-1762(05)70584-8

Nagesh, S., Basha, A. J., & Singh, T. D. (2015). Dynamic performance analysis of high-speed flexible coupling of gas turbine engine transmission system. *Journal of Mechanical Science and Technology, 29*(1), 173-179.

Patel, N. R., Oza, H. H., Gohel, M. V., Parmar, A. B., & Kadivar, J. V. (2014). Prevention of failure within the working range and enabling a design of automatic flexible cushion coupling *International Journal of Engineering Science and Innovative Technology (IJESIT), 3*(1), 485-493.

Pathan, S., & Khaire, P. (2014). Experimental study to identify the effect of type coupling on unbalance using frequency spectrum analysis *IOSR Journal of Mechanical and Civil Engineering, 11*(3), 13-16.

Sekhar, A. S., & Prabhu, B. S. (1995). Effects of coupling misalignment on vibrations of rotating machinery. *Journal of Sound and Vibration, 185*(4), 655-671.

Veale, K. L., & Roberts, L. W. (2011). *Efficiency management within an industrial environment*. Paper presented at the Industrial Engineering and Engineering Management (IE&EM), 2011 IEEE 18Th International Conference on 3-5 Sept. 2011.

Vibration control, S. s. i. s. (2015). http://www.easyflex.in/

Xu, M., & Marangoni, R. (1994). Vibration analysis of a motor-flexible coupling-rotor system subject to misalignment and unbalance, Part I: theoretical model and analysis. *Journal of Sound and Vibration, 176*(5), 663-679.

AUSTRALIAN JOURNAL OF ENGINEERING AND TECHNOLOGY RESEARCH (AJETR)
Vol. 2, Issue 1 - 2017

DETERMINATION OF TECHNICALLY FEASIBLE DEVELOPMENT STRATEGY TO PRODUCE UNCONVENTIONAL TIGHT GAS SAND RESERVOIR

Temoor Muther
Mehran UET Jamshoro, Pakistan

Naveed Ahmed Ghirano
Mehran UET Jamshoro, Pakistan

Saleem Qadir Tunio
Dawood UET Karachi, Pakistan

Asadullah Memon
Mehran UET SZAB Campus Khairpur Mirs', Pakistan

Abdul Haque Tunio
Mehran UET Jamshoro, Pakistan

ABSTRACT:

Exploitation of unconventional resources is changing the global energy landscape day by day. The depletion of conventional resources and high oil and gas demands have shifted the attention towards such resources. Their development is also very challenging. However, advancement in technologies such as hydraulic fracturing and horizontal drilling boost up the exploitation tendency of these invincible assets.

This paper deals with the determination of technically feasible development strategies in unconventional tight gas sand reservoir. Tight reservoirs have been characterized by low porosity and low permeability. Hence, a single-porosity simulation model of tight gas sand reservoir has been developed which describes the behavior of gas flow in small pores of the reservoir.

Various development strategies can be employed for tight gas reservoirs. The selection of best strategy involves the technical and economic feasibility of reservoir. The strategies include Vertical well, Horizontal well, Vertical well with hydraulic fracture and Horizontal well with hydraulic fractures. Sensitivity analysis has been carried out by considering all these wells separately in the base model and their effects on average reservoir pressure, production rate, and cumulative production have been identified. This study is concluded by a recovery factor comparison chart which analyses these strategies and a best selection is made. This study will serve as a prototype to select best and feasible development technology in various basins having tight gas formation.

Keywords: Tight gas, Development Strategies, Production Optimization

1. INTRODUCTION:

A reservoir is termed as tight if it has low matrix permeability about 0.1 md or less and a matrix porosity of about 10 percent. A tight gas reservoir contains gas in its small pores. They have low productivity as compared to conventional reservoirs. According to Tight Gas Policy-2011, Pakistan, it is defined as a reservoir with natural gas that has an effective permeability of less than 1.0 md (clause-

5). From a study conducted, the proven tight gas reserves in various basins and horizons of Pakistan comes under the range of 24 - 40 TCF. Sui Upper Limestone, Pirkoh Limestone, Habib Rahi Limestone, Sembar Sands & Siltstones and Lower Goru Tight Sands are important candidates of TGR in Pakistan.

There have been a lot of technologies introduced to enhance the productivity of Tight Gas Reservoirs. The economic development of Tight Gas Reservoirs requires proper designing and handling of both the reservoir and the wellbore.

2. MODEL DESCRIPTION:

The unconventional tight reservoir in this study has an average permeability of around 0.00363 md with 6% of porosity. The kv/kh ratio is assumed to be 0.1. The reservoir has no natural fractures, therefore, a single porosity simulation model is used in this study to quantify the flow the behavior in the small pores of tight sand. For base case, a vertical well is installed with the simulated reservoir (Fig. 1). The well is perforated in 2nd layer of simulated reservoir.

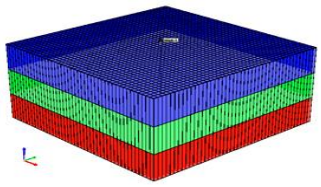

Figure 1: Simulation model with vertical well (Base Case)

3. DEVELOPMENT OF TIGHT GAS RESERVOIR:

Tight gas reservoir can be developed by four possible ways. The strategies include vertical well, vertical well with fracture, horizontal well, and multistage fractured horizontal well.

3.1. Vertical Well:

Since tight gas reservoir has low permeability, therefore, vertical well will not provide required production rate and it would not be economically justifiable for production. From Figure 2, it is evident that well is producing at a very low production rate which is not technically feasible for the company. The recovery factor is also very low as shown in Figure 3.

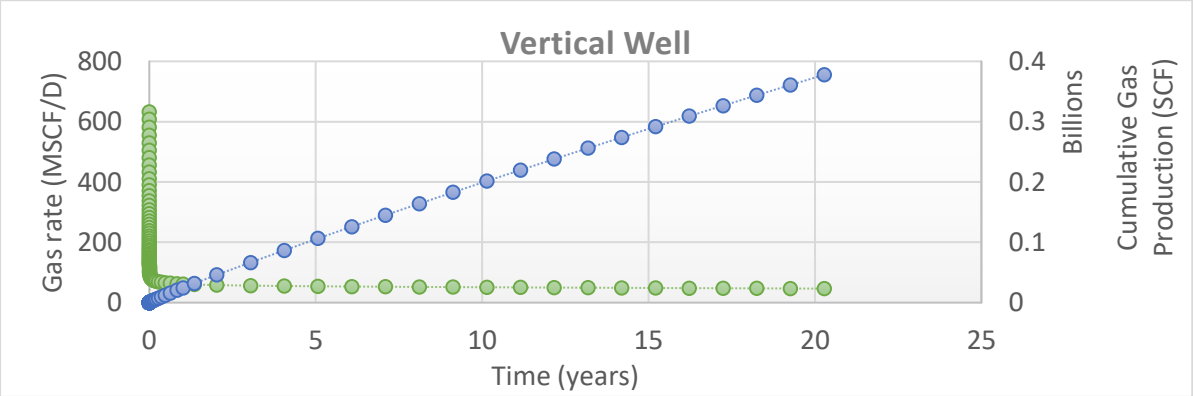

Figure 2: Production response of Vertical Well

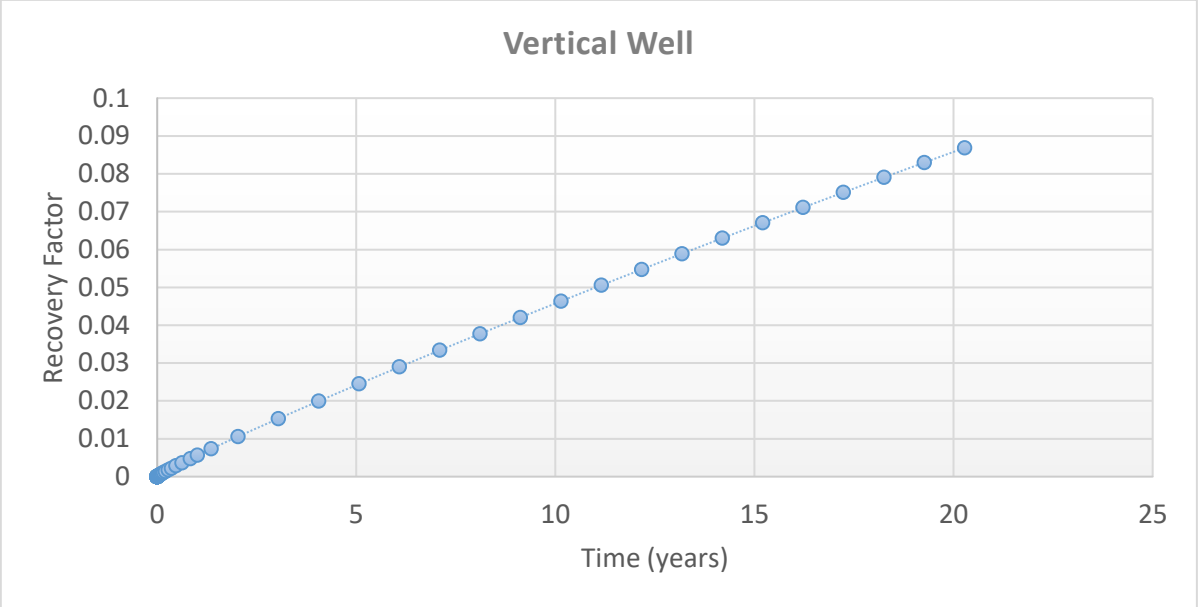

Figure 3: Recovery Factor of vertical well

Furthur, the pressure depletion is also low which results in less production of gas as shown in Fig. 4.

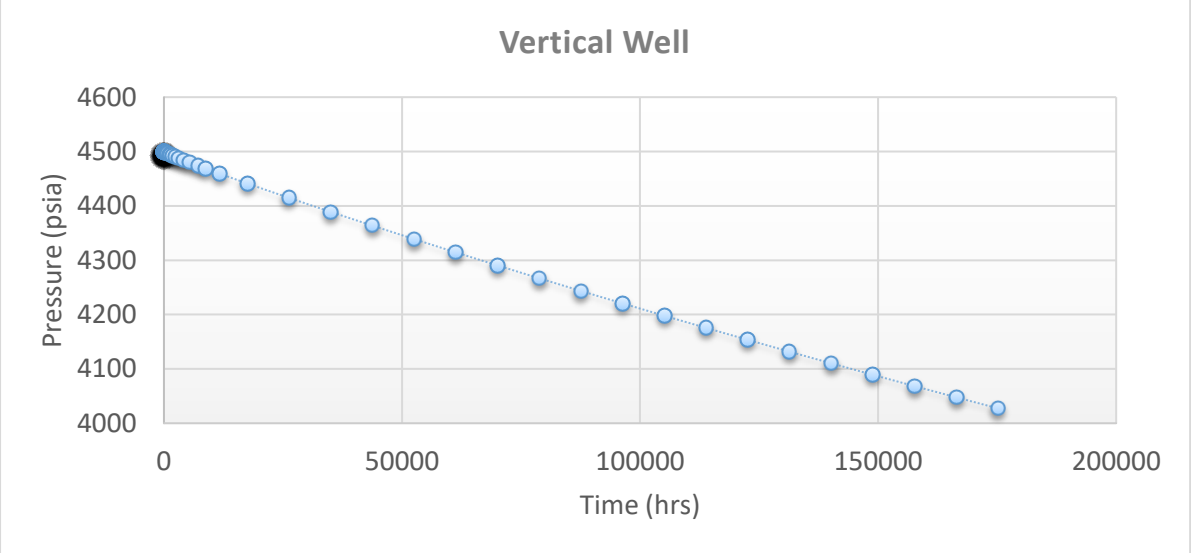

Figure 4: Pressure response up to 20 years

3.2. Vertical Well with Fracture:

The next strategy is to create a fracture perpendicular to vertical well. This would allow gas to flow more easily from reservoir to well as compared to vertical well. This will result in increased production (Fig. 5). Fracture half-length highly affect the production in this strategy. The fracture half-length, in this case, is 300 ft. The fracture is developed by introducing transmissibility multipliers and local grid refinement. This increased production results in increased recovery factor of gas as shown in Figure 6. Also, the pressure depletion is more than simple vertical well which causes more production as compared to vertical well. This depletion is shown in Figure 7.

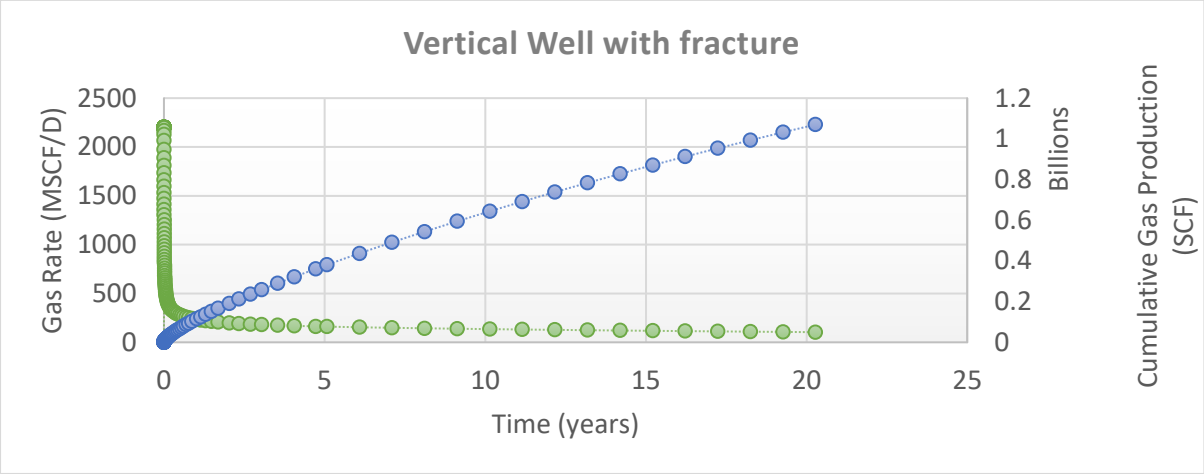

Figure 5: Production profile of Vertical Well with fracture upto 20 years.

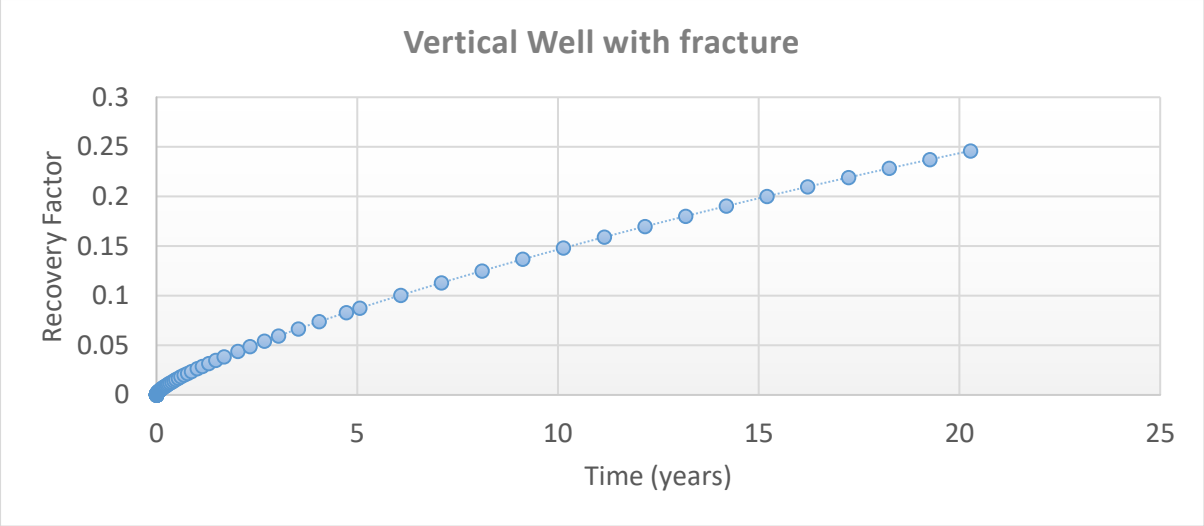

Figure 6: Recovery Factor of vertical well with fracture up to 20 years

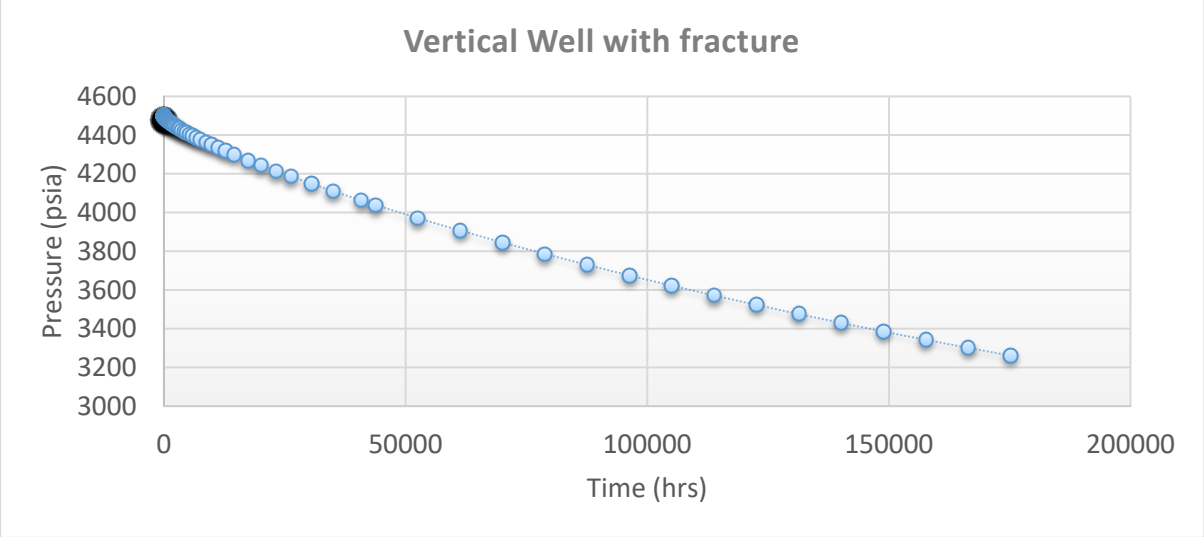

Figure 7: Pressure response up to 20 years (Vertical well with fracture)

3.3. Horizontal Well:

The horizontal well is drilled at an angle of 90^0 from the vertical well. It provides more exposure to reservoir area than the above techniques and hence greater production as evident from Figure 8 and Figure 9. Also, the pressure depletion is more than vertical and vertically fractured well (Figure 10).

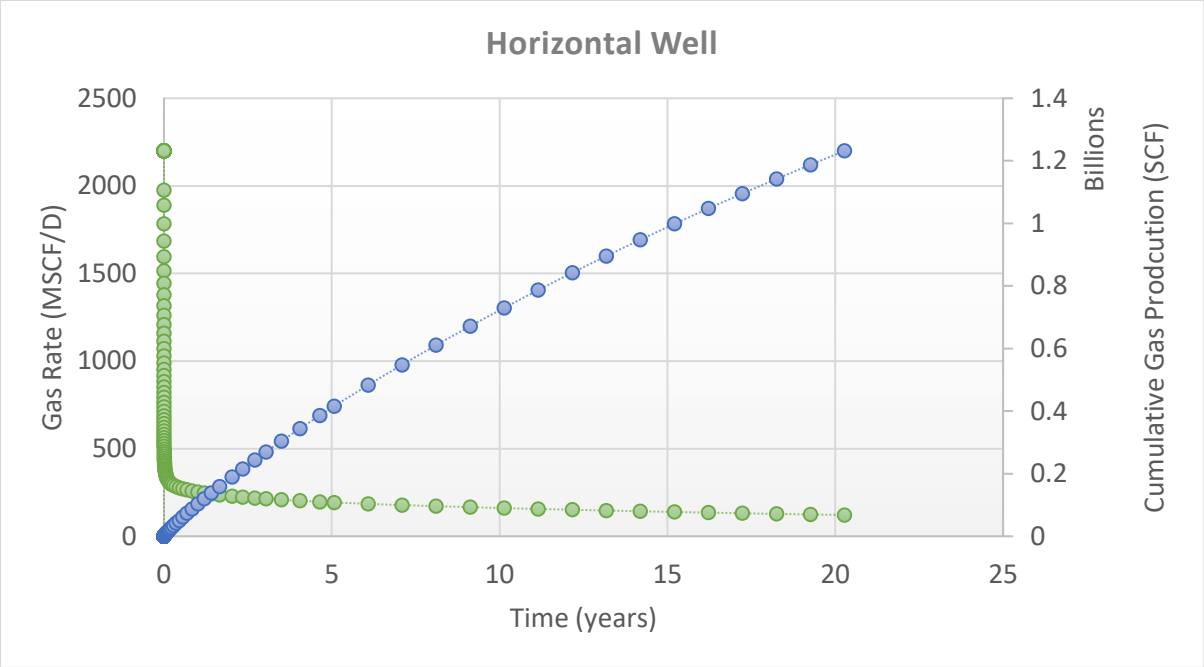

Figure 8: Production profile of 20 years of production (horizontal well)

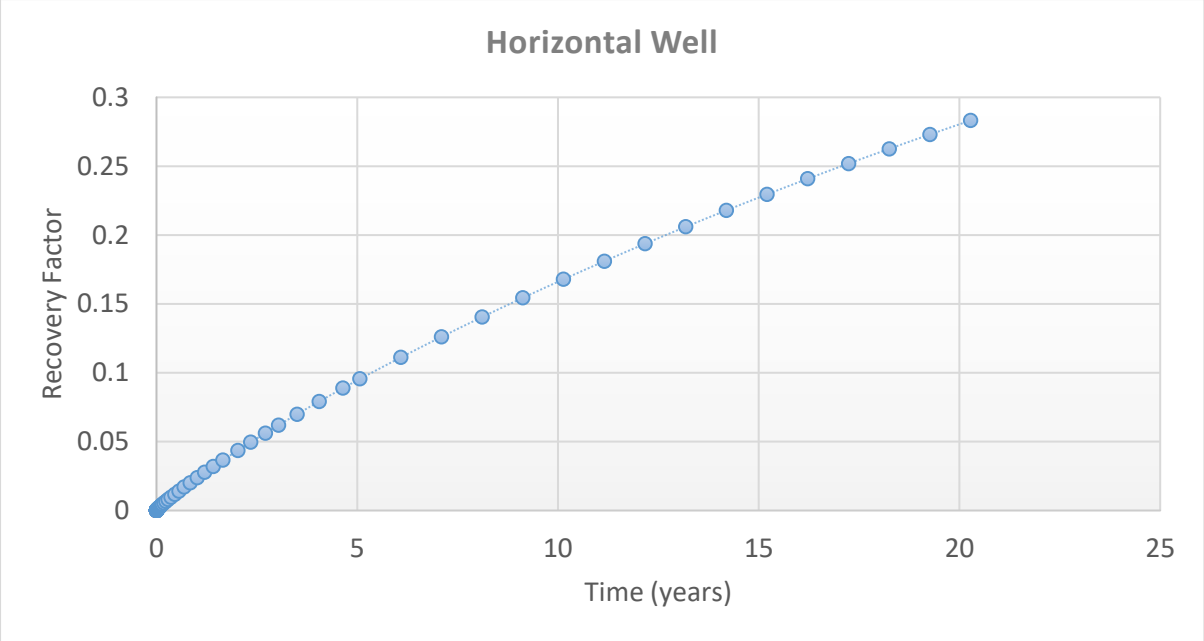

Figure 9: Recovery Factor of horizontal well up to 20 years

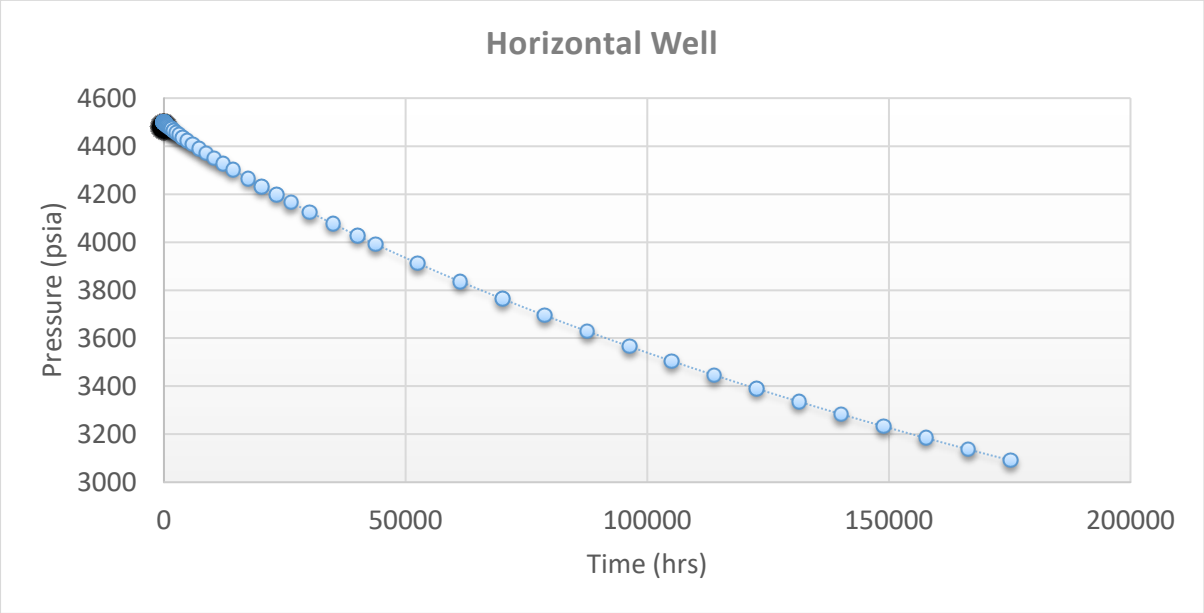

Figure 10: Pressure response up to 20 years (Horizontal Well)

3.4. Multi-stage hydraulically fractured Horizontal Well

In this strategy, horizontal well is drilled and fractures are created over the entire horizontal well. This simulated case consists of 1000 ft of horizontal well length with around 10 hydraulic fractures. This strategy not only have greater contact area with reservoir but also higher stimulated reservoir volume (SRV) because of fractures. This results in higher pressure depletion (Fig. 11), more gas production (Fig. 12) and higher gas recovery factors (Fig. 13).

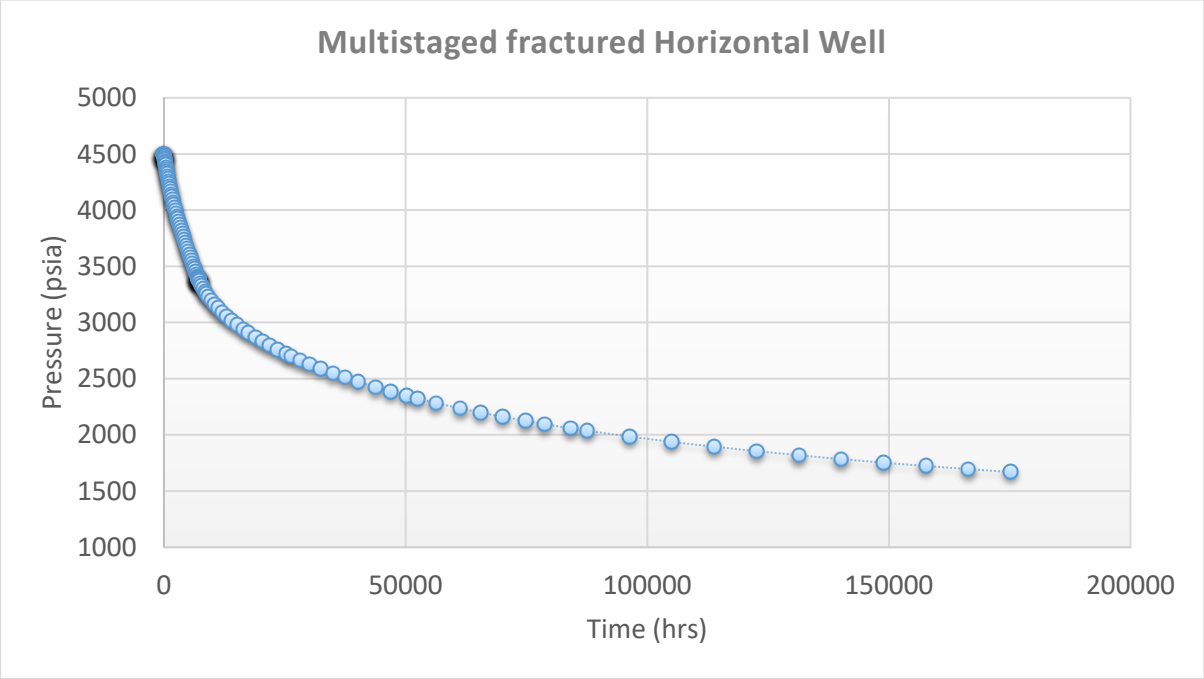

Figure 11: Pressure response up to 20 years (multi-stage hydraulically fractured horizontal well)

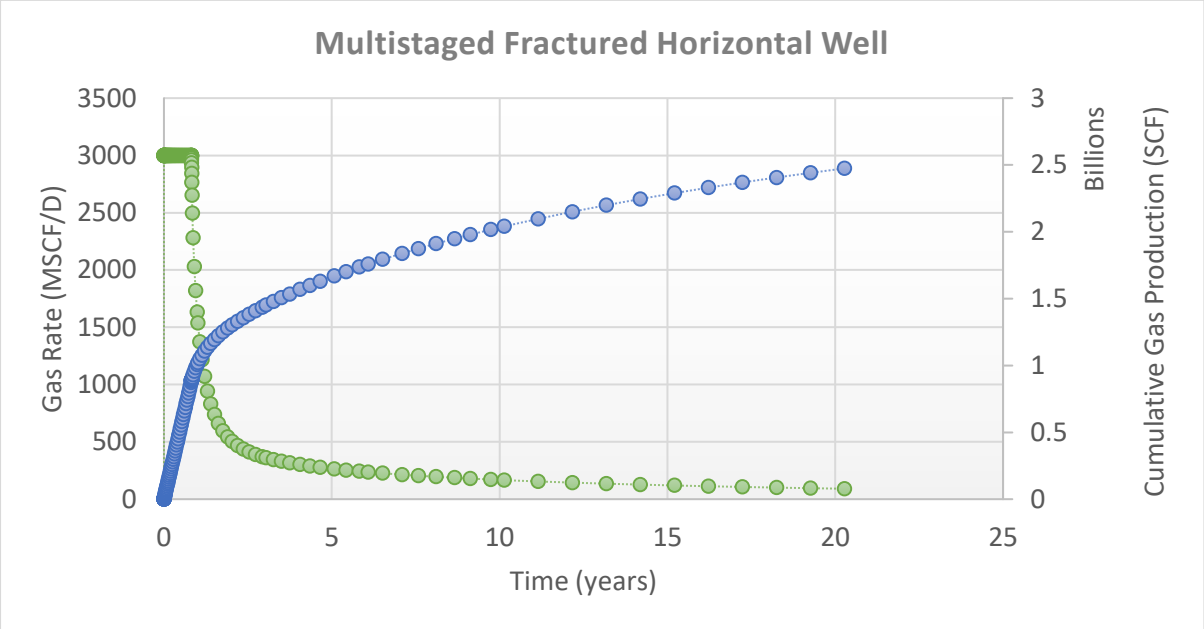

Figure 12: Production profile of 20 years of production (Multistaged hydraulically fractured horizontal well)

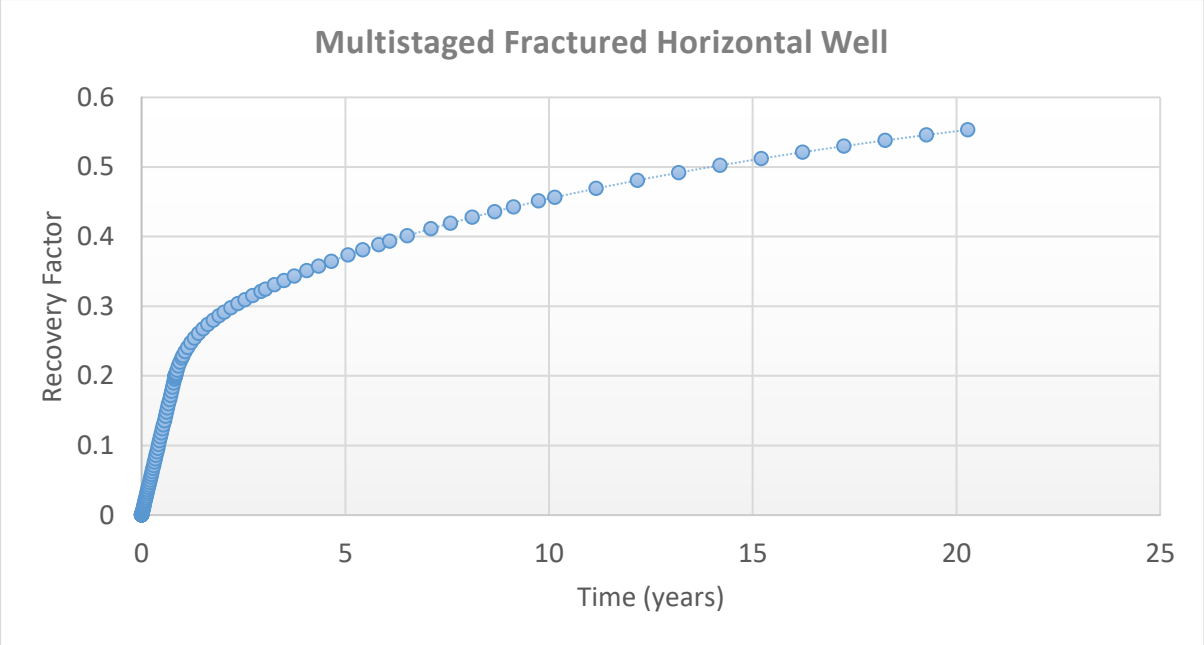

Figure 13: Recovery Factor of multistaged hydraulically fractured horizontal well up to 20 years

4. RESULTS AND DISCUSSION:

After analyzing Figure no: 2, 5, 8 and 12, it has been found that multistage hydraulically fractured horizontal well provides greater production rate and cumulative production as compared to other technologies. The production rate observed during 20 years of production of reservoir from multistage hydraulically fractured horizontal well is way much higher than other technologies. Also, the

cumulative production from such strategy is about 2.47 BSCF which is 6.67 times higher than reservoir base case. Figure 14 and figure 15 shows the comparison of production rates and gas cumulative production respectively of all the above four types of wells.

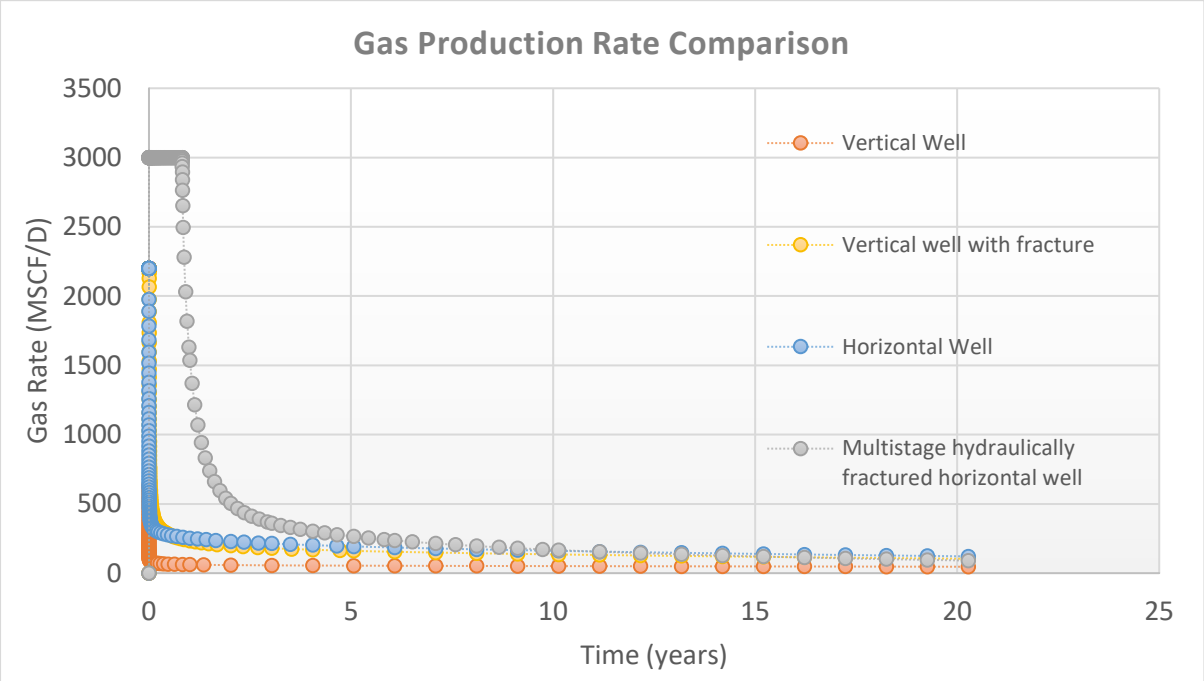

Figure 14: Production rate comparison up to 20 years of production.

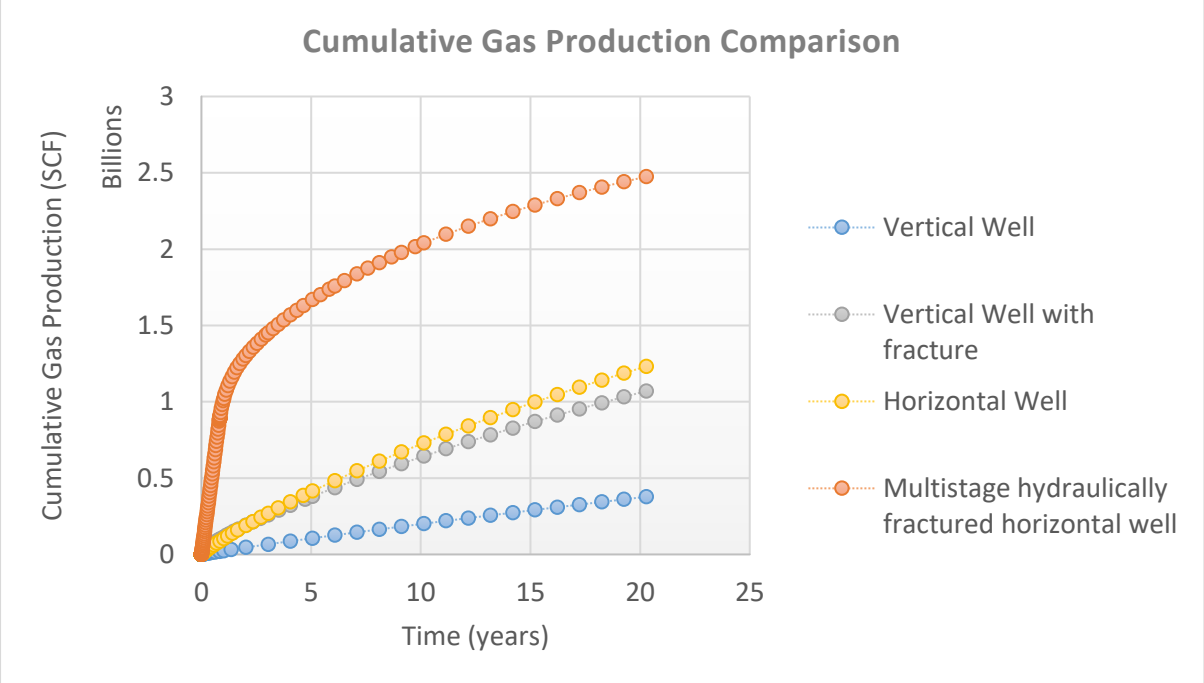

Figure 15: Gas Cumulative Production comparison up to 20 years of production.

It has been also found through the analysis of simulated reservoir that Gas Recovery Factor of multistage hydraulically fractured horizontal well is 55.34% while horizontal well, vertical well with fracture and vertical well has Recovery Factor of 28.32%, 24.59% and 8.6% resp. as shown in Figure 16. Hence, technically multistage hydraulically fractured horizontal well is the best candidate for tight gas reservoir. But, economic constraints must also be taken into consideration while selecting such wells. These percentages may vary depending upon the characteristics of reservoir.

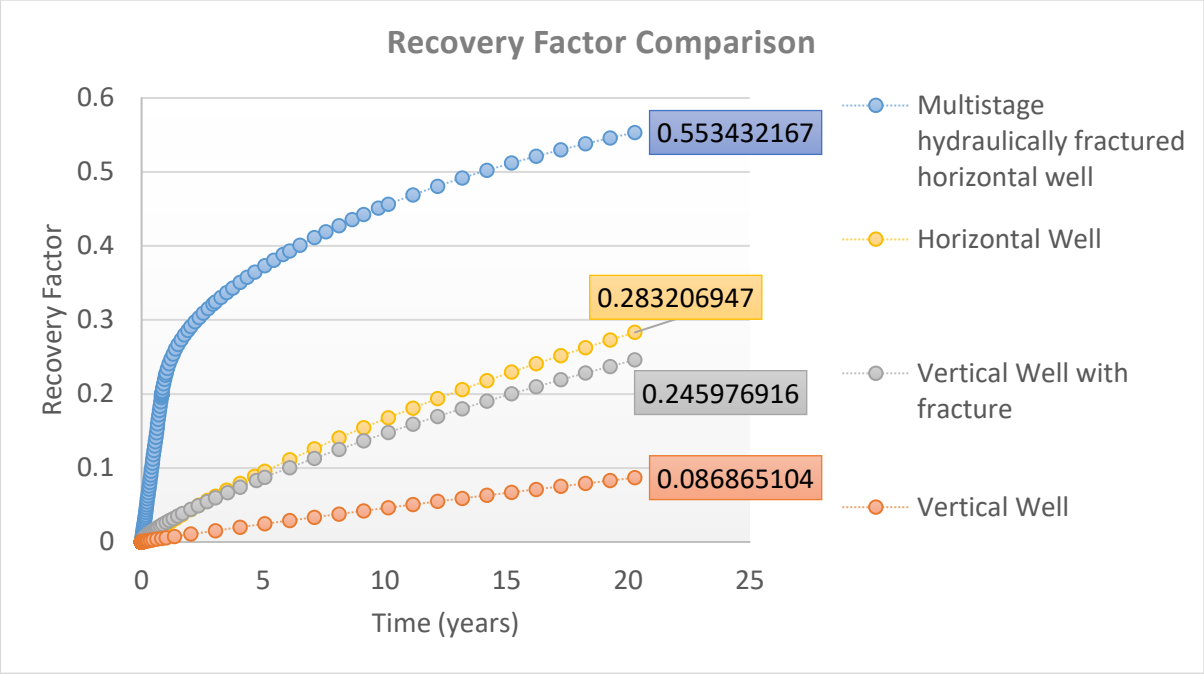

Figure 16: Gas Recovery Factor Plot

5. CONCLUSION

It is a known fact that large amount of hydrocarbons trapped in unconventional tight resources. However, their development is highly dependent on advanced production enhancement techniques and economics. This work focuses on the production obtained by different development strategies in a tight gas reservoir. It has been found in this study that higher production rates, cumulative production, and recovery rates can be observed with multi-staged hydraulically fractured horizontal well technically. Still, while selecting any well economic constraints must also be determined.

6. ACKNOWLEDGEMENT

We would like to express our gratitude to Mehran University of Engineering and Technology, Jamshoro and SZAB Campus Khairpur Mirs', for granting us the permission to publish this paper.

7. REFERENCES:

[1] KishoreKumar et al. (2017). *Optimization of Fracturing Technique for Successful Exploitation of Tight Gas Reservoirs of Mandapeta Field*. SPE-185421-MS.

[2] Mei Yang et al. (2016). *Integrated Hydraulic Fracture Design and Well Performance Analysis. Unconventional Oil and Gas Resources Handbook*. Pg. 361–386.

[3] Domingo Mata et al. (2016). *Hydraulic Fracture Treatment, Optimization, and Production Modeling. Unconventional Oil and Gas Resources Handbook*. Ch. 8, 215–242.

[4] Ghazanfer Raza Abbasi et al. (2016). Hydraulic Fracture Modelling Approaches in Numerical Simulation. International Journal of Chemical and Environmental Engineering Vol. 7, No. 2.

[5] Xinfang Ma and Xiaoying Li. (2015). *Parameters optimization of stimulated reservoir volume of fractured horizontal wells in tight gas reservoirs*. International Journal of Latest Research in Science and Technology Vol. 4, Issue 5, 2015, 136-140.

[6] Quanshu Li et al. (2015). *A review on hydraulic fracturing of unconventional reservoir*. Petroleum Volume 1, Issue 1, 2015, 8–15.

[7] Yu Didier Ding et al. (2014). *Numerical Simulation of Low Permeability Unconventional Gas Reservoirs*. SPE/EAGE European Unconventional Resources Conference and Exhibition, 25-27 February, Vienna, Austria. SPE 167711.

[8] J. Ostojic et al. (2012). *Production performance of hydraulic fractures in tight gas sands, a numerical simulation approach.* Journal of Petroleum Science and Engineering. Pg. 75-81.

[9] Shahab Alam. (2011). Potential of Tight Gas in Pakistan: Productive, Economic and Policy Aspects. Search and Discovery Article #80149.

[10] Dilhan Ilk et al. (2010). *Production Analysis and Well Performance Forecasting of Tight Gas and Shale Gas Wells*. SPE Eastern Regional Meeting, 13-15 October, West Virginia, USA. SPE-139118.

[11] Boyun Guo et al. (2007). *Petroleum Production Engineering, A Computer-Assisted Approach*. Pg. 252-265.

[12] S. Zahid et al. (2007). *Development of Unconventional Gas Resources: Stimulation Perspective*. SPE Production and Operations Symposium, Oklahoma, USA. SPE 107053.

AUSTRALIAN JOURNAL OF ENGINEERING AND TECHNOLOGY RESEARCH (AJETR)
Vol. 2, Issue 1 - 2017

SHAPE MEMORY EFFECT AND PERFORMANCE OF A NITINOL ENGINE

Vyavahare P.V
School of Mechanical and Building Sciences, VIT University Chennai, India

Karthikeyan C.P
School of Mechanical and Building Sciences, VIT University Chennai, India

ABSTRACT

This paper mainly focuses on the parameters that affect power output of Nitinol heat engine and phase transformation characteristics of Nitinol wire. In order to conduct this study, a two-pulley engine is fabricated and tested for power generation. Thermal parameters influencing the phase transformation of the Ni-Ti wire are determined. Results show that temperature of bath has a significant impact on power output. A mathematical model is developed for nitinol engines using the shape memory effect. Efficiency estimated using the model developed is compared with the Carnot efficiency. The comparative results of the efficiency were found to be inversely proportional to each other.

Keywords: Shape memory alloy, transformation temperature, phase transformation, austenite, martensite.

1. Introduction

Despite several deformations, shape memory alloys (SMA) can still remember their predetermined shape. SMA can be austenite, martensite or a mixture of them depending on the temperature. Normally nitinol transforms between the high temperature phase called B2 phase (also called as austenite - denoted by P) and the low temperature phase called B19 phase (also called as martensite, denoted by M). However due to thermal and mechanical effects such as thermal cycling, chemical composition, heat treatment, deformation may appear as an intermediate phase known as rhombohedral or R-phase (denoted by R) between the transformation of austenite to martensite which result in a two-stage transformation. Numerous elements can influence the transformation characteristics in NiTi-based shape memory alloy: variation in nickel content, after solution treatment aging, combined thermo-mechanical treatment, thermal cycling, doping with ternary alloying elements and processing techniques [1]. There are many factors which affect the power output of nitinol engine such as dimensions of the sink, diameter of nitinol wire, centre distance between two pulleys, number of turns of wire, bath temperature. Another factor of interest in the testing of the SMAs is heating/cooling rate which is impacted by heat transfer for a prolonged period, as observed in most of SMA's. Until now there are many publications which concentrate on the thermal and mechanical effects on the transformation behaviour of NiTi SMA [2]. However, the study of different parameters and transient study of SMA is still limited till date.

2. History of SMA

While conducting experiments with an alloy of gold (Au) and cadmium (Cd), an interesting phenomenon was discovered by Arne Olandder in 1932. When cooled, the Au-Cd alloy could be plastically deformed and then be heated to return to predetermined shape. This phenomenon is called the Shape Memory Effect (SME) and the alloys that show this behavior are called Shape Memory Alloys (SMA). At the Brussels World's fair, researchers Chang and Read demonstrated the Shape Memory Effect in 1958. By lifting a weight using an Au-Cd SMA, they showed that the SME could be used to perform mechanical work. After this, further research has been carried to determine other materials demonstrating the same phenomenon. In 1962, a group of U. S. Naval Ordnance Laboratory analysts, lead by William Beuhler, unearthed a huge revelation in the field of SME and SMA. An alloy of nickel and titanium was being tested for heat and corrosion resistance and they came to know that the alloy of nickel and titanium also exhibits SME phenomenon. The Ni-Ti SMA was found to have some advantages over already discovered alloys; they were significantly less expensive, easier to work with, and less dangerous (from health standpoint). These factors create interest and motivate others to research in the Shape Memory Effect and applications of shape memory effect [3].

2.1. Principle of Operation

Shape Memory alloys are the alloys of metallic materials which, when subjected to suitable thermal procedure, return to their original position. Au-Cd, Cu-Sn, Cu-Zn-(X), Cu- Al-Ni, In-Ti, Ni-Al, Ni-Ti, Fe-Pt, Mn-Cu, and Fe-Mn-Si are some examples of these alloys. Between the two different phases, called austenite and martensite, a temperature and stress based shift occurs in the material's crystalline structure and thus the shape memory effect (SME) is observed. Soft phase is called martensite phase while hard phase is called austenite phase. Following is a simple example to explain SME in action.

Consider the SMA in austenite phase. If it is cooled below its phase transition temperature, the crystalline structure will change to hard phase, i.e. the martensite phase. If bar is plastically deformed by any means, say bending, and heated above transition temperature then the bar will return to its original position due to phase transformation from martensite to austenite. Let us make this phenomenon simpler by a simplified two-dimensional representation of the material's crystalline arrangement, as shown in Figure 1. Every single box represents a grain of material with border representing grain boundary. Due to grains, a heavily twinned structure is formed; this means that the grains are oriented across grain boundaries in a symmetric order. The twinned structure permits the interior cross section of individual grains to change while keeping the same interface with contiguous grains. Therefore, Shape Memory Alloys are fit for encountering large macroscopic deformations while maintaining considerable order within their microscopic structure. For instance, if a bit of SMA begins as austenite [Figure 1a], the interior nuclear grid of every grain is cubic, making grains with pretty much right points.

If phase transformation temperature is reached by cooling action, the crystalline structure changes to martensite [Figure 1b] and the grains breakdown to the structures like jewels. Note that the grains are oriented in different directions for different layers. Presently, if adequate anxiety is connected, the martensitic structure shown in Figure 1b will begin to yield and "de-twin" as the grains re-situate, such that they are all balanced in the same direction [Figure 1c]. This conduct can be better comprehended by looking at a regular anxiety strain bend for the martensite stage [Figure 2].

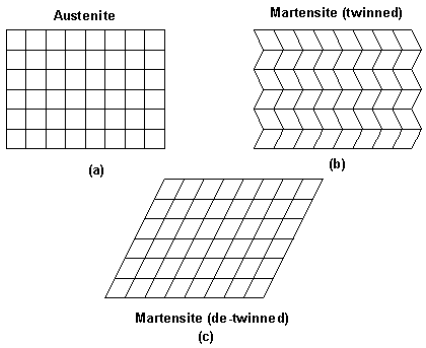

Figure 1. Material Crystalline Arrangement during the Shape Memory Effect

At first, for little hassles, the structure shown in Figure 1b acts flexibly from area 0 to 1. At position 1, the material yields and de-twinning happens somewhere around 1 and 2. At 2, the martensitic structure is totally de-twinned as shown in Figure 1c. In the blink of an eye, a second flexible area happens from 2 to 3. At 3, an enduring plastic distortion starts that is not recoverable by the SME.

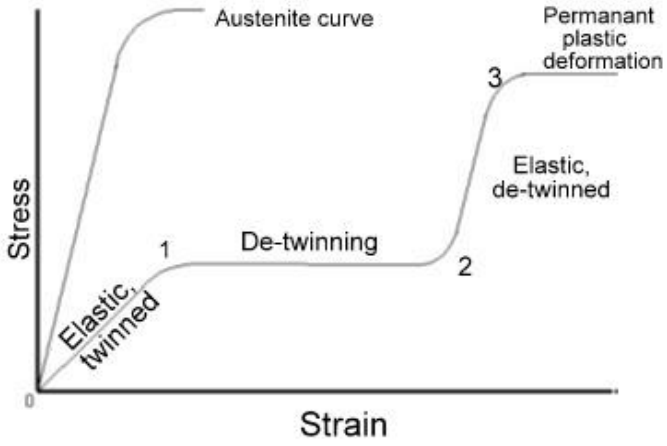

Figure 2. Stress -Strain Relationship of a Shape Memory Alloy

2.2. Nickel-titanium (Ni-Ti) shape memory alloy

Out of all the Shape Memory Alloys that have been developed so far, Nickel-Titanium (Ni-Ti) has proven to be the most beneficial and flexible in engineering applications. Some of the following characteristics of Ni-Ti make it better than the other SMA's: better ductility, recoverable motion is fast, excellent corrosion resistance (comparable to series 300 stainless steels), high biocompatibility, stable transformation temperature, and the ability to be electrically heated for shape recovery.

Ni-Ti SMA is the paired, equiatomic intermetallic compound of nickel and titanium. It is made up of approximately 50 atomic% Ni and 50 atomic% Ti. The valuable qualities of the intermetallic compound are moderate solvency range for overabundance Ni or Ti as well as for most other metallic elements, and ductility comparable to most ordinary alloys. The solvency permits Ni-Ti to be alloyed with different components which enables improvements in mechanical properties and stage change temperature (where stage change temperature is taken to mean AF). Adding additional Ni to the binary compound (up to 1% extra) strongly depresses the phase transformation temperature and increases the yield strength of the austenite. Iron and chromium can likewise be added to bring

down the transition temperature. By shifting these and different components, the change temperature can be fluctuated from –200 to 110°C *(*- 325 to 230°F). Copper can be used as an additive to decrease the hysteresis and lower the deformation stress (de-twinning stress) of the martensite. Table 1 shows the key physical properties of equiatomic Ni-Ti SMA.

Table 1 Properties and phase transfromation of Nitinol

Properties	Austenite	Martensite
Melting temperature, ° C	1300	
Density, g/cm^3	6..54	
Resistivity, Ω-cm	Approx. 100	Approx. 70
Thermal conductivity, W cm/^{o} C	18	8.5
Corrosion resistance	Similar to 300 series stainless steel or titanium alloys	
Young's Modulus, GPa	Approx. 83	Approx. 28
Yield strength, Mpa	195 to 690	70 to 140
Ultimate tensile strength, MPa	895	
Transformation temperature, ° C	-200 to 110	
Latent heat of transformation, ° C	167	
Shape memory strain	8.5% maximum	

2.3. Manufacturing and shaping of Nitinol

Manufacturing Nitinol SMA and shaping it for a specific purpose is very tough task. Inert atmosphere has to be maintained while melting Ti as it is a very reactive element. Plasma-arc melting, electron-beam melting, and vacuum induction melting are some of the common methods used during this process. Standard hot-forming and cold-working processes are used in order to initially shape the Ni-Ti ingots. During cold working, alloy must annealed frequently as it gets work harden very quickly. By minimizing the stress needed to de-twin the martensite and increasing the strength in the austenite phase, we can improve SMA's performance. For this, we can use processes like work hardening and heat treatment processes. Machining Ni-Ti through cutting methods is difficult, as is welding, soldering, and brazing. For creating specific shapes grinding, shearing, and punching are better methods. The "memory configuration" that is giving shape memory to SMA is done by holding the part in desired shape, and then heat-treating at 500 to 800°C (950 to 1450°F). Prefabricated SMA elements like wire, rod, ribbon, strip, sheet, and tubing are provided by companies like Dynalloy, Inc. and Shape Memory Applications, Inc. This companies also provides custom element to user specification.

3. Methodology

3.1 Modeling

Model consists of simply two pulleys. A nitinol wire of 0.5 mm diameter is run between two pulleys.

Two pulleys were made up of glass. Diameter of the bigger pulley is 70mm and diameter of the smaller pulley is 40mm. Center distance between the two pulleys can be varied by fixing adjustable bolt at different positions. Solidworks model of two pulley system helps to visualize the model and the challenges in fabrication.

3.2 Experimental setup

The engine [Figure 3a], generates power by using nitinol wire loop. The loop made of nitinol runs in between the two pulleys. Hot water on hot side and cool ambient air on cool side is used by this device in order to perform action. The smaller wheel of engine is partially dipped in a hot liquid. Memory given to the nitinol loop wire in engine is 'straight' shape. Whenever a part of loop gets in contact with a hot liquid, it gets heated above its transition temperature and tries to straighten out. Figure 3a explains the phenomenon. From Figure 3b, it is clear that at position 1, nitinol wire is straight and cool. As the wire travels from position 1 to position 2, it gets bent around the small glass pulley and comes in contact with hot liquid. As the wire moves from position 2 to position 3, it comes in contact with hot water and thus gets heated above its transition temperature due to which it tries to straighten out. As the wire tries to straighten out, it takes form the form shown by dotted line. While doing so, the wire exerts a tugging force of magnitude F along the loop. As the wire moves from position 3 to 4, it comes in contact with ambient air due to which its temperature decreases and, thus, austenite phase starts converting to martensite phase. As the wire moves from position 1 to position 4, it travels over the bigger pulley and a sufficient long time is available for the wire to cool below its transition temperature; the wire get ready for another cycle. In simple words, one side of loop stiffens due to high temperature while the other side i.e. air side of loop, cools and relaxes. A wheel pulley rotates due to mechanical force. Sometimes it becomes necessary to jump start the engine by giving rotation to the bigger pulley manually. Interestingly, the engine hasn't a set rotational direction. Whichever way it is started it will continue to rotate. The engine can also be powered by using solar energy. A magnifying lens focusing sunlight on the smaller glass wheel also supplies sufficient temperature gradient to power the engine.

(a)

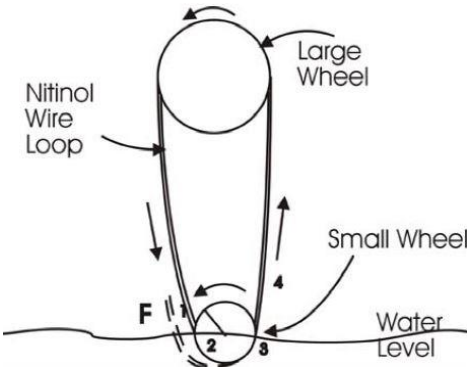

(b)

Figure 3. Working principle of nitinol engine

3.3 Experiments performed

Aim of this experiment is to find out variation of speed of nitinol engine with respect to decrease in temperature of bath. Water is takeen as a heating fluid as it is easily available and it has many advantages over other fluids as heating source. Water is heated to 90 degrees Celsius with help of conventional heating process and then the heating source is removed. Water is then poured in a flask and nitinol engine is placed over the flask. The temperature on cool side is room temperate which was found to be 32 degrees Celsius during the experiment.
As explained in working principle in the above section, the engine starts rotating. Speed of engine is measured with the help of laser tachometer. Figure 4 shows the laser tachometer used for measuring speed of nitinol engine in RPM. As the time passes, temperature of water bath goes on decreasing due to heat loss to surrounding. Variation in speed of the engine is measured with the help of laser tachometer.

Figure 4. Laser tachometer

4. Results and Discussion

4.1. Transient analysis: -

Table 2 shows the variation of speed of engine with respect to decrease in temperate of water bath. Figure 5 shows the output of these results in graphical form. From Table 2 and the aforementioned graph we can conclude that,

- Engine does not start unless temperature of bath reaches 45 degrees Celsius
- From 45 to 75-degree Celsius speed goes on increasing with the bath temperature
- After 75-degree Celsius, speed remains constant irrespective of increase in temperature of bath

Table 2 (a) and (b) Variation of speed with temperature of bath

(a)

S. No	Temperature (degree Celsius)	RPM
1	90	180
2	87	180
3	84	180
4	81	180
5	78	180
6	75	157
7	72	129

8	69	110
9	66	100

(b)

S. No	Temperature (degree Celsius)	RPM
10	63	93
11	60	86
12	57	82
13	54	80
14	51	75
15	48	75
16	45	72
17	42	0
18	40	0

Figure 5. Graph of temperature Vs speed

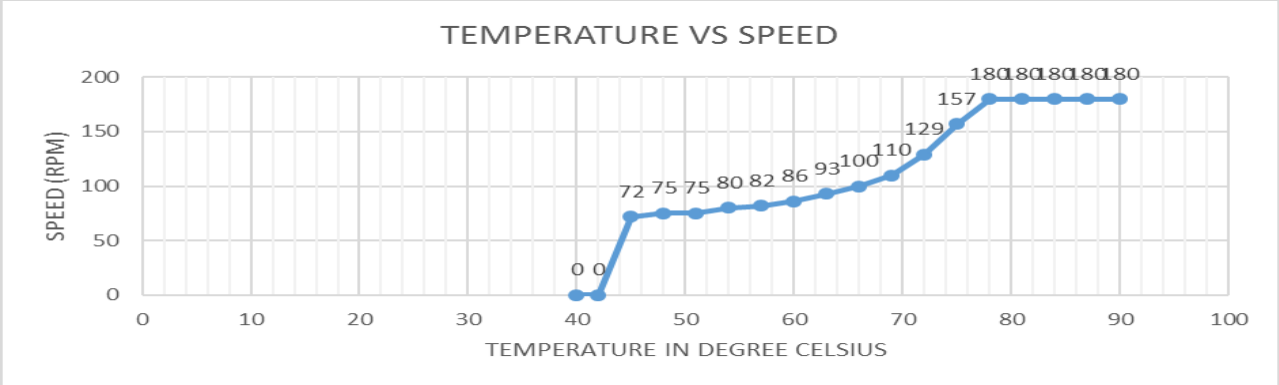

5. Mathematical model for finding efficiency

NITINOL engine is fed by the heat energy of LP water by means of heat transfer at the boundary of Wire – LP water. Let us consider this process similar to heat transfer of metal surface at the boundary with the moving water. Then, the intensity of the flow of heat transfer will be equal to: [21]

$$W= (\sigma_0 + \sigma_1\sqrt{v}\ )\ S_W\ \Delta T \qquad \text{Watt} \tag{1}$$

Where, V is the velocity of heated section of NITINOL engine with the length of l_w relative to water, $\Delta T=T_{warm} - T_{cool}$ is the temperature gradient (thermal head) – the difference between the temperatures of LP water, T_{warm} (hot) and T_{cool} (cold) water, and σ_0 ,σ_1 are the coefficients of heat transfer equal to [21]

$$\sigma_0=350\ W/m^2k\ ,\ \sigma_1=2100\ (W/m^2k).(s/m)^{1/2} \tag{2}$$

The contact surface Sw of wire with LP water for engine is determined by,

$$S_W=n2\pi r_0 w=1*2\pi*0.5*10^{-3}*0.37= 1.16238*10^{-3}\ mm^2 \tag{3}$$

Where r_0 = radius of nitinol wire which is 0.5 mm in our case

And l_w = length of nitinol wire running between two pulleys =370 mm in our case

Apparently, W is the sum of two summands:

$$W= W_Q+W_A \quad (4)$$

Where, WQ is a part of W consumed continuously for heating of wire at inverse martensitic transition M→A, and WA is a part of W at the expense of which engine develops the power.

Q is the quantity of heat transferred to wire for specific time at operating conditions, necessary for M→A transition

$$Q=M.C_P.\Delta T \quad \text{Watt} \quad (5)$$

The value C_P is the average value of the product of specific heat capacity of nitinol C, from the experiment, it is known that in the case of nitinol [21]

Where ,

$$C_P=5.2*106 \text{ J/m}^3\text{k} \quad (6)$$

And M= mass flow rate of wire through fluid (m^3/s)

$$M=\pi r^2_0 V \quad (7)$$

By definition, the thermal efficiency is the relation between the work and the quantity of heat received by engine at heating, i.e.

$$\eta=W_A/Q \quad (8)$$

Here W_A is considered instead of W because only W_A is a part of work developed by engine while other part i.e. W_Q is absorbed by engine

Hence,

$$W_A= W/2 \quad (9)$$

Now, let us find thermal efficiency of engine according to Carnot, for comparing Carnot efficiency of engine with actual efficiency consider the readings obtained while performing experiment of temperature vs. speed.

At 90 degrees' Celsius temperature of water, speed given by NITINOL engine was N=180 RPM

According to Carnot, efficiency is determined as

$$\eta_K =1- (T_{cool} / T_{Warm}) \quad (10)$$

In this case, T_{COOL} = Temperature of cool air (i.e. room temperature) = 305 K T_{WARM}= Temperature of hot water = 363 K.

Putting this values in Eq(10), we get

(11)

$$\eta_k = 0.1597 = 15.97\%$$

Now for finding actual efficiency of engine we will make use of Eq (8),

Putting values of Eq(2) and Eq(3) in Eq(1) and substituting ΔT=363-305=58 k, we get

$$W=(350+2100^*)*1.16238*10\text{-}3*58 \quad (12)$$

$$0\text{Now } V= (\Pi DN/60) \quad (13)$$

Where D= diameter of rotating wheel = 70 mm

$$V = \frac{\pi * 0.07 * 180}{60}$$

$$V= 0.6597 \text{ m/sec} \quad (14)$$

Putting Eq (14) in Eq (12), we get,

$$W= 138.58 \text{ W} \quad (15)$$

From Eq (9)

$$W_A= \frac{138.58}{2} = 69.29 \text{ W} \quad (16)$$

Now from Eq (5),(6) AND (7),

$$Q=M.C_P.\Delta T$$

$$Q=\pi*(0.5*10^{-3})^2*0.6597*5.2*10^6*58$$

$$Q=156.2753 \text{ W} \quad (17)$$

Putting Eq (16) and Eq (17) in Eq (8), we get

$$\eta = \frac{69.29}{156.27} = 0.4433 = 44.33\% \quad (18)$$

We can compare the Carnot and actual efficiency of nitinol engine now by using Eq (11) and Eq (18); actual efficiency of nitinol engine is greater than Carnot efficiency. This happens because nitinol engine does not require any work output for its operation like Carnot cycle requires. Thus, it is not limited to Carnot efficiency. However, Carnot efficiency of each case is obtained just for comparison with other engine working on Carnot cycle.

For different cases, comparison between actual and Carnot efficiency is tabulated in Table 3.

The tabulated results are represented by graph in Figure 5.

Table 3. Efficiency calculation

Sr. no	T_{cool} (K)	T_{warm} (K)	ΔT (K)	V_{rel} (m/s)	W (w)	W_A (w)	Q (w)	η_k	η
1	305	363	58	0.6597	138.59	69.29	156.27	0.1597	0.4434
2	305	360	55	0.6597	131.42	65.71	148.19	0.1527	0.4434
3	305	357	52	0.6597	124.25	62.12	140.10	0.1456	0.4434
4	305	354	49	0.6597	117.08	58.54	132.02	0.1384	0.4434
5	305	351	46	0.6597	109.91	54.95	123.94	0.1310	0.4434
6	305	348	43	0.5754	97.11	48.55	101.05	0.1235	0.4805
7	305	354	49	0.4728	102.18	51.09	94.61	0.1384	0.5399
8	305	342	37	0.4030	72.39	36.19	60.91	0.1081	0.5942
9	305	339	34	0.3665	64.08	32.04	50.90	0.1002	0.6294
10	305	336	31	0.3408	56.79	28.39	43.15	0.0922	0.6570
11	305	333	28	0.3151	49.76	24.88	36.03	0.0840	0.6904
12	305	330	25	0.3000	43.63	21.81	30.69	0.0757	0.7107
13	305	327	22	0.2924	37.99	18.99	26.27	0.0672	0.7228
14	305	324	19	0.2748	32.04	16.02	21.33	0.0586	0.7511
15	305	321	16	0.2748	26.98	13.49	17.96	0.0498	0.7511
16	305	318	13	0.2638	21.59	10.79	14.01	0.0408	0.7704

From Table 3, we conclude that efficiency of engine goes on increasing as the temperature gradient decreases. This happens because the decrease in W is very less as compared to the decrease in Q. Due to this ratio, efficiency increases.

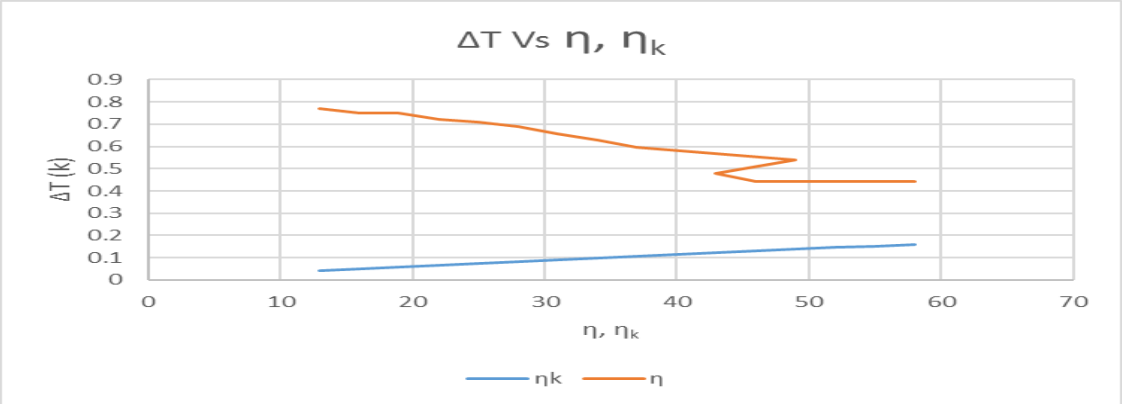

Figure 5. Graph of temperature difference Vs efficiency

6. Summary

Thermal parameters influencing the speed of the Ni-Ti engine are determined. Results show that the temperature of bath plays a major role on power output. From mathematical results we can conclude that the actual efficiency of nitinol engine is inversely proportional to the temperature gradient.

7. References

1. Zheng, Y., Cui, L., Schrooten, J., 2004. Temperature memory effect of a nickel–titanium shape memory alloy. Appl. Phys. Lett. 84-1, 31.

2. Kurita, T., Matsumoto, H., Abe, H., 2004. Transformation behavior in rolled NiTi. J. Alloys Compd. 381, 158–161.
3. Huang, W.M., 2005. Transformation front in shape memory alloys. Mater. Sci. Eng. A 392, 121.
4. Huang, X., Liu, Y., 2001. Effect of annealing on the transformation behavior and super-elasticity of NiTi shape memory alloy. Scr. Mater. 45, 153–160.
5. Kurita, T., Matsumoto, H., Sakamoto, K., Abe, H., 2005. Transformation behavior of shock-compressed Ni48Ti52. J. Alloys Compd. 400, 92.
6. Liu, Y., McCormick, P.G., 1990. Factors influencing the development of two-way shape memory in NiTi. Acta Metall. Mater. 38-7, 1321–1326.
7. Liu, Y., Humbeeck, J.V., Stalmans, R., Delaey, L., 1997. Some aspects of the properties of NiTi shape memory alloy. J. Alloys Compd. 247, 115–121.
8. Liu, Y., Yang, H., Voigt, A., 2003. Thermal analysis of the effect of aging on the transformation behavior of Ti 50.9 at.% Ni. Mater. Sci. Eng. A 360, 350.
9. Chrobak, D., Str ´o˙ z, D., Morawiec, H., 2003. Effect of early stages of precipitation and recovery on the multi-step transformation in deformed and annealed near-equiatomic TiNi alloy. Scr. Mater. 48-5, 571
10. Otsuka, K., Wayman, C.M., 1998. Shape Memory Materials. Cambridge University Press.
11. Somsen, C., Z¨ahres, H., K¨ astner, J., Wassermann, E.F., Kakeshita, T., Saburi, T., 1999. Influence of thermal annealing on the martensitic transitions in Ni–Ti shape memory alloys. Mater. Sci. Eng. A 273–275, 310–314.
12. Lahoz, R., Puertolas, J.A., 2004. Training and two-way shape memory in NiTi alloys: influence on thermal parameters. J. Alloys Compd. 381, 130–136.
13. Frick, C.P., Ortega, A.M., Tyber, J., Maksound, A.El.M., Maier, H.J., Liu, Y., Gall, K., 2005. Thermal processing of polycrystalline NiTi shape memory alloys. Mater. Sci. Eng. A 405, 34–49.
14. Gorbet, R., and Wang, D., 1998, “A Dissipativity Approach to Stability of a Shape Memory Alloy Position Control System”, IEEE Transactions on Control Systems Technology, Vol. 6, No.

MULTI-AREA LOAD FREQUENCY CONTROL (LFC) FOR POWER SYSTEM USING LINEAR QUADRATIC GAUSSIAN (LQG) CONTROLLER

Muddasar Ali
Department of Electrical Engineering, Army Public College of Management & Sciences (APCOMS), (U.E.T) Taxila, Pakistan

Muhammad Ejaz Hassan
Department of Electrical Engineering, Army Public College of Management & Sciences (APCOMS), (U.E.T) Taxila, Pakistan

ABSTRACT:

Nowadays power demand is increasing continuously and the biggest challenge for the power system is to provide good quality of power to the consumer under changing load conditions. When real power changes, system frequency gets affected while reactive power is dependent on variation in voltage value. That is why real and reactive power is controlled separately. For satisfactory operation, the frequency of power system should be kept near constant value. Continuous change in frequency by variation of load is a big challenge for the generating unit to compensate it as quickly as possible. Many techniques have been proposed to obtain constant value of frequency and to overcome any deviations. The Load Frequency Control (LFC) is used to restore the balance between load and generation by means of speed control. The main goal of Load Frequency Control (LFC) is to minimize the frequency deviations to zero. Load Frequency Control (LFC) incorporates an appropriate control system, which is having the capability to bring the frequencies of the Power system back to original set point values or very near to set point values effectively after the load change. This can be achieved by using conventional controller but the conventional controller is very slow in operation. Modern and optimal control systems enjoy a lot of advantages over conventional controllers. They are much faster than conventional controller and give better stability response than conventional controllers. In this research paper, Linear Quadratic Regulator (LQR) and Linear Quadratic Gaussian Controller (LQR+ Kalman Filter) are applied for two areas Load Frequency Control (LFC) in power system using MATLAB/SIMULINK software package. Reduction in settling time and frequency deviation was successfully achieved by Using Linear Quadratic Gaussian (LQG) Controller.

Keywords:

Load Frequency Control (LFC), Conventional Controller, Linear Quadratic Regulator (LQR), Kalman Filter, Linear Quadratic Gaussian (LQG) Controller.

1. INTRODUCTION:

Power system is used for the conversion of natural energy to electric energy. For the optimization of electrical equipment, it is necessary to ensure the electric power quality. During transmission, both the active and reactive power balance must be maintained between the generation and utilization. When either frequency or voltage changes equilibrium point will shift. Good quality of electrical power system demands that both the voltage and frequency to be fixed at desired values irrespective of

change in loads that occur randomly. It is in fact impossible to maintain both active and reactive power without control which would result in variation of voltage and frequency levels. To cancel the effect of load variation and to keep frequency and voltage level constant, a control system is required. The active and reactive powers have a combined effect on the frequency and voltage. Frequency is mostly dependent on the active power and voltage on reactive power. Thus the issue of controlling power systems can be separated into two independent problems.[1] The active power and frequency control is referred to as Load Frequency Control (LFC). LFC is a very important issue in power system operation and control for supplying sufficient and reliable electric power with good quality. With an increasing demand, the electric power system becomes more and more complicated. The power system is subjected to local variations of load in random magnitude and duration. As the load varies, the frequency related with this area is affected. Frequency transients must be eliminated as soon as possible. The generators in a control area always vary their speed (speed up or slow down) for maintaining the frequency and the relative power angle to the predefined values with tolerance limit in both static and dynamic conditions. Frequency should remain nearly constant for satisfactory operation of power system. Frequency deviation can directly impact on a power system operation, system reliability and efficiency. Large frequency deviations can damage equipment and degrade load performance. Overload can ultimately lead to a system collapse.[2] Variation in frequency adversely affects the operation and speed control of induction and synchronous motors. Various control strategies have been proposed and investigated by several researchers for LFC design in power systems. Many classical approaches have been used to provide supplementary control which will drag the frequency to normal operating value within very short time. This extensive research is due to the fact that LFC constitutes an important function of power system operation where the main objective is to keeping the frequency fluctuations with in pre-specified limits.[3] In this research Paper, Linear Quadratic Regulator (LQR) and Linear Quadratic Gaussian Controller (LQG) are applied for two areas LFC in power system. Reduction in settling time and frequency deviation is successfully achieved by Using LQG Controller.

2. BRIEF LITERATURE SURVEY:

Pradipkumar Prajapati has presented various Conventional controllers for Multi Area Load Frequency Control in the power system. A comparison was made between PID controller and PI controller in terms of performance aspect in multi areas power systems. Simulation results showed that the PID controller outperformed the PI controller in terms of less frequency deviation and settling time.[1] Gajendra Singh Thakur used PI and PID controller to solve the Load Frequency Control problem of single area power system. Simulation results show that PID controller has better performance than the PI controller because it reduced the settling time and minimized overshoot. PID controller with simple approach can provide better performance comparing with the conventional PI controller. Simulation results show that the superior performance of the system using Z-N Tuned PID controller.[2] Mohinder Pal used PI controller for Load Frequency Control in the power system. It is seen that Integral Controller results in a stable frequency. With the proper choice of control parameters, frequency deviations can be effectively controlled. Due to disturbances in the power system frequency deviates. To overcome this problem Integral Controller is used.[3] Mohammed Wadi presents the analysis of an optimal LQR controller and Legendre Wavelet Function. A comparison was made between an LQR optimal controller and an optimal controller based on Legendre Wavelet Function in

terms of performance in single area power systems. Simulation results showed that the optimal controller based on Legendre wavelet function approximation method outperformed the LQR controller in terms of less frequency deviation and steady state error; while both had the same settling time. A numerical example demonstrated the effectiveness of the proposed optimal control via Legendre Wavelets Function over LQR controller.[4]

3. LOAD FREQUENCY CONTROL:

In a large electrical power system, nominal frequency depends significantly on the balance of produced and consumed active power. As the peak demands do not have any certain time, they may occur at any random time of the day in the power system. When active power imbalance occurs in any part of the system, it results in changes in the frequency of the entire system. If there is any sudden load change occurring in a control area of power system, then there will be frequency deviation. The generators in a control area always vary their speed together (speed up or slow down) for maintaining the frequency to the predefined values with tolerance limit in both static and dynamic conditions.[4] The main objective of LFC is to maintain the frequency constant by means of speed control. Industrial loads connected to electrical power system are very sensitive to the quality of electrical energy, mainly the frequency component. Thus, the steady-state frequency error in the system must stay within acceptable values in order to keep the balance. Figure 1 shows the relationship between system frequency and load which is inversely proportional.[8]

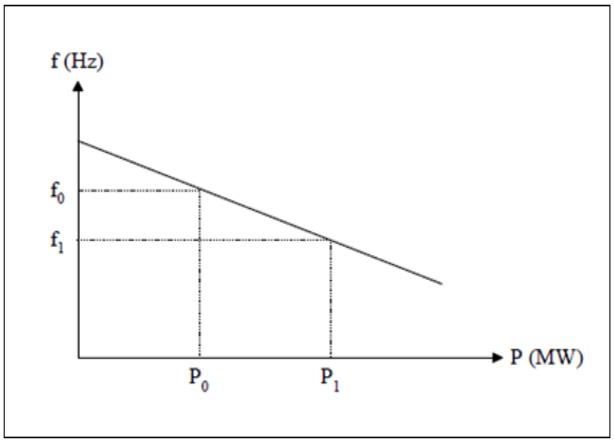

FIGURE 1: VARIATION OF LOAD FREQUENCY CHARACTERISTIC

Possible increase in load reduces the nominal frequency of the system. This alternation in frequency is sensed by a regulator in the primary control loop; subsequently, the rotational speed of the turbine is increased leading to an increase in the produced power.[5] Frequency deviations can directly impact power system operation, system reliability and efficiency. Large frequency deviations can damage equipment, degrade load performance, overload transmission lines and adversely affect the performance of system protection schemes. These large-frequency deviation events can ultimately lead to a system collapse. Variation in frequency adversely affects the operation and speed control of induction and synchronous motors. Due to dynamic nature of the load, continuous load change cannot be avoided but the system frequency can be kept within sufficiently small tolerance levels by adjusting the generation continuously using LFC.[8] Figure 2 gives the schematic diagram of load frequency control for power system. In this control method, a frequency sensor senses the change in frequency and gives the signal Δf. The LFC senses the change in frequency signal and the increments real powers ΔP, which will indirectly provide information about incremental state error. These sensor signals are amplified, mixed and transformed into a real-power control signal ΔPc. The valve control mechanism

takes ΔPc as the input signal and provides the output signal, which will change the position of the inlet valve of the prime mover.[6]

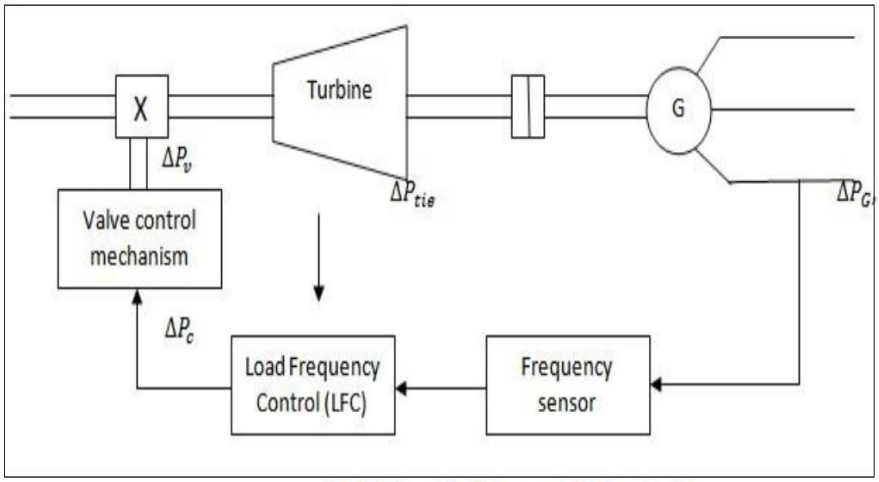

FIGURE 2: BLOCK DIAGRAM OF LOAD FREQUENCY CONTROL (LFC) FOR POWER SYSTEM. [8]

4. LINEAR QUADRATIC REGULAOR (LQR) CONTROLLER:

This is a technique that is applied in the control system design which is implemented by minimizing the Performance Index of the system variables. Here we have discussed the design of the optimal controllers for the linear systems with Quadratic Performance Index, which is also known as the Linear Quadratic Regulator or LQR Controller. The aim of the optimal regulator design is to obtain a control law u*(x, t) which can move the system from its initial state to the final state by minimizing the Performance Index. The Performance Index is selected to give best trade-offs between performance and cost of control. The Performance Index which is widely used is the Quadratic Performance Index and is based on minimum error and minimum energy criteria.[7-8]

Consider a plant:

$$X(t) = Ax(t) + Bu(t) \qquad (1)$$

The aim is to find the Vector K of the control law,

$$U(t) = -K(t)*x(t) \qquad (2)$$

It minimizes the value of the Quadratic Performance Index J of the form,

$$J = \int_{to}^{t} (x'Qx + u'Ru)dt \qquad (3)$$

Where Q is a positive semi definite matrix and R is real symmetric matrix. The choice of the elements of Q and R allows the relative weighting of individual state variables and individual control inputs.[9]

To obtain the solution we make use of the method of Langrange Multipliers. The problem reduces to the minimization of the following unconstrained Equation,

$$L[x, \lambda, u, t] = [x'Qx + u'Ru] + \lambda' [Ax + Bu - \dot{X}] \qquad (4)$$

The optimal values determined are found by equating the partial derivative to zero.

$$\frac{dL}{d\lambda} = AX^{*}+BU^{*}-\dot{X}^{*}= 0 \quad , \quad X^{*} = AX^{*}+ BU^{*}$$

$$\frac{dL}{du} =2RU^{*} + \lambda'B =0 \quad , \quad U^{*} = \frac{-1}{2}R^{-1}\lambda'B$$

$$\frac{dL}{dx} =2X'Q+ \lambda'+\lambda'A =0 \quad , \quad \dot{\lambda} = \dot{-}2QX^{*}-A'\lambda$$

Assume that there exists a symmetric, time varying positive definite matrix P (t) satisfying,

$$\lambda =2P(t)\,X^{*} \qquad (5)$$

Substituting Equation 2 into (U^{*}) gives the optimal closed-loop control law,

$$U^{*}(t) = -R^{-1}B'P(t)\,X^{*} \qquad (6)$$

Obtaining the derivative of Equation 5,

$$\dot{\lambda}=2(\dot{P}X^{*}+P\dot{X}^{*}) \qquad (7)$$

By using equation 7 and $\dot{\lambda}$, we obtained,

$$P(t) = -P(t)A - A'P(t) - Q + P(t)BR^{-1}B'P \qquad (8)$$

The above equation is referred to as Matrix Riccati Equation. For linear time invariant systems, since $\dot{P}$=0, when the process is of infinite duration tf =∞ and Equation 8 becomes,

$$PA + A'P(t) + Q - PBR^{-1}B'P=0 \qquad (9)$$

One of the important properties of LQ-Regulators is that they guarantee nominally stable closed-loop system, provided certain conditions are met.[8]

The MATLAB Control System toolbox can be used for the solution of the Riccati Equation. Choosing the weight matrices Q and R usually involves some kind of trial and error and they are usually chosen as diagonal matrices.[10] The solution of LQR results in an asymptotically stable closed-loop system if,

1. The system (A, B) is controllable.
2. R>0
3. $Q=C^{T}C$ Where (C, A) is observable.

The definition of optimal control system is designing the control law in order to find out the feedback gain matrix 'K' such that the given Performance Index will be minimized. The LQR design procedure is in stark contrast to classical control design, where the gain matrix K is selected directly.[6] To design the optimal LQR, the design engineer first selects the design parameter weight matrices Q and R. Then, the loop time response is found by simulation. If this response is unsuitable, new values of Q and R are selected and design is repeated. The parameter weight matrices Q and R can be written as,[9]

$$Q=C^{T}C \quad , \quad R=1 \qquad (10)$$

The MATLAB code is written in MATLAB-R2011. The MATLAB command to obtain feedback K-Matrix is,[8]

$$[K, P]=lqr2\ (A, B, Q, R) \qquad (11)$$

The optimal gain vector K for Area 1 & Area 2 in Power system for LFC is obtained by using Equation 11,

Feedback K-Matrix of Area1=K_1= [-0.086 -0.507 -0.909]

Feedback K-Matrix of Area2=K_2= [-0.077 -0.529 -0.914]

5. KALMAN BUCY FILTER:

The LQR solution is basically a state-feedback type of controller which requires that all the states must be available for feedback. Designing a control system is required for estimating the state vector, based upon a measurement of the output given by equation 12 & 13 and known input u. This optimal observer is commonly known as Kalman Filter. In addition, the combination of state feedback and Kalman observer will always result in stable closed loop systems. The Kalman Filter provides us with a procedure of designing observers for multivariable plants. This observer is guaranteed to be optimal in the presence of noise signal. Consider a plant with the following state space representation.[9]

$$\dot{X}= AX + BU + \omega \qquad (12)$$

$$Y =CX +DU +v \qquad (13)$$

Where,

A, B, C are the plant's state coefficient matrices.

ω is the process noise vector.

v is the measurement noise vector.

The state space solution of the above equation was first provided by R.E.Kalman and R.S Bucy.

The Optimal observer (Kalman Filter) is given by,

$$\hat{\dot{X}} = A\hat{X}+BU+L(Y-C\hat{X}) \qquad (14)$$

Where $\hat{X}$ is the estimate of state x and L is the gain matrix of Kalman Filter. The observer gain L is computed as,

$$L=\sum C^{T} R^{-1} \qquad (15)$$

The $\sum$ is found as the positive semi-definite solution of,

$$A\sum + \sum A' + Q - \sum C^{T} R^{-1} C \sum = 0 \qquad (16)$$

The Equation 16 is very similar to the LQR solution known as Riccati Equation. The Q and R matrices represent the intensity of the process and sensor noise input and it can be selected by the user. These matrices are known as co-variance matrices. Their size is a measure of how strong the noise is: the larger the size, the more random or intense the noise hence it is called the noise intensity. Finally the mathematical condition for the design of Kalman Filter is that the matrices Q and R are positive semi definite and the system must be observable. [9]

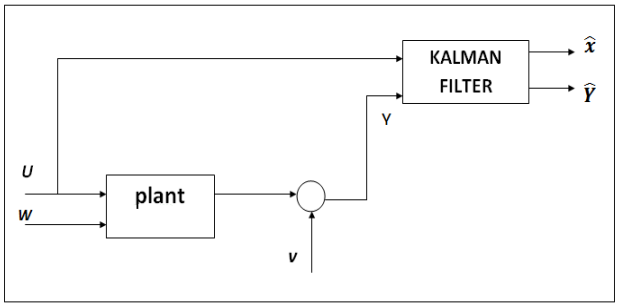

FIGURE 3: BLOCK DIAGRAM OF KALMAN FILTER FOR LFC. [9]

The Kalman filter Optimal Gain Matrix L is calculated with W and V matrices at the nominal operating point as follow,[5]

$$W=10*B^{T}*B \qquad (17)$$

$$V=0.01*C*C^{T} \qquad (18)$$

The MATLAB code is written in MATLAB-R2011. The algebraic Riccati Equation can be solve using the specialized Kalman Filter MATLAB command lqe .The MATLAB command to obtained observer gain L of Kalman Filter is given by,[5]

$$[L, S] = lqe\ (A, B, C, W, V) \qquad (19)$$

Where,

L is the returned Kalman Filter optimal gain.

S (∑) is the returned solution to the Riccati Equation.

The observer gain L of Kalman Filter for Area 1 & Area 2 in Power system for LFC is obtained by using Equation 19,

$$\text{L-Gain of Kalman Filter for Area 1=L}_1=\begin{bmatrix}-4.9329\\-0.0162\\939.230\end{bmatrix}$$

$$\text{L-Gain of Kalman Filter for Area 2=L}_2=\begin{bmatrix}-4.366\\-0.0150\\673.4705\end{bmatrix}$$

6. LINEAR QUADRATIC GAUSSIAN (LQG) CONTROLLER:

LQR was designed which is the cause of minimization of the Quadratic Objective Function. The Kalman Filter was also introduced with LFC in presence of noise process w and measurement noise v.[10] The combination of LQR with the Kalman Filter forms an Optimal Compensator which is called as Linear Quadratic Gaussian (LQG) Controller. The optimal compensator design process is the following, [5]

1. Design an optimal regulator (LQR) for a linear plant using full-state feedback. The regulator is designed to generate a control input U (t), based upon the measured state-vector X.
2. Design Kalman Filter for the plant assuming a known control input U (t) a measured output Y(t) including noises w & v.
3. Combine the separately designed optimal regulator and Kalman Filter into an optimal compensator that generates the input vector U (t), based upon the estimated state-vector $\hat{X}$ rather than the actual state vector X, and the measured output Y (t). The plant equation and the problem solution is now repeated. [5]

$$\dot{X} = AX + BU + \omega \quad (20)$$

$$Y = CX + v \quad (21)$$

The Control-Law of LQR is now given by,

$$U(t) = -K(t) * \hat{X}(t) \quad (22)$$

The Kalman Filter state-space equation is given by,

$$\dot{\hat{X}} = A\hat{X} + BU + L(Y - C\hat{X}) \quad (23)$$

By putting Equation 22 of LQR in Equation 23 of Kalman Filter, the state-space equation of LQG-Controller is given by,

$$\dot{\hat{X}} = (A - B*K - L*C + L*D*K) * \hat{X} + L*Y \quad (24)$$

Where,

K & L are the optimal regulator and Kalman Filter gain.

$\hat{X}$ is the estimated state vector.[9]

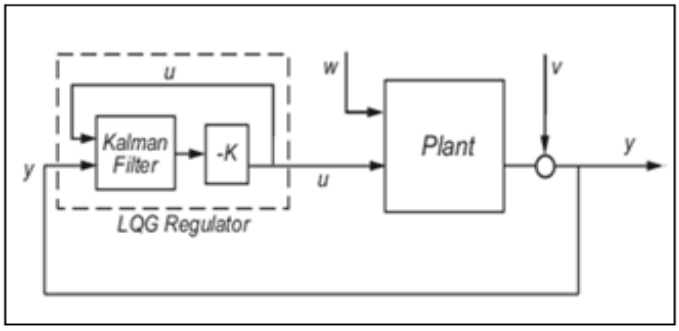

FIGURE 4: BLOCK DIAGRAM OF LQG-CONTROLLER FOR LFC. [5]

Using MATLAB's Control System Toolbox, a state-space model of the closed-loop system, can be constructed as follows.[5]

Sysp =ss (A, B, C, D); (25)

sysc = ss (A-B*K-L*C+L*D*K ,L,K ,zeros (size (D'))) (26)

syscl = feedback(sysp,sysc); (27)

Where,

sysp = State-space model of the plant (LFC).

Sysc= State-space model of the LQG compensator.

syscl = State-space model of the closed loop system.

7. SIMULATION AND RESULTS :

A comparison of LFC (uncompensated) without any controller, with LQR Controller and finally with LQG Controller has been observed. The comparison is made in terms of performance with respect to frequency deviation and settling time as shown in Table 1. The parameters of the numerical example, is solved using MATLAB as shown in Table 2. In addition, the solution of an example consists of three scenarios with LFC: the first one contains no controller (uncompensated LFC), the second scenario used LQR Controller and finally the last scenario used LQG Controller.

A. FIRST SCENARIO:

In the first scenario, MATLAB simulation of Load Frequency Control (LFC) is constructed using Simulink and solved without using any controller. Figure 5 and Figure 6 show the Simulink diagram of LFC and the frequency deviations respectively,

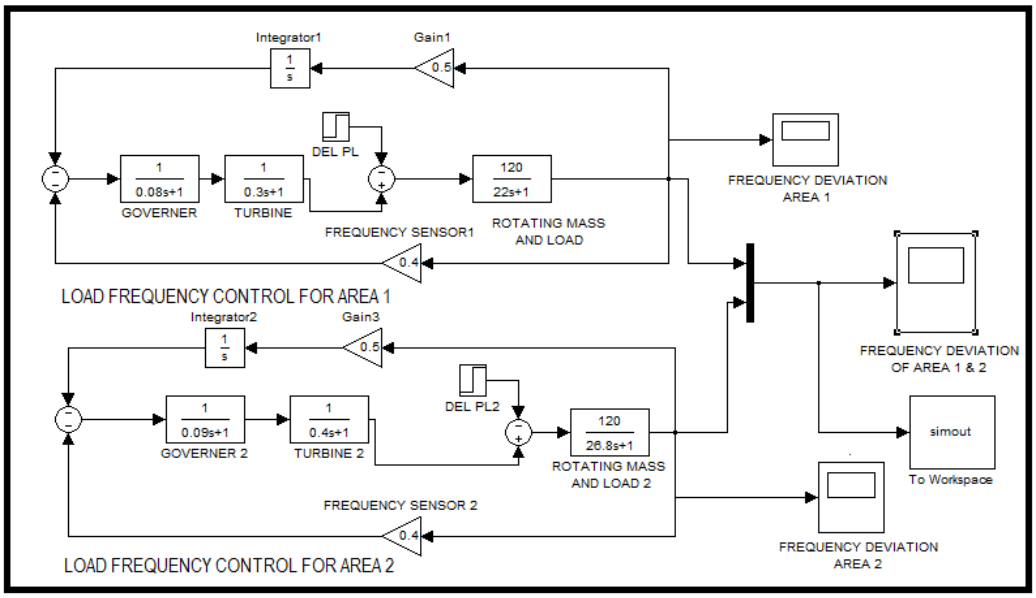

FIGURE 5: SIMULINK MODEL OF FIRST SCENARIO FOR TWO AREA LFC WITHOUT ANY CONTROLLER.

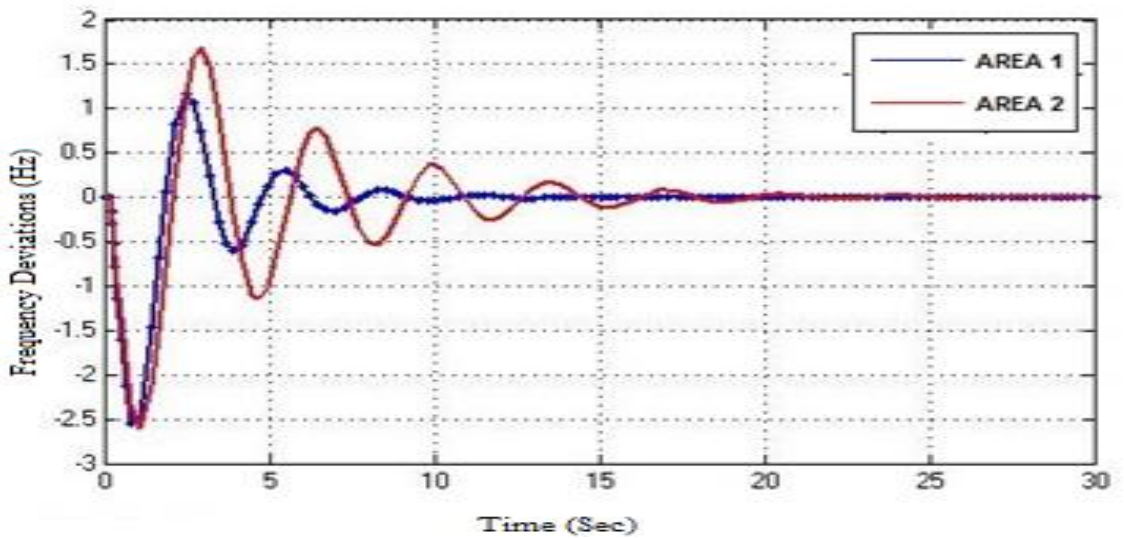

FIGURE 6: FREQUENCY DEVIATION OF FIRST SCENARIO FOR TWO AREA LFC WITHOUT ANY CONTROLLER. (UNCOMPENSATED LFC)

B. SECOND SCENARIO:

In the second scenario, LQR optimal controller is designed in which K-gain vector is used as a feedback to reduce the frequency deviations and settling time of LFC in the power system. The LQR controller is designed using Equation 11 in M-file and by using Simulink in MATLAB. The simulink diagram and the frequency deviations are shown in Figures 7 and 8 respectively,

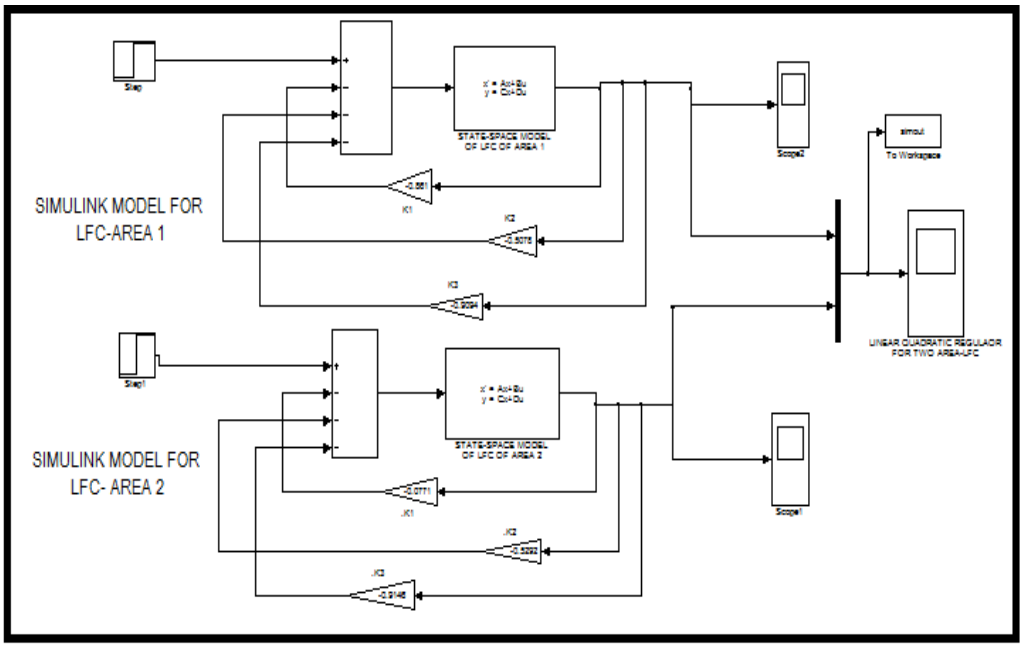

FIGURE 7: SIMULINK MODEL OF SECOND SCENARIO FOR TWO AREA LFC WITH LQR_CONTROLLER.

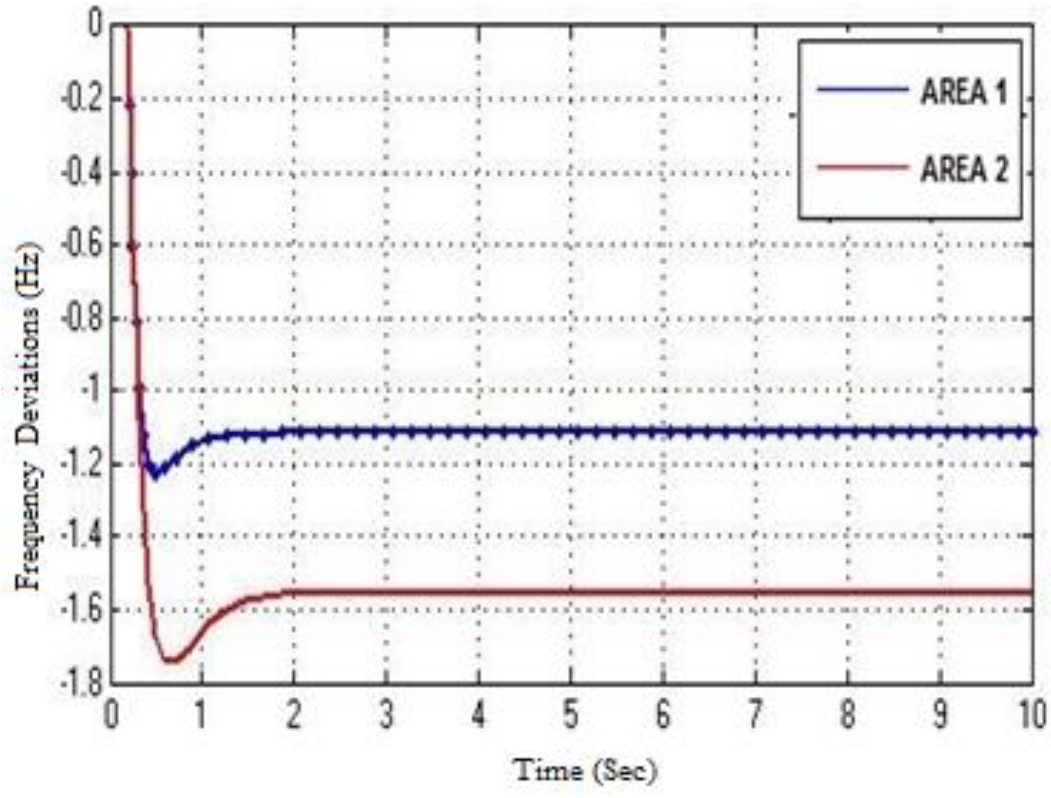

FIGURE 8: FREQUENCY DEVIATION OF SECOND SCENARIO FOR TWO AREA LFC WITH LQR _CONTROLLER.

C. THIRD SCENARIO:

In the final scenario, the LQG Controller is designed which is used as a feedback in two area of LFC, to reduce the frequency deviations and settling time in power system. The LQG controller is designed

using Equations 25 to 27 in M-file and MATLAB. The frequency deviation is shown in Figure 9 respectively,

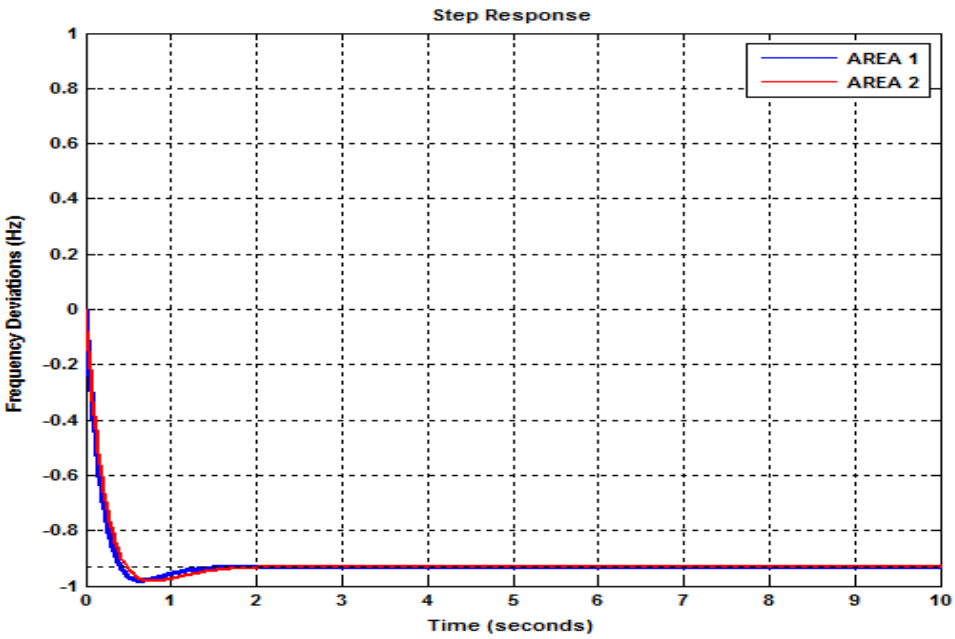

FIGURE 9: FREQUENCY DEVIATION OF THIRD SCENARIO FOR TWO AREA LFC WITH LQG_CONTROLLER.

8. DISCUSSION

Table 5.1 shows the performance of LFC by various control strategy over frequency deviations and settling time for two area LFC in power system.

S #	PARAMETER	AREA	UNCOMPENSATED LFC	LFC WITH LQR_CONTROLLER	LFC WITH LQG_CONTROLLER
1	FREQUENCY DEVIATION (Hz)	1	1.1 to -2.5	0 to -1.23	0 to -0.9
		2	1.5 to -2.5	0 to -1.7	0 to -0.98
2	SETTLING TIME (Sec)	1	11 Sec	1.5 Sec	1.1 Sec
		2	21 Sec	2 Sec	1.38 Sec

TABLE 1: COMPARATIVE ANALYSIS OF DIFFERENT CONTROLLERS WITH LOAD FREQUENCY CONTROL (LFC) IN POWER SYSTEM.

In this research paper, first an optimal LQR Controller is designed for LFC in the power system. Then the states are estimated by Kalman Filter. Then, by combining both LQR and Kalman Filter an optimal compensator called Linear Quadratic Gaussian (LQG) is designed which recovers the responses of optimal LQR-regulator in the presence of estimated states. The performance of LQR and LQG Controllers are shown in the above simulations of Figure 8 & 9. From the above simulations, it is clear that the LFC without any controller has more frequency deviations as compare to LQR and LQG controllers. It is clear from the graphical representation of the step response that the settling time is

more in an uncompensated system than that for a compensated system while using LQR and LQG controllers and the system reached faster to a steady state in compensated system with these advance control techniques.

9. CONCLUSION

This research paper contains designing of a controller that can produce optimal results with LFC in power system. Two Controllers with LFC were studied into account. It was seen that a feedback controller called LQR Controller with LFC was better than the uncompensated system in terms of frequency deviation and settling time. The Linear Quadratic Gaussian (LQG) Controller is designed to provide the best results in terms of both frequency deviation and settling time and achieved required reliability under changing load conditions.

10. FUTURE WORK

1. The parameters in this research work were taken as constant throughout the whole operation, but there may be parameter uncertainty due to wear and tear, temperature Changes, imperfection of component, aging effect and environment changes etc. So, during controller designing, variation of these parameters may be taken in to consideration.

2. The LFC for Power System can be designed by using PID controller via different optimization techniques, like Genetic Algorithm (GA), Particle Swarm Optimization (PSO), Simulated Annealing (SA) and Artificial Neural Network (ANN) etc and results can be compare with Linear Quadratic Gaussian (LQG) Controller.

11. APPENDIX

S #	TWO AREA POWER SYSTEM PARAMETER
1	F=50Hz
2	D=8.34e-3
3	Kr_1=0.5
4	Kr_2=0.4
5	Tr_1=10.0s
6	Tr_2=11.0s
7	Tg_1=0.08s
8	Tg_2=0.09s
9	Tt_1=0.3s
10	Tt_2=0.4s
11	H_1= 0.09166
12	H_2= 0.108033

TABLE 2: TWO AREA POWER SYSTEM PARAMETERS.

ACKNOWLEDGEMENT

The first author is thankful to Dr. Muhammad Ejaz Hassan, Associate Professor & Head, Department of Electrical Engineering, Army Public College of Management & Sciences (APCOMS) Rawalpindi, (U.E.T) Taxila, Pakistan for his valuable suggestions and necessary recommendations.

REFERENCES

[1] Pradipkumar Prajapati, "Multi-area Load Frequency Control (LFC) by Various Conventional Controllers" 978-1-4673-9925-8/16/$31.00 2016 IEEE.

[2] Gajendra Singh Thakur, "Load frequency control (LFC) in Single area with traditional Ziegler-Nichols PID Tuning controller" International Journal of Research in Advent Technology, Vol.2, No.12, December2014 E-ISSN: 2321-9637.

[3] Mohinder Pal, "To Control Load Frequency by using Integral Controller", International Journal of Innovative Research in Science, Engineering and Technology (An ISO 3297: 2007 Certified Organization) Vol. 3, Issue 5, May 2014.

[4] Mohammed Wadi, "Optimal Controller for Load Frequency Control via LQR and Legendre Wavelet Function", Journal of Automation and Control, 2015, Vol. 3, No. 2, 43-47 Available online at http://pubs.sciepub.com/automation/3/2/2 Science and Education Publishing DOI:10.12691/automation-3-2-2.

[5] ALI M. YOUSEF," Improved Power System Stabilizer by Applying LQG Controller", Advances in Electrical and Computer Engineering, ISBN: 978-1-61804-279-8.

[6] P.Suresh Kumar," Load Frequency Control Of Multi Area Power System Using Fuzzy And Optimal Control Techniques", International Journal of Recent Trends in Engineering & Research (IJRTER) Volume 02, Issue 08; August - 2016 [ISSN: 2455-1457.

[7] Shyam K. Joshi," Analysis of load frequency control using PID Controller" ,International Journal of Emerging Technology and Advanced Engineering Website: www.ijetae.com (ISSN 2250-2459, ISO 9001:2008 Certified Journal, Volume 4, Issue 11, November 2014.

[8] Power System Analysis by Hadi Saadat.

[9] Design of Feedback Control Systems, by Stefani, 4th Ed.

[10] Modern control design with MATLAB by Ashish Tewari.

AUSTRALIAN JOURNAL OF ENGINEERING AND TECHNOLOGY RESEARCH (AJMFR)

Vol. 2, Issue 1 - 2017

DESIGN OF ROBUST CONTROLLER FOR AUTOMATIC VOLTAGE REGULATOR (AVR) IN POWER SYSTEM

Khadija Jalal
Department of Electrical Engineering, Army Public College of Management & Sciences (APCOMS), (U.E.T) Taxila, Pakistan.

Muhammad Ejaz Hassan
Department of Electrical Engineering, Army Public College of Management & Sciences (APCOMS), (U.E.T) Taxila, Pakistan.

ABSTRACT:

Due to ever increasing load demand, electrical power system is operating under highly stressed conditions. Any internal or external disturbance can produce oscillations in the power system. Power system oscillations and their damping is a major challenge for electricity supply industry. Load state changing as dynamic system behaviour will change the current flow in the generator system that result in armature voltage and terminal voltage change. Inductive loads leads to a voltage drop and capacitive load leads to a voltage rise and result in variation of voltage from its rated value. To overcome this problem the generator excitation is controlled by Automatic Voltage Regulator (AVR) which is widely used to deal with the issues of maintaining terminal voltage and improving transient stability of the power system. AVR incorporates an appropriate control system which is having the capability to bring the voltage of the Power system back to original set point effectively after the load change. This can be achieved by using Conventional controllers but these controllers are very slow in operation. The H∞ controller can be used with AVR to get faster and better results. The H∞ control method provides good robust performance under changing load disturbances. In this paper, H∞ controller is designed for AVR. The adjustments in the parameters of the weight functions are achieved by "Automatic Weight Selection Algorithm" The simulations are done using MATLAB software. Reduction in settling time, overshoot and voltage deviation were successfully obtained by using Robust H∞ controller with AVR in Power system.

Keywords: Automatic Voltage Regulator (AVR), Conventional Controllers, Robust H∞ controller, Automatic Weight Selection Algorithm.

1. INTRODUCTION

The Power system is mainly concerned with the generation of electric power from sending to receiving end as per consumer requirements with minimum amount of losses. Power system network is designed to operate at certain nominal frequency and terminal voltages. Any deviation to this may cause dynamic instability within the system which may leads to overall system collapse and may cause damage to connected equipment. Change in reactive power mainly affects the system voltage while change in real power is sensitive to change in system frequency. Therefore real and reactive powers are controlled separately with the use of well control equipment in the generation, substation or distribution substation. The power system researchers round the globe are working meticulously to maintain these two vital parameters at nominal level. Control equipment for the generation is usually used to regulate the supply of active and reactive power. Thus, a control

system cancels the effect of the random load changes and to keep the frequency and voltage, at standard values. The growth in size and complexity of electric power systems along with increase in power demand has initiated the need for intelligent systems that combine different techniques and methodologies **[1].** The automatic control system detects these changes and initiates in real time as set of control actions which will eliminate as effectively and quickly as possible the state deviations. The Automatic Voltage Regulator (AVR) plays an essential role to regulate the voltage magnitude and reactive power whereas active power and system frequency is controlled by Load Frequency Control (LFC). Over the past few decades, several control techniques have been developed. The classical proportional-integral-derivative (PID) controller is the well known among them. Therefore, many methods have been used for fine tuning the PID controller parameters. The setting of the PID controller parameters is cumbersome, especially in industrial systems that have nonlinearities, high order, and delay time. Generally, it is difficult to achieve the best performance of the system by using these methods **[2-6].** A variety of controller design techniques are available in literature, among these, H∞ are one of the most popular techniques for controller designs which ensure robustness, disturbance rejection and perfect stability of the system. The main purpose of the controller is that it can capture bounded uncertainties and reject disturbance **[7].** The control objective of the H∞ controller is to achieve the design parameters by minimizing the norm of the closed loop system **[8].** This Paper explains H∞ controller design procedure for AVR. This technique is mainly applied in linear domain and results in better robustness. Most important task in H∞ controller design method is the selection of weight functions. There are usually two weights in the design process. One is input weight and the other is output weight. These weights are used to normalize the input and output command **[11].** The adjustments in the parameters of the weight functions are achieved by "Automatic Weight Selection Algorithm" **[12].** The advantage of H∞ controller is that the control effort generated by this technique is under limits and can be easily applied to the plant.

II. LITERATURE REVIEW

Hany M. Hasanien proposed the Genetic Algorithm method to optimally design a PID controller in the Automatic Voltage Regulator for improving the step response of terminal voltage. The proportional gain, the integral gain, the derivative gain, and the saturation limit were chosen to define the search space for the optimization problem. As a result of this proposed approach, fast design and an accurate performance prediction were achieved. Therefore, when this proposed approach is applied, it is more efficient in raising the precision of optimization **[1].** Hestikah Eirene Patoding and Eodia T. Lobo proposed the right location for the installation of a PID controller in the AVR system installed after load changes input (before the AVR system) so that the load changes the affect voltage can be set. AVR's performance becomes lighter in controlling the voltage on the existing tolerance. P and PID controllers conducted in disturbance conditions or changes in load indicated that the PID controller is better than the P controller to control the voltage in times of load changes **[2].** Ashok Singh proposed ZN Tuned controller which is more effective means for improving the dynamic performance of the AVR and LFC. The proposed controller still achieves good dynamic performance when the other controller such as PID Controller and without controller response. The simulation results show that the proposed controller can perform an efficient search that achieves better performance criterion through also, the ZN tuned controller response is more superior **[3].**

III. AUTOMATIC VOLTAGE REGULATOR (AVR)

The heart of the excitation systems lies in the voltage regulators. It is a device that serves the output voltage change and provides corrective actions to take place for an isolated generator feeding a load. The Automatic Voltage Regulator (AVR) functions to maintain the bus bar voltage constant.

The AVR has the following objectives, **[13]**

1. To keep the system voltage constant so that the connected equipment operates satisfactorily.

2. To obtain a suitable distribution of reactive load between machines working in parallel.

3. To improve stability of the Power system.

The AVR senses the terminal voltage and adjust the excitation to maintain a constant terminal voltage. It also maintains the reactive power at the required level. The schematic diagram of a simplified AVR is shown in Fig. 1.

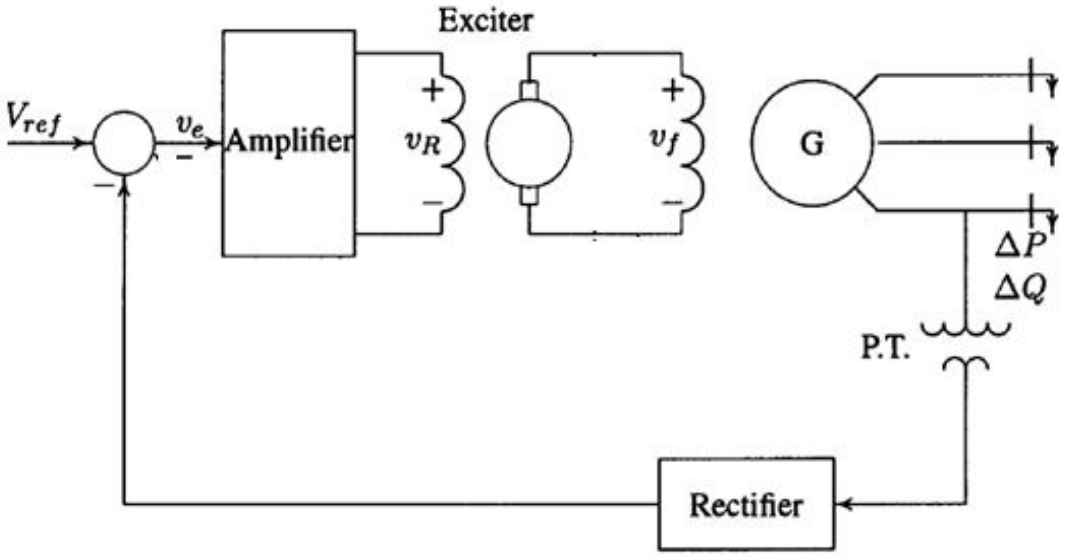

FIGURE 1: GENERAL MODEL OF AVR [18]

IV. MATHEMATICAL MODELING OF AUTOMATIC VOLTAGE REGULATOR

In control system design, initially mathematical modeling of the system is performed. Without mathematical modeling it is almost impossible to design a controller for the system. Controller can be designed by using the practical results of the system but directly performing on practical system, is a risky task. By mathematical modeling, one can conduct proper analysis of the system. Hence, it is important to develop a mathematical model for checking the performance and stability of the Automatic Voltage Regulator **[18]**.

AMPLIFIER MODEL

The excitation amplifier may be rotating amplifier, magnetic amplifier or modern electronic amplifier. The amplifier is represented by gain with K_A symbol and time constant T_A and the transfer function is given as:

$$\frac{V_R(s)}{V_e(s)} = \frac{K_A}{1+T_A} \quad (1)$$

The value of K_A ranged from 10 to 400, Time constant T_A ranged 0.02 to 0.1 seconds.

EXCITER MODEL

As the output voltage of exciter is nonlinear function so there is no simple relationship between field voltage and terminal voltage. In simplest form the transfer function of exciter ignoring the saturation or other nonlinearities can be represented by single time constant T_E and gain K_E:

$$\frac{V_F(s)}{V_R(s)} = \frac{K_E}{1+T_E} \quad (2)$$

The value of K_E range 10 to 400, Time constant T_E between 0.5 to 1 seconds.

GENERATOR MODEL

In linearized model the transfer function relating the generator terminal voltage to its field voltage can be represented by gain K_G and time constant T_G and the transfer function is given as:

$$\frac{V_t(s)}{V_F(s)} = \frac{K_G}{1+T_G} \quad (3)$$

The value of K_G range 0.7 to 1.0, Time constant T_G ranged 1.0 to 2.0 from full load to zero loads.

SENSOR MODEL

Voltage is sensed by potential transformer. It is then rectified through bridge rectifier. Sensor is modelled with a simple first order transfer function,

$$\frac{V_t(s)}{V_F(s)} = \frac{K_R}{1+T_R} \quad (4)$$

The Value of T_R ranged from 0.001 to 0.06 second.

COMPLETE MODEL OF AVR

Figure 2 shows the Automatic Voltage Regulator obtained by combining all the models from equation 1 to 4, with generator terminal voltage (V_T) as output to the reference voltage (V_{ref}) as input,

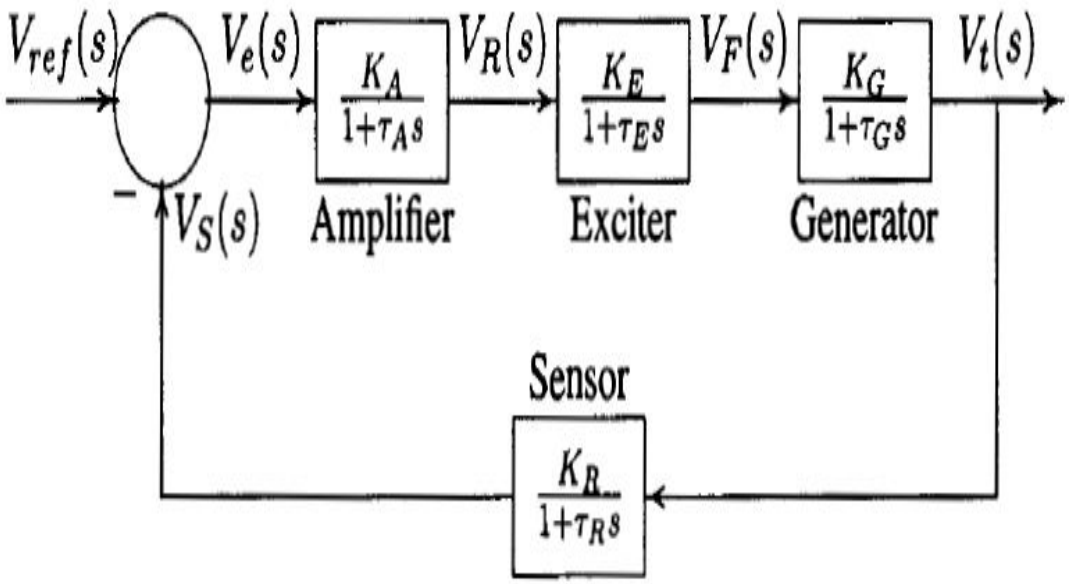

FIGURE 2: MATHEMATICAL BLOCK DIAGRAM OF AVR [18]

V. H∞ CONTROL DESIGN TECHNIQUE

The H∞ control method is utilized for stabilization and good robustness in term of performance. A controller is designed for a specific task and its theme is to control the magnitude of closed loop Transfer Function from input to output. The main advantage of H∞ control design method over the other classical control methods is its relevance to multivariable system's problem. All the H∞ control problems can be formulated in to a general control configuration. Let G (s) is the open loop transfer function of the plant and K(s) is the controller transfer function such that the closed loop system performs robustness and good performance. The controller K(s) will be derived keeping three criterions **[19].** They are,

1. Stability criterion: It states that the roots of the characteristic equation 1+G (s) K(s) = 0 should lie in the left half side of s plane.

2. Performance Criterion: It states that the sensitivity, $S(s) = \frac{1}{1+G(s)K(s)}$ to be small for all frequencies where disturbances and set point changes is large. Sensitivity is the transfer function between the output and disturbances of a system.

3. Robustness criterion: It demands for stability and performance to be maintained not only for the nominal model but also for a set of neighboring plant models that result from unavoidable presence of modelling errors. H∞ problem can be expressed in many areas of control. Due to such importance, it is very important to introduce a general model of such design so that everyone can use it according to their requirements. Figure 3 shows the general representation of control, **[19]**

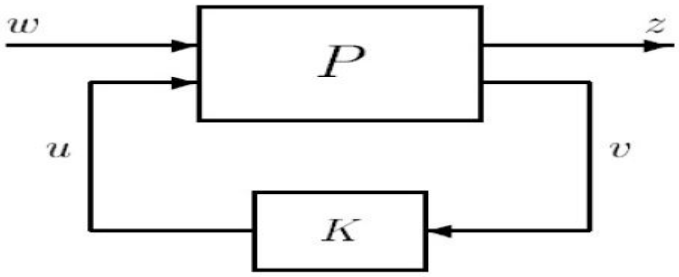

FIGURE 3: H∞ CONTROL GENERAL BLOCK DIAGRAM [19]

VI. H∞ ALGORITHM

H∞ controller synthesis splits a complex control problem into two separate sections, one dealing with stability, the other dealing with performance. The sensitivity function, S, and the complementary sensitivity function, T, are used in the controller synthesis. Sensitivity function is the ratio of output to the disturbance of a system and is given by equation, **[26]**

$$\mathbf{S} = \frac{\mathbf{1}}{(\mathbf{1}+\mathbf{GK})} \qquad \textbf{(5)}$$

The other function is called 'Complementary Sensitivity Function (T)'. This is a transfer function from reference input 'r' to output 'y' and is given by equation,

$$\mathbf{T} = \frac{\mathbf{GK}}{(\mathbf{1}+\mathbf{GK})} \qquad \textbf{(6)}$$

The ultimate aim of the robust control is to reduce the effect of disturbance on output. So sensitivity S and the complementary function T are to be reduced. For obtaining that it is enough to reduce the magnitude of |S| and |T|. This can be done by making $|S(j\omega)| < \frac{1}{W1(j\omega)}$ and $|T(j\omega)| < \frac{1}{W2(j\omega)}$. Where, W1 and W2 are the weight function assigned by the designer. W1 is the performance weighting function to limit the magnitude of the sensitivity function.

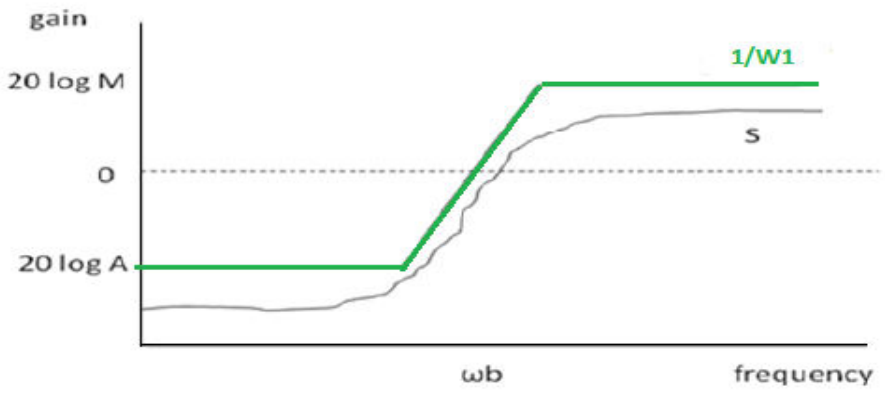

FIGURE 4. DESIRED NATURE OF FREQUENCY PLOTS OF PERFORMANCE WEIGHT FUNCTION AND SENSITIVITY FUNCTION [26]

W2 is the robustness weighting function to limit the magnitude of the complementary sensitivity function.

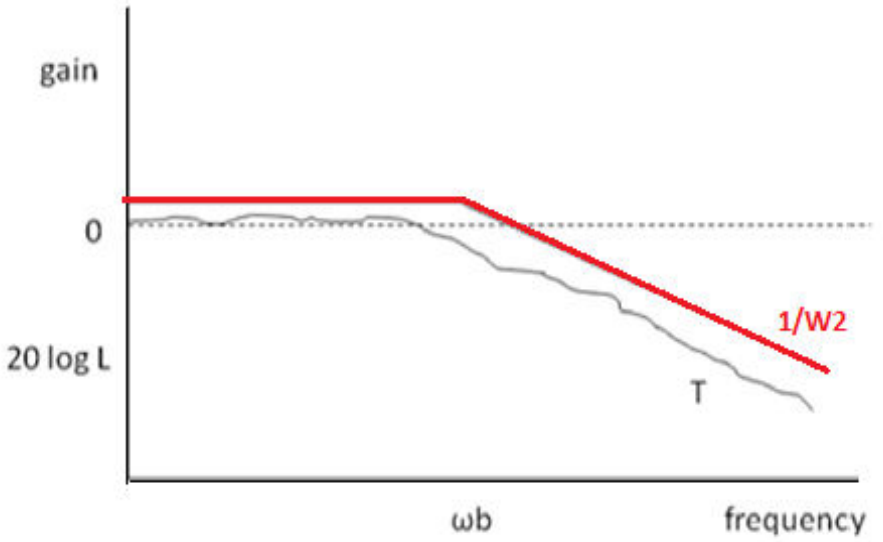

FIGURE 5: DESIRED NATURE OF FREQUENCY PLOTS OF ROBUSTNESS WEIGHT FUNCTION AND COMPLIMENTARY SENSITIVITY FUNCTION [26]

As mentioned earlier the robust controller is synthesized in order to make the H∞ norm of the plant to be as low as possible. In order to obtain this condition weight functions are added to the plant for loop shaping. The weight functions are in fact lead-lag compensators which can shape the frequency response of the system in the desired way. Loop shaping is done to make the frequency response of the plant with the weight functions to come in the desired manner. In loop shaping the parameters of the weight functions are changed to make the frequency response of the whole system to remain within limits **[15].** The control synthesis requires the plant transfer function, controller transfer function and the various weight functions to augment together. Thus an augmented plant model is made as shown in Fig 6.

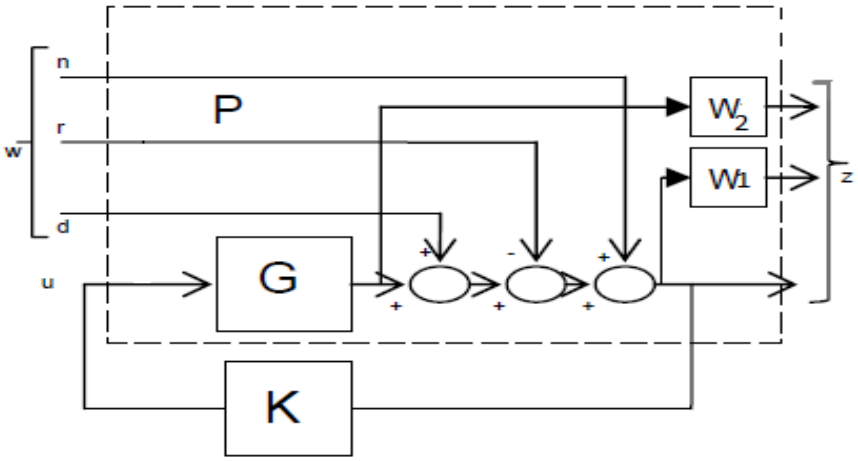

FIGURE 6: AUGMENTED PLANT MODEL FOR THE SYNTHESIS OF H∞ CONTROLLER

VI. AUTOMATIC WEIGHT SELECTION ALGORITHM

The choice of weights is very important in H∞ controller design as it counters the uncertainties and disturbances in the system.If in some cases there are no uncertainties in the model then these weights are used to increase the performance, robustness and stability of the system. Once, these weights are designed, they are used for the construction of H∞ controller. The controller designed will minimize the singular values of the closed loop transfer function of the Sensitivity function S and Complementary Sensitivity function T [25].As mentioned in the robust control theory the synthesis of the controller requires the selection of two weight functions. The work done by Jiankun Hu, Christian Bohn, H.R. Wu [17] suggests some methods for the selection of these weight functions for different plant transfer functions. **[17]** The works shown in reference also describes some ways for designing robust controller for uncertain plants. In all these design procedure the weighting functions are selected using trial and error method and later the H∞ controller is synthesized by loop shaping technique. An iteration work with assumed initial values is conducted to find out the weight functions. It is very difficult to achieve simultaneously meet all the requirements for the synthesis of robust controller. After many trial and error methods, a systematic procedure for the synthesis of H∞ controller is identified for AVR. This novel method makes adjustments in the parameters of the weight functions and enables the control synthesis algorithm to converge to a feasible solution for AVR in power systems meeting all the requirements of robust control. Even though there are no methods available for selecting the transfer functions for weight functions, certain generalization can be done by understanding the loop shaping procedure. Such an empirical formula to determine the performance and robustness weights for a general H∞ control problem is suggested by skojested **[26]** and is given in equations 7 and 8,

$$w1 = \frac{s/M + w_b}{s + w_b A} \qquad (7)$$

$$w2 = \frac{Ls + 1}{2(0.5Ls + 1)} \qquad (8)$$

Where W_1 is the performance weighting function, W_2 is the robustness weighting function, 'w_b' is the cut off frequency, 'M' is the gain for high frequency disturbances and 'A' is the gain for low frequency control signal and L is a constant. The plots, Fig 4 & Fig 5 show the nature of $\frac{1}{W1(j\omega)}$,S and $\frac{1}{W2(j\omega)}$, T to be satisfied for the synthesis of H∞ controller. This can be made by closely shaping the $\frac{1}{W1(j\omega)}$ and $\frac{1}{W2(j\omega)}$ plots. This loop shaping technique consists of adjusting the various parameters of the weight functions. A generalization is made on how these parameters are to be varied to closely shape the curves to make a robust H∞ controller synthesis algorithm. The flow chart of the automatic weight selection algorithm is shown in Fig 7. The objective of the algorithm is to modify the weights until the various performance criterions specified in robust control theory is met. As per the robust control criterion, the algorithm searches for a minimum value of cost function γ along with shaping the closed loop responses of sensitivity function, and complementary sensitivity function.

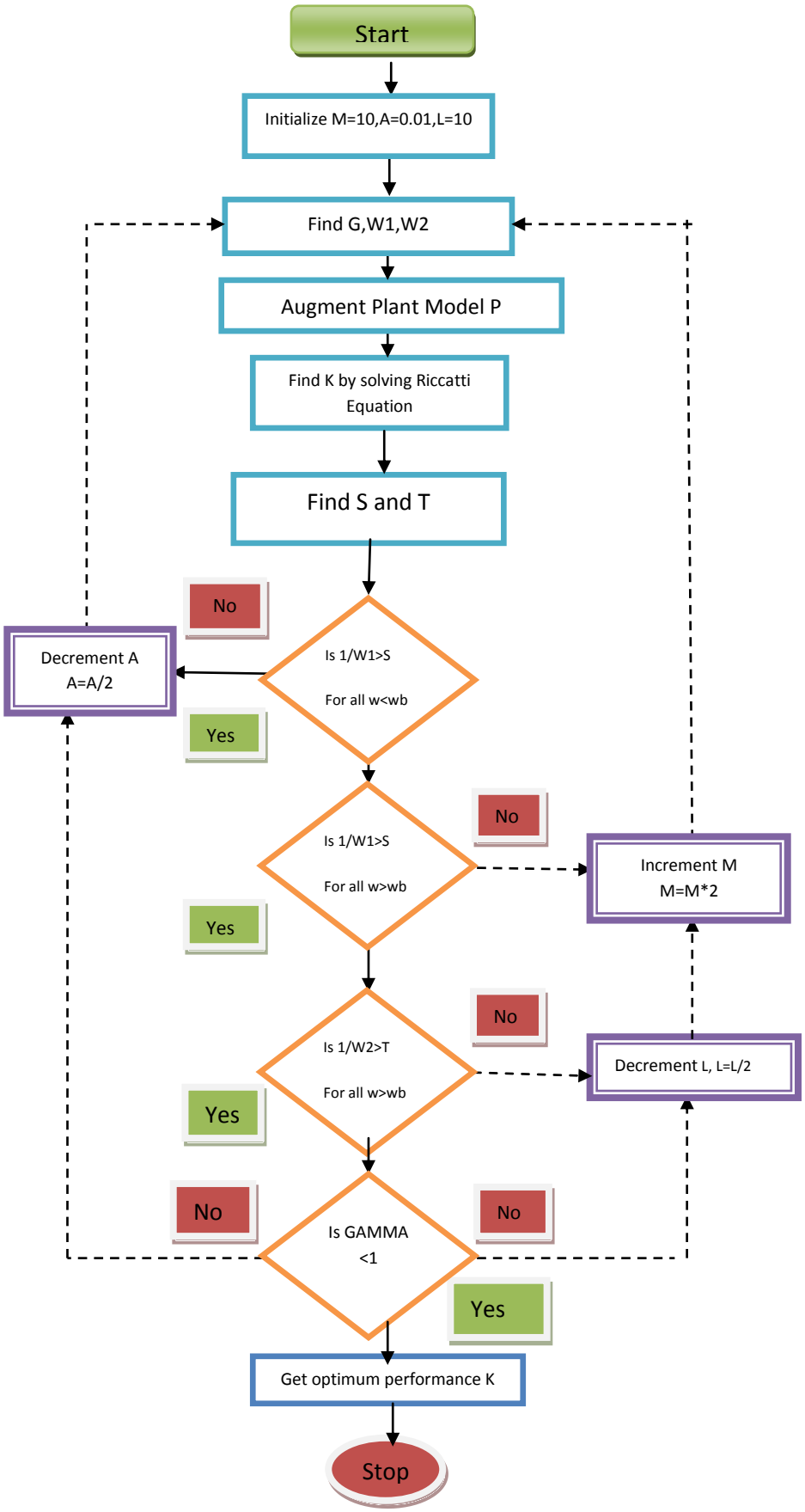

FIGURE 7: AUTOMATIC WEIGHT SELECTION ALGORITHM

VII. SIMULATION AND RESULTS

RESPONSE OF AVR WITHOUT ANY CONTROLLER

The MATLAB-Simulink model of the AVR system without any controller is shown in figure 8. A step reference voltage signal of amplitude 1 pu is applied to the system.

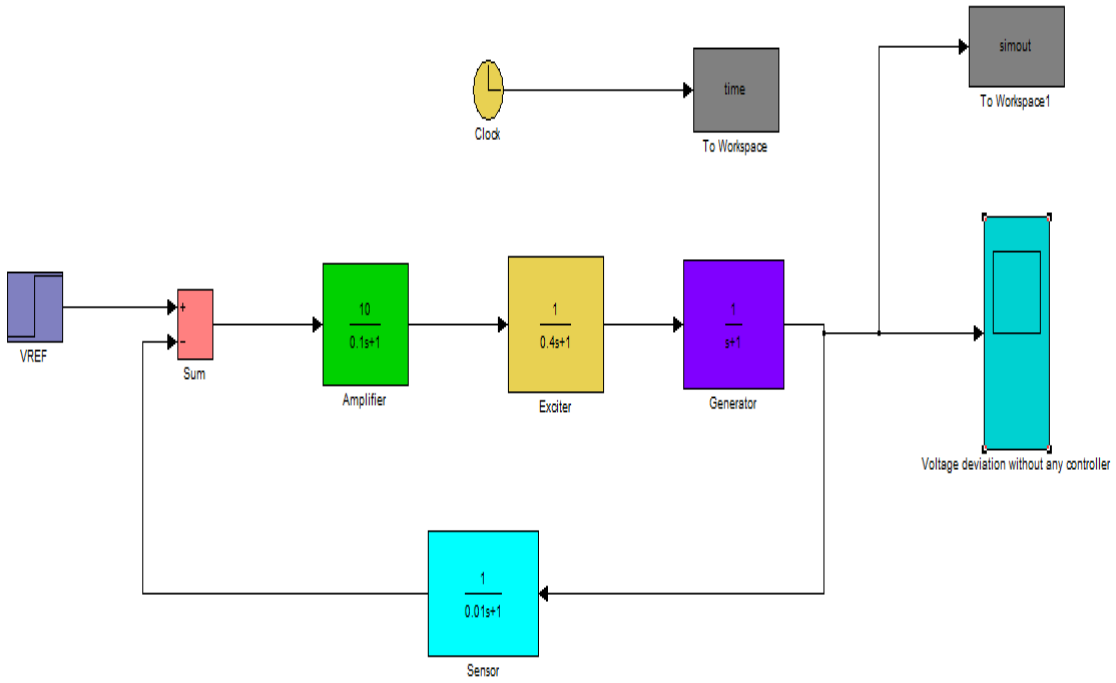

FIGURE 8: SIMULINK MODEL OF AVR WITHOUT ANY CONTROLLER

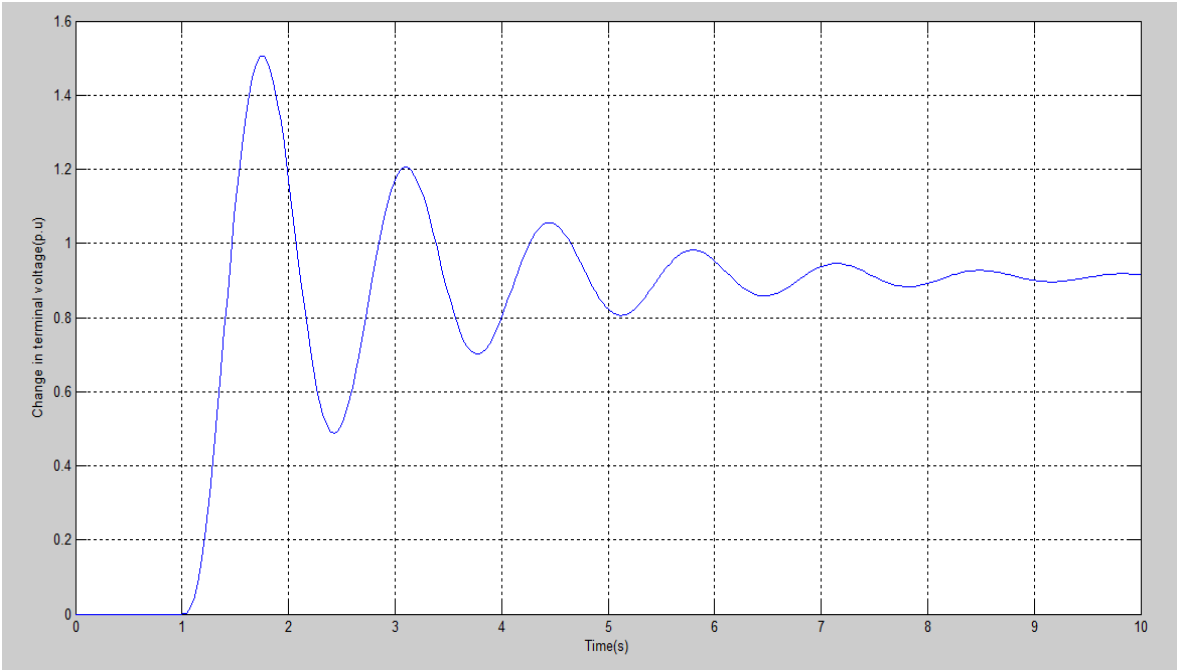

FIGURE 9: STEP RESPONSE OF CHANGE IN THE TERMINAL VOLTAGE WITHOUT ANY CONTROLLER

H∞ CONTROLLER DESIGN FOR AVR

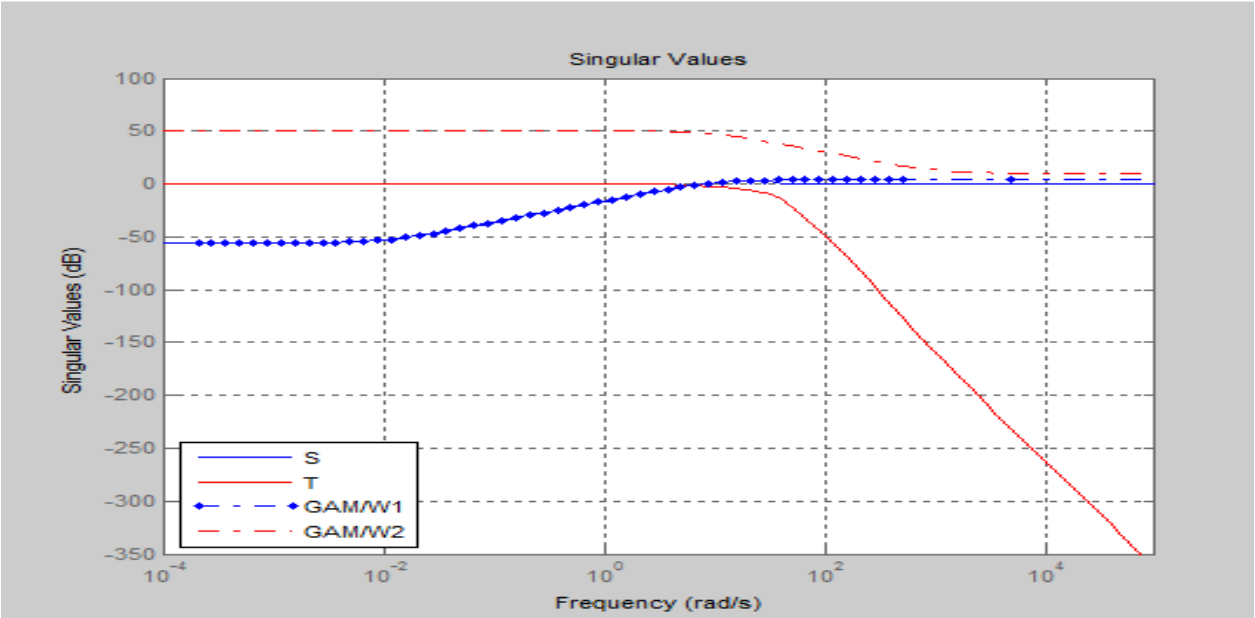

FIGURE 10: SINGULAR VALUES OF AVR

INPUT WEIGHTING FUNCTION

W1 is the input weighting function. It is used to limit the magnitude of the sensitivity function as shown in figure 11. W1 is obtained by using automatic weight selection algorithm,

$$W1 = \frac{0.1(s+10)}{(s+0.01)}$$

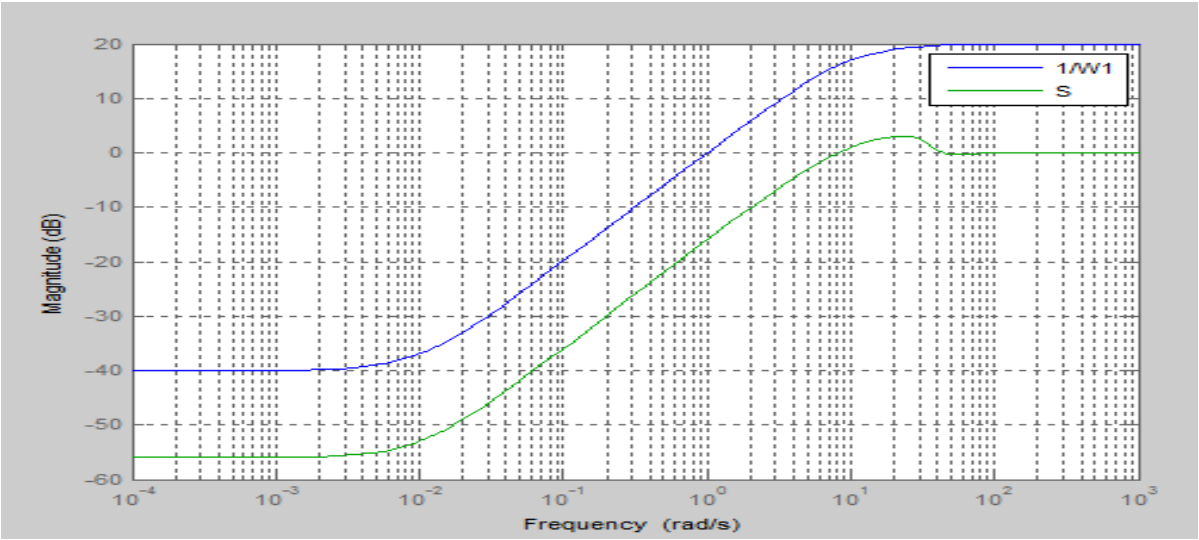

FIGURE 11: INPUT WEIGHTING FUNCTION '1/W1' LIMITING THE MAGNITUDE OF SENSITIVITY FUNCTION 'S'

OUTPUT WEIGHTING FUNCTION

W2 is the robustness weighting function. It is used to limit the magnitude of the complementary sensitivity function 'T' as shown in figure 12. W2 is obtained by using automatic weight selection algorithm,

$$W2 = \frac{0.005(s+10)}{(s+1000)}$$

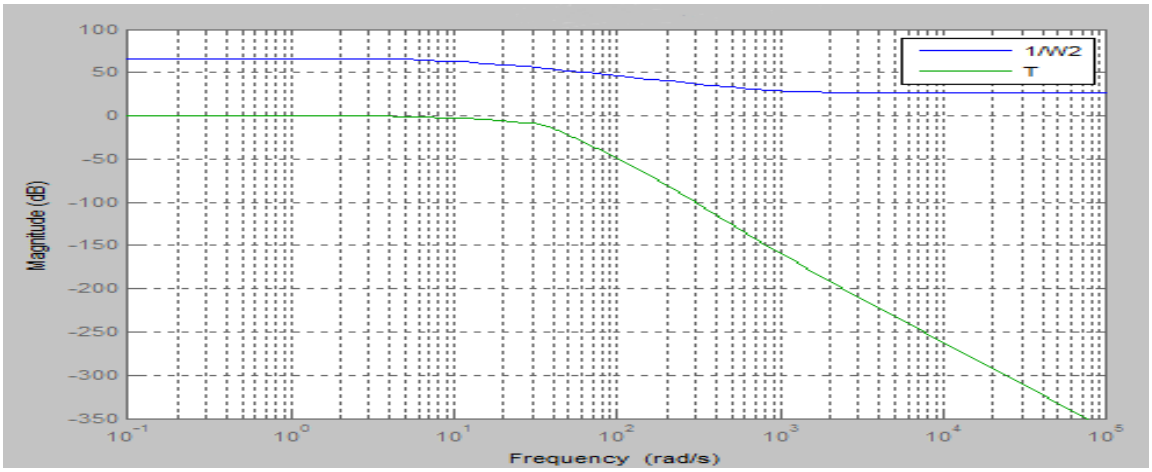

FIGURE 12: OUTPUT WEIGHTING FUNCTION '1/W2' LIMITING THE MAGNITUDE OF COMPLEMENTARY SENSITIVITY FUNCTION 'T'

RESPONSE OF AVR USING H∞ CONTROLLER

As we know that our system was unstable before H∞ Controller. Now we have designed H∞ Controller and performed a closed loop analysis. We can see from the figure 13, that the system has become stable and tracks the reference input. Settling time of the closed loop system is 0.448 seconds second and rise time is 0.22 seconds.

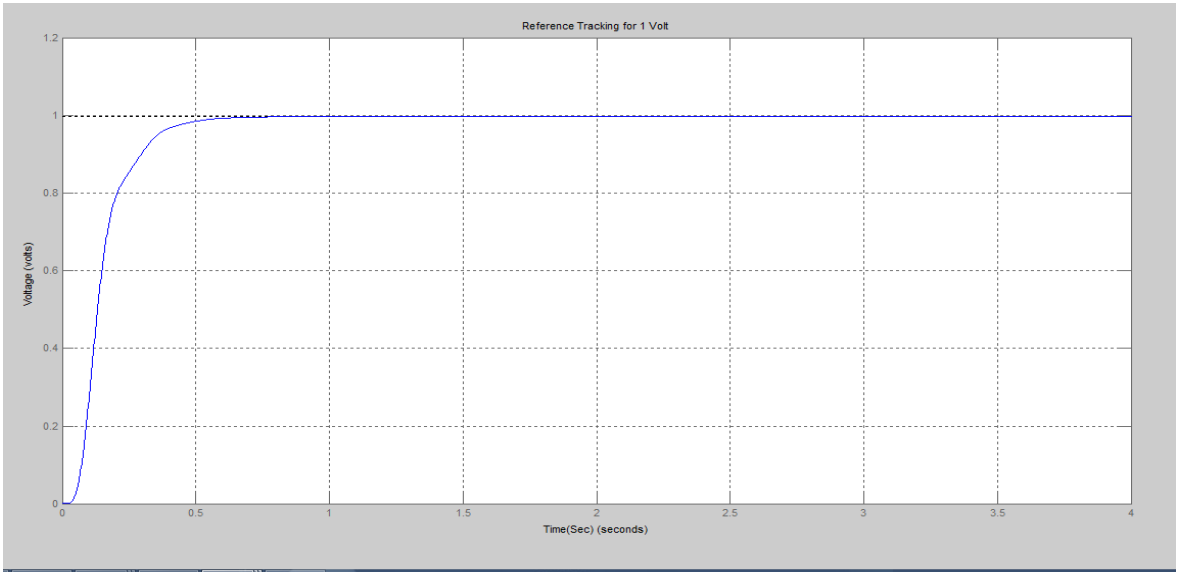

FIGURE 13: STEP RESPONSE OF CHANGE IN THE TERMINAL VOLTAGE WITH H∞ CONTROLLER

S#	PARAMETERS	AVR WITHOUT CONTROLLER	AVR WITH H∞ CONTROLLER
1	% Overshoot	50.75	0
2	Rise time	0.468	0.2
3	Settling time	7.1	0.448

Table 1: COMPARISON OF AVR WITH AND WITHOUT H∞ CONTROLLER.

REFERENCE TRACKING

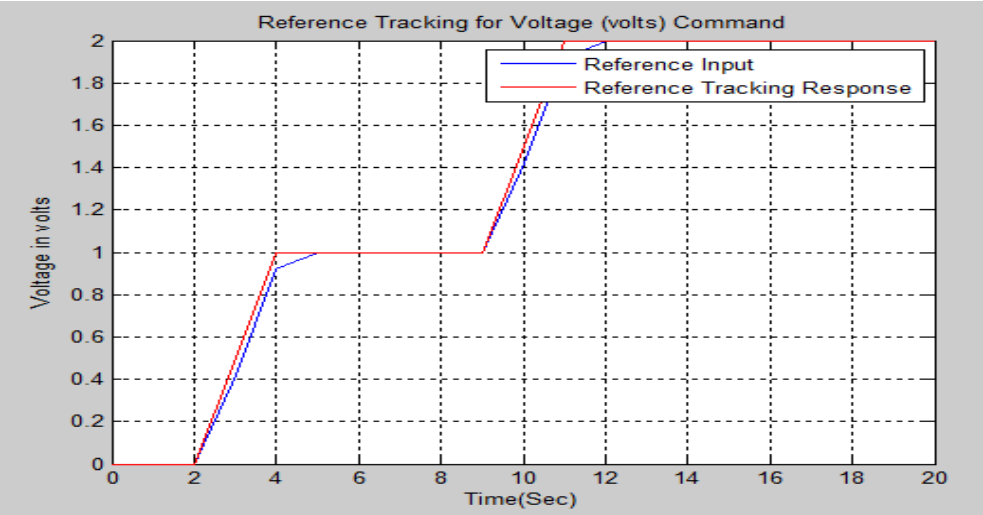

FIGURE 14: REFERENCE TRACKING RESPONSE OF AVR

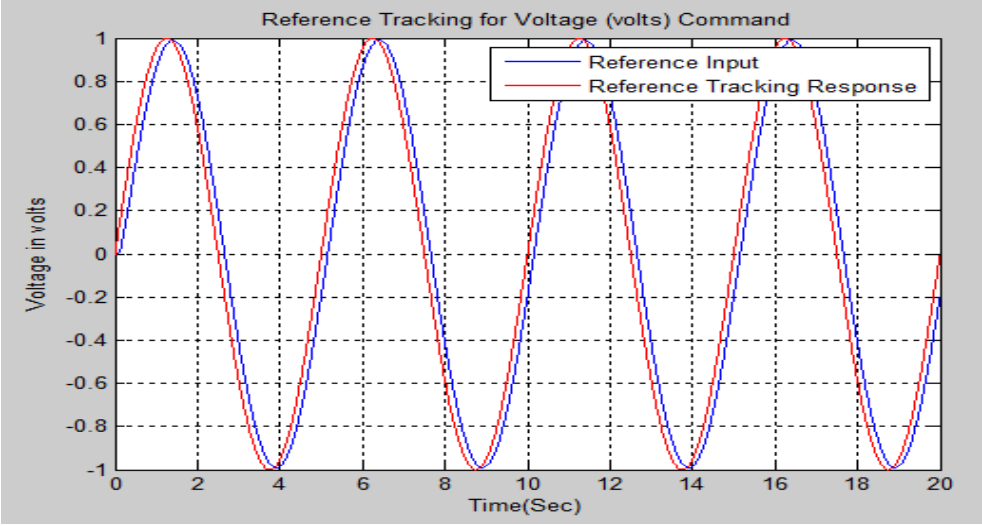

FIGURE 15: SINUSOIDAL RESPONSE OF AVR

CONCLUSION

It has been shown that H∞ control technique can effectively be applied with AVR. The results show that the performance of AVR using H∞ control is high compared to conventional AVR. The tuning of weighting functions using 'Automatic Weight Selection Algorithm' enables the control synthesis algorithm to converge to a feasible solution meeting all the requirements of robust control. Simulations results show the efficient working of the controller. Simulation contains the closed loop step response of the system. It was found that the system becomes stable and tracks the reference input. Reduction in Settling time and rise time is observed. The controller is also tested for voltage deviation, the AVR will attain the required voltage corresponding to the given reference voltage command. The simulation results show that the proposed controller is robust against disturbances. At the completion of this research, there are many key points which are learnt about the H∞ design procedure. H∞ controller has the capability to maintain stability and robustness of AVR under the presence of load disturbances in power system. The control effort generated by this technique is under limits and can be easily applied to the plant.

APPENDIX

Name of Parameter	Gain	Time Constant
Amplifier	K_A=10	T_A=0.1
Exciter	K_E=1	T_E=0.4
Generator	K_G=1	T_G=1
Sensor	K_R=1	T_E=0.01

TABLE 2: PARAMETERS OF AVR

ACKNOWLEDGEMENT

The first author is thankful to Dr. Muhammad Ejaz Hassan, Associate Professor & Head, Department of Electrical Engineering, Army Public College of Management & Sciences (APCOMS) Rawalpindi, (U.E.T) Taxila, Pakistan for his valuable suggestions and necessary recommendations.

REFERENCES

[1] Hany M. Hasanien, "Design Optimization of PID Controller in Automatic Voltage Regulator System Using Genetic Algorithm Method", IEEE Systems Journal, VOL. 7, NO. 4, DECEMBER 2013

[2] Hestikah Eirene Patoding, Eodia T. Lobo, Matius Sau, "Modeling Control of Automatic Voltage Regulator with Proportional Integral Derivative, International Journal of Research in Engineering and Technology", Volume: 04 Issue: 09 September -2015

[3] Ashok singh, Rmeshwar Singh, Rekha kushwah, "Automatic Voltage Regulator and Automatic Load Frequency Control of Electric Power Plant with optimal tuning PID" , International Journal for Research in Applied Science & Engineering Technology (IJRASET), Volume 3 Issue X, IC Value: 13.98 ISSN: 2321-9653, October 2015

[4] Hwan Il Kang, Min Woo Kwon, "Comparative Study of PID Controller Designs Using Particle Swarm Optimizations for Automatic Voltage Regulators", IEEE Systems Journal, 978-1-4244-9224-4/11, 2011

[5] Z.-L. Gaing, "A particle swarm optimization approach for optimum design of PID controller in AVR system", IEEE Trans. Energy Convers,vol. 19, no. 2, pp. 384–391, Jun. 2004.

[6] V. Mukherjee and S. P. Ghoshal, "Intelligent particle swarm optimized fuzzy PID controller for AVR system", Electr. Power Syst. Res., vol. 77,no. 12, pp. 1689–1698, 2007.

[7] P.Mitra, S.Chowdhury, "Performance of a Fuzzy LogicBased Automatic Voltage Regulator in Single andMultiMachine Environment, IEEE Systems Journal",10.1109/UPEC.2006.367644,04 June 2007.

[8] A. Visioli, "Tuning of PID controllers with fuzzy logic," IEE Proc. Control Theory Appl., vol. 148, no. 1, pp. 1–8, Jan. 2001.

[9] R. A. Krohling and J. P. Rey, "Design of optimal disturbance rejection PID controllers using genetic algorithms," IEEE Trans. Evol. Comput, vol. 5, no. 1, pp. 78–82, Feb. 2001.

[10] D. Devaraj and B. Selvabala, "Real-coded genetic algorithm and fuzzy logic approach for real-time tuning of proportional-integral-derivative controller in automatic voltage regulator system," IET Generation Transmission Distribution, vol. 3, no. 7, pp. 641–649, 2009.

[11] J. Zhang, J. Zhuang, H. Du, and S. Wang, "Self-organizing genetic algorithm based tuning of PID controllers," Inform. Sci., vol. 179, no. 7, pp. 1007–1018, Mar. 2009.

[12] H. M. Hasanien and S. M. Muyeen, "Design optimization of controller parameters used in variable speed wind energy conversion system by genetic algorithms," IEEE Trans. Sustainable Energy, vol. 3, no. 2, pp.200–208, Apr. 2012.

[13] D. E. Goldbert, "Genetic Algorithm in Search, Optimization and Machine Learning. Reading, MA: Addison-Wesley",1989.

[14 G. Zames, "Feedback and complexity, special plenary lecture addendum", IEEE Conference on Decision and Control, 1976.

[15] D. McFarlane and K. Glover, "A loop shaping design procedure using H∞ synthesis", IEEE Transactions on Automatic Control, 37:759–769, 1992.

[16] B. Shafai H. Oloomi, "Weight selection in mixed sensitivity robust control for improving the sinusoidal tracking performance", Proceedings of the 42nd IEEE Conference on Decision and Control Maui, Hawaii USA, Dec 2003.

[17] John E. Bibel and D. Stephen Malyevac, "Guidelines for the selection of weighting functions for h∞ control", January 1992.

[18] Hadi Saadat, Power System Analysis Tata McGraw-Hill series publishing companay Limited New Delhi, India 2002

[19] Stefani, Design of Feedback Control Systems ,4th Ed.

[20] J. W. Helton,"Operator theory and broadband matching". Proceeding of IEEE Allerton Conference, 1979.

[21] A. Tannenbaum, On the blending problem and parameter uncertainty in control theory. 1977.

[22] M. G. Ortega M. Lopez-Martinez, C. Vivas, “Multivariable nonlinear H∞ controller for laboratory helicopter”. Proc. of 44th IEEE conference on Decision and Control and European Control Conference, Seville Spain, 2005.

[23] M.G. Ortega M M. Lopez-Martinez and F.R. Rubio, “An H∞ controller of the twin rotor laboratory equipment”, Proceeding of 11th IEEE International Conference on Emerging Technologies and Factory Automation (ETFA03), 2003.

[24] J. C. Doyle K. Zhou and K. Glover, Robust and Optimal Control. Prentice- Hall, 1996.

[25] F.R. Rubio M.G. Ortega, “Systematic design of weighting matrices for the H∞ mixed sensitivity problem”, Journal of Process Control, 14:89–98, 2004.

[26] Sarath Nair, “Automatic Weight Selection Algorithm for Designing H Infinity controller for Active Magnetic Bearing”, January 2011.